Implication of Future Carbon Dioxide Injection on Selected Niger-Delta Reservoir Rocks and Fluids.

By

ADEBAYO Thomas Ayotunde

(CUGP070199)

A Thesis Submitted in the Department of Petroleum Engineering, School of Engineering, College of Science and Technology to the School of Postgraduate Studies

As part of the requirements for the award of the degree of Doctor of Philosophy (Ph.D) in Petroleum Engineering of Covenant University, Ota, Ogun State, Nigeria

July 2013

Certification

We hereby certify that this thesis is an original research work carried out independently by Thomas Ayotunde ADEBAYO under our supervision in partial fulfillment of the requirements for the award of the Degree of Doctor of Philosophy (Ph.D) in Petroleum Engineering of Covenant University, Ota, Ogun State, Nigeria.

Prof. Churchill T. Ako
(Supervisor)
Professor of Chemical Engineering
Department of Petroleum Engineering
Covenant University, Ota, Nigeria.

Prof. Frederick K. Hymore
(Co-supervisor)
Professor and Head
Department of Chemical Engineering
Covenant University, Ota, Nigeria.

Dedication

To God Almighty, the only One Who is worthy of praise and adoration; Who was and is and is to come; Who can kill and makes alive.

Acknowledgement

Success is based on the ability to get the right help at the right time. I hereby acknowledged all those who were helpful to me at the time of need. Without the collective effort of the many rivers, the ocean might have dried up.

My special thanks go to my immediate family for their moral support and understanding. It is only a man that has peace that can achieve tangible things in life. A peaceful wife and peaceful children are beyond all that money could obtain. I say a big thank you to Glorious, Divinefavour, Divinefaithfulness, Divinecovenant, Divinefulfillment and Divinegreatness.

I acknowledge the tremendous effort of my supervisors, they were almost more eager for the completion of this research than I. They were sources of encouragement especially in the time of discouragement due to prolonged challenges in accessing the right equipment. Prof. Ako is a father and Prof. Hymore is always eager to know the level of progress on the work. They took much time in going through the work and giving quality advice that led to a new vision on the research process. Prof. Omoleye of Chemical Engineering Department and Prof. Kehinde Okonjo of Chemistry Department, Covenant University, were of tremendous help in given useful information and corrections that were of great help in the completion of the work.

Table of Contents

List Of Figures

List of Tables

List of Abbreviations and Symbols

AAS	Atomic Absorption Spectrometer.
CCS	Carbon capture and storage
CO_2	carbon dioxide
K/k	permeability
SEM	scanning electronic microscope
SC	super critical
OBM	water-in-oil mud (oil-based mud)
WBM	water based mud
S_{wirr}	irreducible water saturation
P1, P2	porosimeter pressure readings.
MilliDarcy	unit of pressure equivalent to 9.869233×10^{-16} square meters
C_p'	shear stress peak parameters
C_r	shear stress residual parameters
Ø	porosity
φ_r	the effective residual stress friction angle
φ_p'	the effective peak stress friction angle

Abstract

Mitigation against increasing carbon dioxide, CO_2, in the atmosphere is uppermost in environmental research due to its negative effects and the most effective approach is in the area of underground carbon storage. In this research, a model was developed to study the possible alteration of porosity and permeability during CO_2 injection to Kwale sandstone reservoir, Kwale shales, Imeri oil sand and Ota Kaolinitic clay. The proposed model combined the Timur model irreducible water saturation equation and the Coates-Dumanoir permeability equation, to describe CO_2 injection influence on the Kwale reservoir permeability. The proposed model gave permeability values ranging from 0.06 milliDarcy to 92.46 milliDarcy for the Kwale sandstones and shale; 2.01 to 10.2 milliDarcy for Imeri oil sand and 1.8 to 10.2 milliDarcy for Ota Kaolinitic clay samples. In comparison, the Timur model gave permeability values from 0.0 to 634 milliDarcy; Tixier values range from 0.0 to 10053 milliDarcy; Coates-Dumanoir gave values of 6.68 - 8550 milliDarcy while Aigbedion gave values ranging from -3.7 to 5.94 milliDarcy. The published Kwale sands permeability ranges from 0.8 to 87 milliDarcy. During this research it was discovered that the injection of CO_2 into Kwale sandstones resulted in an increase in the porosity of the sandstone, which is an indication of possible reaction between the injected CO_2 and the formation. This made the Kwale sandstone formation a potential CO_2 storage reservoir. It was concluded that the black Kwale shale lacked storage integrity as the stored gas may migrate to nearby reservoirs. The grey shale is recommended for CO_2 storage as there was observed increase in porosity which is an indication of possible reaction with the CO_2 to form new minerals which will make the gas to remain underground. Imeri oil sand formation is too porous and is recommended, with reservation, as a potential CO_2 storage reservoir. The Ota Kaolinitic clay with its moderate initial porosity and reducing porosity with CO_2 injection is a potential storage reservoir for CO_2. It was observed that there is no single equation to describe the permeability variation with time for the samples considered but the permeability is a second degree polynomial in time and porosity immediately after injection but has an exponential relationship with the time/porosity after some days of injection. Moreover, research was conducted on the possible leakage of the stored CO_2 to a nearby formation being drilled or produced. It was

observed that this leakage will create drilling problems due to its side effect on the properties of the drilling mud and the oil in place. CO_2 leakage into a nearby producing reservoir will affect the property of the producing oil negatively and there may be need for further treatment of the crude at the surface.

Chapter 1

INTRODUCTION

1.1. Background Of The Study

The most important on-going research is in the area of climatic change and its negative effect on the environment. Most of this research is concentrated on the environmental impact of petroleum production and product utilization and is mostly on the sequestration of carbon dioxide, CO_2, its storage and possible injection into reservoirs for enhanced oil production or for storage purpose. It has been observed that CO_2 emission into the atmosphere can be reduced through its application in food products canning, application in oil recovery and CO_2 sequestration and storage.

Sequestration can be of the surface or geological in application. Surface sequestration involves the use of forest or plants to absorb CO_2 gas as a mitigating factor for the reduction of atmospheric CO_2. Geological sequestration involves the sub-surface injection of captured atmospheric carbon dioxide to displace methane from underground coal deposits, enhance the recovery of oil from the sub-surface and storage in abandoned oil or saline reservoirs. The process of CO_2 mitigation is depicted in Figure 1.

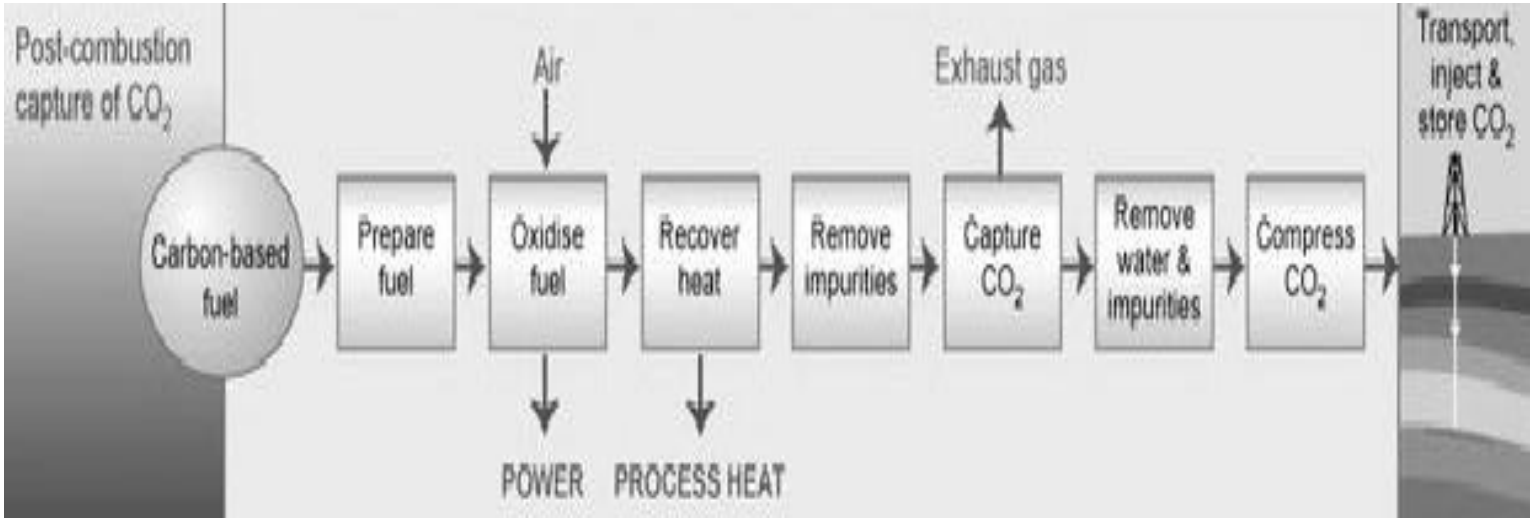

Fig. 1: Typical Process Of Combustion CO_2 Mitigation
(Source: Scottish Centre for Carbon Storage)

Much work has been done on carbon capture and storage (CCS) in the developed countries but virtually no recorded research is available on the Niger-Delta environment. Unfortunately, Niger-Delta reservoir characteristics are quite unique and different from the carbonate, silicate and basaltic reservoirs where most of the research has been concentrated. Niger-Delta reservoirs are mostly made of sandstone, with varying degrees of shale content and growth fault structure. Since CO_2 storage is dependent on the ability of the CO_2 to react with and remain in the storage structure, there is need for research on the lithological characteristics of the desired storage reservoir as this will reveal the ability of the reservoir to serve as a secure storage. Moreover, the sandy nature of the Niger-Delta reservoirs is currently causing sand production problem in the region.

Nigerian environment also contributes to the emission of the CO_2 that is creating the world environmental problem as a result of present power generation challenges in Nigeria forcing people to consume more combustible fuel, coupled with gas flaring and uncontrolled CO_2 emission. Therefore, the country needs to consider removal of the CO_2 from the atmosphere as a matter of urgency.

Owing to the present economic situation that makes funding for research difficult, there is a high probability that Nigeria may end up importing the CCS technology/process, employed in the developed countries, instead of going into new researches that is specifically applicable to the sub-surface nature of her reservoirs. This could result in serious problems in the Niger-Delta sandstone reservoirs. This research reported in the thesis is intended to correct this and to serve as a basis for the general application of CCS technology in Nigeria.

This research examines the challenges associated with storing captured CO_2 in the Niger-Delta reservoirs. The major questions requiring adequate responses are:

1. Will there be formation of secondary porosity and improved/impaired permeability?
2. Will the present problem of sand production be addressed or compounded as a result of reactions between CO_2 and the reservoir fluids/matrix leading to porosity variation?

3. Will the sub-surface formation adjacent to, or those underlying, the power generation plants be good candidates or suitable storage for CO_2 that may be captured from the power plants?
4. What is the possible negative effect of future leakage of the stored CO_2 on exploration activities in the Niger-Delta environment?

1.2. Research Objectives

This research examines:

1. Anticipated problems associated with future storage of captured CO_2 in Niger-Delta reservoirs.
2. Possible alterations of the reservoir matrix and fluid properties.
3. Consequences of the reservoir alterations on storage safety.
4. Consequences of matrix alteration on exploration activities in nearby fields and on oil production and separation.

1.3. Scope of Study

Considering the data available on Nigerian industries, the scope of the research was based on the effects of injected CO_2 on reservoirs that are close to the sources of high CO_2 pollution namely:

1. The gas turbine generation plants in Nigeria listed in Table 1.1 below, with special consideration of Ughelli thermal power plant, Sapele Gas turbine, Omotosho power plant and Afam power plant.
2. Olorunsogo power plant and Ewekoro cement manufacturing complex.
3. Egbin power plant and the Lagos/Ogun industrial complexes. This concentration of industries is a good source of CO_2 capture candidates.

Table 1.1: Power Generation Plants in the Niger-Delta Region

(Sources: *Daily Times NG*, 30th Jan. 2013; Adelere, 2012; Eberhard and Gratwick, 2012)

Power station	**Community**	**Type**	**Capacity**	**Installed Capacity**	**Major sub-surface formations**
Afam Power Station	Afam	Gas turbine	420 MW	420 MW	Afam clay, Niger- Delta complex
Egbin Thermal Power Station	Egbin, Lagos State	Gas-fired steam turbine	1320 MW	It has six 220 MW independent units.	Oshosun formation (Benin formation)
Sapele Gas turbine Power Station	Sapele, Delta State	Gas turbine	225 MW	300 MW	Niger-Delta formation (adjacent to Kwale oil fields)
Olorunsogo Phase I and II Power Station	Olorunsogo, Ogun State	Gas turbine	160 MW	700 MW (Phase I/II)	Ewekoro limestone; Kaolinitic clay; oil sand
Omotosho Power Station (Phase I and II)	Omotosho, Ondo State	Gas turbine		335 MW (Phase I) 450 MW (Phase II)	Ondo State Oil sand
Ughelli Thermal Power Station	Ughelli, Delta State	Gas-fired steam turbine	330 MW	972 MW	Niger-Delta complex (adjacent to Kwale oil fields)
Geregu Power Plant	Geregu, Kogi State	Gas turbine		414 MW 434 MW (Phase II)	Middle Niger Basin complex

Sapele turbine power plant is included as a candidate for future CO_2 capture operation and it is adjacent to the Sapele and Kwale oil fields. This is because the *Leadership Newspaper* of July 04, 2012 quoted the speech of the Nigerian Minister of Information, Labaran Maku, stating that "Sapele Power Plant has began Operation and is expected to inject 225 MWs To National Grid".

In the actual sense, every country contributed to CO_2 emission and yet not all have abandoned oil reservoir for CO_2 storage. This necessitated the consideration of other readily available potential CO_2 storage reservoirs. Clay was considered because all countries have clay underground and the captured CO_2 can then be stored in the clay. Oil sand was also considered in this research as potential CO_2 storage reservoir because of its vast deposit in the world. Moreover, Ehlig-Economides and Economides (2010) estimated from calculations that the volume of CO_2, either in liquid or supercritical gas form, to be disposed cannot exceed more than 1% of the available oil reservoir pore space. This implies that most of the past estimates on available underground reservoir volumes for CO_2 storage are in excess of 5000 to 20000 percent. This necessitated the reason to look beyond abandoned oil reservoirs and consider other underground rocks that can serve as potential storage facility.

The research therefore focuses on the following:

1. Kwale sandstones and shale reservoirs, Niger-Delta region, as a storage candidate for CO_2 that is expected to be captured from Sapele, Ughelli and Afam power plants. This includes the following:
    - Investigation of the possibility of reaction between Niger-Delta reservoir sandstone grains (Kwale reservoir) and compressed CO_2, resulting in the formation of new compounds that enhanced or destroyed the cementation property of the reservoir.
    - The possibility of instability in the reservoir structure was investigated by considering the possibility of alteration of the porosity and permeability of the Niger-Delta reservoir. Such a porosity change may lead to lower or higher underground oil sand production in an area already facing sand production problem.
    - Investigation of the possibility of reaction between injected CO_2 and the water layer that is connected to a producing reservoir, resulting in the formation of weak carboxylic acids.

2. Ota Kaolinitic clay, member of Oshoshun formation complex.
   Investigation involved the possibility of CO_2 storage in the Ota Kaolinitic clay underlying the Olorunsogo power generating plant and located adjacent to Lagos/Ogun industrial complex and also near Egbin thermal power plants as a future candidate CO_2 storage reservoir.

1. Nigeria oil sand reservoir (Imeri Oil sand, Ogun State)
   Investigation was made of the possibility of CO_2 storage in the oil sand sub-surface as candidate CO_2 storage reservoir adjacent to Egbin, Omotosho and Olorunsogo power generation plants and the Lagos/Ogun industrial complex. This is because the power plants and the industrial complex are possible future CO_2 captured sources.

2. Also considered was the CO_2 effect on the Niger-delta crude and simple drilling fluids. This is to mitigate against possible CO_2 leakage from stored Niger-Delta reservoir to nearby reservoir with production or exploration activities. Nigerian Bonny light crude and simple drilling fluids were considered.

Sedimentary characterization of the formation adjacent to Olorunsogo power plants I/II and Egbin thermal plant in the study area is summarized in Table 1.2.

Table 1.2: Formations Underlining Lagos/Ogun Study Area. (Based on the works of Omatsola and Adegoke, 1981, Adegoke, 1977, Ogbe, 1972, Agagu, 1985, Kogbe, 1976 and Jones and Hockey, 1964).

Basin	Group	Members	Characteristic features
Dahomey Basin		Coastal plain sands	This is the youngest sedimentary unit in the eastern Dahomey Basin. It probably overlay the Ilaro Formation unconformable, but convincing evidence as to this is lacking (Jones and Hockey, 1964). It consists of soft, poorly sorted clayey sand and pebbly sands
		Ilaro Formation	A sandstone unit with mainly coarse sandy estuarine deltaic and continental beds and with rapid lateral facies change. It is the most intensive formation in the Idiroko, Ilaro and Ewekoro environment. It overlies the Oshoshun formation.
		Oshoshun Formation	It is a sequence of mostly pale greenish-grey laminated phosphate marls, light grey white-purple clay with interbeds of sandstones. It also consists of clay stone underlain by argillaceous limestone of phosphatic and glauconitic materials in the lower part of the formation. The sedimentation of the Oshoshun Formation was followed by a regression.
	Imo group	Akinbo Shale Formation	It is made up shally limestone about 12.5m thick which tends to be sandy and is of gritty sand to pure grey and with little clay. Lenses of limestone of Ewekoro Formation are found in this formation.
		Ewekoro Formation	It is mostly limestone in characteristic features and contains an average of 89.2% CaO, 1.9%MgO, 1.5% Al2O3, 5.7% S_iO_2 and 5.9% Fe_2O_3 (Akinmosin, 2005)
	Abeokuta Group	Araromi Formation	It is a sand formation and it is overlain by dark-grey shale and inter-bedded limestone and marls occasional lignite bands
		Afowo Formation	Made up of coarse to medium- grained sandstones with variable interbeds of shale, siltstones and clay.
		Ise Formation	Made up of continental sands, grits and siltstones

The Ota kaolinitic clay used in this research is a sequence of light grey and white-striped purple clay with interbeds of sandstones. This is a characteristic feature of the Oshoshun formation and is regarded as a member of that formation. A borehole was sunk at Benja- Ota and it encountered series of white kaolinitic clay followed by a thin sandstone layer and by pink kaolinitic clay. Two open, 0.9 meter diameter, wells dug around Idiroko Road at Onibuku-Ota and Canaanland-Ota area which are within 2 kilometers radius of the Benja–Ota environment, gave the same characteristic strata. Below this depth is a very thick layer of clay which is very problematic during drilling since it creates drill string differential sticking.

1.4. Methodology

The research was laboratory based while literature and past models were used for inference purposes. The laboratory analysis was divided into four major parts and the laboratory experiments monitored the following:

1. Implication of injecting CO_2 directly to zones of different formation fluids such as gas, oil and water zones.
   - Laboratory reactions between CO_2, brine and Kwale reservoir rocks at high pressure and the study of alteration of the reservoir rock properties.
   - Laboratory reaction between CO_2 and a typical Bonny light crude.
   - Investigation on the possible formation of secondary porosity and enhanced/impaired permeability of the reservoir.

2. Implication of injecting CO_2 into the Kaolinitic clay underlying the Olorunsogo power plant using Ota Kaolinitic clay as a representative candidate.

3. Implication of injecting CO_2 into an oil sand zone and possible alteration of properties of the oil sand.

4. Irreducible water saturation evaluations were carried out using a centrifuge and drying method analyses.

5. Implication of CO_2 leakage from stored Niger-Delta reservoir to nearby wells being drilled. This is in the form of crude oil and drilling mud contamination.

Thereafter, permeability variation was modeled using available models since permeability variation is directly related to variation in effective porosity variation that was measured in steps 1 to 3 above.

1.5. Limitations of Research.

The expected limitation in this research is the inability to attain very high pressure, which is the condition for deep wells in the Kwale fields. The $40^{o}C$ ($104^{o}F$) temperature and 10337 KN/m^2 (1500 psi) pressure used represented shallow wells in that field.

Moreover, the Kwale fields sandstone samples available were obtained at 973 - 1020 meters (3200 - 3350 feet) sub-surface, which represented shallow wells. The oil operating companies in Nigeria are usually reluctant to release drill cores or cuttings to external persons as these are regarded as company secrets. This creates a limitation to extension of the study to very deep wells, which may be preferable candidates for CO_2 storage in the Kwale field.

The oil sand used is from an outcrop at Imeri village, Ijebu east, Ogun State and it has an extensive sub-surface deposit. Two boreholes were previously sunk by Government but only one was partially successful. The sticky nature of the oil sand deposit makes the sinking of boreholes difficult and very expensive. Unfortunately, there were no available rock samples from the previously dug boreholes due to non-preservation of the samples. Hence, this research used shallow samples as a representation that will give a pointer to what is to be expected at this reservoir, with respect to effects of CO_2 contact with the oil sand reservoir rock during the gas storage.

1.6. Experimental Considerations/Assumptions

Assumptions were made in this thesis on the possibility of an increase/reduction in reservoir porosity for various Niger-Delta sandstone and shale reservoir rock types. This is as a result of the dissolution of part of the rock grain minerals/cementing materials by the injected CO_2 gas. This dissolution was assumed to be the result of a

possible reaction between the reservoir rock matrix and the injected fluid and is not due to the pressure of injection.

Also considered is a change in the physical properties of the Imeri oil sand sample injected with CO_2. This experiment was carried out bearing in mind the location of industrial CO_2 sources around the vicinity of this oil sand deposits. This was mainly because five (5) thermal power generation plants are located within a 70 km (229,885feet) radius of the deposit while the hydrocarbon reservoirs are much farther than this. Moreover, the oil sand is also a type of hydrocarbon deposit and the future *in*-situ exploitation of this oil sand will create reservoirs that will be available for CO_2 storage. The gas turbine power plants located within the 70 km radius of the oil sand are Olorunsogo I/II, Omotosho I/II and Egbin power plants with total capacity of 2805 Mega Watts.

Moreover, the changes in the physical properties of Ota kaolinitic clay sample injected with CO_2 was considered. This was because the kaolinitic clay is located in the sub-surface under the Olorunsogo thermal power plant I & II and the Ewekoro cement complex. It will be a cheaper CO_2 storage reservoir, due to extra transportation cost to be expended, if the captured CO_2 from these plants/complex is taken to far away abadoned oil fields for storage.

The possible changes in the physical properties of the Bonny light crude sample contaminated with CO_2 was considered in the research. It is practically impossible to inject CO_2 into a reservoir without affecting the physical properties of the fluid in the reservoir. Any effect on the property of the crude, by the CO_2 gas, may have a negative influence on the future surface treatment of oil production from the reservoir, especially if the CO_2 injection process doubles as CO_2 storage and enhanced oil production. Moreover, the thesis was carried out with expectation of a leakage from the CO_2 stored reservoir into a nearby oil reservoir. This is due to unforeseen sub-surface deformation that may lead to the CO_2 storage reservoir structural failure.

The effect of a possible leakage of stored CO_2, as kick gas, on drilling activities in Niger-Delta was considered, due to the characteristic growth-fault of the Niger Delta coupled with the sand production challenges. It was rightly be assumed that, there might be a future leakage of stored CO_2 to a nearby formation due to the faults. Since

the research is based on the implications of future CO_2 storage in the Niger-Delta. Consideration was therefore given to possible contamination of the drilling mud being used during future drilling operation in a nearby reservoir/field. Experiments conducted focused on the effects of CO_2 kick on the properties of simple water-based drilling fluid and an oil-based drilling fluids.

1.6.1. Experimental Consideration For The Kwale Sandstone Samples

Sub-surface hydrocarbon reservoir conditions that are available for possible CO_2 injection are:

1. Sub-surface reservoir rock located in oil zone
2. Sub-surface reservoir rock located in the gas zone
3. Sub-surface reservoir rock located in the water zone

Other reservoir conditions that could be obtainable are

1. Sub-surface methane hydrates rocks.
2. Other types of sub-surface water reservoir rock.

Because reservoir rocks are also of two types, oleophilic and hydrophilic, the following are therefore practically obtainable in the sub-surface hydrocarbon reservoir rocks:

1. Oleophilic oil reservoir rocks.
2. Hydrophilic oil reservoir rocks.
3. Oleophilic water reservoir rocks.
4. Hydrophilic water reservoir rocks.
5. Oleophilic gas reservoir rocks.
6. Hydrophilic gas reservoir rocks.
7. Hydrophilic dry sub-surface rocks.

In order to satisfy some of the above reservoir conditions with the CO_2 injection, the following experiments were carried out:

a. Two core samples were soaked in crude oil and then injected with CO_2.
b. Two core samples were soaked in water and then injected with CO_2.
c. Two dry core samples were injected with CO_2 gas.

Since the used Kwale sandstone and shales reservoir core cuttings were not dried, it was assumed that it retained its common nature, which is mostly hydrophilic for sandstone and oleophilic for shales in the Niger-Delta environment.

In conclusion, this thesis establishes the bases for CO_2 injection in the Niger-Delta environment for oil reservoirs, clay reservoirs and oil-sand reservoirs. Presently, there are no available data on these reservoirs. Clay and oil sand reservoirs were considered as candidate CO_2 storage reservoirs because of the present continuous production in the Niger-Delta region, which presently make the oil reservoirs unavailable for CO_2 storage. Presently, the abandoned fields are being re-developed under the marginal field development programme of the Nigerian Government.

Further work is expected to continue using the bases established in this research and focusing on deeper formation zones.

Chapter 2

LITERATURE REVIEW

Gardner (2009) stated that "makers of biofuels and plastics and chemicals made from crops want U.S. Senators to change the climate bill to give them free pollution permits that would be needed to emit greenhouse gases under the legislation". The free pollution permits was considered for power Generation Company by the US Senate climate bill (Cowan and Gardner, 2010) but was temporarily abandoned in later part of 2010 with no limit to carbon emissions (Haroon, 2010). This implies that as one problem is solved by eliminating the use of fossil fuels due to their high carbon pollution, the same problem of pollution is expected to subsist with the new fuels system. This implies that the best approach to the problem is not to get rid of the fossil fuels but to intensify process of reducing atmospheric CO_2. The makers of the alternative motor fuel ethanol and plastics from renewable biomass, are asking for permission to be allowed to go ahead with carbon pollution for the next 38 years. They requested that the U.S. Senate should give them 1 to 5 percent of the emissions permits in a cap and trade program outlined from 2012 to 2050. The biofuels industry, which manufactures bio-plastics and chemicals, and is smaller than the oil refining industry which makes similar products, are actually asking for more permission to pollute more than the oil refining. The oil refining industry has been given 2 percent of the pollution permits under the bill. The reason that was that given by the biofuels and plastics industry was that, their plants produces products that are renewable and so should get a share of the permits.

Some studies proved that biofuels are carbon pollutants just like the fossil fuel (Liptow and Tillman, 2012; Weiss *et al*, 2012). The studies stated that the advantage of biofuels over fossil fuel, is that they pollute less. An example that was cited, is that ethanol made from corn has CO_2 emissions about 50 percent lower than those of the corresponding weight of gasoline. This ascertion is an indication that the biofuels are also carbon pollutants like fossil fuels. From the above, it can be seen that unless the weight volume of biofuel required for a given task, is less than half of the equivalent volume of the fossil fuel, biofuels may end up being higher carbon pollutants. There is an uncertain claim that cellulosic ethanol, a second generation fuel made from presently special non-food crops, is cleaner and has lower carbon emmision than ethanol

biofuels. If this comes to reality, then biofuels may be better than fossil fuels but when will it be available.

All this boils down to the fact that there will still be a need for CCS even when the use of fossil fuels ends. It is therefore pertinent to focus on the development of the CCS now.

2.1. Carbon Dioxide Sequestration

Qi (2009) modified a streamline-based simulator and used it to solve CO_2 transport in aquifers and oil reservoirs, in order to propose a design strategy for CO_2 injection to maximize storage in both aquifers and oil reservoirs. The consideration for CO_2 and brine injection added a solid and an extra liquid phase to the simulator such that there was a modification from two-phase to three-phase consisting of an aqueous phase, a hydrocarbon phase and a solid phase and a four-component (water, oil, CO_2 and salt) simulator specialized for CO_2 injection. The solid phase was added in the expectation that CO_2 injection would result in the formation of salt. Relative permeability changes and variations in the trapped non-wetting phase saturations due to hysteresis were considered on a block-by-block basis. The study of the design was also extended to oil reservoirs. In all these, an Eclipse simulator was used as the main simulator. The design was extended to the injection of high-pressure, supercritical CO_2 into a North Sea field, Maureen. He used 72 by 82 by 39 grid-blocks using a simple Eclipse 100 simulator. The Maureen field is an abandoned oil reservoir and consists mainly of submarine sandstones with the reservoir and fluid properties cited in Table 2.1.

Also investigated by Qi, was the effect of salt (halite) precipitation during dry supercritical CO_2 injection using a modified streamline-based simulator. In the study, the sensitivity of relative permeability, grid size and brine salinity to salt precipitations obtained, concluded that salt precipitation can be a very important effect to be considered when dry CO_2 is injected into a high salinity reservoir. This is because the observed result proved that just after 2 years of CO_2 injection, about 20% of the permeability of the reservoir was reduced. This will have serious effect on the injectivity effectiveness of the injector and also on the fluid flow within the reservoir. Unfortunately, in the research, consideration was not given to the possibility of improved permeability but only to damaged permeability near the wellbore. The major

assumption made during his research was that both CO_2 and brine were injected and then followed by brine injection alone. This resulted in over 80% of the CO_2 becoming immobile in the pore space and concluded that for thousands of years, the CO_2 will only form carbonate in the rock and will not migrate upward.

This assumption may not be totally correct since there is a possibility that the carbonate formed could easily be eroded by water infiltration from another reservoir, resulting in the formation of new compounds which may migrate upward due to the formation of a secondary porosity because of the carbonation reaction. Moreover, consideration was not given to the possibility of altered chemical composition of the rock matrix due to parallel reactions, between the injected CO_2 and the rock sediments and also the reaction between CO_2 and water forming weak acids which then reacts with the rock matrix. These two reactions tend to alter the porosity and the permeability of the formation as well as the mobility ratio of the fluids in the sub-surface. Consideration should also have been given to the incomplete dissolution of CO_2 in water due to the large volume of the CO_2. This will make part of the CO_2 to remain in the gaseous state.

In this thesis, some considerations were given to the dissolution of CO_2 in water and possible formation of salts. Also considered are expected resultant changes in porosity and permeability due to chemical reaction and salt precipitation.

Table 2.1: The Reservoir and Fluid Properties of Maureen Field.

(Qi, 2009)

Reservoir Properties		**Fluid Properties**	
Reservoir Area: 7200 m x 6000 m x 457 m (23645 ft x 19704 ft x 1500.8 ft)		Oil Gravity	850 - 876 kg/m^3 (53.1- 54.7 lb/ft^3)
Net to Gross Ratio	60 % - 84 %	Oil Viscosity	$7.3X10^{-4}$ Pa s
Average Porosity	18 % - 22 %	Oil Compressibility	$1.5X10^{-3}$ /MPa
Average Permeability	50 – 1000 mD	Water Viscosity	0.00035 Pa.s
Average Water Saturation	26 - 39 %	Water Density	1050 kg/m^3
Temperature	116^{o}C	Water Compressibility	$4.15X10^{-4}$ /MPa
Reservoir Pressure	26.5 MPa (3843 psi)	Rock Compressibility	$2.9X10^{-3}$ /MPa
		CO_2 Viscosity	$6X10^{-5}$ Pa.s
Oil Water Contact	2640 m	CO_2 Density	731 kg/m^3
Formation Volume Factor	1.37 rB/STB	Gas Oil Ratio	311 scf/stb
		Bubble Point Pressure	14.2 MPa (2059.5 psi)

Watson (2007) carried out a simulation study to determine the possibility of injected CO_2 early breakthrough to wellbores when used for the flooding of reservoirs. He stated that bentonite in cements are affected by CO_2 injection. This implies that when a well is cemented with cement that contains bentonite, it will end up being a storage risk during CO_2 storage in the reservoir containing the well. He stated that since Alberta wells are capped with cement bridge plugs, they are subject to serious failure in the presence of CO_2. This implies that if injected CO_2 breaks through to the cement plugs, the integrity of the storage is not guaranteed if the cementing cannot resist the reaction of the acidic gas.

Houston (2007) stated that there is a possibility that injecting CO_2 underground will cause it to react with the water and the minerals in order to be stabilized. He also assumed that, the gas will migrate into the sub-surface local environment instead of remaining as a giant gas bubble which will end up seeping to the surface. Contrary to the general belief that reactions might take place over hundreds or thousands of years, their study discovered that if CO_2 is injected into rocks, reactions will occur quickly, making the gas less likely to escape. This assertion was made based on data obtained from the Miller oilfield in the North Sea, where British Petroleum had been pumping sea water into the oil reservoir to enhance the flow of oil. It was discovered that as the analysis of the produced water was carried out during oil production, minerals was found to have developed and dissolved as the water travelled through the field. The overall assumption they made was that, there must have been a reaction between CO_2, water and the reservoir rock and that the reaction was beneficiary to CO_2 storage due to the formation of a trap.

Information from *Columbia Education Online* (2013), suggested that the stages of natural CO_2 sequestration and storage reactions are as follows:

1. Carbon dioxide is removed from the atmosphere by dissolving it in water and forming carbonic acid

$$CO_2 + H_2O \rightarrow H_2CO_3 \text{ (carbonic acid)}$$

2. Carbonic acid erodes the rocks, yielding bicarbonate ions, other ions, and clays

$$H_2CO_3 + H_2O + \text{silicate minerals} \rightarrow HCO_3^- + \text{cations } (Ca^{++}, Fe^{++}, Na^+, \text{etc.}) + \text{clays.}$$

3. Calcium carbonate is precipitated from the calcium and bicarbonate ions are formed in (2) above in seawater by marine organisms like coral such that:

$$Ca^{++} + 2HCO_3^- \rightarrow CaCO_3 + CO_2 + H_2O$$

In this thesis, assumption has been made that all possible reactions will take place between the injected CO_2 and the formation (Columbia Education Online, 2013). This resulted in the permeability or porosity being enhanced/altered in Niger-Delta reservoir leading to serious leakage of undissolved CO_2 back to the atmosphere. Hence, it is necessary to study the safety of Niger-Delta reservoirs for CO_2 storage integrity as the use of water mass as CO_2 storage is not recommended in the Nigerian environment. This was to guide against a repeat of the Cameroon's Lake Nyos CO_2 leakage disaster of 1986. Moreover, as a major oil-producing country and an extensive user of refined oil, Nigeria is a major contributor to carbon emission and needs to reduce this emission.

The inference made from one of the oldest CO_2 storage operations in the world, which is located at Sleipner with over 1 million tons of CO_2 injected into a saline aquifer reservoir within a twelve-year period serves as the basis for most popular belief in the suitability of reservoirs for CO_2 storage. It was initially concluded that CO_2 can be stored permanently in the Sleipner reservoir of the Utsira formation due to the initial success of the project (Bickel *et al*, 2007). It was even erroneously assumed that it could hold the whole of Europe's CO_2 emissions for years, based on assumption that the Sleipner storage is secured and has infinite storage capacity. Unfortunately, this assumption was disproved when a Statoil Hydro operated project was abandoned in 2008 after the discovery of leaked process-water from the Utsira formation. Moreover, a study by the Norwegian Petroleum Directorate proved that the CO_2 storage capacity of the Utsira formation is of highly limited capacity (Semere, 2007; Haugan, 2004; Greenpeace, 2008).

This justifies the necessity to study the alterations in the chemical and physical properties of the reservoir sand, arising from the chemical effect of ejected CO_2 on the reservoir fluids and matrix. The Utsira sand failure was probably as a result of the non-consideration of the chemical effect of injected CO_2 on the sand. Study should have been made on the ability of the compound formed by this CO_2 injection to cause permeability damage in the sand, resulting in erosion of the sealing component of the reservoir rock.

Zweigel *et al* (2004) carried out investigations on the reservoir geology of the Utsira formation. The investigation was based on actual CO_2 injection into sands of the Miocene-Pliocene Utsira Formation at the Sleipner fields in the North Sea. The highly porous (35%–40%) and extremely permeable Utsira sands are organized into approximately 30 m thick homogenous strata. The strata are separated by thin 1 m thick, low-permeability shale layers, which are assumed to contain potential fluid pathways of erosive or deformational origin. The research indicated that there is a 6.5 m thick shale layer close to the top of the sands which separates an eastward thickening sand wedge from the main sand package below. Migration simulations indicate that the migration pattern of CO_2 below the shale layer would differ strongly from that within the sand wedge above. Time-lapse seismic data acquired prior to the start, and after three years, of injection confirmed a reservoir model based on these findings and showed that the thin shale layers act as temporary barriers and that the 6.5 m thick shale layer does not fully inhibit the upward migration of CO_2.

2.1.1. Carbon Dioxide Reaction During Sequestration

Garner *et al* (2011) carried out experiments to compare and model pure gas sorption isotherms (CO_2 and CH_4) for well-characterized coals of different maturities to determine the most suitable coal for CO_2 storage on the basis that CO_2 injection in unrecoverable coal seams is applicable for both storage and methane recovery processes. The experiments were carried out with CO_2 and CH_4 gases at 25°C and from 1 to 50 bars in order to determine CO_2 and CH_4 adsorption on several coals using a gravimetric adsorption method. The CO_2 adsorption capacities obtained are from 0.5 to 2 mmol/g of dry coal. When the experimental results were analyzed using Langmuir, Tóth and Temkin sorption isotherm model equations, the experimental isotherms displayed Langmuir type I character with a reversible adsorption that is limited to a monolayer; the Langmuir equation fitted the experimental data reasonably well. For the CO_2 storage efficiency, the Tóth and Temkin models appear to be more reliable than the Langmuir model.

Singleton (2007) carried out the risk analyses and implications of the geological storage of CO_2. The research addressed the public perspective of CCS and its public acceptance. The study concluded that the risks involved in geological storage are not

considered to be worse than those of existing fossil fuel energy technologies. He addressed how geological storage is perceived by the public; how to improve the perspective and also to check if financial compensation can be used to improve the public acceptance of energy facilities. It is assumed that the carbon is stored on the seafloor in layers of limestone. Moreover, he assumed that some of the carbonate formed undergoes transformation to form free CO_2 as it ages and returned the CO_2 to the atmosphere in a reaction suggested as follows:

$$CaCO_3 + SiO_2 \rightarrow CO_2 + CaSiO_3$$

Berger and Young (1979) investigated the reaction of calcium silicates with carbon dioxide and water. It was discovered that calcium silicates with different Ca-Si ratios have different reaction kinetics that are dependent on the Ca-Si ratio of the reactant. The research also indicated that the activation energy for the carbonation reaction ranged from 41.02 KJ/mol (9.8 kcal/mol) for Ca_3SiO_5 to 95.86 KJ/mol (22.9 kcal/mol) for $CaSiO_3$ giving major reaction products of calcium carbonate and calcium silicate hydrates as intermediates. The final stable reaction products consist of calcium carbonate and a highly polymerized hydrous silica gel. In the course of the reaction, it was also discovered that two forms of $CaCO_3$ were formed, calcite and aragonite. Calcite is formed during the carbonation of Ca_3SiO_5, β-Ca_2SiO_4, and γ-Ca_2SiO_4 when free water is present. Aragonite is formed in the carbonation of $CaSiO_3$ and absence of free water. They also discovered that the extent of reaction was dependent on the pressure of the CO_2 as the reaction decreases rapidly at CO_2 pressures less than 0.12 atmosphere while at pressures between 0.12 and 54 atmospheres, the carbonation reaction increases slowly. It was concluded that temperature and relative humidity have significant influences on the rate of carbonation.

Chadwick (2009), in an investigation on flow process evolution in aquifers during CO_2 injection, discovered that increase in induced pressure serves as limitation to the rate at which CO_2 can be injected into regional saline aquifers with large storage capacity. Generic flow models were generated to examine the effects on reservoir pressure evolution of various reservoir parameters such as dimensions, permeability, porosity, presence and type of seal. It was concluded that CO_2 injection involves dominantly single-phase flow processes in much of the reservoir and surrounding adjacent strata, with additional two-phase flow effects around the CO_2 plume itself. They also concluded that large and thick aquifers, even without any significant flow barriers, can

accept high injection rates of up to 10 million tons of CO_2 per year and yet without undue pressure effects. It was also concluded that flow barriers, such as faults increase induced pressures considerably and that any reservoirs with such features require extreme careful site characterization and operational planning before using them for large CO_2 storage projects.

The principles established from the generic modelling were applied to a real aquifer storage operation at Sleipner in the North Sea. Here, CO_2 is being injected into the Utsira Sand, a large relatively homogeneous reservoir. Modelling indicates that any pressure increase should be negligible. Observed wellhead pressures show a small rise in value, which can be attributed to temperature changes in the fluid column in the wellbore. Pressure changes in the reservoir are likely to be very small.

Rochelle *et al* (2004), in a research on the impact of chemical reaction on CO_2 storage in deep geological structures, discovered that immediately after injection, the CO_2 will be stored as a free phase within the host rock. After some time, it will dissolve into the local formation water and initiate a variety of geochemical reactions. They stated that there are chemical reactions that might occur once CO_2 is injected underground which tends to have impacts on long-term CO_2 storage. Some of these reactions may be beneficiary or detrimental to CO_2 storage. Some may chemically contain or 'trap' the CO_2 as dissolved species resulting to formation of new carbonate minerals. They stated that these processes are dependent on the structure, mineralogy and hydrogeology of the specific lithologies concerned. The processes also depended on the chemical stability of the engineered features (principally, the cement and steel components in the well completions). They therefore concluded that individual storage operations will have to take account of local geological, fluid chemical and hydro-geological conditions.

The Rochelle research is applicable to the study of integrity of formation to store CO_2 but the inclusion of the well completion characteristics is assumed to be unnecessary as it has little or no effect on the reaction of a large volume of injected CO_2. Instead of this well completion characteristics, consideration should have been given to the cementation component of the strata and not the cementation of the injection well.

The possibility of alteration of the chemical properties of hydrocarbon reservoir fluids was also not considered by Rochelle, but this is a major consideration in this thesis.

This is because the alteration of reservoir fluids will result in alteration of production and separation processes.

Klaus (2002), in a research discovered that carbonate chemistry offers permanent solutions to the disposal problem of sequestration of waste CO_2 which require methods that store several trillion tons of CO_2 safely for a long time. Since the long-term storage of this CO_2 has lots of uncertainty and hazards, he researched into the formation of carbonates from CO_2 and metal oxides in exothermic reactions. It was suggested that the carbonates formed can be safely and permanently kept out of the active carbon stocks in the environment. He also suggested that there is a need for the development of an extractive minerals industry that provides the base ions for neutralizing carbonic acid.

2.2. Carbon Dioxide Storage in Aquifer

The solubility of CO_2 in water is similar to the solubility of some other gases in water and therefore it is a function of temperature, pressure and salinity of the water. Experimental work has proved that the solubility of CO_2 in fresh water increases with increasing pressure and decreasing temperature (Crawford et al, 1963).

Jens et al (2008) carried out research on the large-scale impact of CO_2 storage in deep saline aquifers with reference to corresponding pressure response in stratified systems. The main objective of the research was to investigate the three-dimensional region of influence during/after injection of CO_2 and evaluating the possible implications for shallow groundwater resources. They also considered the effects of interlayer communication through low-permeability seals. They prepared a two-dimensional radial symmetric model representing a CO_2 storage site with a deep saline aquifer underlying sandstone/shale. It was assumed that the storage formation into which CO_2 is injected is a 60 m thick aquifer 1 and is located at a depth of between 1140 and 1200 m below the ground surface. The storage formation is bounded at the top by a sealing layer 100 m thick Aquitard 1, followed by a sequence of a 60 m thick aquifers (aquifers No.2 - 7) and 100 m thick sealing layers (Aquitard No.2 - 7) as depicted in the model (Fig. 2.1). Their simulation results indicated that there was pressure buildup in the storage formation even up to 100 km distance away from the injection zone, whereas the lateral distance migration of brine is rather negligible. In the research

model, they estimated the areal effect of CO_2 injection in the reservoir to be as depicted in the Fig.2.2 and this is dependent on possible brine leakage into a nearby abandoned well.

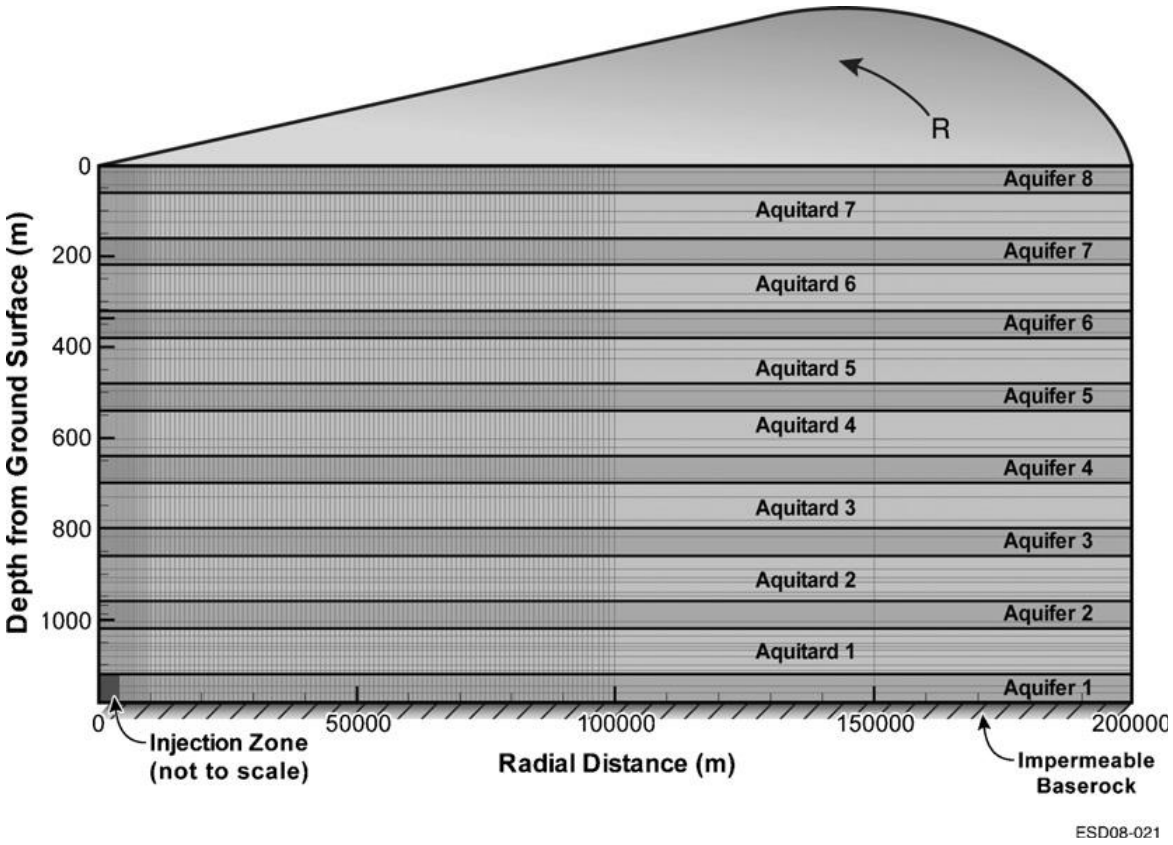

Fig.2. 1: Assumed model for investigating effect of CO_2 injection (adapted from Jens et al, 2008)).

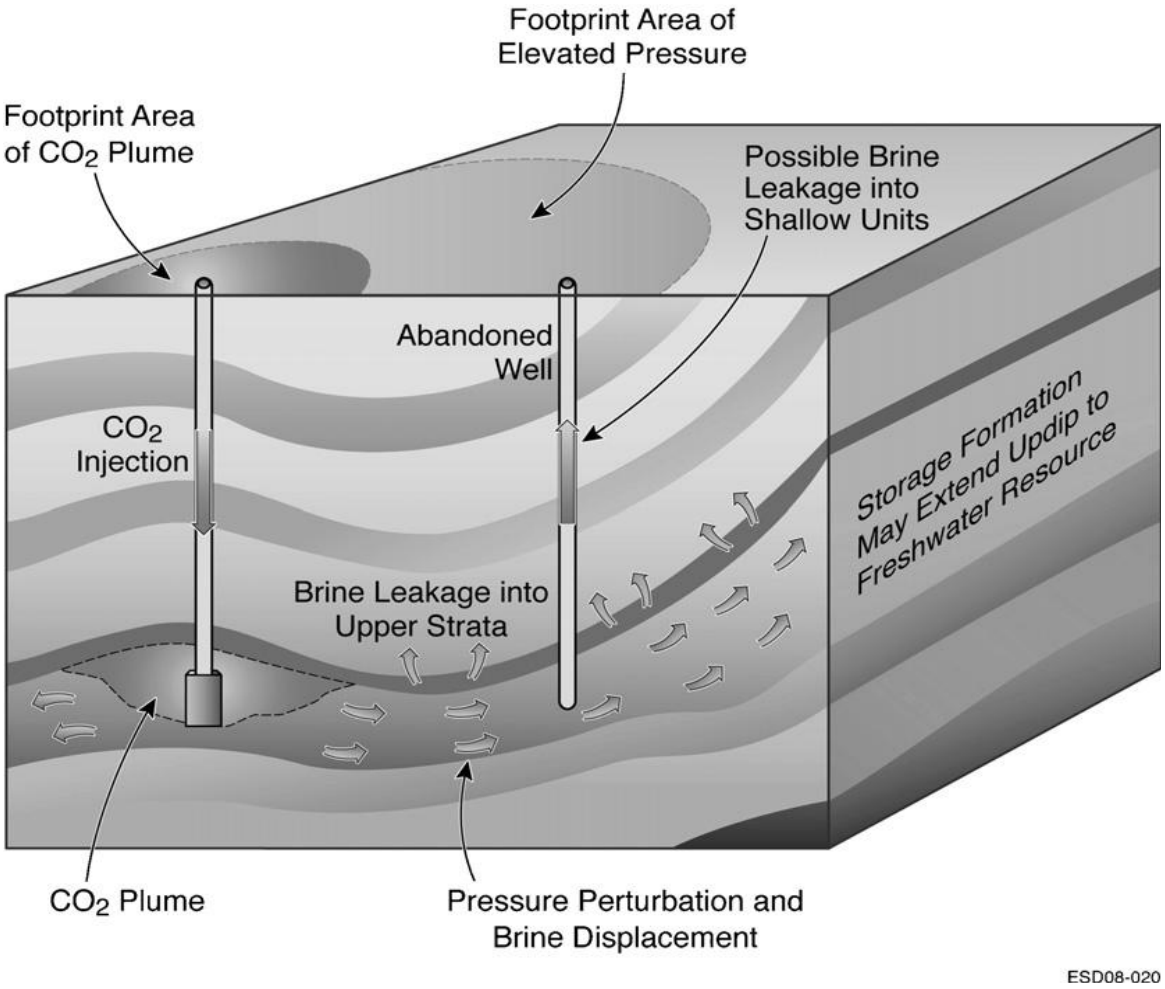

Fig.2. 2: Possible Areal Pressure Influence of Injection of CO_2

(adapted from Jens et al, 2008)

Juerg *et al* (2009), in their research in a CarbFix pilot project, discovered that the long-term retention time and environmental safety of the CO_2 storage in sub-surface reservoirs is a function of the interaction of the injected CO_2 with the reservoir fluids and rocks. They concluded that the storage of CO_2 as solid magnesium or calcium carbonates in basaltic rocks may provide such a long-term and thermodynamically stable storage solution. This is because basaltic rocks, compounds of magnesium and calcium silicate, provide the alkaline earth metals necessary to form solid carbonates. The in-situ mineralization of CO_2 was studied by them and the project involves the capture and separation of flue gases at the Hellisheidi Geothermal Power Plant. This was followed by the transportation and injection of the CO_2 part of the flue gas fully dissolved in water at high pressures and at a depth ranging between 400 and 800 m. Before the CO_2 injection, a reservoir characterization study was conducted, including soil CO_2 flux measurements, geophysical survey and tracer injection tests. This was done to determine the reservoir area available for chemical reaction between the CO_2 and the rock matrix.

Chang *et al* (1996), presented a three-dimensional and three-phase compositional model for simulating CO_2 flooding with special consideration to CO_2 solubility in water using implicit pressure, explicit saturations (IMPES) and implicit models. In their model, CO_2 was assumed to dissolve in the aqueous phase while all other hydrocarbon components were either in the oil or gas phase. The exception to this was the water phase that was assumed to exist on its own as a liquid phase and as a vehicle for CO_2 solubility. The oil phase and the gas phase densities and fugacities were modeled by a cubic equation of state in order to approximate the process of gas injection for enhanced recovery process. He stated that the "CO_2 solubility was computed using a CO_2 fugacity coefficient table that is converted internally from input CO_2 solubility data as a function of pressure at reservoir temperature". Two different types of simulations were carried out. One was without CO_2 in water and another with CO_2 soluble in the water phase. The simulations used various correlations for the solubility of CO_2 in water and other properties of CO_2 saturated water. The process followed in the simulation was:

- Data for CO_2 solubility in water were obtained from the literature.

- Water formation volume factor, water compressibility and water viscosity data were obtained either experimentally or from correlations and were entered as functions of pressure but at reservoir temperature.
- The CO_2 solubility in water was converted into a fugacity coefficient table as a function of pressure.
- The fugacity coefficients were then used to compute the solubility of CO_2 in water during the simulation runs, using the equality of component chemical potential constraint.
- Lastly, the water formation volume factors, compressibility and viscosities were then computed as functions of the amount of CO_2 dissolved in the water.

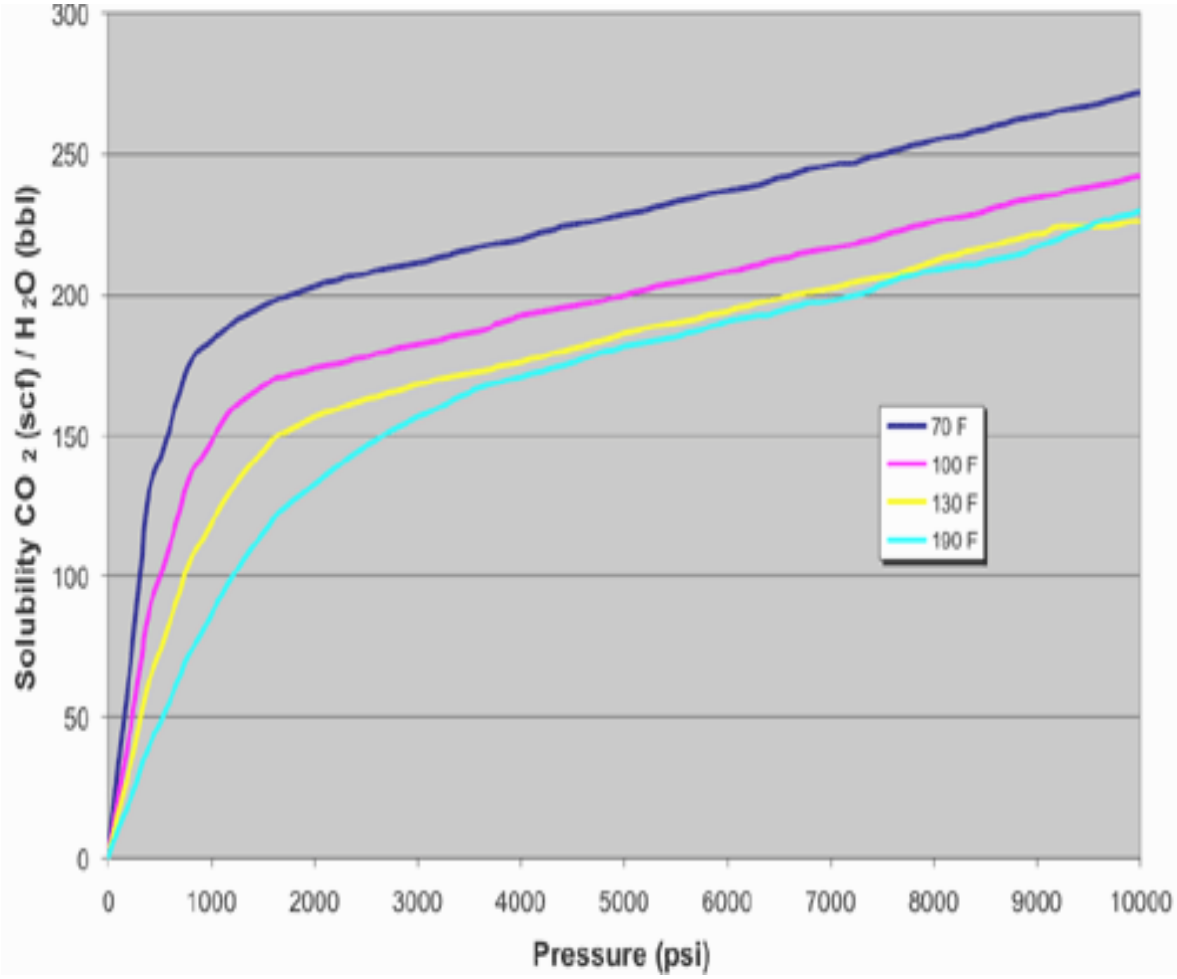

Fig. 2.3.1: CO_2 Solubility in Water

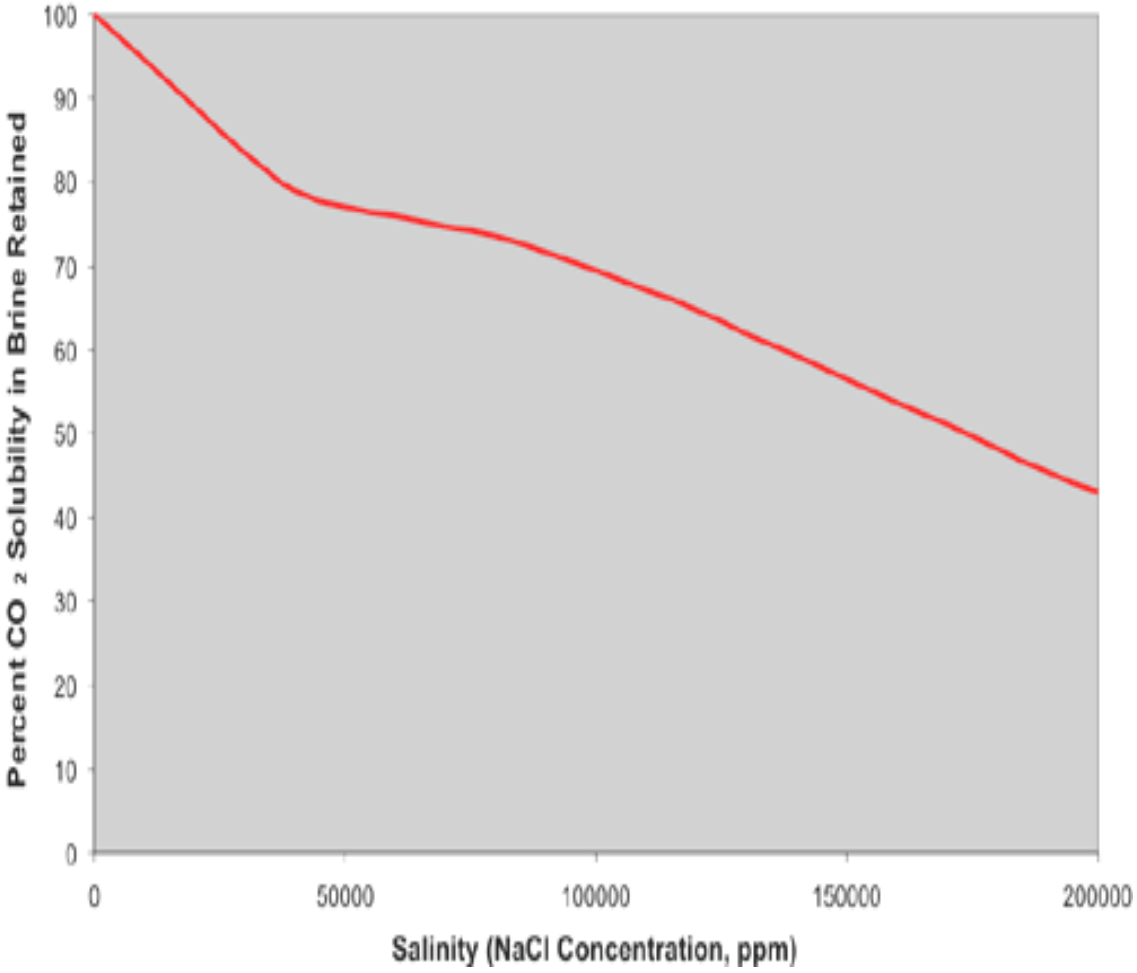

Fig. 2.3.2: CO_2 Solubility in Brine

An experimental model was used to observe the phenomenon of active phase change qualitatively, using a silicon model to represent the pore structure of Berea sandstone saturated with water and then flooded with CO_2. Digital photographs were employed to study the CO_2-water displacement front and the active phase change phenomenon was observed visually. A control experiment was set up using nitrogen as an inert gas. This is because the solubility of nitrogen in water was assumed to be negligible. CO_2, on the other hand, is a gas that is highly soluble in water and it was observed that the residual water saturation decreases with every cycle of drainage and imbibitions. Moreover, it was observed that as CO_2 dissolved, it was able to diffuse into the smallest pore spaces without necessarily overcoming capillary entry pressure. It was also observed that as CO_2 evolved out of solution it displaced the water that was previously immobile into higher-permeability pathways and this additional mobile water ended up impeding the flow of CO_2 such that the relative permeability of CO_2 became less than that of nitrogen.

Jennie and Keith (2008) considered the geochemical reactions that enhance the transformation of CO_2 gas into dissolved or solid phase carbon. This involves the liberation of cations to neutralize carbonic acid. The research was on CO_2 storage in the sub-surface using geochemical approaches. Also presented were various geochemical approaches and their potentials and limitations. It was assumed that though geochemical approaches have limitations, yet it has a unique potential to contribute to CO_2 reductions in better ways than both the physical and biological carbon storage. This is because geochemical approaches require less technological expansion over the existing infrastructure for direct removal of CO_2 from the atmosphere than the other two. They summarized the many approaches to storing the carbon emitted from the burning of fossil fuels as follows:

i. Location approach. That is land, ocean, or geological storage
ii. Mechanism of storage. That is biological, chemical or physical processes

They further stated that the biological approach, which is basically forest sequestration, uses the photosynthetic process to capture and convert atmospheric CO_2 into organic carbon. The chemical approaches rely on interaction between the CO_2 and the sub-surface in the form of a chemical reaction to transform the injected gaseous CO_2 into

dissolved or solid-phase carbon. The physical approaches rely on barriers that will trap the gas-phase CO_2 in the sub-surface. They concluded with the following applications of CO_2 mechanism of storage.

Table 2.2. Application of Carbon Storage by both Location and Mechanism of Storage

Process Mechanism	**Land surface Application**	**Ocean Application**	**Geological Application**
Biological	CO_2 storage enhances carbon content of soils. It helps in re-forestation processes.	It helps in the ocean fertilization and serve as biological pump.	It helps in the use of anaerobic content of soils reactions to reduce CO_2 to CH_4 in strongly reducing environments.
Chemical	It is applicable in industrial production of stable carbonates.	It helps in the acceleration of $CaCO_3$ dissolution. It serves as source of additional alkalinity.	It resulted into the sub-surface dissolution of carbonates/silicates when brine is acidified by injected CO_2.
Physical	-	It resulted into formation of 'lakes' of liquid CO_2.	It helps in the physical confinement of gas phase CO_2 in underground formations.

Zekri *et al.* (2009), in an experiment to study the effect of supercritical CO_2 injection on limestone formation in the presence of brine and asphaltenic crude, made use of ten core flooding experiments under reservoir conditions of 27470 KN/m^2 (4000 psia) pressure and 121^{o}C temperature. The experiments involved the use of limestone rock cores representing different carbonate oil field and saturated with actual reservoir fluids of filtrated brine and asphaltenic crude oil. The asphaltene content of the produced crude oil, the water and mineralogical rock analyses, were used together with the scanning electron microscopic (SEM) photos of the rock pores to evaluate the effect of a supercritical CO_2 flood on the permeability and mineralogical variation characteristics of the cores. It was proposed that the calcite dissolution and/or precipitation is the major reason for permeability improvement and/or impairment. It was concluded that the extent of permeability damage, depends on the fabric of the rocks, the salinity of the brine, and the initial core permeability.

2.3. Carbon Dioxide Sequestration Applications.

Nazir *et al.* (2011) suggested that CO_2 in flue gases from the brick manufacturing industry is a contributor to the green house gas emission especially in developing countries like Pakistan. This is because firewood and coal are used as primary fuels in kilns for brick manufacturing in Pakistan. They, authors, suggested that the CO_2 emissions to the environment from these brick kilns should be captured. They developed a simulation model in order to mitigate carbon emissions from the brick kiln. They were able to capture 96% of the CO_2 emitted from the brick kilns by using their model.

Zain *et al.* (2001), in an investigation on CO_2 sequestration in Malaysia for enhanced oil recovery used the Dulang Field, due to the availability of CO_2 source and also due to the large quantity of data available for that field. They investigated the oil - CO_2 interaction and characterized the oil. The method used involves the application of phase behaviour, vapourization and displacement tests. They discovered that CO_2 miscible enhanced oil recovery was not possible for that field either at the stage of their investigation or even at the initial pre-production stage of the reservoir. This is because they obtained a Multiple Contact Miscibility Pressure (MCMP) of 22270 KN/m^2 for produced CO_2 and 23028 KN/m^2 of hydrocarbon gas pressure. Though this was achieved using equation of state, but the initial reservoir pressure was only 12411

KN/m^2. They, authors, concluded that the vaporization ranges from 2 - 5% with the produced gas at an operating reservoir pressure of 9652 – 12411 KN/m^2. Based on this, they suggested that the potential recovery process is an immiscible process and a gas mixture containing high CO_2 content should be used in order to minimize cost. It was concluded that alternative technique of water-alternating-gas (WAG) process may improve the mobility control and sweep efficiency for enhanced recovery.

Stavins (2009) researched into CCS for over ten years with special interest in biological sequestration using the forest as storage. The research was basically on the cost implication of a change in land-use and carbon sink; on factors affecting the cost of carbon sequestration in forest sink as a consequence of climate change and on an economic review of carbon sequestration in general. The research focus was on costs and not on the reactions that could be initiated by carbon dioxide storage in forests or sub-surface reservoirs.

Soren (2004) investigated the technical feasibility of CCS technology. He estimated that it costs between $200 and $250/ton of carbon captured. He suggested that the immediate prospects favour CCS for electric power plants and certain industrial sources, with storage in depleted oil and gas reservoirs as opposed to aquifers. This is due to the possibility of a pay-back when extra oil/gas is produced from the depleted reservoir following the injection of captured CO_2.

2.4. Kwale Reservoir, Niger Delta Environment

Ekine and Iyabe (2009) carried out a petrophysical characterization of the Kwale Field reservoir. They used well log data from the deep parts of the six wells they considered and these were used in the petrophysical characterization of the field. They discovered the presence of twelve distinct sand units using available sonic, gamma-ray, matrix density and restivity logs. They concluded that the porosity of the reservoirs in the field reduces downwards, an average of 19% at shallow depths and 13% at the deepest sands. They also concluded that the available wells data analyzed gave between 52.5 and 88.5% average water saturation.

In their conclusion, they reported that the permeability obtained is between 3.158 x 10^{-12} and 2.7633 x 10^{-11} m^2 (3.2 and 28.0 mD). They concluded that more research is required before a final conclusion can be drawn on these assertions. The results they obtained are reported in Tables 2.3 to 2.5 and are of paramount importance to this thesis since the Kwale Field is one of the points of focus of this thesis.

In line with Ekine and Iyabe research, the Kwale field is being considered as a candidate for CO_2 storage in the sense that the porosity is low and the permeability is very low. Even when there is an erosion of the reservoir as a result of the CO_2 injected, there is a possibility that the reservoir will still maintain its storage integrity. Moreover, the field is close to a cluster of turbine power generation plants at Sapele and ughelli in Delta State.

Table 2.3.: Lateral % Porosity Distribution in Kwale Sands

[Ekine and Iyabe, 2009]

Sands	Kwale-1	Kwale-2	Kwale-5	Kwale-6	Kwale-8	Kwale-10
A	-	21	19	-	-	17
B	19	18	19	19	-	17
C	21	19	19	17	-	-
D	20	20	18	17	-	18
F	17	18	17	17	15	17
G	17	19	17	17	13	16
H	17	17	11	16	13	-
I	-	16	17	15	12	-
J	-	16	14	14	12	-
K	-	19	13	13	12	-
L	16	17	13	11	-	-
M	14	-	11	12	11	-

Table 2.4.: Lateral Water Saturation Distribution in Kwale Sands

[Ekine and Iyabe, 2009]

Sands	Kwale-1	Kwale-2	Kwale-5	Kwale-6	Kwale-8	Kwale-10
A	-	74	-	-	-	17
B	45	75	69	76	-	17
C	32	82	77	71	-	-
D	48	85	73	74	-	18
F	53	93	78	69	-	17
G	50	75	82	74	-	16
H	36	91	89	67	76	-
I	-	75	71	63	92	-
J	-	82	90	90	92	-
K	-	75	74	73	92	-
L	41	81	66	81	58	-
M	57	-	51	55	54	-

Table 2.5: Lateral Permeability Distribution in Kwale Sands

[Ekine and Iyabe, 2009]

Sands	Kwale-1	Kwale-2	Kwale-5	Kwale-6	Kwale-8	Kwale-10
A	-	16	-	-	-	37
B	28	8.1	12	10	-	27
C	87	8.6	9.4	7.0	-	-
D	31	10	10.8	6.4	-	24
F	16	5.2	9.4	7.4	-	13
G	18	8.1	5.2	7.4	-	68
H	27	4.3	5.2	6.0	1.9	-
I	-	4.8	6.5	5.1	1.1	-
J	-	4.0	6.9	1.8	1.1	-
K	-	10.2	1.8	2.0	1.1	-
L	16	5.4	1.9	0.8	2.3	-
M	4.6	-	1.9	2.5	3.7	-

2.5. Nigerian Oil Sand Reservoir

Akinmosin et al (2010) stated that outcrops of oil sands in southwest Nigeria contain saturated and aromatic hydrocarbon components. The bituminous sands are enriched in saturates with about 28.7 to 24.1 volumetric percent and also aromatic hydrocarbons of about 27.53 to 23.59%.

Akinmosin and Gbolahan (2010) carried out a geochemical analysis of oil sand deposits in western Nigeria covering Ogun, Ondo and Edo States. In their research, samples were obtained mostly in three regions: south west Eregu, south west Oniti/Oniparaga and south east of Obamuwasan camp. The map of the sample area is shown below in Fig. 2.4. The aim of their research was to establish the heavy metals and radioactive metals in the oil sand. The Inductively Coupled Plasma-Mass Spectrometry (ICP-MS) was employed for the geochemical analysis. The results indicated that the following trace elements are present: As, Cd, Cr, Cu, Ni, Pb and Zn and the radioactive elements of Zr, Pb, Sr and U. The analyzed concentrations of these elements are presented in Table 2.6. The implication of these results is that they gave the amount of metals that are expected to react with either the CO_2 gas injected or the acidic solution formed between the injected CO_2 and the reservoir water. It was assumed that if these trace elements are reactive with the CO_2 or the weak acid, then chemical erosion will take place, resulting in the formation of new substances which will either lead to a reduction or an increase in porosity and/or permeability.

Table 2.6: Concentration of Elements Obtained From Geochemical Analysis (Akinmosin and Gbolahan, 2010)

	Components	Concentration, ppm
1	V	5-90
2	Cr	2.3-58.5
3	Ni	4.1-331
4	Zn	4 - 33.7
5	As	0.2-2
6	Pb	1.4-36.6
7	Cu	0.8-54.3
8	U	0.1-4.2
9	Th,	0.4-18.9
10	Pb	1.4-36.6
11	Sr	2.4-138
12	Rb,	1.3-24.1
13	Zr	3-26

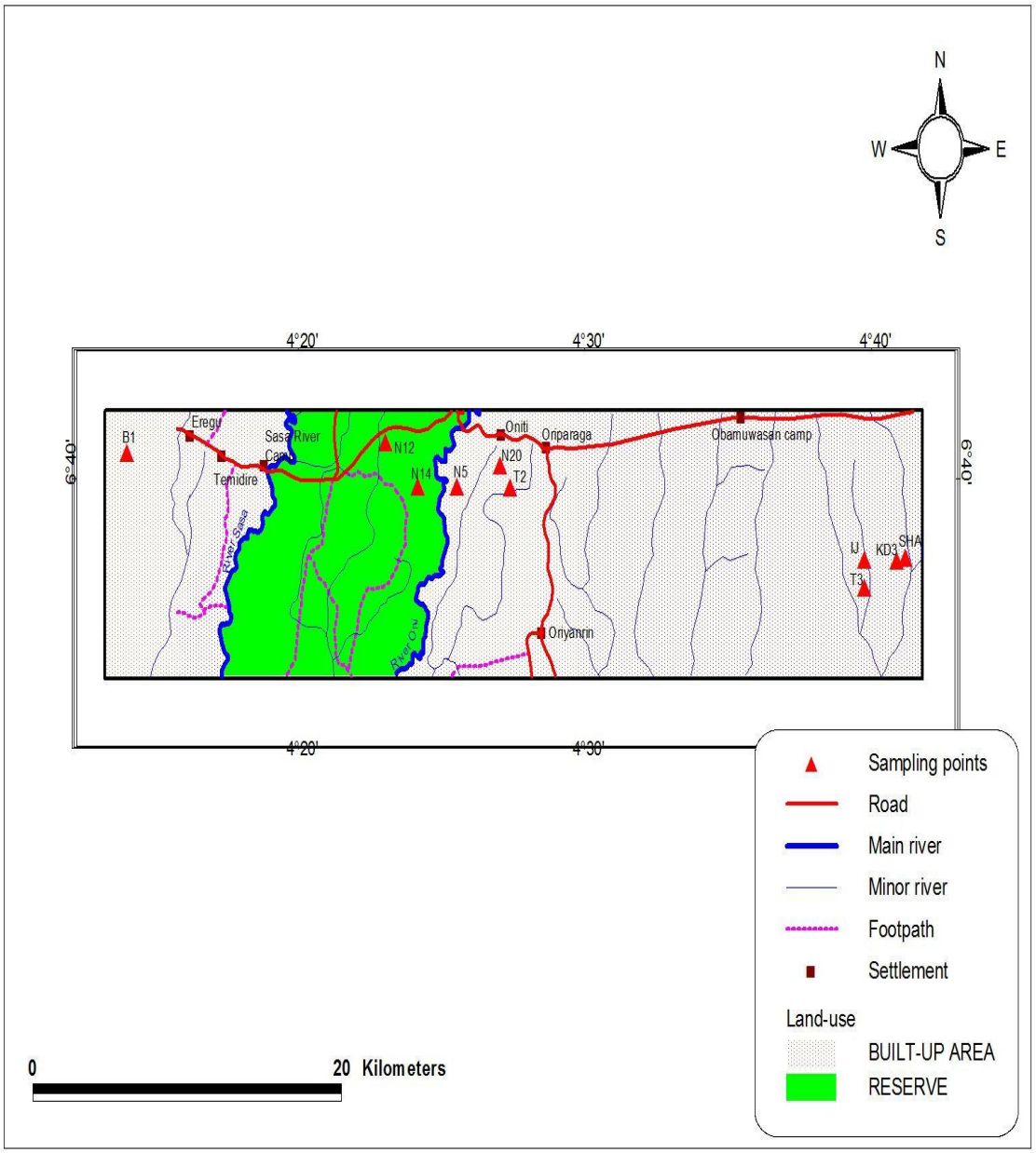

Fig.2.4.: Western Nigeria Oil Sand Sampling Area Map (Akinmosin and Gbolahan 2010)

Adewusi (1992) reviewed the extent of oil sand deposits in Nigeria and stated that it will eliminate some unnecessary oil importations. He enumerated the negative impact of importation of bitumen on the Nigerian economy, especially since it could easily be processed locally. He also suggested appropriate production technology options and their environmental implications, as well as government's expected role in ensuring an accelerated and long-term oil sands development in the country.

Online Nigeria (2013) stated that as far back as 1908, efforts were made concerning oil sand exploitation in Nigeria by the Nigerian Bitumen Corporation, which was a German company, but World War I put an end to the exploitation of this resource. In 1937, the company that came later for oil exploitation did not show much interest in bitumen exploitation. The company, Shell-D'Arcy, owned by Shell and Royal Dutch, preferred to explore the Owerri environment for crude oil. World War II also hindered further exploration but work was resumed at the end of the war by Shell-BP Company. By June 5, 1956, a total of 28 wells have been drilled together with 25 bore holes. All the holes were dry. An economic discovery was made at Oloibiri, Bayelsa State with an initial production rate of 5,100 barrels per day. Though the oil sand in Nigeria is extensive, success in the crude oil exploitation has destroyed any desire for exploitation of heavy crude from the oil sand. In 1992, Nigeria wasted over 216 million pounds sterling to import heavy crude from Venezuela to serve as a feedstock to the Kaduna Refinery for the production of lubricants and greases. This was at the rate of 50,000 barrels per day, a volume that is insignificant if the vast oil sand deposits in Nigeria, estimated at 31 billion barrels of heavy crude, are exploited.

Ola (1991) researched into the determination of the geotechnical properties of Nigerian oil sand and discovered that the oil sand samples used had an average of 5% clay and 3-5% bitumen with well graded silt. The results obtained indicated an *in situ* compressive strength of about 450 kN/m^2 and a ratio of tensile to compressive strength of about 22%. It also stated that peak shear strength parameters, C_p', of $15kN/m^2$ and peak stress friction angle, φ_p', of 19° were obtained while the residual parameters, C_r, of 0 and effective residual stress friction angle, φ_r, of 18° were also obtained. He stated that the compacted oil sands have characteristics of over consolidated soil with a pre-consolidating pressure of 140 kN/m2. He concluded that the average Nigerian oil sand behaved like soft sandstone.

Various samples of oil sands were taken in Agbabu, Looda, Ilubinrin and Ofosu areas of Ondo State, Nigeria (Febisola, 1998). The samples were obtained from outcrops, trenches, pits and boreholes. The physico-chemical analyses of these samples gave results for physical properties such as a softening point of 44°C to 52°C; a ductility of 0.1 mm to 1.3 mm and a penetration of 80 mm to 1OO mm. The rheological properties of the oil sands indicate that they are of sufficiently good quality to be used in road construction. The chemical properties obtained are as follows: hydrocarbon content 7.2% to 18.2% by weight; resins content 32.0% to 34.0% by weight.; and sulphur content 5.0 ppm to 10.0 ppm. The Ofosu sample had the highest sulphur content. It was also discovered that the bitumen of the oil sands has high content of naphtenes, aromatic hydrocarbons and asphaltenes that are similar to those of conventional crude oils and can therefore be upgraded as alternative crude and as a potential feedstock for the petrochemical industry.

Okechukwu (1999) carried out research on the composition of Nigerian oil sand bitumen using ion-exchange, ferric chloride coordination chromatography for the separation of acids, bases and neutral nitrogen compounds. Thereafter, the remaining hydrocarbon fraction was separated into saturates, mono-aromatics, di-aromatics, poly-aromatic and polar compounds, using dual packed columns of silica-alumina gels. On comparison with the Utah and the Athabasca bitumen data, with respect to hydrocarbon/non-hydrocarbon distribution and the high-boiling petroleum fraction of the non-distilling portion, it was discovered that there was a close resemblance to the Canadian oil sand when simulated with distillation data obtained for the Nigerian oil sand samples and chromatographic separation data.

Akinmosin *et al.* (2011) obtained twelve core oil sand samples. Based on the similarities in their physical and textural characteristics using scanning electron microscope studies, SEM, (VEGA TESCAN/LMU-SEM), it was concluded that the oil sands contained minerals such as kaolinite, k-feldspar, pyrite crystals, corrosion quartz and corrosion feldspar which had been precipitated as pore filling cement. Analysis of the SEM images also showed 2-4 µm micro pores and 2-5 µm fractures.

The SEM images of the constituent minerals are as shown in Fig. 2.5 and 2.6.

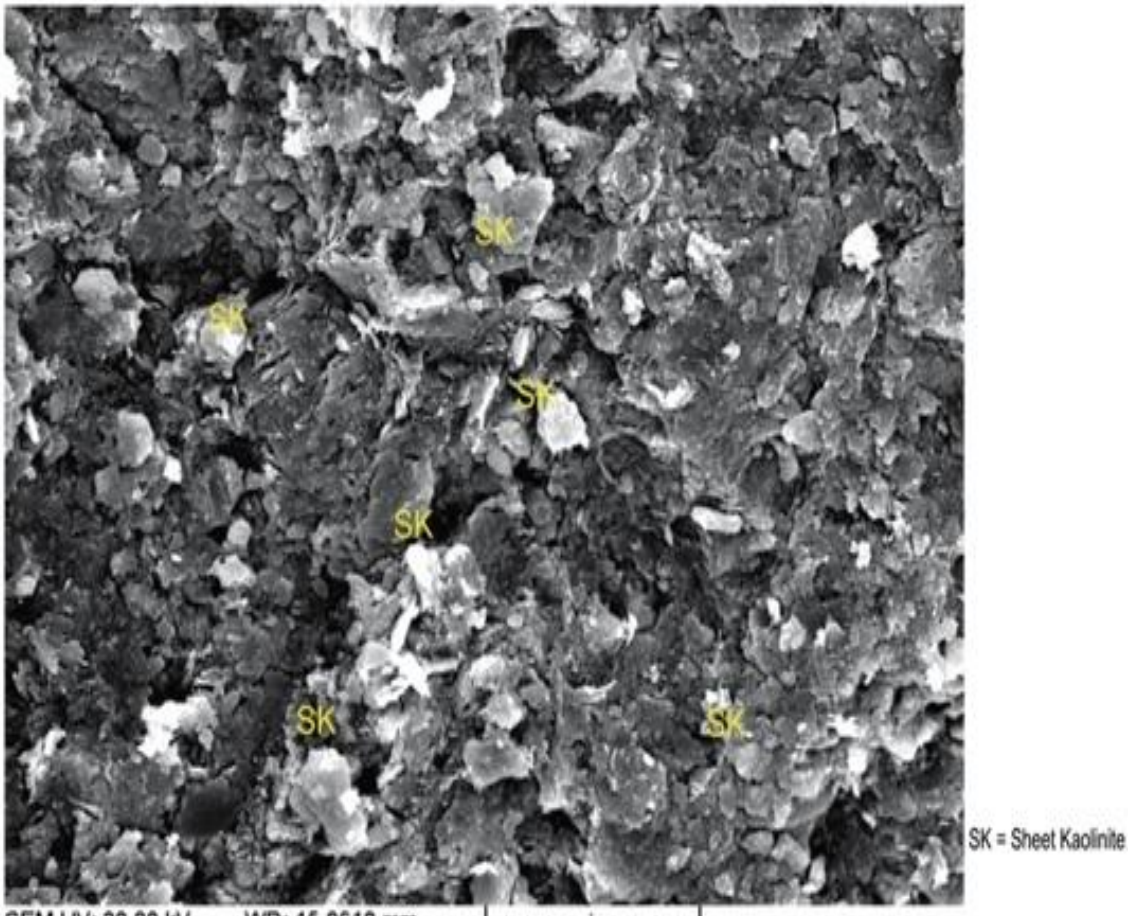

Plate I: Scanning electron micrograph of sheet kaolinite.

Fig. 2.5: SEM for Sheet Kaolin Component (Akinmosin *et al., 2011*)

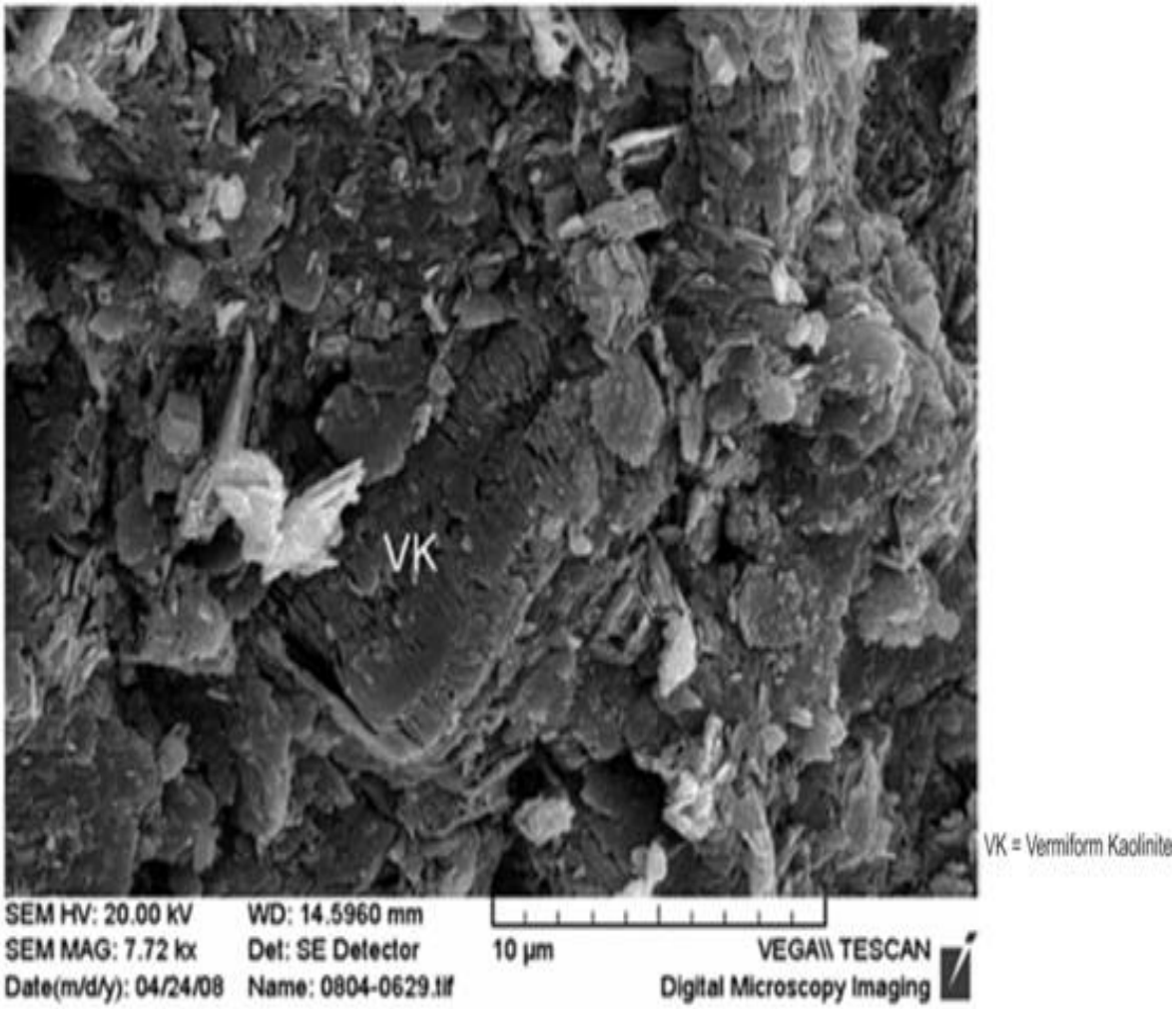

Fig. 2.6: SEM for Vermiform Kaolin Component (Akinmosin *et al., 2011*)

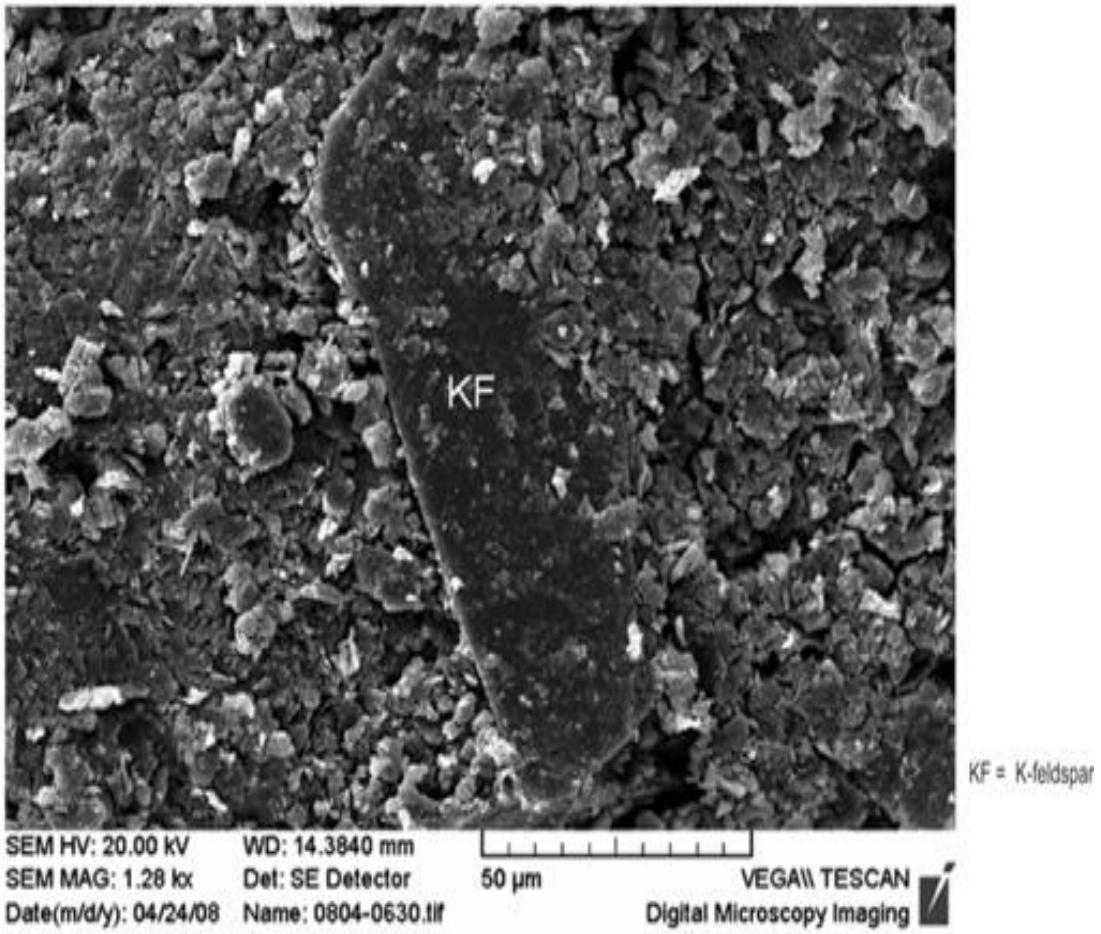

Plate 3: Scanning electron micrograph of k-feldspar

Fig. 2.7: SEM for K-Feldspar Component (Akinmosin *et al.*, *2011*)

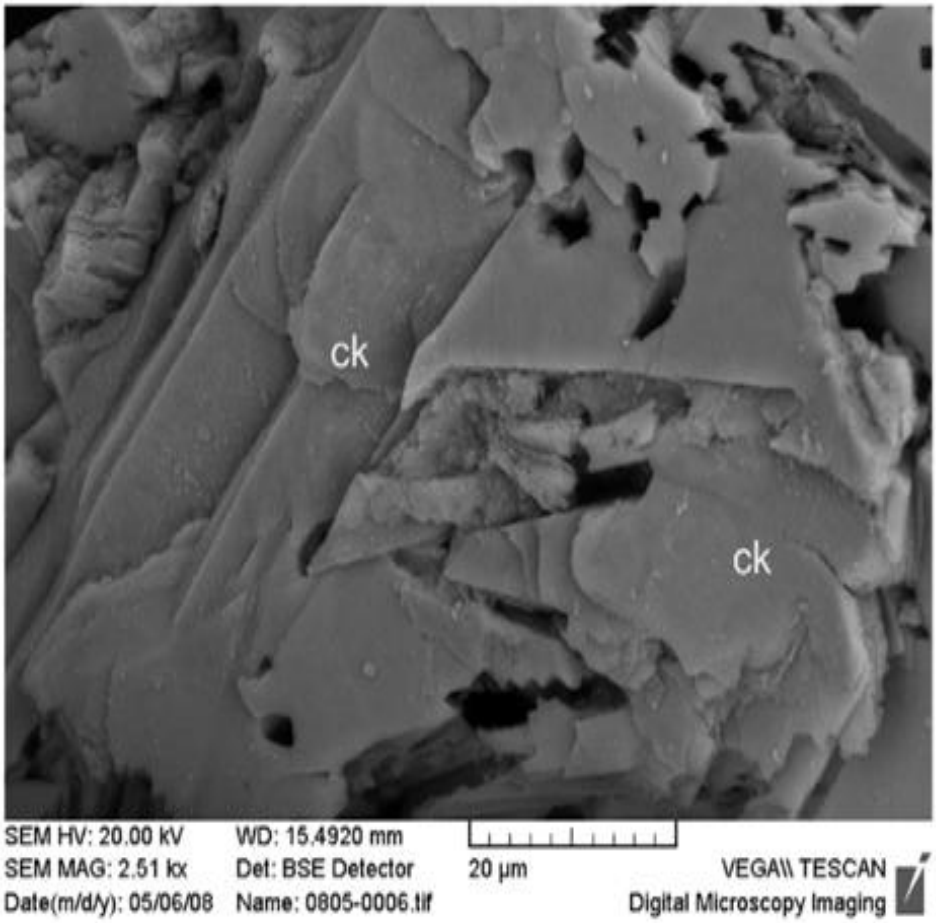

Plate 4: Scanning electron micrograph of corrosion k-feldspar.

Fig. 2.8: SEM for Corrosion Feldspar Component (Akinmosin *et al., 2011*)

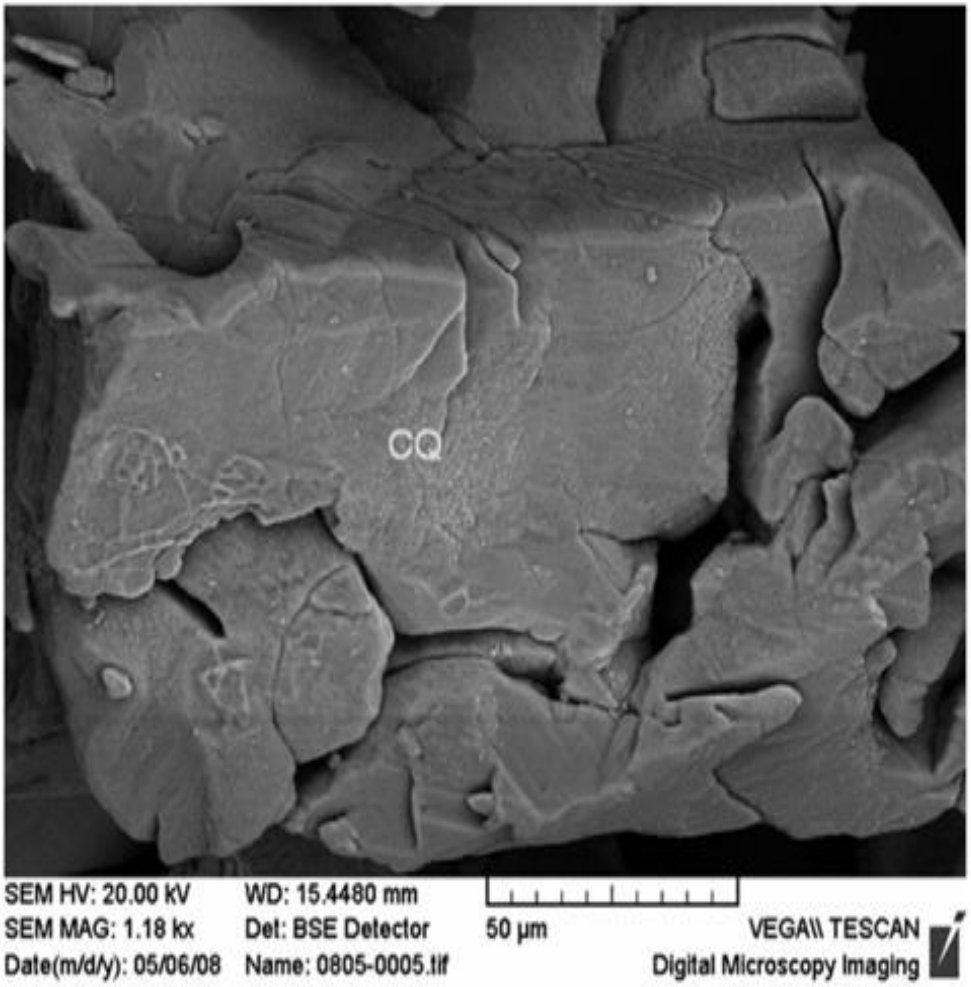

Plate 5: Scanning electron micrograph of corrosion quartz.

Fig. 2.9: SEM for Corrosion Quartzite Component (Akinmosin *et al., 2011*)

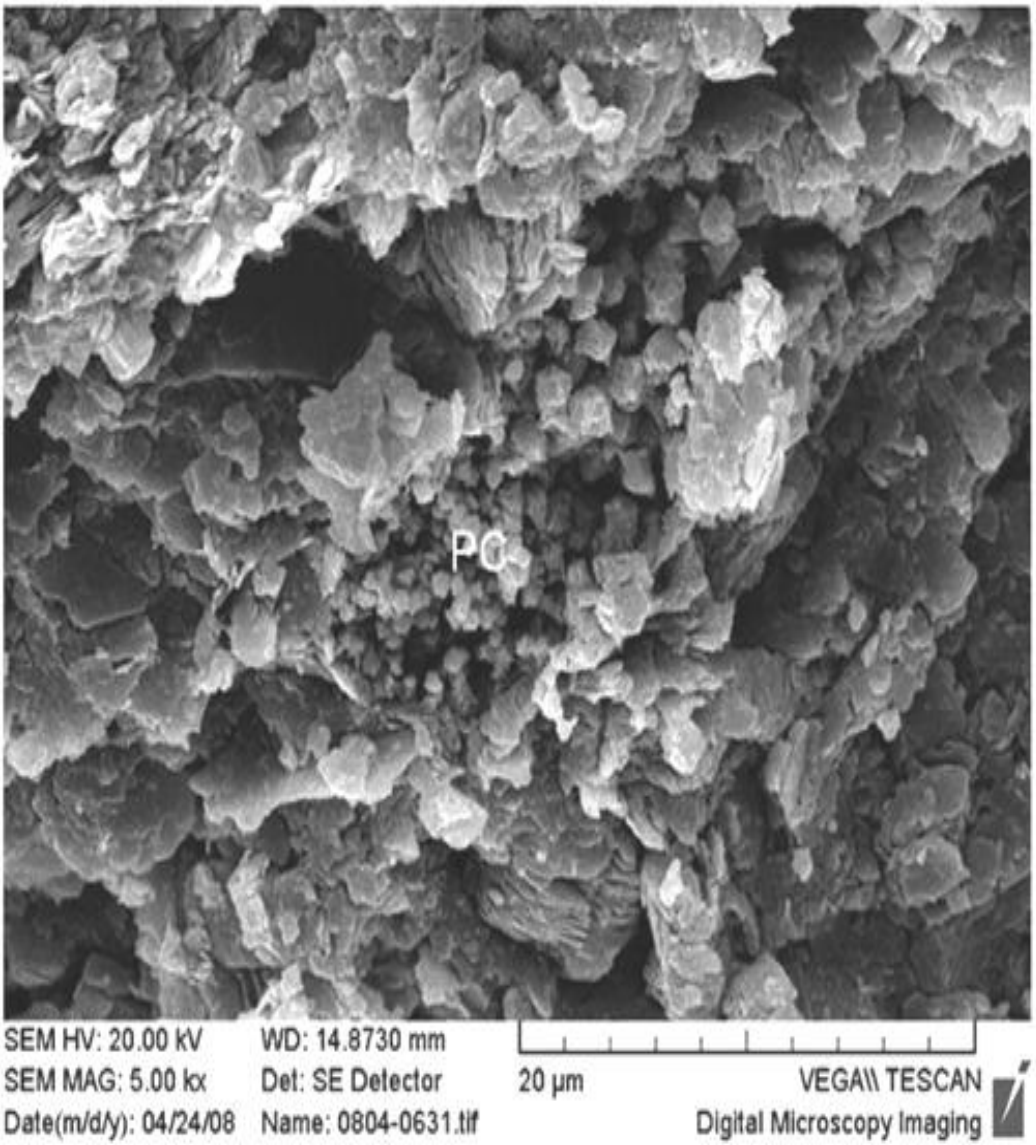

Plate 6: Scanning electron micrographs of pyrite crystals

Fig. 2.10: SEM for Pyrite Crystals Component (Akinmosin *et al., 2011*)

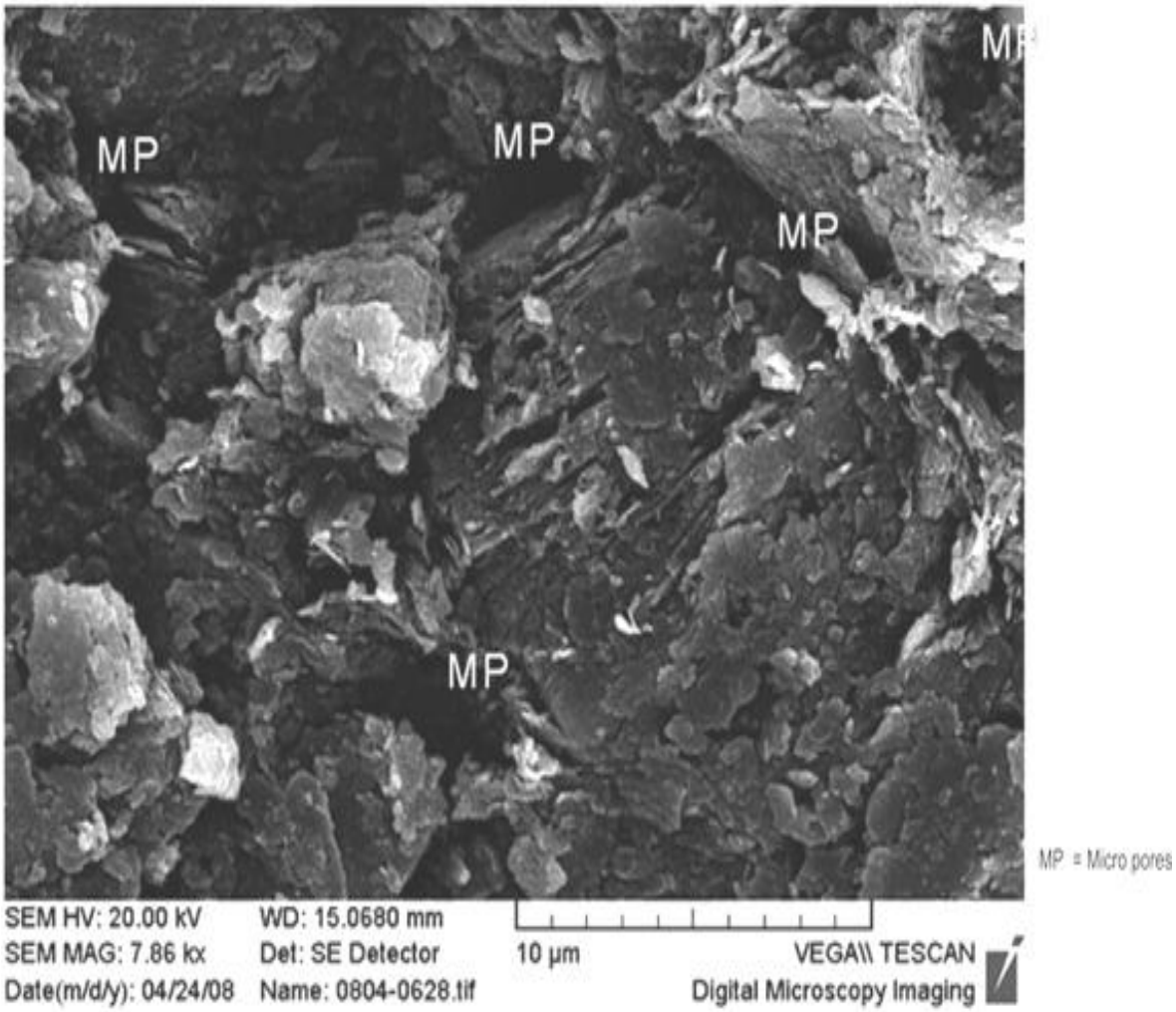

Plate ™: Scanning electron micrographs of micro pores

Fig. 2.11: SEM for Micro Pores (Akinmosin *et al.*, *2011*)

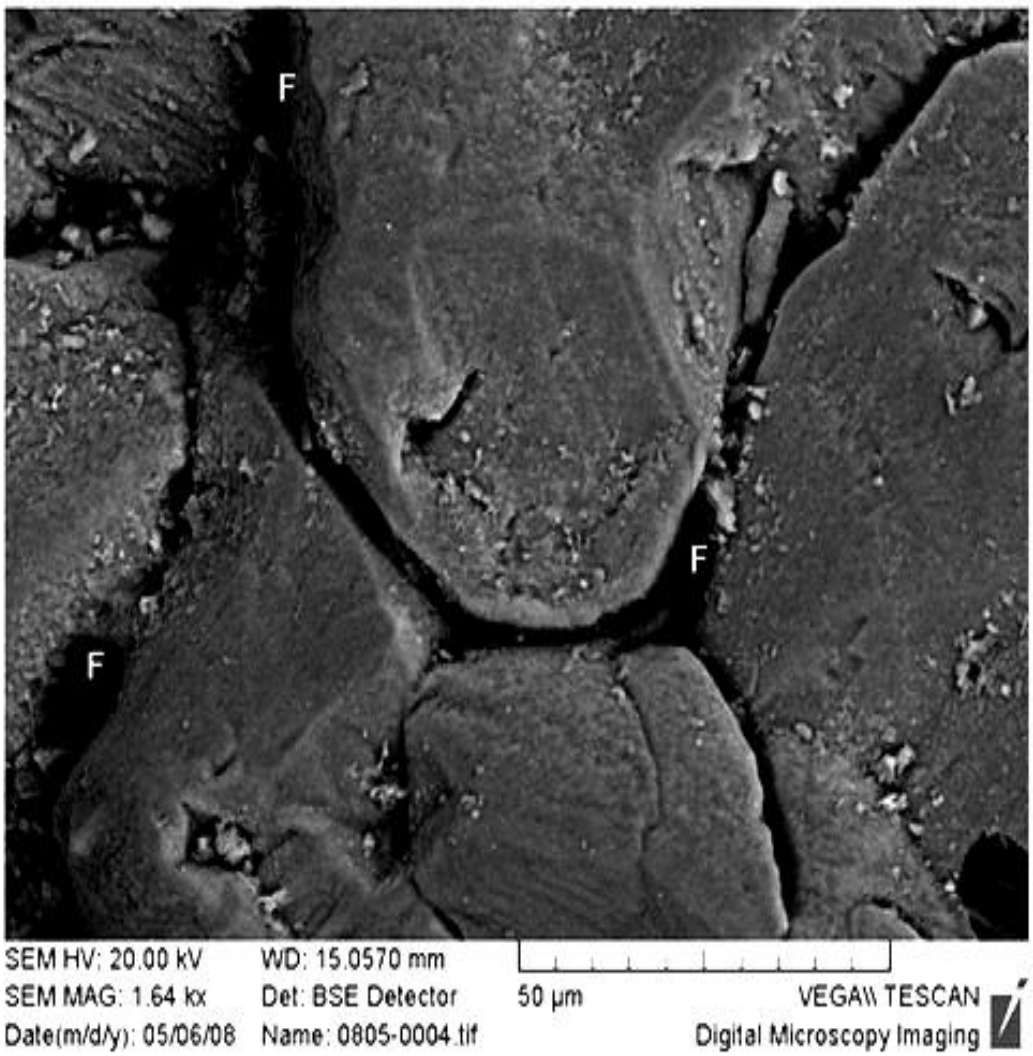

Fig. 2.12: SEM for Fracture (Akinmosin *et al., 2011*)

This Akinmosin *et al* research, is directly related to this thesis since Imeri oil sand could be regarded as a member of the Afowo oil sand group and both are members of the Abeokuta group.

2.6. Ota Kaolinitic Clay, Member of Oshoshun Formation.

Kaolin is found in Ogun, Kogi, Imo, Rivers, Anambra, Bauchi, Kebbi, Ondo, Ekiti, Akwa-Ibom, Katsina and Plateau States of Nigeria (www.ngsa-ng.org/otherminerals.pdf).

Badmus and Olatinsu (2009), from their research on the geological mapping and characterization of the Ewekoro formation, concluded that the resistivity values of limestone rock samples collected from the study area have revealed that the limestone of Ewekoro formation has various degrees of qualities. This was characterized by their resistivity and permeability values. They reported that their results also revealed "the occurrence of limestone in all the locations within the third and fourth geo-electric layers with resistivity values ranging from 10 to 100 kWm and a thickness ranging from 15 to 90 m". The laboratory analysis method used gave the resistivity values ranging from 6 to 171 KWm.

The Nigerian kaolin production for a period of 5 years, 2003-2007, is as reported in the Table 2.7 (published by the United States Geological Survey, USGS). This report shows the extent of the vast volume of kaolin available in the country and the untapped volume that will be available for use as possible captured CO_2 storage reservoir.

Table 2.7: Kaolin Production in Nigeria between 2003 and 2007

(United States Geological Survey, www.indexmundi.com/minerals)

Year	**Production (tons)**	**% Change**
2003	52000	-
2004	58000	11.54
2005	93000	60.34
2006	100000	7.53
2007	100000	0.00

Solomon and Murray (1972), state that in a non-aqueous system, kaolin is not an inert compound, but actually takes part in acid-base interactions reactions. Furthermore, it is involved in physical interactions as well. They found that when kaolin is used as a diluent in insecticide powder production, the strength of the surface acid sites of kaolin varies and was dependent on the moisture content. The lower the moisture content the higher the acidic nature of the kaolin sites in the powder. They concluded that dry kaolin will promote or catalyze many chemical reactions but is dependent on the moisture level and that the presence of even of water controls the reaction as small water content will inhibits the reaction.

From the above, there is an indication that kaolin is reactive, especially when there is moisture. This implies that an underground kaolin deposit can be used as a storage for a compound that is reactive towards kaolin. This will make the compound, CO_2 in the case of this thesis, to remain in place until the stored compound is in excess of the amount required for reaction. For this reason, kaolin was considered as a potential candidate reservoir for CO_2 storage in this thesis.

2.7. Permeability Estimations From Porosity.

Timur (1968) gave an accurate relationship for estimating the permeability of sandstones from *in situ* measurements of porosity and from residual fluid saturation from nuclear magnetism log. He suggested that this willould eliminate the expensive coring process. This is because the porosity and the saturations can be obtained from logging while drilling and from drill cuttings. The measurements of permeability (K) were obtained in the laboratory while the porosity (Φ) and residual (irreducible) water saturation (S_{wirr}) were determined using 155 sandstone samples from three different oil fields in North America. He derived an empirical equation for calculating the permeabilities and also derived another equation for estimating residual water saturation in sandstones when the porosity and the permeability are known.

Aigbedion (2007) estimated permeabilities for some Niger-Delta rocks using various correlations; he assumed a model and tested the model against existing models. The work was on permeability modelling in a Niger Delta reservoir that had no core data. He expanded the work of Timur (1968) who worked on the establishment of a correlation relating permeability, porosity and residual water saturation for sandstone

reservoirs. He also considered the work of Coates and Dumanoir (1981) and of Tixier (1949). The models used by Aigbedion are as follows:

Timur's model (1968)

$$K = 0.136\frac{\emptyset^{4.4}}{S_{wirr}^{2}} \qquad \text{…..2.6.1}$$

Tixier's 1949 model

$$k^{1/2} = 250.\frac{\emptyset^{3}}{S_{wirr}} \qquad \text{…..2.6.2}$$

Coates-Dumanior's 1981 permeability model

$$k^{1/2} = 100.\emptyset^{2}\frac{(1 - S_{wirr})}{S_{wirr}} \qquad \text{…..2.6.3}$$

In the above equations 2.6.1. to 2.6.3

K (or k) is the permeability (milli Darcy)

Ø is the porosity

S_{wirr} is the irriducible water saturation

Aigbedion (2004) proposed the following linear permeability model for the Niger-Delta:

$$\text{Log K} = -0.83565 + 13.069\emptyset \qquad \text{…..2.6.4}$$

Anomohanran and Chapele (2012) used the Tixier and Timur empirical models to estimate the permeabilities of three sand layers each of 39 wells, in a field using available data on porosity and water saturation. They used the Kriging interpolation technique in the estimation of the permeability distribution of the field. Experimental work was also done for the determination of the permeabilities from core samples. These authors observed that there was a strong correlation between the core and estimated permeabilities. They later used the estimated permeability values for the first layer as input data in the Kriging interpolation process and found that the permeability ranges from 0.81 to 3.98 Darcy, with the Tixier empirical model. The Timur model yielded a permeability range of 0.97 to 3.80 Darcy. For the second layer, the estimated permeabilities from the two models were closer than for the first layer. The Tixier model gave permeabilities ranging from 0.40 to 3.69 Darcy while the Timur model

gave a range of 0.38 to 3.59 Darcy. For the third layer, the Tixier model ranged from 0.20 to 0.95 Darcy and the Timur model from 0.30 to 1.10 Darcy. They concluded that there was consistency in the values of the permeability distribution obtained for the two models and that there was a decrease in permeability with increasing depth.

2.7.1. Permeability Model Proposal

From the above, it may be observed that while the other authors incorporated the saturation factor in the estimation of the permeability from the porosity, Aigbedion found that permeability is a direct function of porosity and that the saturation factor may be negligible. This he confirmed experimentally. This conclusion is debatable since all formations/sands may not behave exactly the same way. A better model is proposed in this thesis to take care of the changing porosity as CO_2 gas injection proceeds.

Considering the fact that irreducable water saturation is constant for a particular reservoir under natural production conditions, then the equations above can be re-written as follows:

Timur Model. $K = C_1.\emptyset^{4.4}$ …..2.4.5

Coates and Dumanoir's Model $K = C_2.\emptyset^{4}$ …..2.4.6

Tixier's model $K = C_3.\emptyset^{6}$ …..2.4.7

Aigbedion's model $K = 10^{C_4 + 13.069\emptyset}$ …..2.4.8

As earlier define, K is the permeability while Ø is the porosity in equations 2.4.5. to 2.4.8. above. C_1, C_2, C_3 and C_4 are constants. This is because S_{wirr} is assumed to be constant for a given sand porosity. This thesis proved that porosity may not be constant when CO_2 is injected into a reservoir and hence, S_{wirr} is also not constant.

The summary of the first three models above is that generally,

$$K = \frac{a\,\emptyset^{b}}{S_{wirr}{}^{c}} \qquad \text{…..2.4.9}$$

In the equation 2.4.9, a, b and c are constants.

In this thesis, permeability variation was investigated with variation in porosity. The porosity is expected to vary with time of CO_2 injection and therefore the irreduceable water saturation S_{wirr} is expected to change with the changing porosity. The following model equations of 2.4.11 and 2.4.15 are being proposed in this thesis since permeability is considered, not as a constant as specified in the above four models, but assumed to change with changing porosity and water saturations.

Proposed porosity variation process in this research is that as injection of CO_2 continues with time, porosity is expected to:

1. Increase rapidly at injection due to injection pressure and at first contact with rock matrix and fluids.
2. Increases slowly as injection continues and rate of reaction reduces.
3. Remains constant or reduces after a long time.

Hence, it is proposed that the following polynomial equation holds for porosity as a function of time of injection.

$$\emptyset_t = a_1.t^2 + a_2.t \quad + a_3 \qquad \text{….2.4.10}$$

In equation 2.4.10 above, a_1, a_2 and a_3 are constants. $\emptyset_t$ is the porosity at a given time. a_1 is assumed to be a function of the reservoir cementation and strength. It is expected that for a compact non-reactive reservoir with little cementing material, a_1 will be negligible since there will no formation of secondary porosity and variation in porosity will be linear and due to fracturing of the formation. For highly reactive reservoir, a_1 is not negligible as porosity will increase rapidly with CO_2 injection, firstly due to reaction and then due to pressure of injection.

The irreducible water saturation at time t is expected to increase or decrease with time such that

$$S_{wirr,\,t} = \text{function } (\emptyset, K) \qquad \text{.....2.4.11}$$

For Kwale sands, available permeability, porosity and water saturation data was applied to obtained the irreducible water saturation as proposed in model equation 2.4.11. above using the four models (appendix B). It was discovered that the Timur and Tixier models gave reasonable irreducible water saturation values with the Timur values being the more accurate values. The Coates-Dunamior model gave almost 100% S_{wirr} values and this is impossible except for rocks in water zone only. Hence, Timur model is chosen as the most appropriate S_{wirr} model for the Kwale sands such that:

$$S_{wirr} = \sqrt{\frac{0.135\emptyset^{4.4}}{K}} \qquad \text{.....2.4.11a}$$

With this model, an equation relating the S_{wirr} and porosity for Kwale sandstone was obtained such that:

$$S_{wirr} = 10.8 * e^{-15.7\emptyset} \qquad \text{.....2.4.12}$$

Application of the Tixier, Timur and Coates-Dunamior models to compute permeability for the measured porosity variation for the Kwale sand gave unreasonable too low values for Timur model, unreasonable too high values for Tixier model and values comparable to available data for the Coates-Dunamior model. Hence, a combination of the Timur S_{wirr} analysis and the Coates-Dunamior permeability equation is proposed to obtain a new model that is best appropriate for the Kwale reservoir permeability variation with porosity.

Coates-Dunamior model equation is as follows:

$$K^{1/2} = 100\emptyset^2 \left[\frac{1-S_{wirr}}{S_{wirr}}\right] \qquad \text{.....2.4.13}$$

Substituting the Timur's S_{wirr} gives

$$\frac{1 - S_{wirr}}{S_{wirr}} = \frac{1 - 10.8 * e^{-15.7\emptyset}}{10.8 * e^{-15.7\emptyset}}$$

…….2.4.14

Substituting this into the Coates-Dunamior model equation gives:

$$K^{0.5} = 100 * \emptyset^2 * \left[\frac{1 - 10.8 * e^{-15.7\emptyset}}{10.8 * e^{-15.7\emptyset}}\right]$$

The proposed permeability-porosity model for the Kwale sandstone/shale reservoirs during CO_2 injection is therefore as follows:

$$K = 100 * \emptyset^2 * \left[\frac{1 - 10.8 * e^{-15.7\emptyset}}{10.8 * e^{-15.7\emptyset}}\right]^2$$

…….2.4.15

Where K is the permeability in milliDarcy

Ø is the porosity in fraction

2.8. Irreducible Water Saturation (S_{wirr})

The Lansing-Kansas City oomoldic limestone has been reported to exhibit a relationship between the irreducible water saturation (S_{wirr}) and the permeability. S_{wirr} increases with reducing permeability (National Energy Technology Laboratory, 2006). The following relationship exist between the percentage S_{wirr} and the permeability

$$S_{wirr} = 35.7e^{-0.46logK} \quad \text{…..2.4.16}$$

where S_{wirr} is in % while K is in mDarcy.

The Tixier, Timur and Coates-Dumanoir permeability models are eachl dependent, in one way or the other, on the irreducible water saturation of the reservoir. The value of the irreducible water saturation has a strong influence on the calculated permeability. Hence, experiments were carried in this thesis to determine the irreducible water saturation of the candidate reservoirs used.

Goetz et al (1996) proposed a drying rate method of analysis for the computation of the irreducible water saturation of a core sample. They stated that the drying rates of water-saturated core samples are of two distinct periods. These are the constant drying rate

and the decreasing drying rate periods. They stated that the drying rate is initially constant and is controlled by the rate of evaporation at the outer surfaces of the sample. During this period, the water in the core has a high degree of hydraulic connectivity and flows by capillary transport to the sample surface. When the level of water saturation decreases, the water loses the connectivity and the drying process goes through a falling rate period. The authors concluded that the transition period between the constant drying rate period and the falling rate period is the beginning of the irreducible water saturation state in the cores. They concluded that the water saturation at this transition stage is the maximum possible irreducible water saturation.

S_{wirr} is also determined by laboratory measurements on core samples using either the porous plate displacement or centrifuge techniques (Goetz et al, 1996). In this thesis, both the centrifuge method and the drying rate method were applied in the determination of the irreducible water saturation of the proposed candidate reservoirs.

Honda and Magara (1982) carried out a theoretical consideration of the irreducible water saturation in mudstone using a capillary model of a porous medium. The air and water absolute permeabilities of the mudstone samples were estimated and it was found that S_{wirr} increases gradually with decrease in porosity of the mudstones. At porosities below 15%, tagged as the critical porosity, the S_{wirr} value is 100%. This implies that below 15% porosity, water saturates the mudstone pores. Their conclusion was that S_{wirr} increases with reducing porosity and vice versa.

2.8.1. Irreducible Water Saturation (S_{wirr}) Variation With Porosity

Estimates of the variation of S_{wirr} with porosity may be made based on the assumption that the irreducible water volume remains constant during the injection that resulted in porosity variation. This is based on the assumption that the rock maintains its wettability during the gas injection. Without this assumption, the expansion of water as the pressure varies will need to be considered. Also the volume change due to the solubility of the injected fluid in water will need to be considered. Moreover, the flooding effect of the injected fluid on the water must be considered.

In the case of CO_2 injection into oil sand resulting in varying porosity, S_{wirr} is expected to vary, since the volume of the irreducible water saturation is assumed to be constant while the pore volume changes. Hence, the irreducible water volume is given as:

$$V_{wirr} = S_{wirr} * Ø_i \qquad \text{(cu.ft/cu.ft of pore space)}$$

Where V_{wirr} = irreducible water volume fraction

S_{wirr} = irreducible water saturation

$Ø_i$ = initial porosity

At a time t after CO_2 injection, the irreducible water volume will become

$$S_{wirr,\,t} = V_{wirr} / Ø_t$$

where $Ø_t$ is the new porosity at time t.

The last equation above was applied in the computation of permeability variation as a function of effective porosity.

Chapter 3.

3.0. EXPERIMENTAL

The experiments were divided into two groups:

1. Effects of injected CO_2 on candidate storage reservoirs. This is sub-divided into:
   a. Kwale sandstone as candidate CO_2 storage reservoir.
   b. Kwale shale (black and grey) as candidate CO_2 storage reservoir.
   c. Ota kaolinitic clay as candidate CO_2 storage reservoir.
   d. Imeri oilsand as candidate CO_2 storage reservoir.

2. Effects of stored CO_2 on fluids. Two sets of experiment were performed in this section.
   a. Effect of stored CO_2 on reservoir crude, Bonny light
   b. Effect of leaked CO_2 from stored reservoir on drilling activity at adjacent reservoir.

3.1. Materials.

The following materials were employed in this research.

3.1.1. Kwale Drill Cutting Samples

Drill cutting samples were obtained from some wells in the Kwale Field in the Niger-Delta at various depths between 975.4 and 1020.1 meters as representation of the reservoir in that area. Samples include:

- Sandstone cuttings
- shale cuttings (grey colouration)
- shale cuttings (black colouration)

Drill cutting samples were of average weight 18.01 g were obtained at a depth of 985.84 m. For sample 3A, the average initial porosity was 37.73%. For sample 3B the avergae porosity was 37.17%. These dry samples were injected with CO_2 and their porosity variations are shown in Fig. 4.7 and 4.8. The cuttings were employed as representative of various possible Kwale reservoir conditions.

i. Crude Oil Impregnated Kwale Drill Cutting

In this section, an investigation is made of a typical abandoned Niger-Delta reservoir into which CO_2 injection is made. The sample is representative of reservoir rock with CO_2 injection at crude oil zone. It also represents an oleophilic (oil-wet) reservoir rock. The drill cutting samples (1A and 1B) were obtained at the depth of 982.45 m and had porosity value of 28.11% and 20.73% respectively. The average weight of each was 17.80g each. The samples were soaked in crude oil before CO_2 injection.

ii. Water Impregnated Kwale Drill Cutting

This is a representative of a reservoir rock with injection at the water zone. The experiment in this section investigates possible porosity alterations when CO_2 is injected into the water zone of a Kwale Field reservoir. It studies the effect of the injection on the reservoir rock located in the water zone. The assumption is that the rock is hydrophilic in nature.

The drill cutting samples were obtained at a depth of 980.3 m and each weighed 17.66 g. Initial porosity values of 20.98% and 48.6% were determined for samples 2A and 2B respectively. Both were soaked with formation water and then injected with CO_2 prior to the porosity experiment. This is a representation of CO_2 injection into a reservoir rock at the water zone.

iii. Dry Kwale Drill Cuttings

The sample is a representation of an extremely depleted oil zone. The research in this section investigates the porosity variation when the reservoir is empty of formation fluid. Though the possibility of the existence of this type of reservoir is slim, it could occur as a result of extreme fluid loss from the reservoir leaving a water wet reservoir totally empty or with a small quantity of dry gas.

3.1.2. Oil sand samples

Samples were obtained at Imeri Village, Ijebu East (Nigeria) as a representative of sub-surface rock samples in the vicinity of the high CO_2 emission Lagos/Ogun industrial zone, which includes industries such as gas turbine power plants, cement companies, breweries, metal recycling plants, metal/plastic bottle manufacturing and other heavy industries.

3.1.3. Kaolinitic clay sample.

Samples were obtained at about 42.7 m depth at Benja, Ota, Ogun State, Nigeria. These serve as representation of the Oshoshun/Ewekoro sub-surface formation under the thermal power generation plants at Olorunsogo I/II, Omotosho and Egbin and also the cement factories in the Papalanto/Ibesse environment. These power plants and cement industries are high CO_2 pollutants and are therefore regarded as potential CO_2 capture sources.

3.1.4. Niger-Delta Bonny Light Crude.

Injection of CO_2 into Bonny light crude oil was also investigated. The aim is to study the effect of injecting CO_2 gas into an oil zone or of a leakage from the CO_2 storage reservoir to a producing zone.

3.1.5. Simple Water-based mud and Oil-based Mud.

Simple water-based mud and oil-based mud were prepared as representatives of drilling mud and the effects of contamination with CO_2 were investigated. This is to represent the possibility of contamination during drilling when there is a leakage of CO_2 gas from the storage reservoir adjacent to a formation being drilled.

3.1.6. Compressed Carbon dioxide gas

Compressed CO_2 gas of over 90% purity was obtained at about 103.41 KN/m^2 in pressurized gas cylinders. This was used for CO_2 injection into the various core samples. It was also employed to replace the nitrogen gas used for the porosity experiment so that the core samples would not be contaminated with nitrogen but with the desired CO_2.

3.2. Analysis Equipment

The analysis was carried out with the following items of equipment.

3.2.1. Core Holder

A modification was initially made to a pressure filter cup to employ it as high pressure vessel, but there were some uncontrollable gas leaks which made pressure maintenance impossible, and no reasonable readings were obtained. The core holder was able to withstand pressures in excess of 6896 KN/m^2 without leakage.

The experimental setup for the CO_2 gas injection is shown in Fig. 3.2. For the porosity measurement, the nitrogen gas of the porosimeter was replaced with CO_2 gas. This was done so that the CO_2 was in permanent contact with the cores throughout the period of the porosity measurements.

Fig. 3.1.: Core Holder (OFI Testing Equipment)

Fig. 3.2: The Experimental Setup For The CO_2 Gas Injection

(Nitrogen gas was replaced with the CO_2 gas for permanent CO_2 - Core contact)

3.2.2. Core Preparation

Cores were prepared from drill cuttings using a core cutter and core drilling machines. The available core drilling machine is the Delta 17-959L driller with the following description:

3.2.2.1. Delta 17-959L Core Drilling Machine

The Delta Model 17-959L (Fig. 3.3) is a heavy-duty 43.2 cm floor model drill press with 3/4 HP, 120/240V induction motor, 1.588 cm capacity chuck and key, cast iron table, rack and pinion elevation mechanism, and external depth stop. The 17-959L has a tilting table with a heavy clamp for various angle drilling The drill press table is fitted with two T-slots for safety purposes to make the work piece immobile during cutting and also for use with various drill press accessories such as fences, stop blocks or clamps. It is attached with 0.7938 cm T-bolts to the table. Side edges and parallel slots are provided for fast work piece clamping. The table raising and lowering handle rotate the table to the desired angle. The table is fitted with a tilt scale located on the knuckle behind it for accuracy. There is a detent pin that can slide in to positive stops of 0, 45 and 90 degrees to give the exact angle. The core drilling machine is fitted with a laser beam cutter. The laser housing assembly is fitted on the drill press column for safety purposes for eyes protection. The laser alignment rod is part of the features of the driller and is used to concentrate the laser beam on the sample, minimize diffusion and ensure safety against stray laser beam. The drill press base is fastened to the floor using the carriage bolts, flat wgreyers and hex nuts. Also available is the Chuck with a Chuck Key that serves as a connector for different drilling accessories to the machine. Light is connected to the headstock for good illumination and for safety purposes during the operation of the machine.

Fig. 3. 3: Delta 17:950L Core Drilling Machine

(OFI Testing Equipment)

3.2.3. Porosity Analysis

This measures the effective porosity of a core sample using digital display of pressure with an operating pressure of 3448 KN/m^2 using helium or nitrogen gas as the recommended injection gas.

The Porosimeter is able to test core samples of 3.81 cm diameter and 5.08 cm length. It has a vacuum pump for evacuating core sample with very low permeability. The unit has an easy calibration and has a lock-in feature for rapid measurements of sample porosity.

It is fitted with air-relief valves to prevent over-pressurization. It is also equipped with a vent as a safety measure in order to eliminate the high pressure after a test has been carried out and before the core holder is opened.

To make the porosity measurement easy, the fitted nitrogen gas was replaced with CO_2 gas during this research so that CO_2 injection and porosity measurement are carried out simultaneously. The principle of operation is very easy as it measures the volume of gas that can be injected into a core sample. Since the injected gas occupies the pore space in the sample, this implies that the volume of gas that a sample can accommodate is equal to the pore volume of that sample.

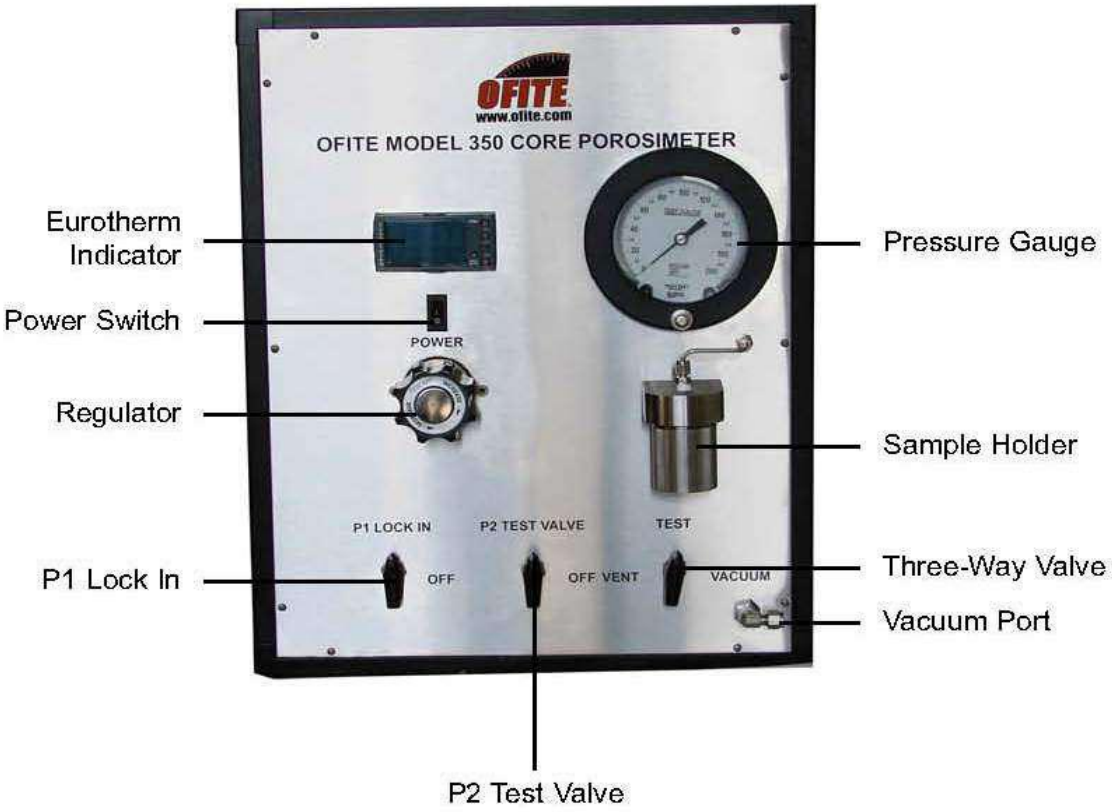

Fig. 3. 4: Model 350 Core Porosimeter

(OFI Testing Equipment)

3.2.4. DRILLING MUD ANALYSIS EQUIPMENT

3.2.4.1. PH meter

Fig. 3. 5: pH Meter (HANNA INSTRUMENTS)

(For measurement of variation in the pH of Bonny light crude and the drilling mud)

3.2.4.2. Viscometer

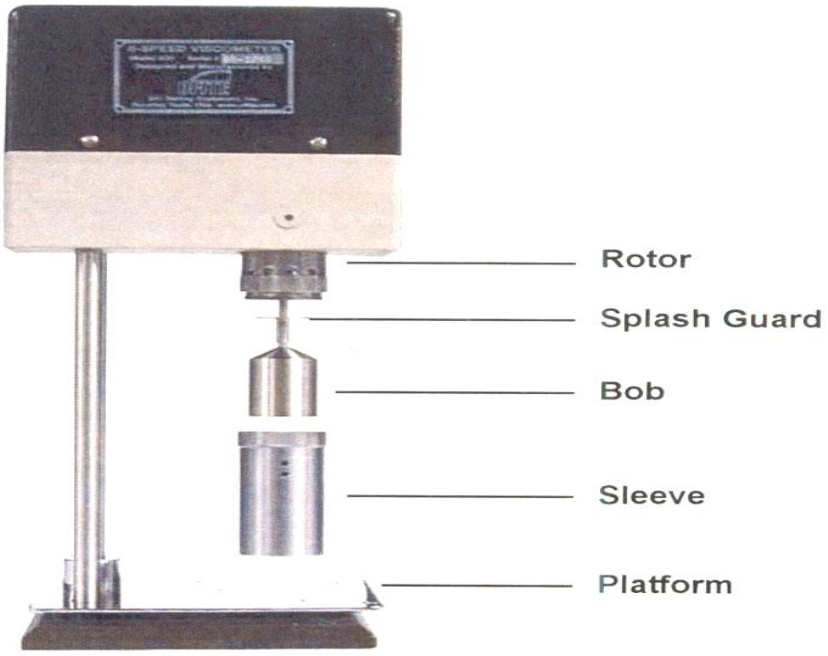

Fig. 3. 6: Vann Viscometer (OFI Testing Equipment)

A pH meter, Fig. 3.5, was used for the measurement of variations in the acidity of the two drilling mud and that of the Bonny light crude when CO_2 was injected into them.

A Vann viscometer, Fig. 3.6, was used for the investigation of the effect of injected CO_2 contamination on the flow properties of the water-based mud, oil-in-water emulsion drilling mud and Bonny light crude oil.

3.2.4.3. Mud Mixer

Hamilton mud mixer (Fig. 3.7) was used in the investigation of the effect of injected CO_2 contamination on the flow properties of the drilling muds. The mixer was used to obtain homogenous mixing so that accurate flow property measurement can be obtained with the Porosimeter.

3.2.4.4. Density Balance

OFITE density balance, Fig. 3.8, was used in the investigation of the change in density and specific gravity of drilling muds and crude oil contaminated with CO_2.

Fig. 3. 7: Mud Mixer

(Hamilton Beach Appliances)

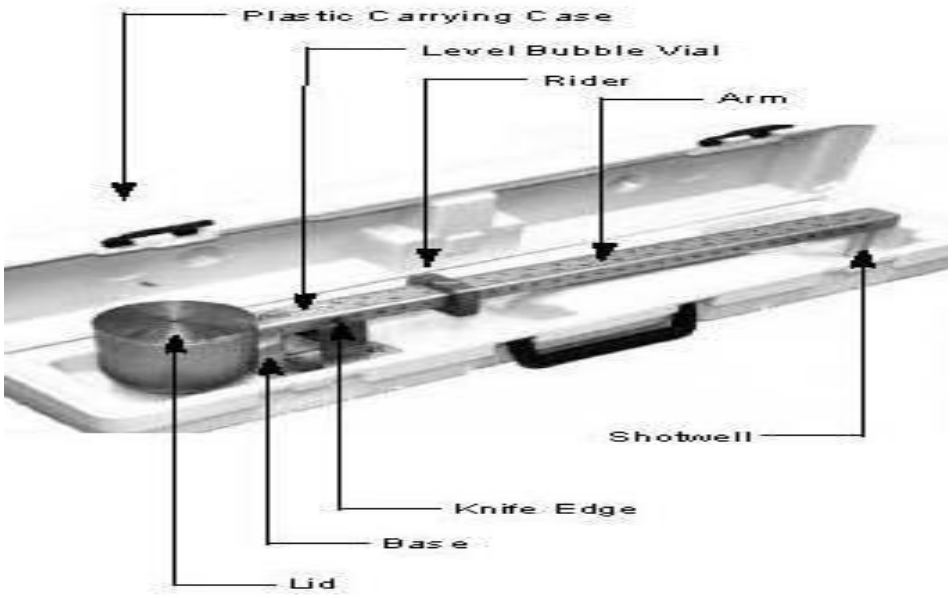

Fig. 3. 8: Mud Density Balance

(OFI Testing Equipment)

3.2.4.5. Resistivity Meter

Fig. 3. 9: Digital Resistivity Meter (OFI Testing Equipment)

The simple digital retivity meter in Fig.3.9, was used in analysis of the resistivity of Bonny crude oil and drilling mud prepared

3.2.5. Sample Analysis With Atomic Absorption Spectrometer (AAS)

This was used in the analysis of the trace metal in the samples used in the research. The trace metals analysed include lead, iron, nickel, manganese and copper. The test for zinc metal was non-conclusive. This analysis was done in order to evaluate possible side reactions, apart from the expected reactions of the major metallic components of each samples. Moreover, the determination gave the extent of impurities in the rock samples. The results for the AAS is reported in the appendix C.8.1 to C.8.5. The AAS that was used is the S-series and is as shown in Fig.3.10.

Fig.3.10: Experimental setup For S-series Atomic Absorption Spectrometer (AAS) Analysis of The Core Samples

3.3. Procedure

The porosity and the irreducible water saturations measurements were carried out in the laboratory. Permeabilities were obtained from models and the literature was used to draw inferences. The laboratory analyses were carried out as reported in items 1, 3 and 4 of section 3.2.1 below.

3.3.1. Kwale Sandstone and Shales As Candidate CO_2 Storage.

The procedure followed were as follows:

1. Porosity analyses were done on 6 different sandstone cuttings and 2 shale cuttings obtained from the Kwale reservoir in the Niger-Delta. Cuttings include.
    a. The volume of each of the cuttings was determined by the water displacement method.
    b. The porosimeter was calibrated to obtain the porosimeter constant.
    c. The cutting sample was placed in the porosimeter and the experiment setup according to the laid dow procedure stipulated in the machine manual.
    d. Porosity readings were taken over a period of 3 to 5 weeks until a constant porosity value was obtained.
    e. Porosity model equations for CO_2 injection were then obtained for each of the samples.

2. Mathematical analysis of the existing porosity, water saturation and permeability data for thirteen Kwale sands were carried out with the assumption that the Kwale field is made up of 13 distinct sands, A to M (Ekine and Iyabe, 2009). In order to model the permeability of the reservoir, the porosity and irreducible water saturation, S_{wirr}, must be known. S_{wirr} is directly related to the initial water saturation, S_w, and it is required in permeability calculations. Hence, the relationships between porosity, permeability and S_w for the Kwale sands were analyzed with the experimental data of Ekine and Iyabe for sands B, C, D, F, G,H, I, K, L and M. This was then applied in the computation of the S_{wirr} using the Tixier, Timur and Coates-Dumanoir models relating porosity, permeability and water saturations. The models were used because they are well established models and provide good representation of the reservoir conditions. They were applied as guides to the expected irreducible water saturation as porosity changes. This was later used for the computation of the permeability of

the eight Kwale sands to obtain appropriate permeabilities for the sand as porosity varies with CO_2 injection.

3. The irreducible water saturation, S_{wirr}, for the Kwale shale sample was determined using both a semi-manual and an automatic centrifuge. The S_{wirr} was also determined with the drying method and the results were compared.
4. The analyses of trace metals in each of the samples were carried out with aid of atomic absorption spectrometer (AAS) using the principle of a flame test. This AAS analysis of the Kwale sandstones and shales samples discovered the heavy metal compositions as a possible determination of reactions products of the metals with injected CO_2 gas.
5. Permeabilities of the Kwale cores were evaluated using established permeability models of Tixier, Timur and modified Coates-Dumanoir. This modified Coates-Dumanoir is the proposed model in this thesis. This is because the Timur model was found to give the most realistic values during the S_{wirr} analysis of the Kwale sand (appendix B); but the Coates-Dumanoir model gave the best permeability values for the sands. Hence a hybrid model using Timur's S_{wirr} equation and Coates-Dumanoir's permeability equation was proposed. Model equations relating combined primary-secondary porosity and corresponding permeability. were then obtained for each of the samples.

3.3.2. Imeri Oil Sand Reservoir As Candidate CO_2 Storage.

The procedure followed is as follows:

1. Experimental determination of variation of porosity of Imeri oilsand with time as CO_2 is injected. Injection of CO_2 gas into Imeri oil sand serves as a representation of the sub-surface rock underlining possible sources of CO_2 capture candidates such as Olorunsogo I and II and Omotosho thermal power generation plants and various cement complexes at Papalanto/Ibesse axis.
2. Experimental determination of the irreducible water saturation for Imeri oilsand using the drying rate method.
3. AAS analysis of the Imeri oilsand to determine the heavy metal composition as a possible determination of metals involved in reaction with injected CO_2 gas.
4. Permeability modelling for the Imeri oilsand samples. The steps for proposed permeability model with time of CO_2 injection is as follows:

- Porosity-time plots from measured data were made.
- Best-fit curves/lines and equations for the plots were obtained.
- Average porosity with the equation obtained in (2) was computed giving an average porosity variation with time.
- With the average porosity, a Modified Coates-Dumanoir permeability was computed with the Timur's S_{wirr}.
- Best fit curves and equations from the Modified Coates-Dumanoir permeability curve were obtained. This described the permeability variation with time of CO_2 injection.

3.3.3. Ota Kaolinitic Clay Reservoir As Candidate CO_2 Storage.

The procedure followed is as follows:

1. Experimental determination of variation of porosity of ota kaolinitic clay with time as CO_2 is injected. The clay serves as a representation of the sub-surface rock underlining possible sources of CO_2 capture such as Egbin, Olorunsogo I and II and Omotosho thermal power generation plants and the cement complexes at Papalanto/Ibesse axis.
2. Experimental determination of the irreducible water saturation for Ota kaolinitic clay using the drying rate method was carried out.
3. Atomic absorption Spectrometer (AAS) analysis of the clay to determine the composition of metals that may be involved in reaction with injected CO_2 gas.
4. For the permeability modelling for the clay sample, the procedure followed is the same as for 3.2.2.(6) above.

3.3.4. Injection of CO_2 into Niger-Delta Bonny light crude

This was carried out to study the effect of CO_2 gas on the reservoir crude oil during CO_2 storage in abadoned oil reservoir. Simple apparatus such as viscometer, density balance, resistivity meter and pH meter were employed in the measurement of the initial properties of the crude such as the density, shear stress, yield point, resistivity and acidity. The procedure was as follows:

a. CO_2 was injected into the crude intermittently for a short period everyday for a total period of 9 days. After each injection, the crude sample is sealed

and allowed to react with the injected CO_2 for a period of 24 hours before measurements were taken.

b. The effects of the injected CO_2 on the density, shear stress and the pH of the crude oil were measured daily before new CO_2 injection.
c. The apparent viscosity of the crude oil was calculated from measured data.

3.3.5. Injection of CO_2 into Simple Drilling Mud Samples

CO_2 was injected into simple water-based mud and oil-based drilling mud (oil-in-water emulsion) and the effects of the gas on the mud properties were measured. This is to represent the effect of possible CO_2 gas kick from stored reservoir to adjacent reservoir being drilled. The procedure followed is same as stated in section 3.2.4 above.

Chapter 4

RESULTS AND DISCUSSIONS

4.1. Results

The results obtained in the course of this research are presented in this section while some of the measured data are presented in Appendix B. The results are presented in two groups:

1. Effects of injected CO_2 on candidate storage reservoirs:
    a. Kwale sandstone as candidate CO_2 storage reservoir.
    b. Kwale black and grey shale as candidate CO_2 storage reservoir.
    c. Ota kaolinitic clay as candidate CO_2 storage reservoir.
    d. Imeri oilsand as candidate CO_2 storage reservoir.
2. Effects of stored CO_2 on fluids:
    a. Effect of stored CO_2 on reservoir crude, Bonny light
    b. Effect of leaked CO_2 from stored reservoir on drilling activity at adjacent reservoir.

4.1.1. Effects Of Injected CO_2 On Candidate Storage Reservoirs

In this section, experiments and calculations obtained as CO_2 gas is injected into some Niger-Delta reservoir rock samples, to study their possibility of serving as candiadte CO_2 storage reservoir is presented. The first experiment carried out was the calibration of the porosimeter.

Porosimeter calibration.

The porosimeter was calibrated in order to correct the accurate determination of the porosity values. Table 4.1 reports the calibration values.

From the table, the expected maximum error reading from the Porosimeter is $\pm$ 0.259%. This was applied in correction of obtained porosity values.

Table 4. 1: Porosity Calibration Measurement

Bulk Volume (cm^3)	Porosimeter constant (cm^3)	PI	P2	V2	V3	Grain volume (cm^3)	porosity
13.43	57.1	11.57	5.17	161.18	127.785	13.396	0.00259

.

P1, P2 are downstream and upstream pressure readings respectively

V2 is the measured volume of the porosimeter core holder cup without a core

V3 is the volume of the porosimeter with installed calibration core

4.1.1.1. Kwale sandstone reservoir as candidate CO_2 storage reservoir.

Presented in this section are the measured variations in Kwale sandstone porosity as CO_2 gas is injected together with the, computation of irreducible water saturation and the permeabilities.

4.1.1.1.1. Experimental Results of Change In Porosity of Kwale Field Reservoir Rock Contaminated With CO_2.

In this section, the porosity measurements for six Kwale sandstone samples are presented. For each zone, two samples were used to represent the sandstone at the oil zone, the water zone and the highly depleted oil zone.

Porosity variation for kwale sample 1A and 1B soaked in crude and injected with CO_2 are presented in Fig. 4.1 and 4.2. The comparison between the measured values for the samples 1A and 1B is presented in Table 4.3.

A. Representative Of Kwale Sandstone Reservoir Rock With Injection At Crude Oil Zone

Sample 1A:

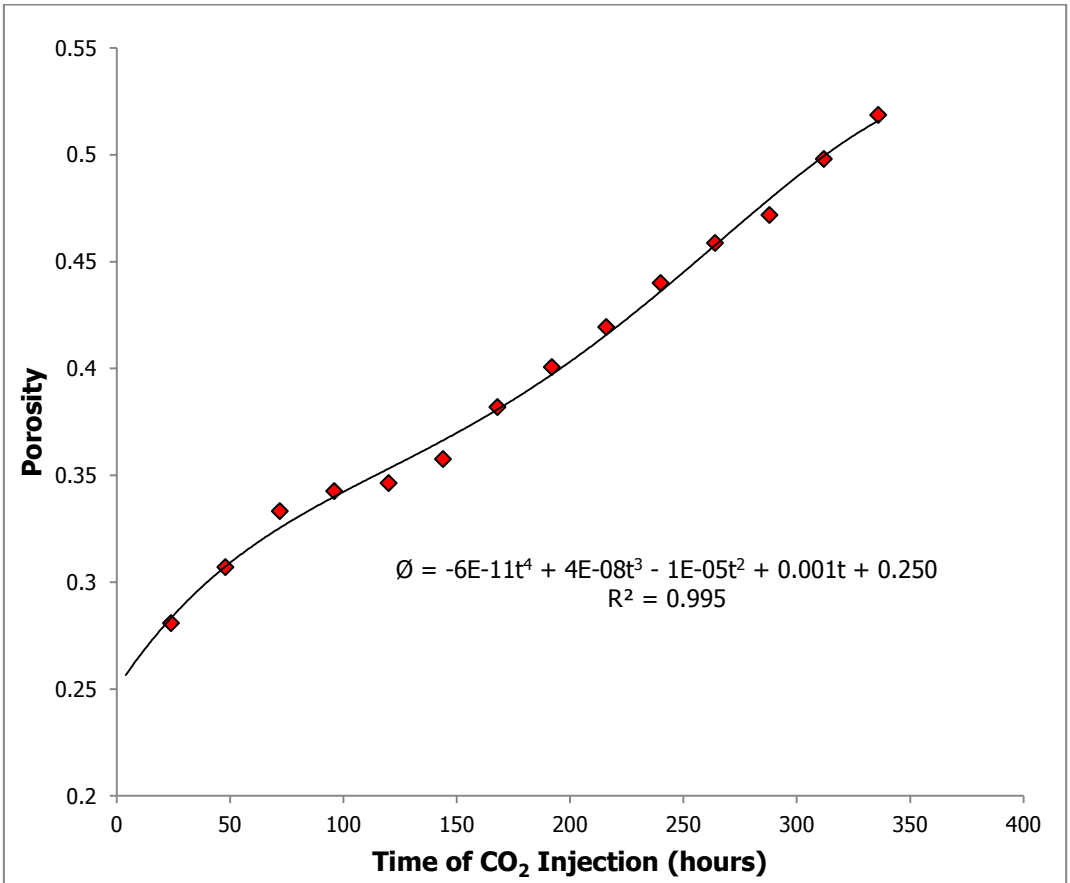

Fig. 4.1: Porosity Variation For Kwale Sample 1A Soaked In Crude & Injected With CO_2

Sample 1B

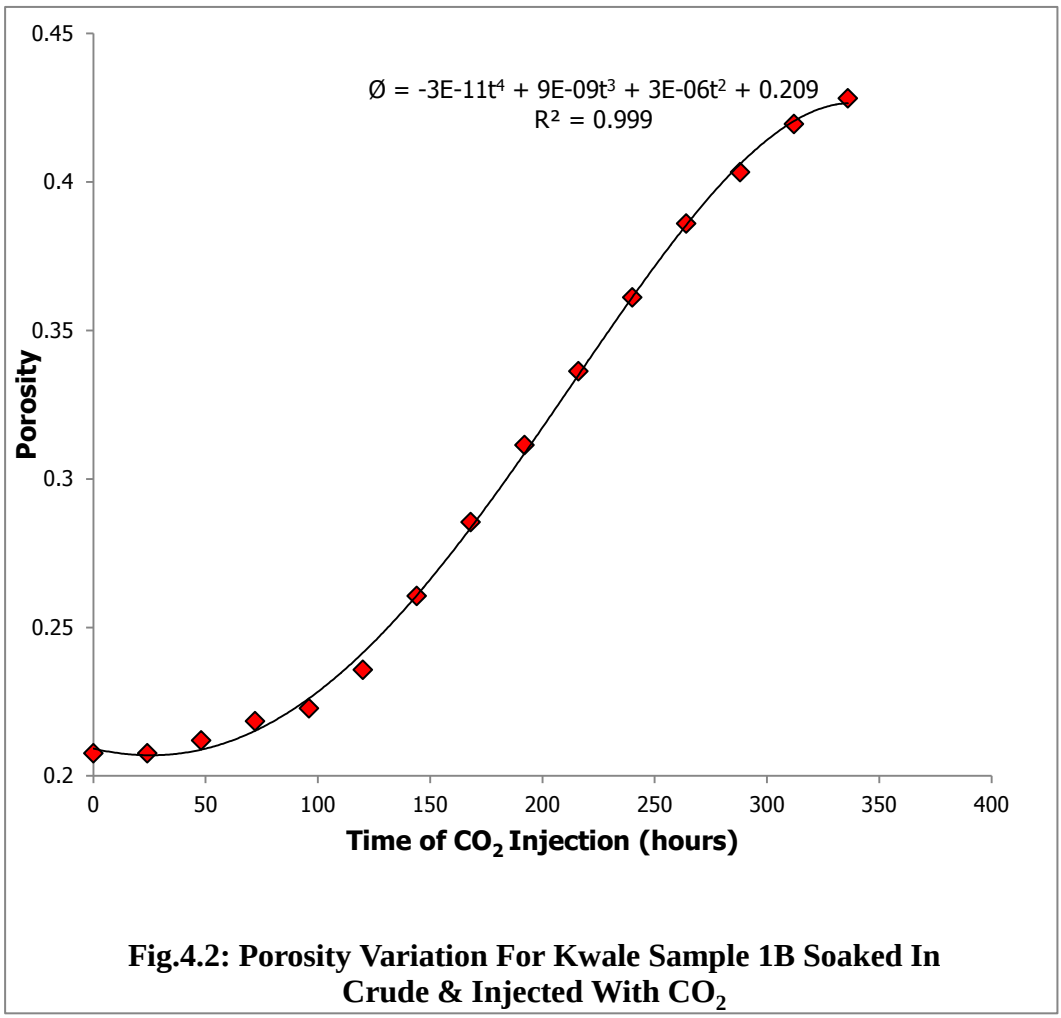

Fig.4.2: Porosity Variation For Kwale Sample 1B Soaked In Crude & Injected With CO_2

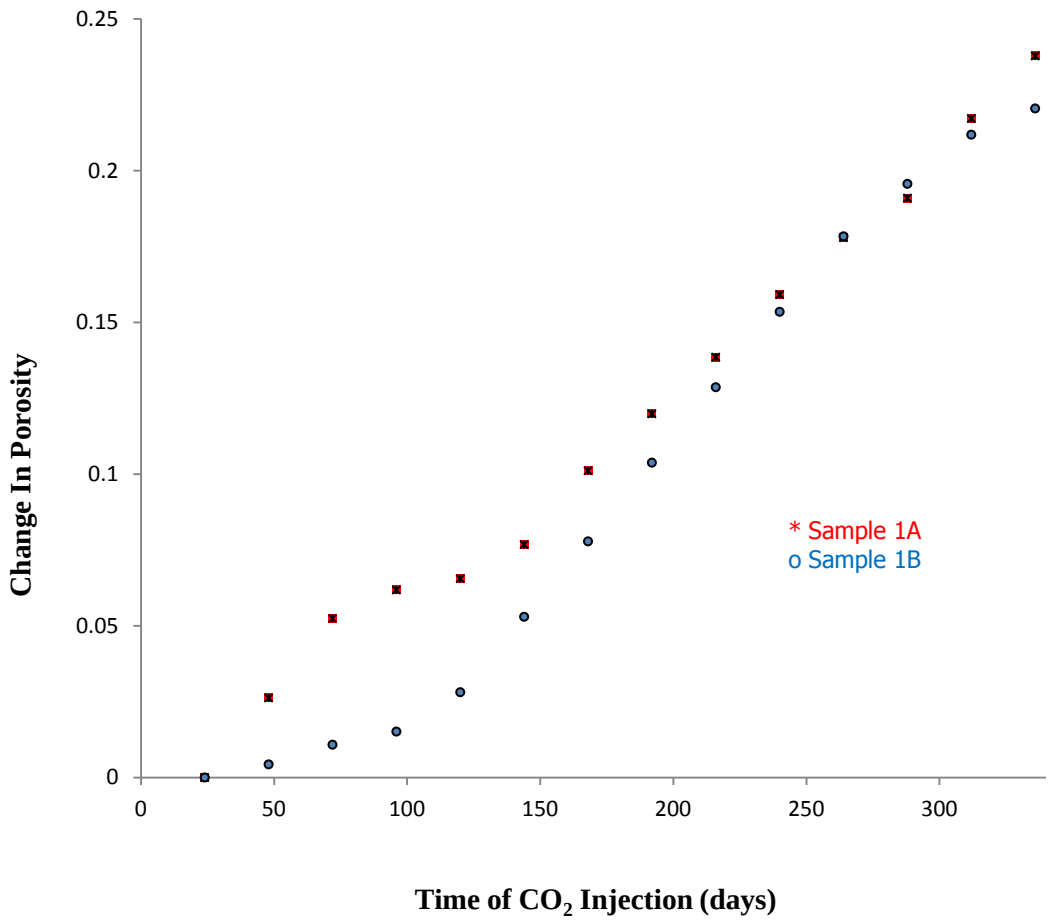

Fig. 4.3: Comparison Between Change in Porosity of Samples 1A & 1B Representing Rock In Crude Oil Zone Injected With CO_2

B. Representative of Kwale Sandstone Reservoir Rock With Injection at Water Zone

Porosity variation for kwale samples 2A and 2B, soaked in formation water and injected with CO_2 are presented in Fig. 4.4 and 4.5. The comparison between the measured values for the samples 2A and 2B is presented in Table 4.6.

Sample 2A

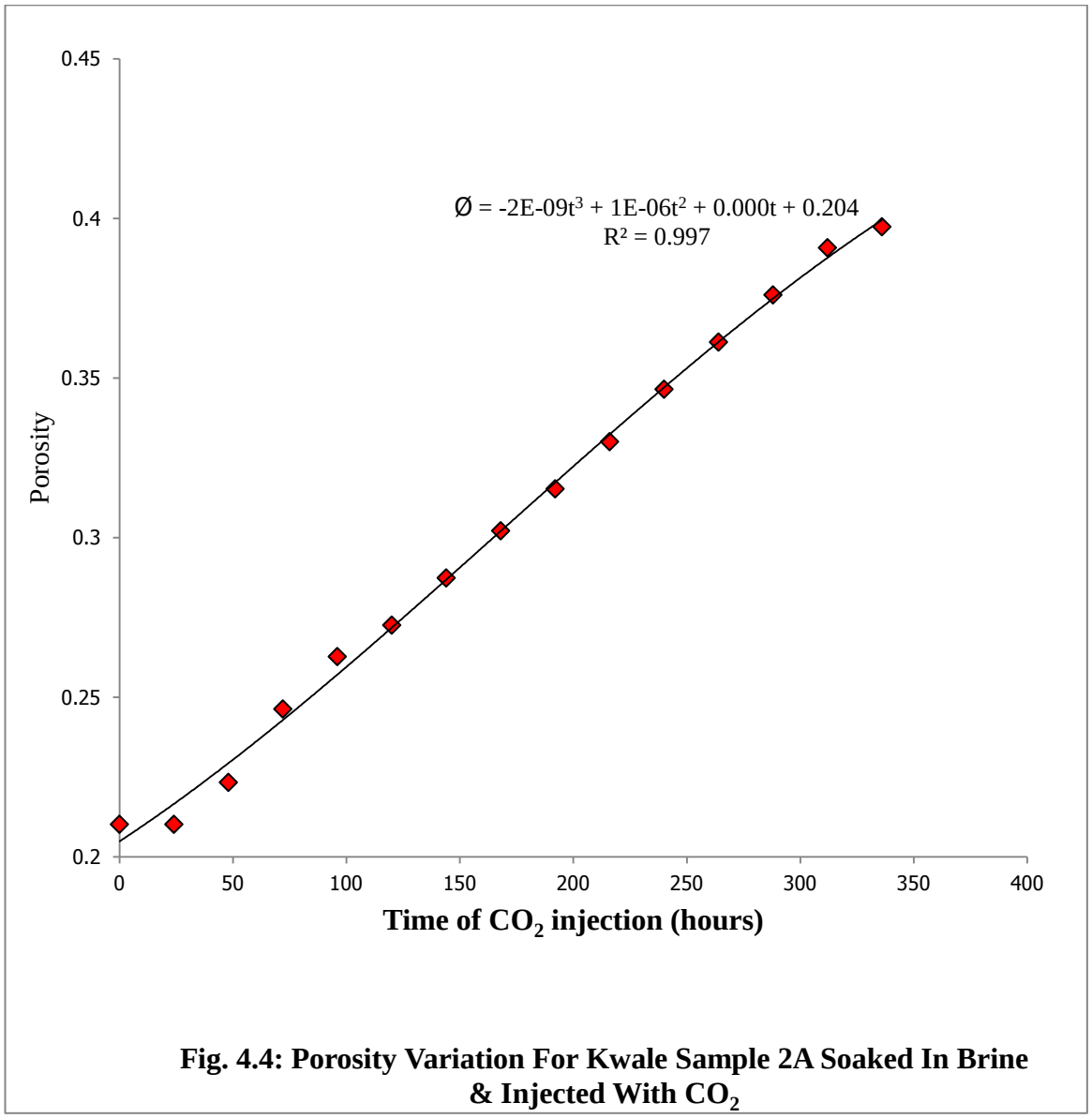

Fig. 4.4: Porosity Variation For Kwale Sample 2A Soaked In Brine & Injected With CO_2

Sample 2B

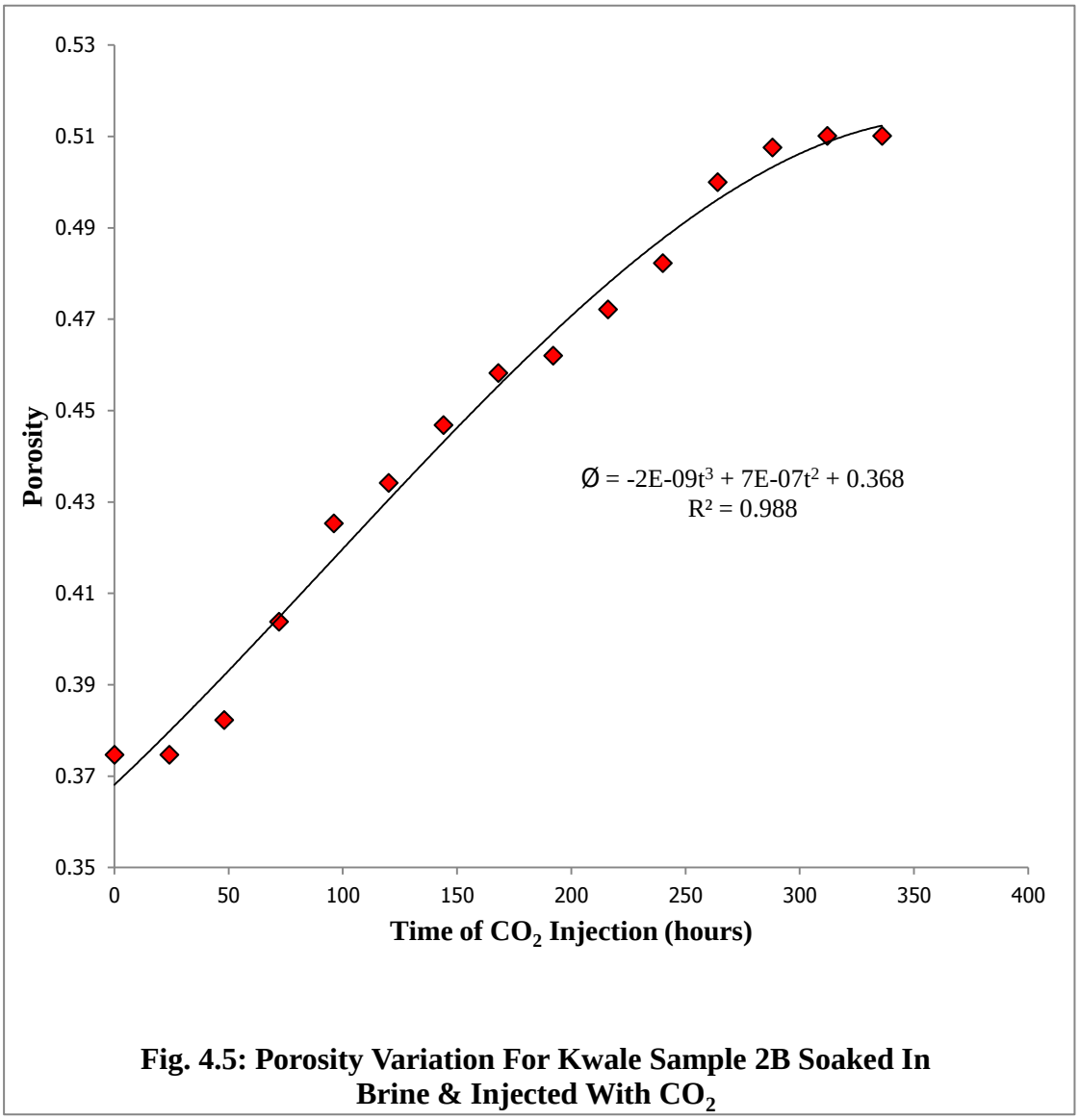

Fig. 4.5: Porosity Variation For Kwale Sample 2B Soaked In Brine & Injected With CO_2

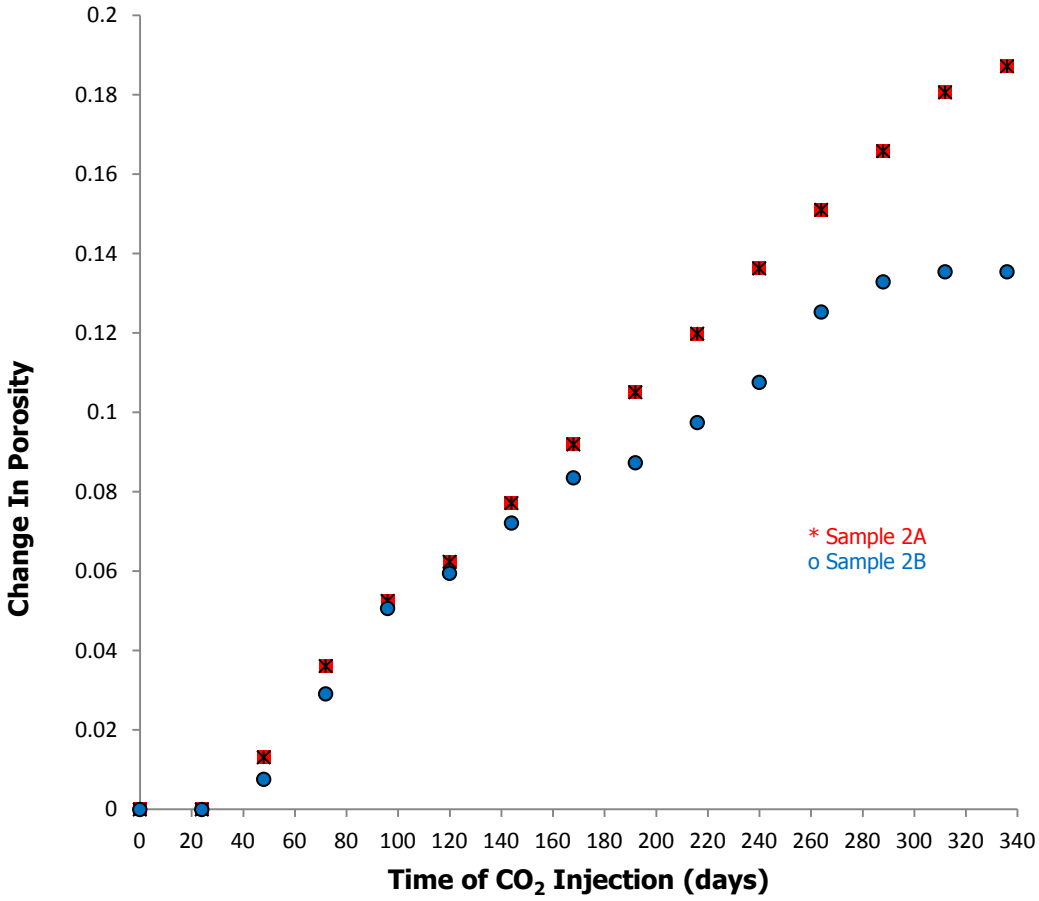

Fig. 4.6: Comparison between change in Porosity For Sample 2A & 2B Soaked In Formation Water & Injected With CO_2

C. CO_2 Injection Into Dry Kwale Sandstone Reservoir Rock or Extremely Depleted Oil Zone

Porosity variation for kwale samples 3A and 3B, dry cores injected with CO_2 are presented in Fig. 4.7 and 4.8. The comparison between the measured values for the samples 3A and 3B is presented in Table 4.9.

Sample 3A.

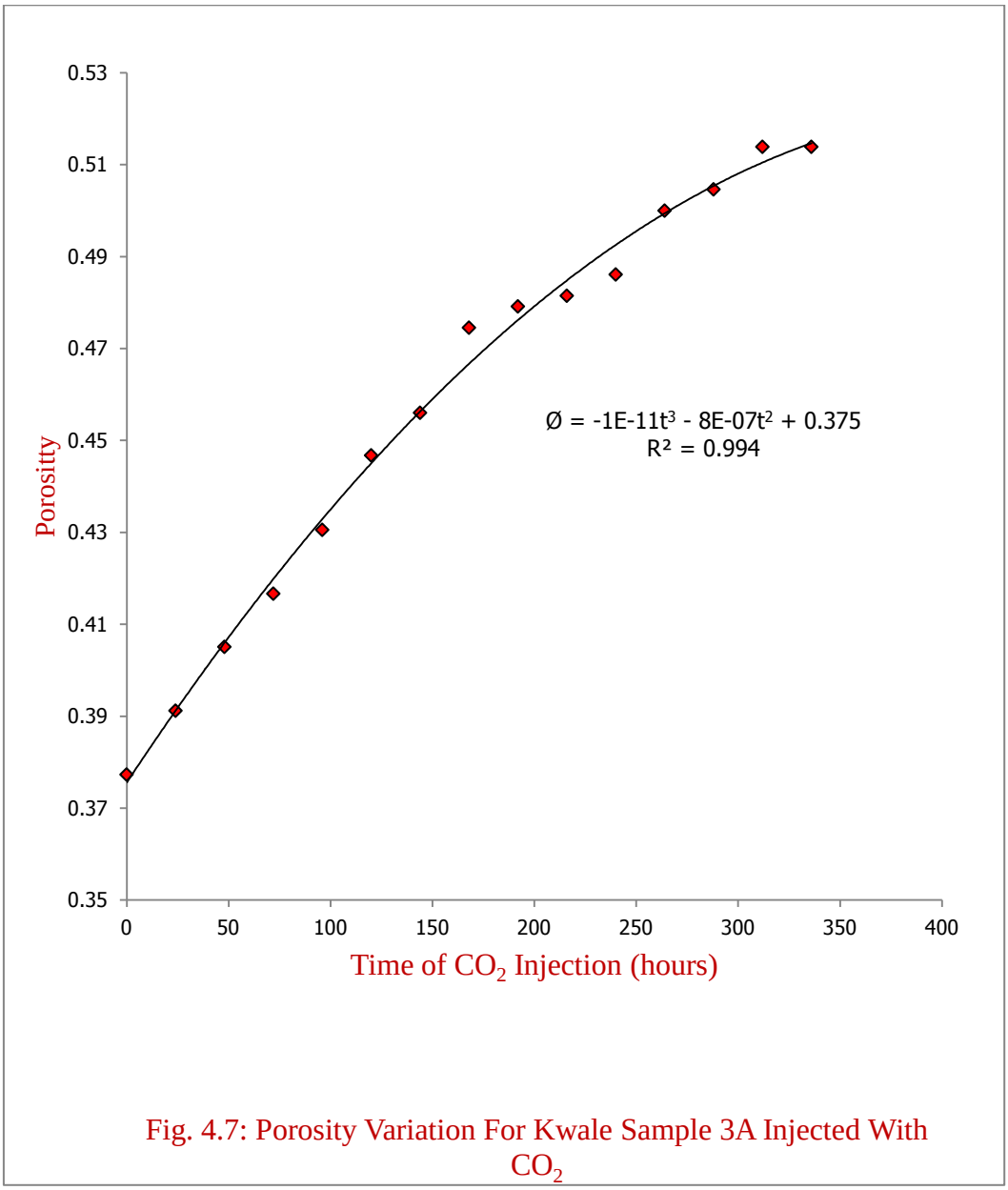

Fig. 4.7: Porosity Variation For Kwale Sample 3A Injected With CO_2

Sample 3B:

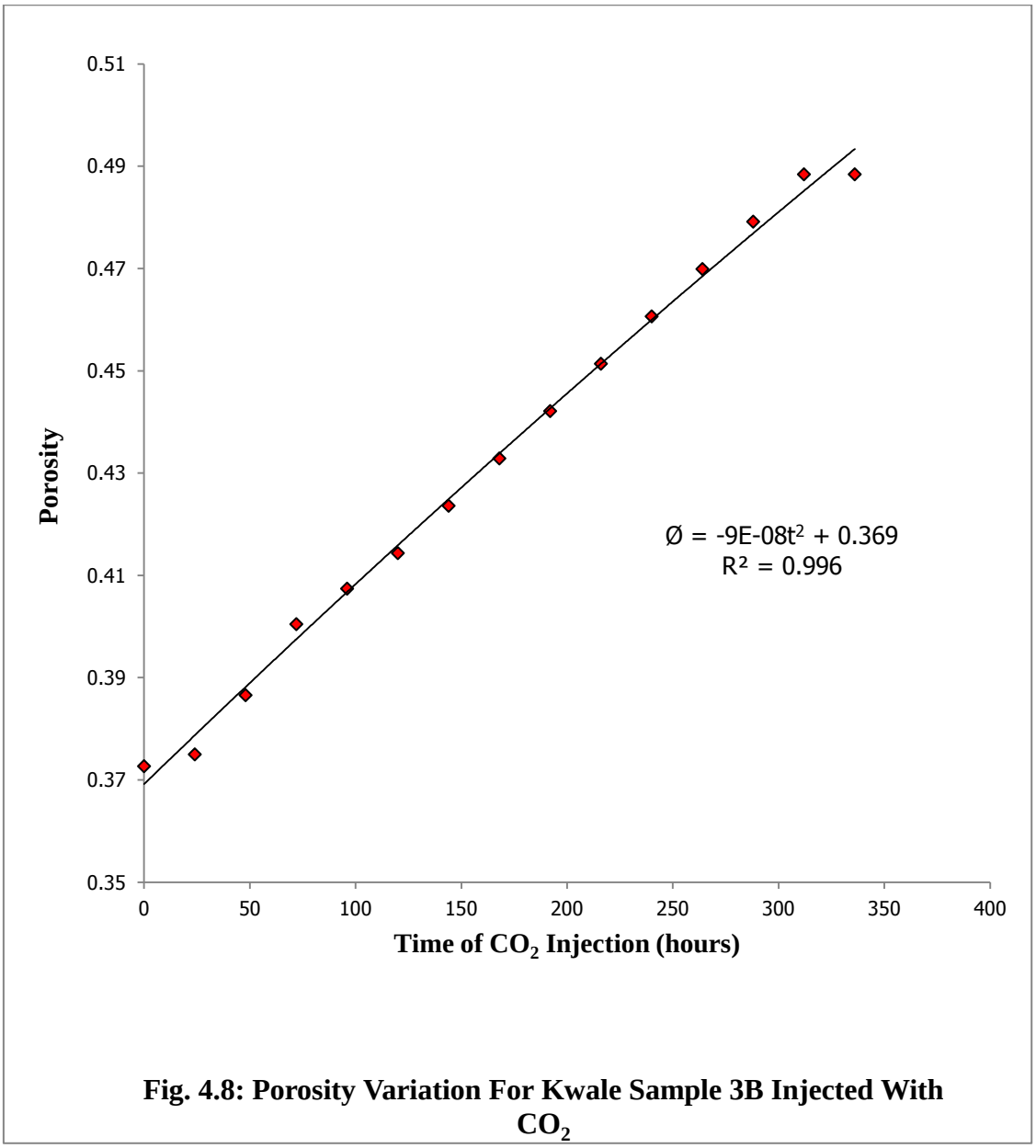

Fig. 4.8: Porosity Variation For Kwale Sample 3B Injected With CO_2

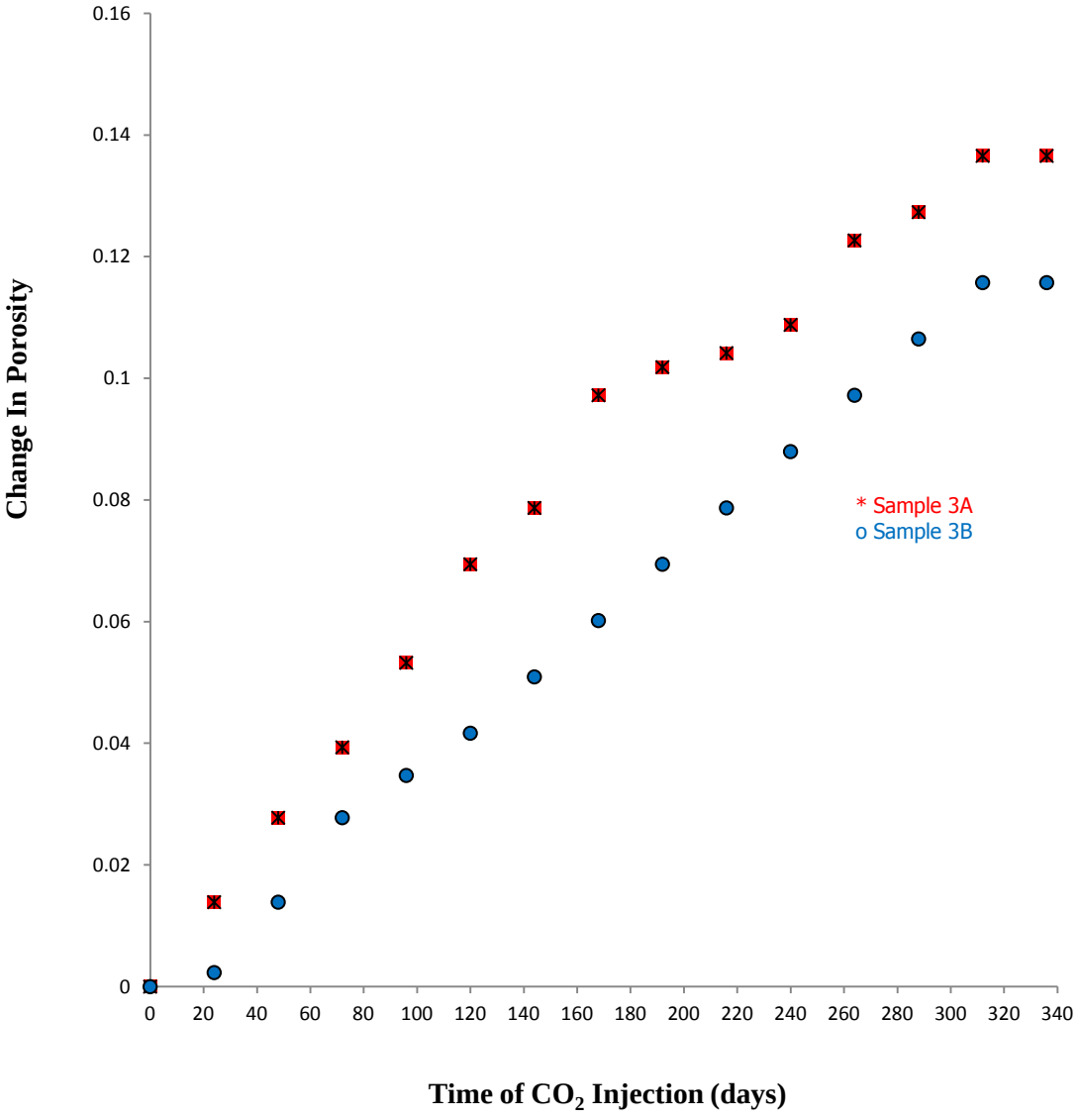

Fig. 4.9: Comparison of Porosity Variations For Dry Core Samples 3A & 3B Injected With CO_2

4.1.1.1.2. S_{wirr} Computation For Kwale Sandstones Samples

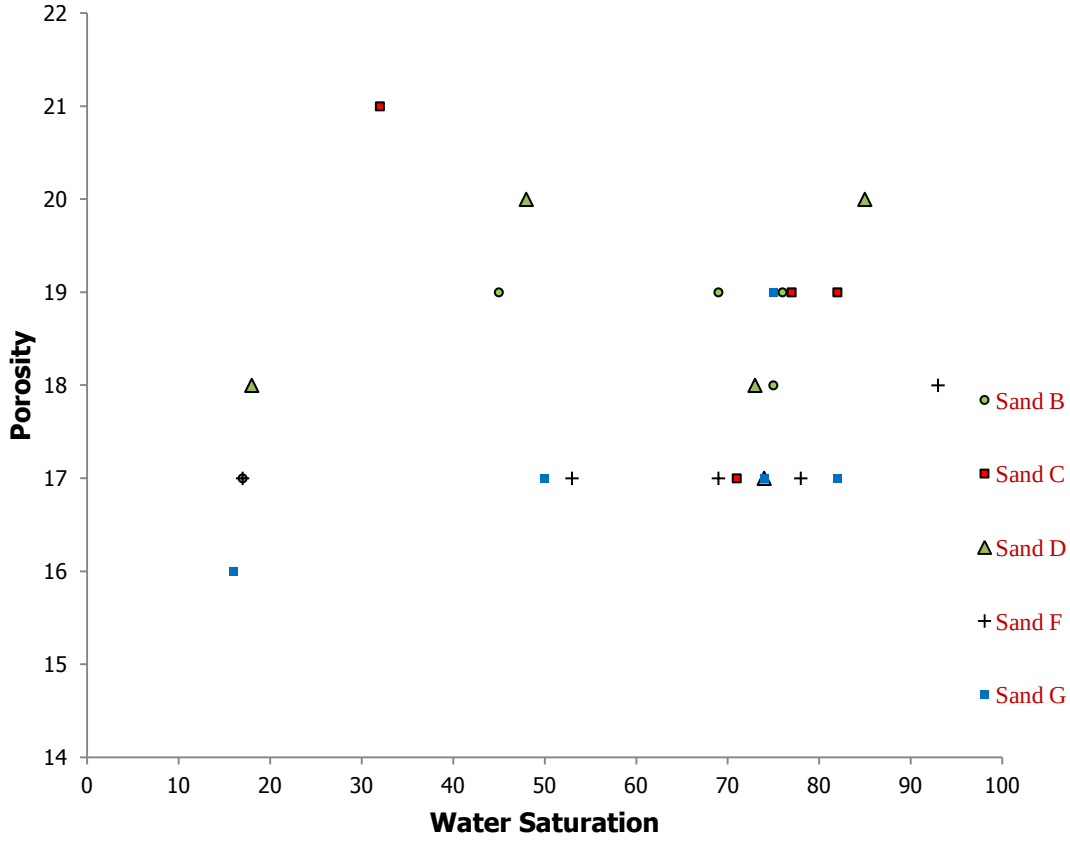

Fig. 4.10a. Porosity-Water Saturation For Kwale Sands

(Adapted from log analysis of Ekine and Iyabe, 2009).

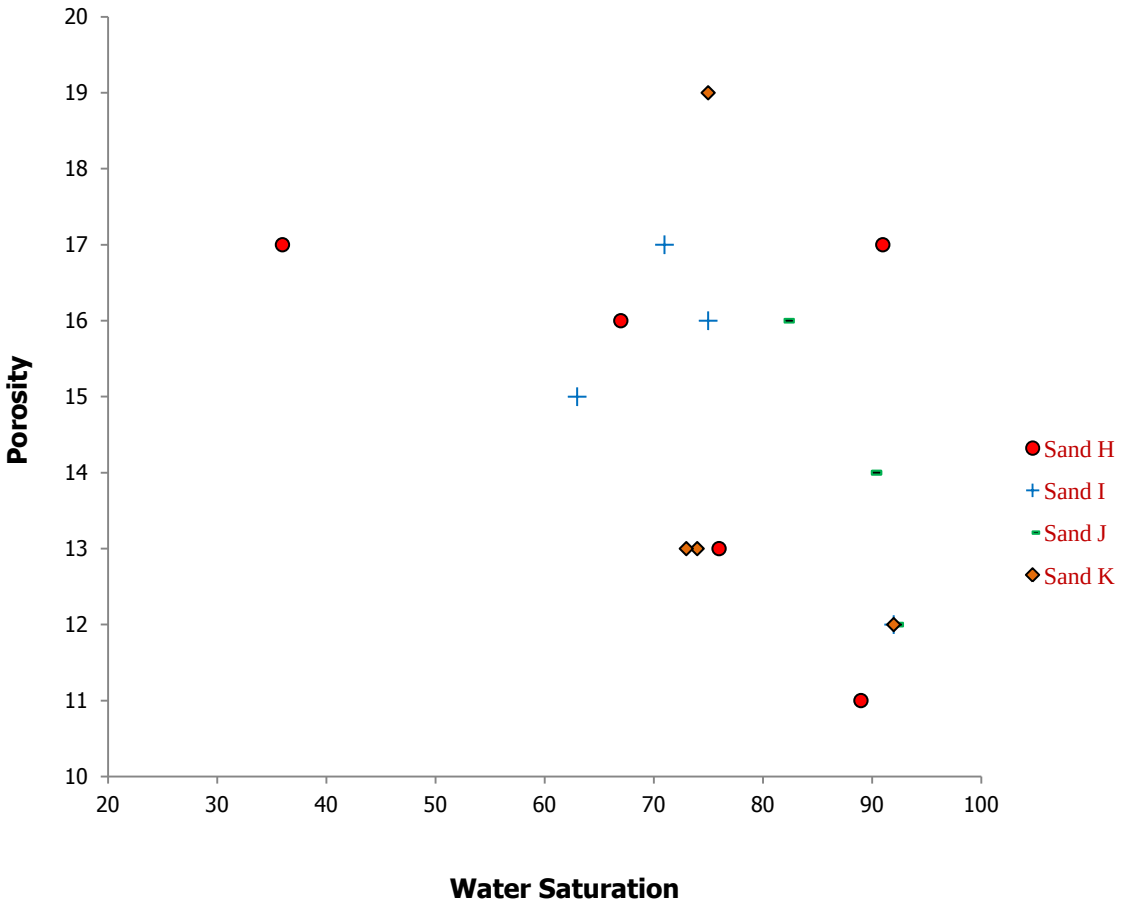

Fig. 4.10b. Porosity-Water Saturation For Kwale Sands H, I, J & K

The variation of the porosity as a function of water saturation for the various Kwale sands, in the absence of CO_2 injection, are plotted in fig. 4.10a and 4.10b. These porosity-water saturations data were employed for modelling the irreducible water saturation, using the Tixier, Timur, Coates & Dumanoir and Aigbedion models to determine the most appropriate model for the Kwale sand when there is neither CO_2 injection nor porosity variation.

As stated in Appendix B, the permeability-porosity relationship obtained graphically is mostly a polynomial in the porosity except for sands H and L. This prooves that the proposed model is right. Based on the available data, the Kwale reservoir sands A and C have average porosities closest to those of the Kwale sandstone samples porosities when compared with other reservoir sands (see Appendix B). Since reservoir C is more dominant than reservoir sand A from the data available, C is therefore used as the basis for the Kwale drill cuttings, and its average water saturation, porosity and permeability are therefore applied for modelling the permeabilities of the Kwale samples (1A-3B) with the Timur and the proposed models. From the plot of porosity versus water saturation for Kwale sand C, two best-fit curves and equations were obtained. For the exponential best fit $S_{wirr} = 10.80e^{-15.7Ø}$ was obtained with a root mean square value of 0.593; the polynomial fit gave $S_{wirr} = -4.465Ø^2 + 162.4Ø – 1409$ with a root mean square value of 0.997**.** Although the polynomial gave a better root mean square value, the S_{wirr} computation gave negative values. Moreover, the exponential fit is more appropriate since the irreducible water saturation value is expected to decrease when there is decreasing water saturation with the injected fluid. Hence, the exponential fit was adopted for the irreducible water saturation computation such that:

$$\mathbf{S_{wirr} = 10.80e^{-15.7Ø}} \qquad \text{.....4.1.}$$

for Kwale sand C. This was therefore applied in the proposed model.

The permeability function is:

$$\mathbf{K = C_1 * Ø^a * (1-S_{wirr})/S_{wirr}} \qquad \text{......4.2.}$$

Where Ø is the porosity

S_{wirr} = irreducible water saturation

K = permeability in milliDarcy (mD)

C_1 and a are constants

Stated in the next section is the results obtained for the calculated permeabilities for the Kwale sandstone core samples 1A, 1B, 2A, 2B, 3A and 3B using the Timur, Tixier, Aigbedion, Coates-Dumanoir models and the proposed permeability model (modified Timur/Coates-Dumanoir).

4.1.1.1.3. Permeability Variations With Kwale Sandstone Porosity Using Timur, Tixier, Coates-Dumanoir, Aigbedion and Proposed Permeability Models

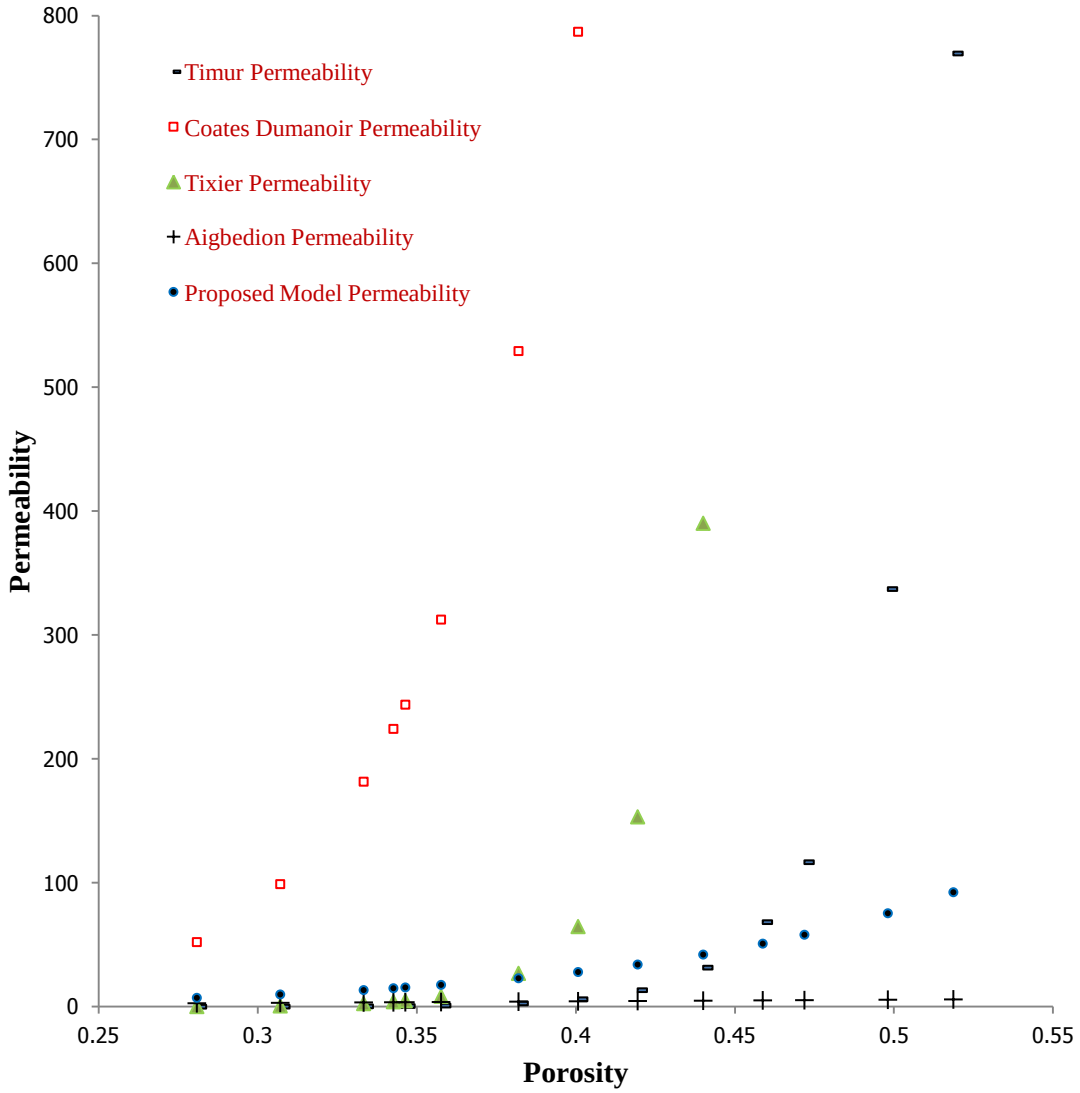

Fig. 4.11: Computed Permeability Values For Different Models and The Proposed Model for Kwale sandstone Sample 1A

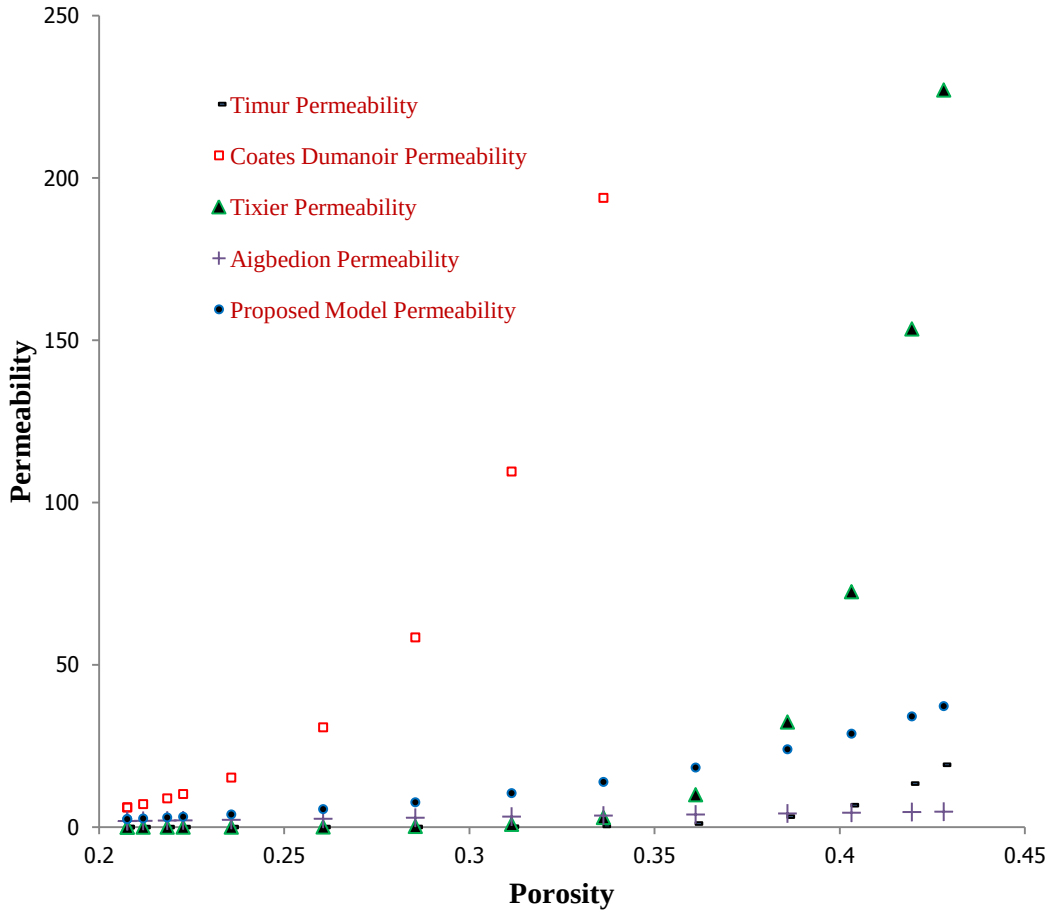

Fig. 4.12: Computed Permeability Values For Different Models and The Proposed Model for Kwale sandstone Sample 1B

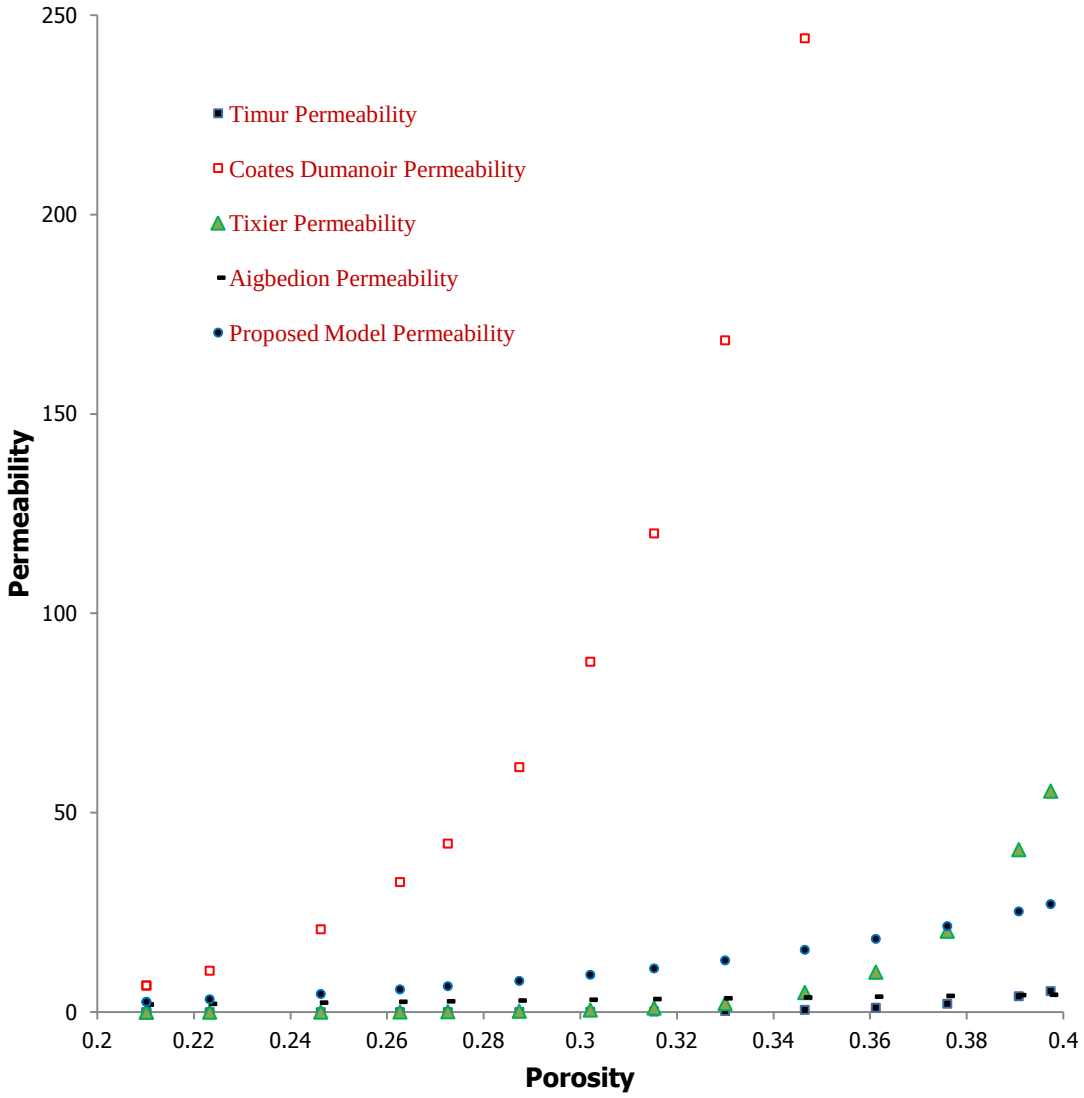

Fig. 4.13: Computed Permeability Values For Different Models and The Proposed Model for Kwale sandstone Sample 2A

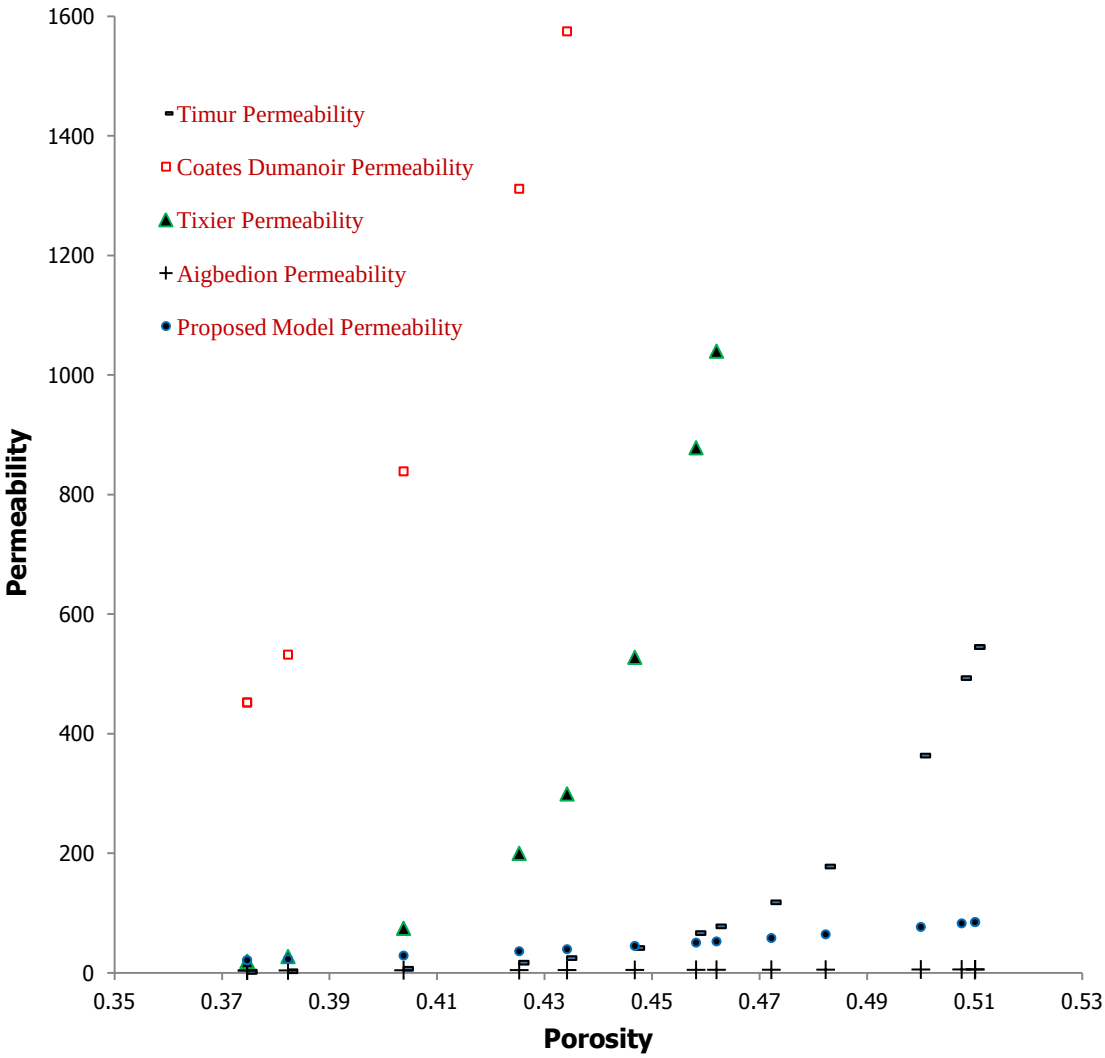

Fig. 4.14: Computed Permeability Values For Different Models and The Proposed Model for Kwale sandstone Sample 2B

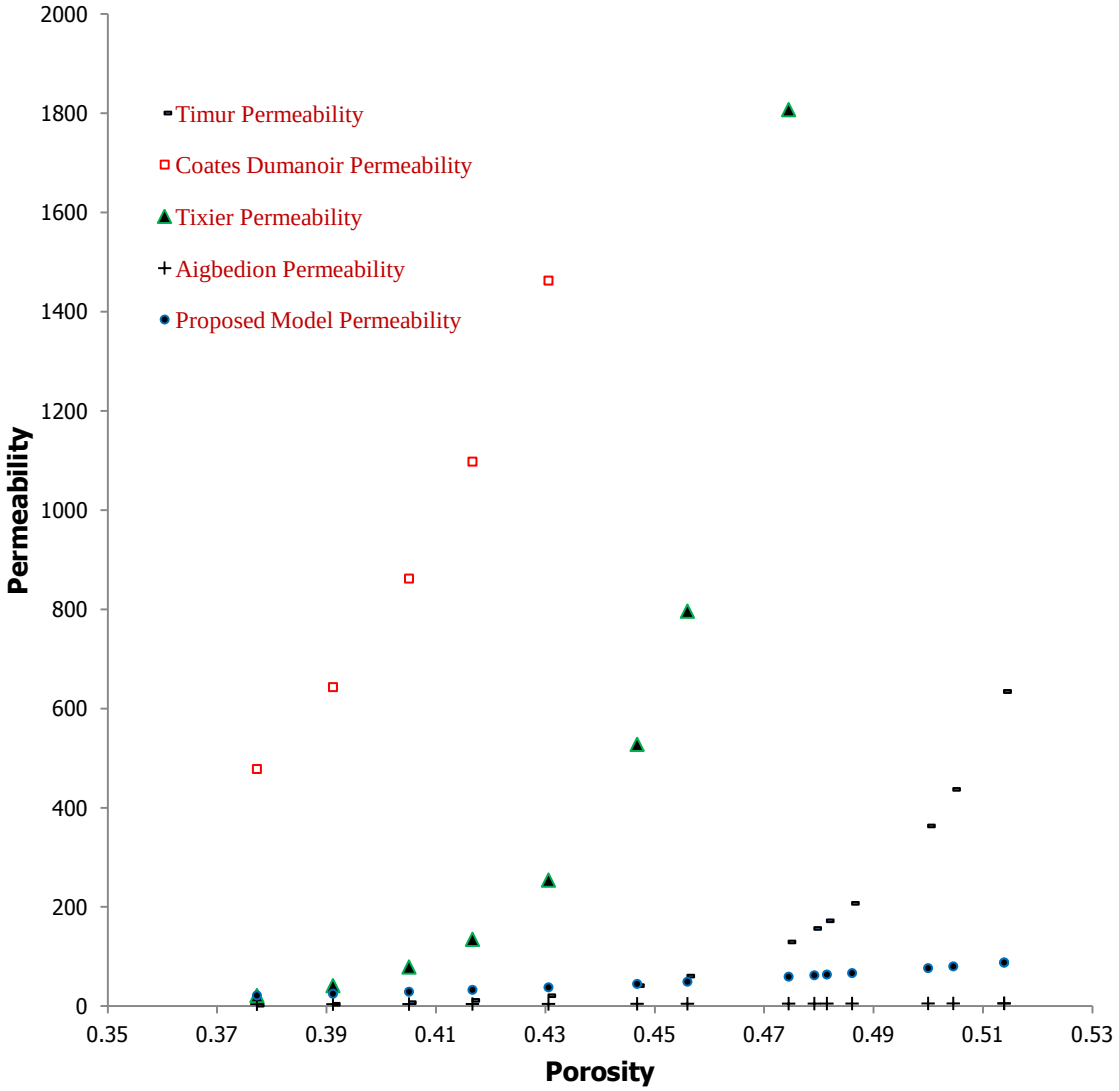

Fig. 4.15: Computed Permeability Values For Different Models and The Proposed Model for Kwale sandstone Sample 3A

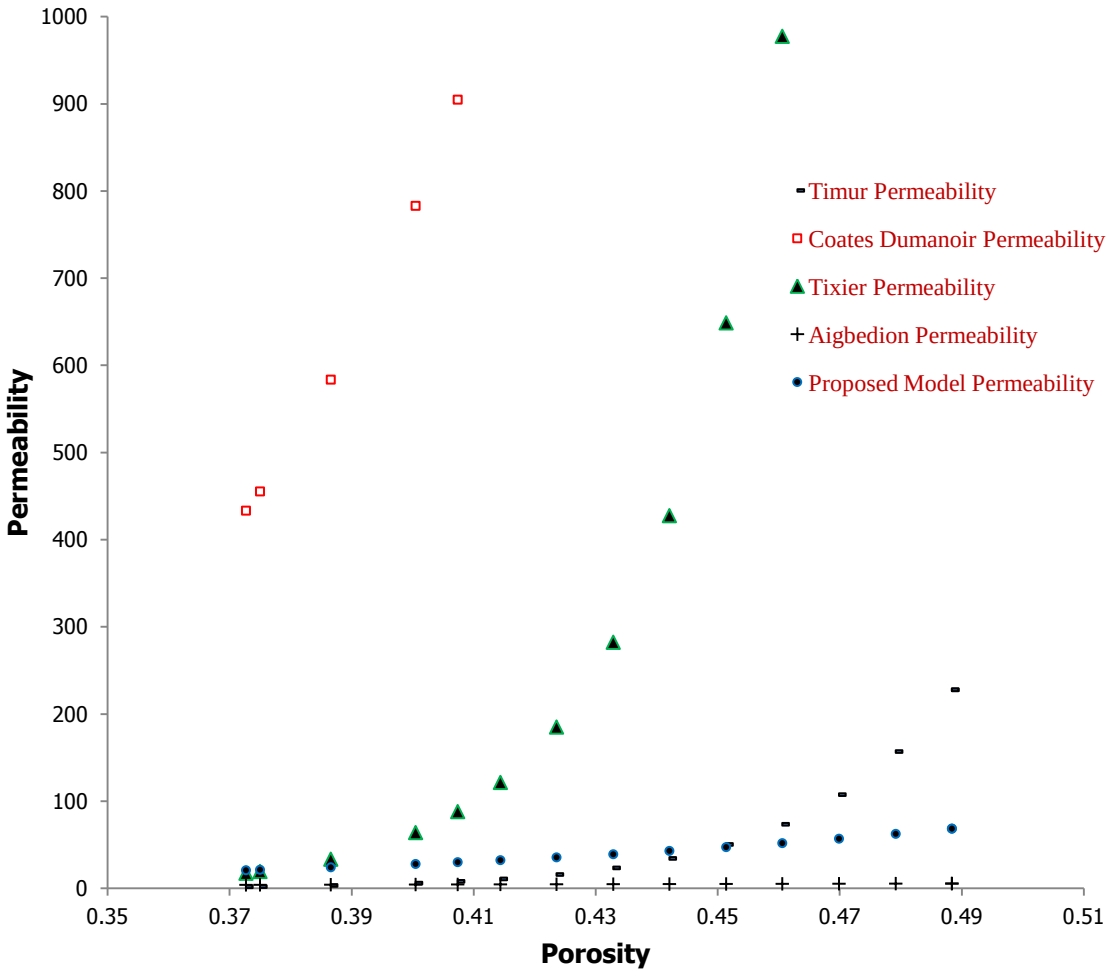

Fig. 4.16: Computed Permeability Values For Different Models and The Proposed Model for Kwale sandstone Sample 3B

4.1.1.1.4. Atomic Absorption Spectrometer (AAS) Analysis For Kwale Sandstones.

Below is the summary of the AAS analysis for the Kwale sandstone samples.

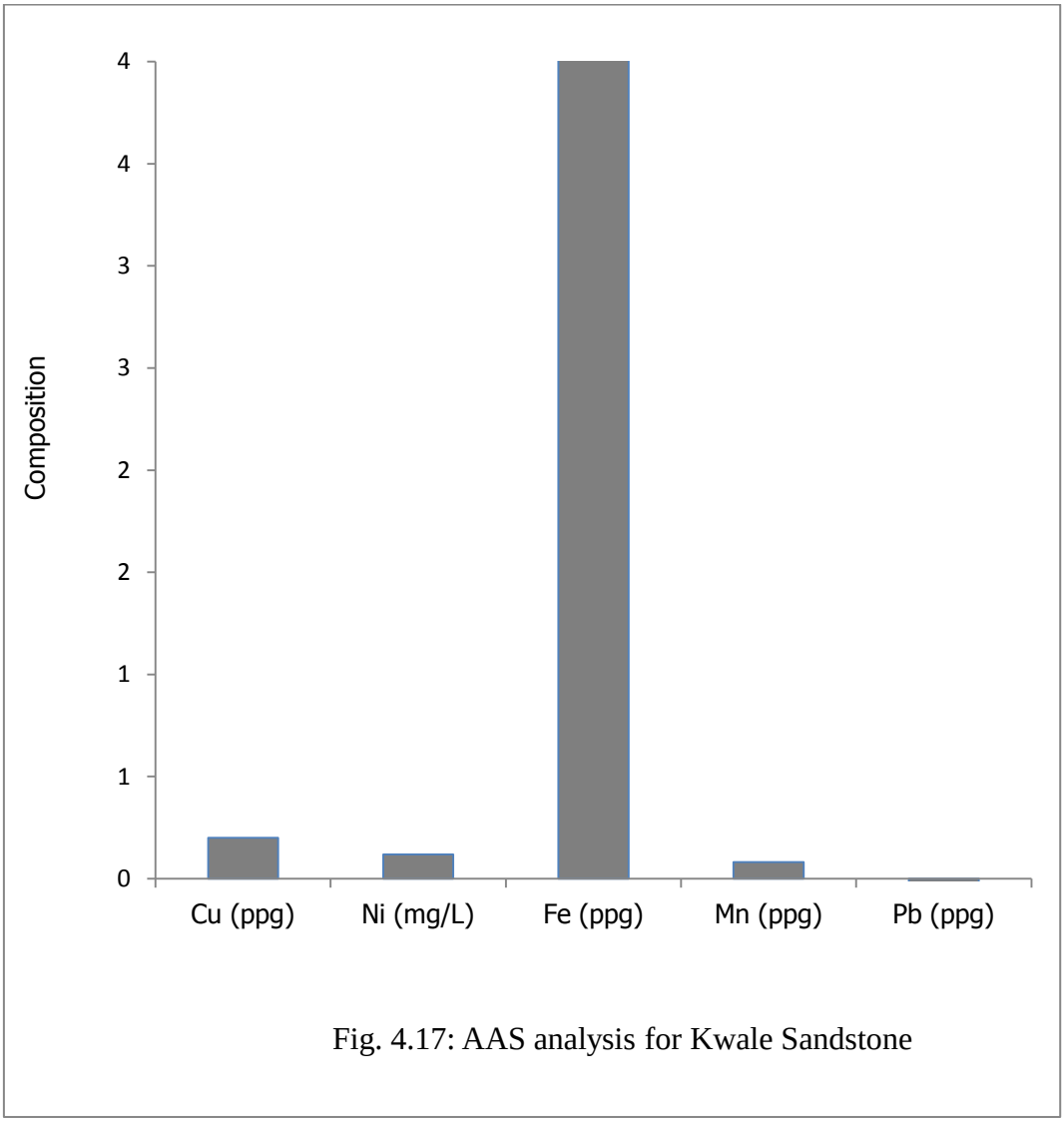

Fig. 4.17: AAS analysis for Kwale Sandstone

(measurements are in parts-per-million, ppm, while that of nickel is in mg/L)

Table 4.2: AAS data For Kwale Sandstone Sample.

	Composition	
	Measured Metal Content , %	Relative to Fe content
Cu	0.1997	0.0235
Ni	0.1191	0.0140
Fe	8.4879	1.0000
Mn	0.0821	0.0097
Pb	-0.1228	-0.0145

4.1.1.2. Experimental Result for The Change In Physical Properties of Kwale Pure Shale Sample Injected With CO_2

The measured porosity values as CO_2 injection increases for the black shale sample is shown graphically in fig.4.18 while the values are as tabulated in Table C.7.

4.1.1.2.1. Kwale Black Shale As Candidate CO_2 Storage Reservoir

4.1.1.2.1.1. Porosity Variation For Kwale Black Shales With CO_2 Injection.

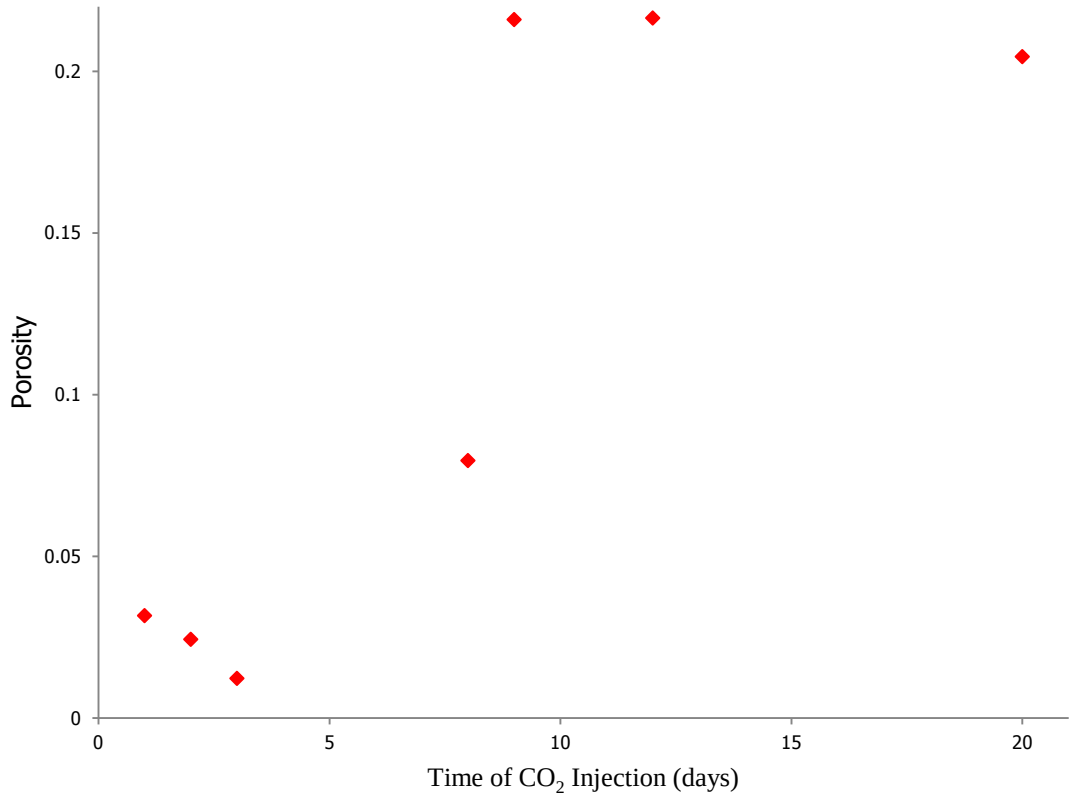

Fig. 4.18: Porosity Variation For Black Shale With Time of Injection

Table 4.3. Best Fit Porosity-Time Analysis For Kwale Black Shale Sample

Time (hrs)	Corrected Porosity	Polynomial best fit		Log. best fit		Exponential best fit	
			Error		Error		Error
1	0.031667	0.0315	0.00017	-0.077	0.10867	0.03081	0.00086
2	0.024346	0.0235	0.00085	-0.0250	0.04936	0.03461	-0.01026
3	0.012265	0.0255	-0.01324	0.0024	0.00987	0.03898	-0.02672
8	0.079629	0.1855	-0.10587	0.14296	-0.0633	0.07293	0.00670
9	0.216002	0.2475	-0.0315	0.15179	0.06421	0.08306	0.13294
12	0.216482	0.4935	-0.27702	0.17337	0.04311	0.12354	0.09294
20	0.204533	1.5895	-1.38497	0.21168	-0.0072	0.36728	-0.16275
Total Error			-1.81158		0.20474		0.03372

Three best fits were obtained at three different time periods and were therefore used for those periods to obtain average porosity equations.

4.1.1.2.1.2. S_{wirr} Variation For Kwale Black Shales With CO_2 Injection.

The calculated irreducible water saturation for the Kwale black shale is as shown in Fig. 4.19.

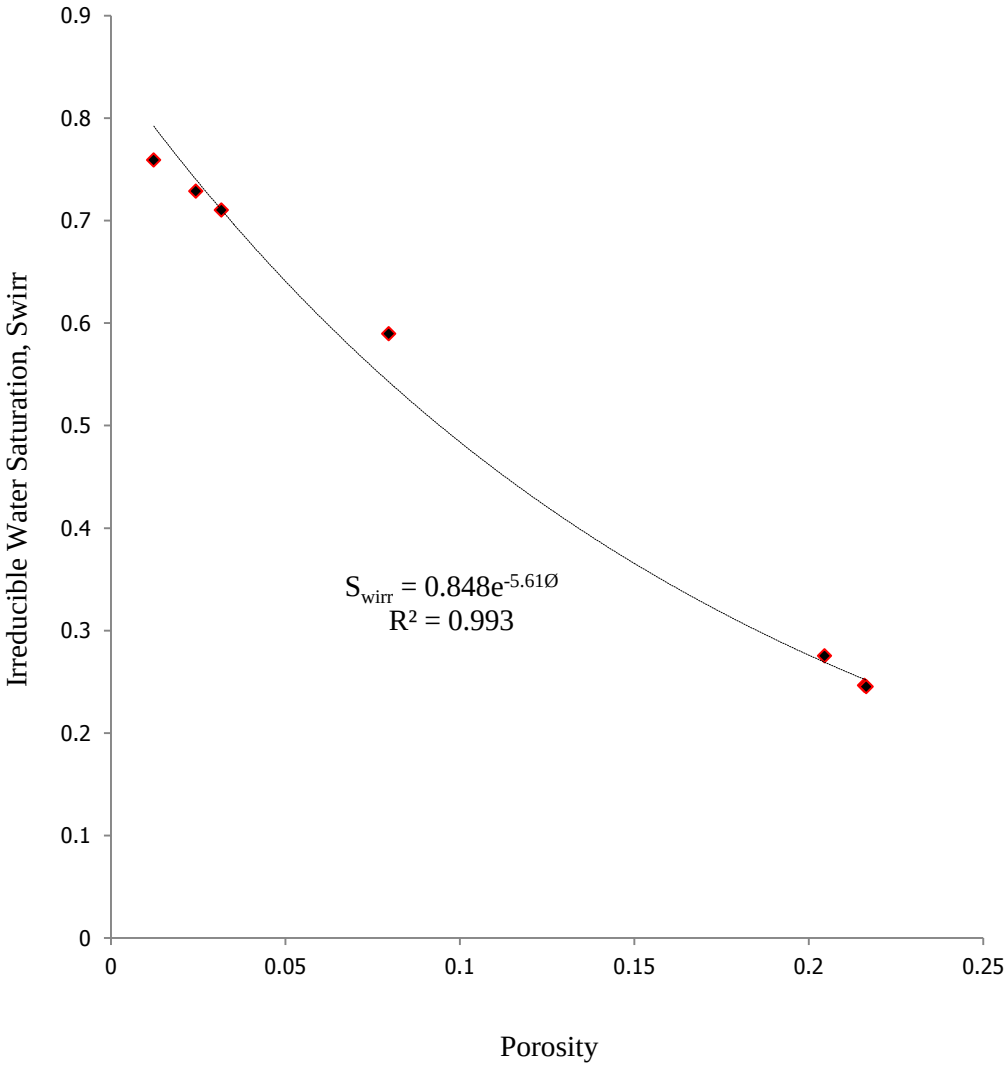

Fig. 4.19: Irreducible water Saturation For Kwale Black Shale

4.1.1.2.1.3. Permeability Computation For Kwale Black Shales With CO_2 Injection.

The calculated permeabilities for the Kwale black shale samples

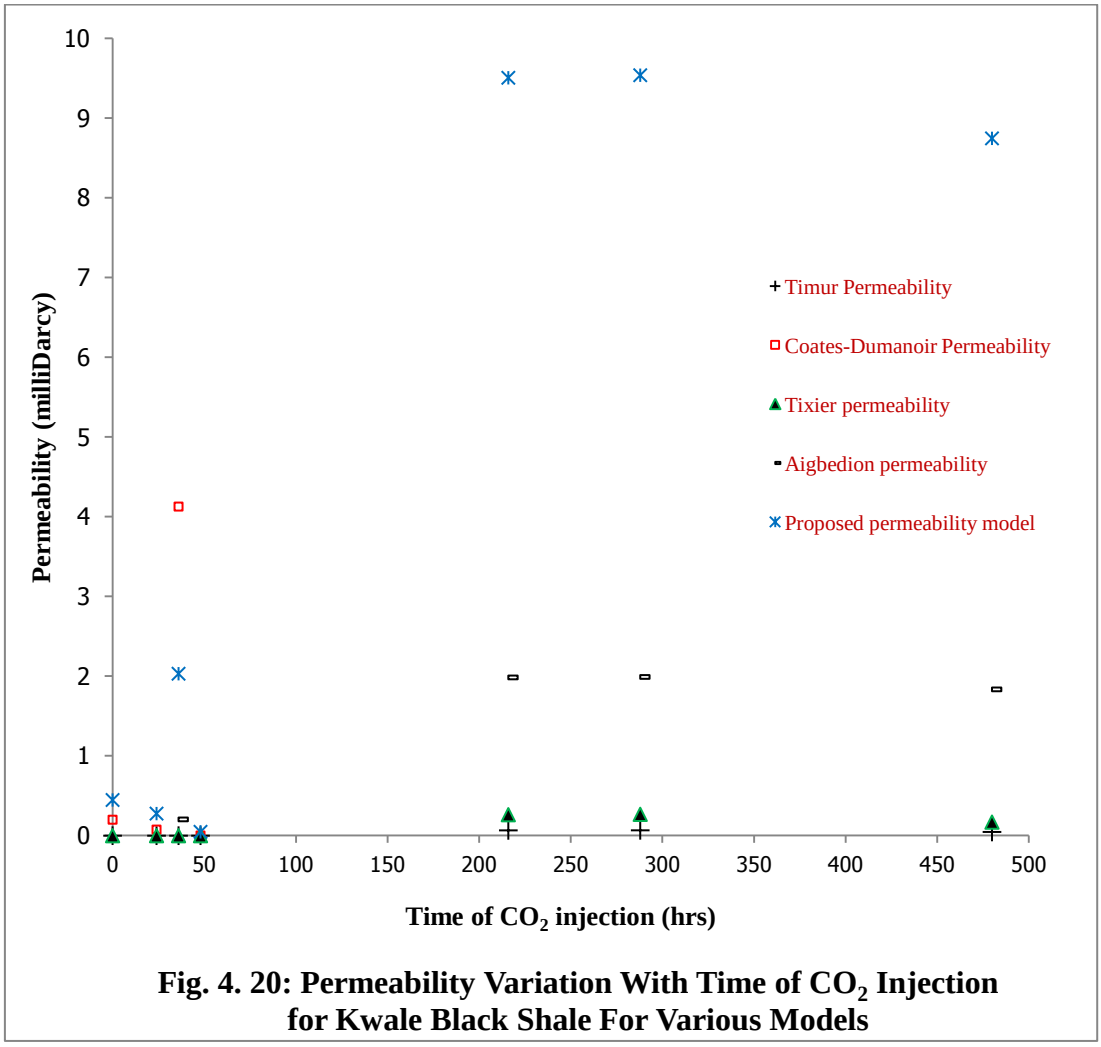

Fig. 4. 20: Permeability Variation With Time of CO_2 Injection for Kwale Black Shale For Various Models

4.1.1.2.1.4. AAS Analysis For Kwale Black Shale Sample

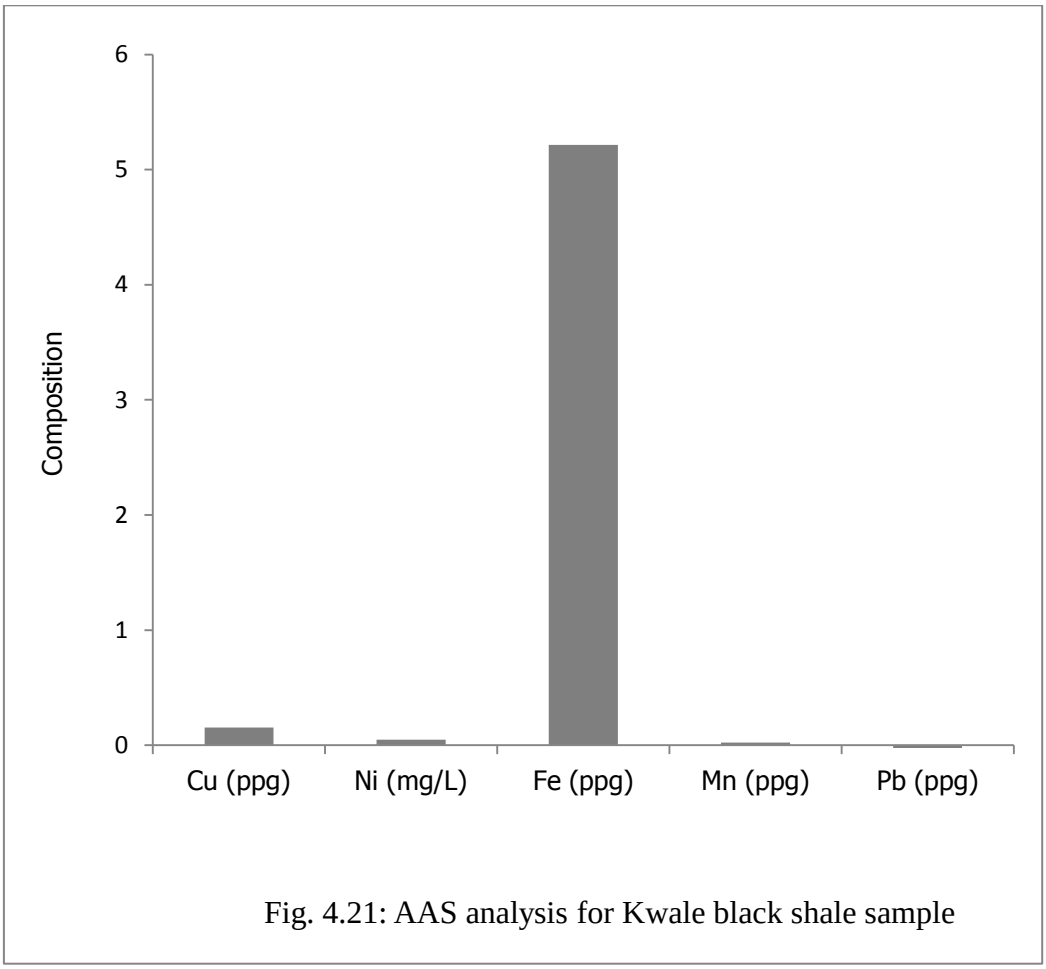

Fig. 4.21: AAS analysis for Kwale black shale sample

Table 4.3: AAS Analysis For Kwale Black Shale sample

	Composition	
	Measured content, %	Relative to Fe content
Cu	0.1536	0.0295
Ni	0.0467	0.0090
Fe	5.2145	1.0000
Mn	0.0237	0.0045
Pb	-0.0791	-0.0152

4.1.1.2.2. Kwale Grey Shale As Candidate CO_2 Storage Reservoir

4.1.1.2.2.1. Kwale Grey Shale Porosity Variation With CO_2 Injection

Measured Porosity For Grey Kwale Shale is presented in fig.4.24.

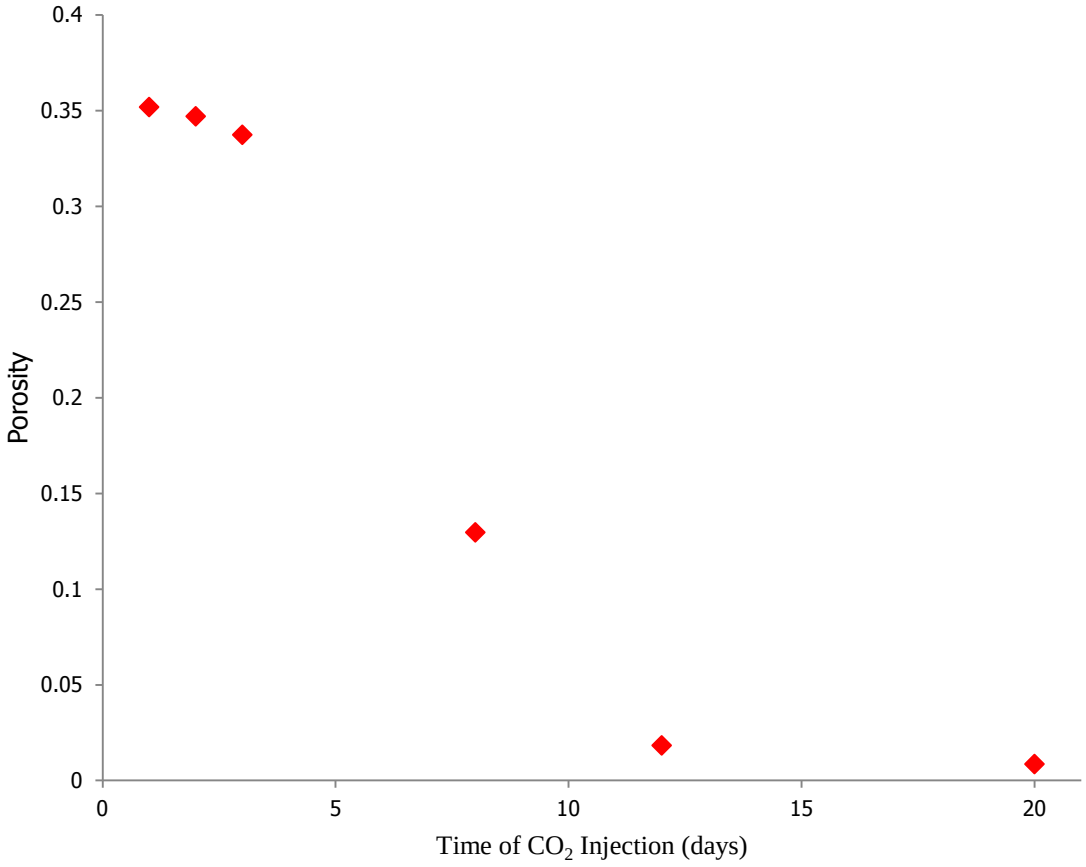

Fig. 4.22: Porosity Variation For Grey Shale With Time of Injection

Table.4.4: Porosity Best Fit Curve Analysis For Kwale Grey Shale Sample

Time (days)	Porosity	Polynomial best fit		Log. best fit		Exponential best fit	
			Error		Error		Error
1	0.35186	0.365	-0.01314	0.395	-0.0431	0.41705	-0.0652
2	0.34703	0.348	-0.00097	0.28603	0.06100	0.33805	0.00898
3	0.33737	0.325	0.01237	0.22521	0.11216	0.27402	0.06335
8	0.129645	0.12	0.009645	0.07808	0.05156	0.09589	0.03376
12	0.01834	-0.152	0.17034	0.0173	0.0011	0.0414	-0.0231
20	0.0086	-0.984	0.9926	-0.0594	0.068	0.0077	0.0009
Total error			1.17085		0.2506		0.0187

From the Table 4.4, the Polynomial, logarithm and exponential fits gave the best fits at different periods and the porosity equation was then based on these in order to obtain the average porosity that was used in the modeling of the permeability. The porosity–time variation for the grey shale is therefore as stated below.

4.1.1.2.2.2. S_{WIRR} FOR KWALE SHALE SAMPLE

The drying rate calculation for the measured water loss with time is as stated in Table 4.5 for grey shale.

Table 4.5: S_{wirr} Determination For Grey Kwale Shale By Drying Rate Method

Time (mins)	Grey shale 1 Weigth (g)	water loss (g)	drying rate (g/min)	Sw
0	1.85	0	0	1
40	1.8	0.05	0.00125	0.8
60	1.8	0.05	0.00125	0.8
70	1.75	0.1	0.00143	0.6
75	1.7	0.15	0.002	0.4
90	1.7	0.15	0.00167	0.4
150	1.6	0.25	0.00167	0

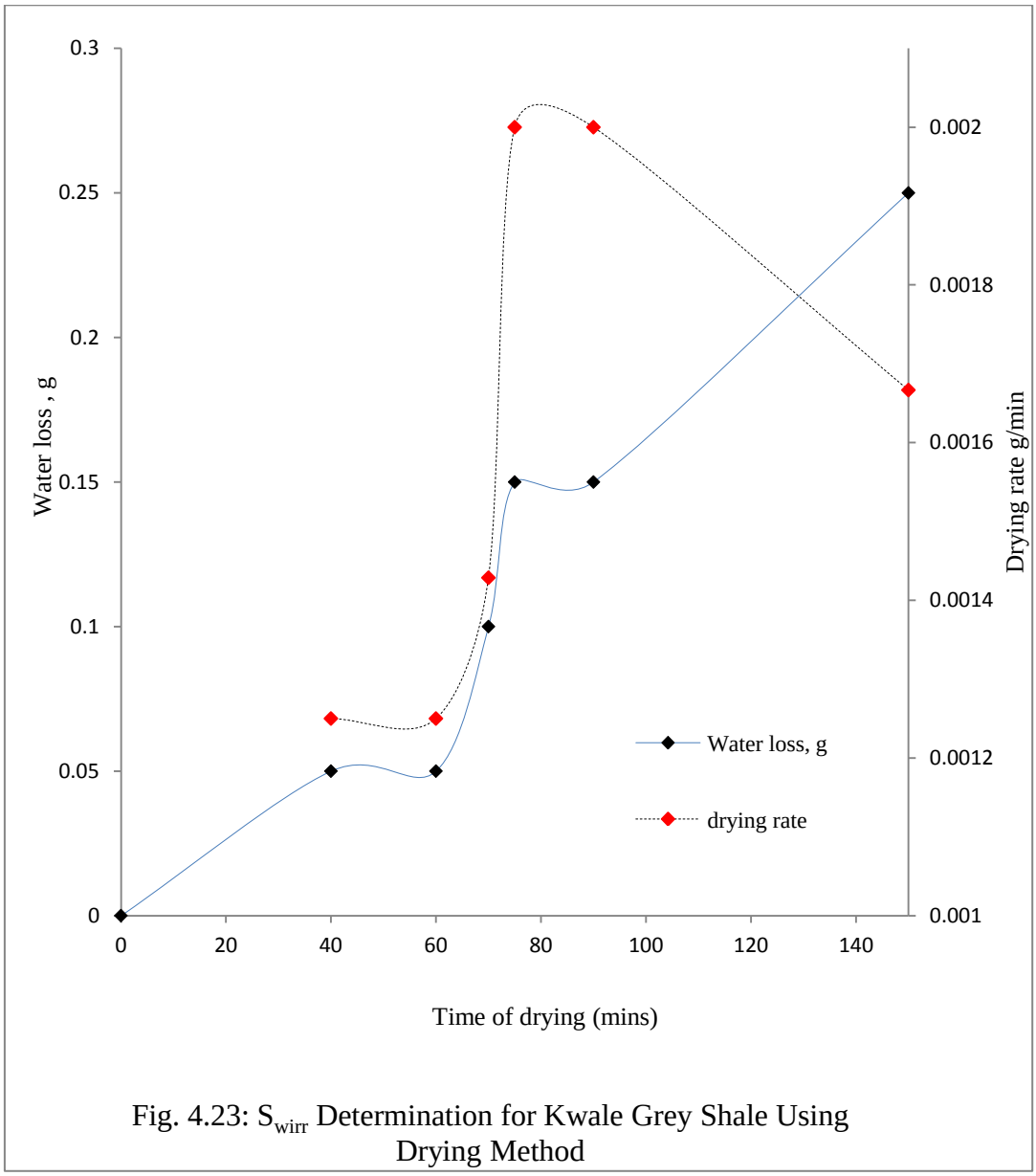

Fig. 4.23: S_{wirr} Determination for Kwale Grey Shale Using Drying Method

Table 4.5.1: S_{wirr} Determination of Kwale Grey Shale Using Automatic Centrifuge Method

Weight Grey shale 2 (g)	water loss (g)	Sw
2.7	0	1
2.6	0.1	0.66667
2.5	0.2	0.33333
Oven dry		
2.4	0.3	0

Table 4.5.2: S_{wirr} Determination of Kwale Grey Shale Using Manual Centrifuge Method

Weight Grey shale 2 (g)	**water loss (g)**	**Sw**
2.4	0	1
2.2	0.2	0.333333
Oven dry		
2.1	0.3	0

4.1.1.2.2.3. Permeability Computation For Kwale Black Shale

The obtained results for the calculated permeabilities for the Kwale grey shale sample using different together with the proposed permeability model.

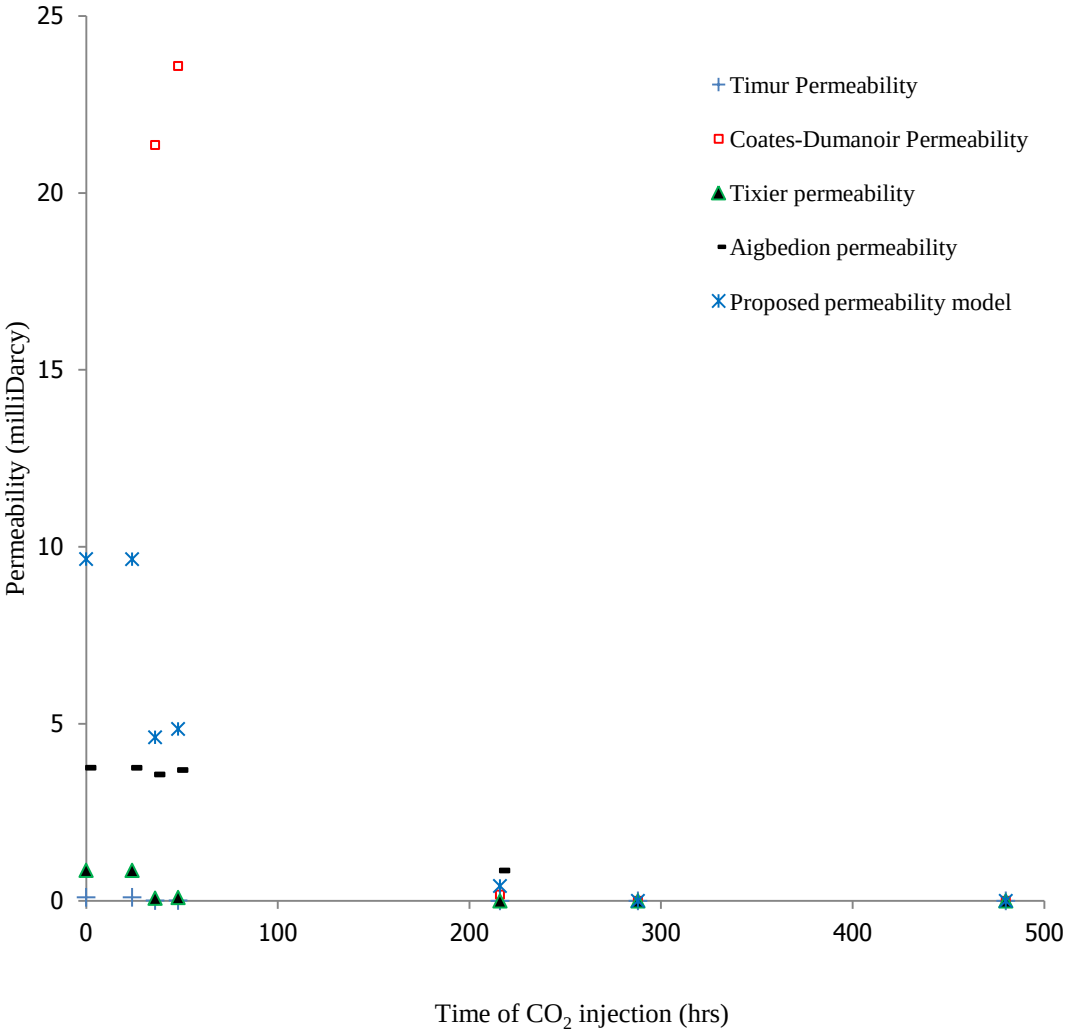

Fig. 4.24: Permeability Variation With Time of CO_2 Injection for Grey Shale For Various Models

4.1.1.2.2.4. AAS Analysis For Kwale Grey shale Sample

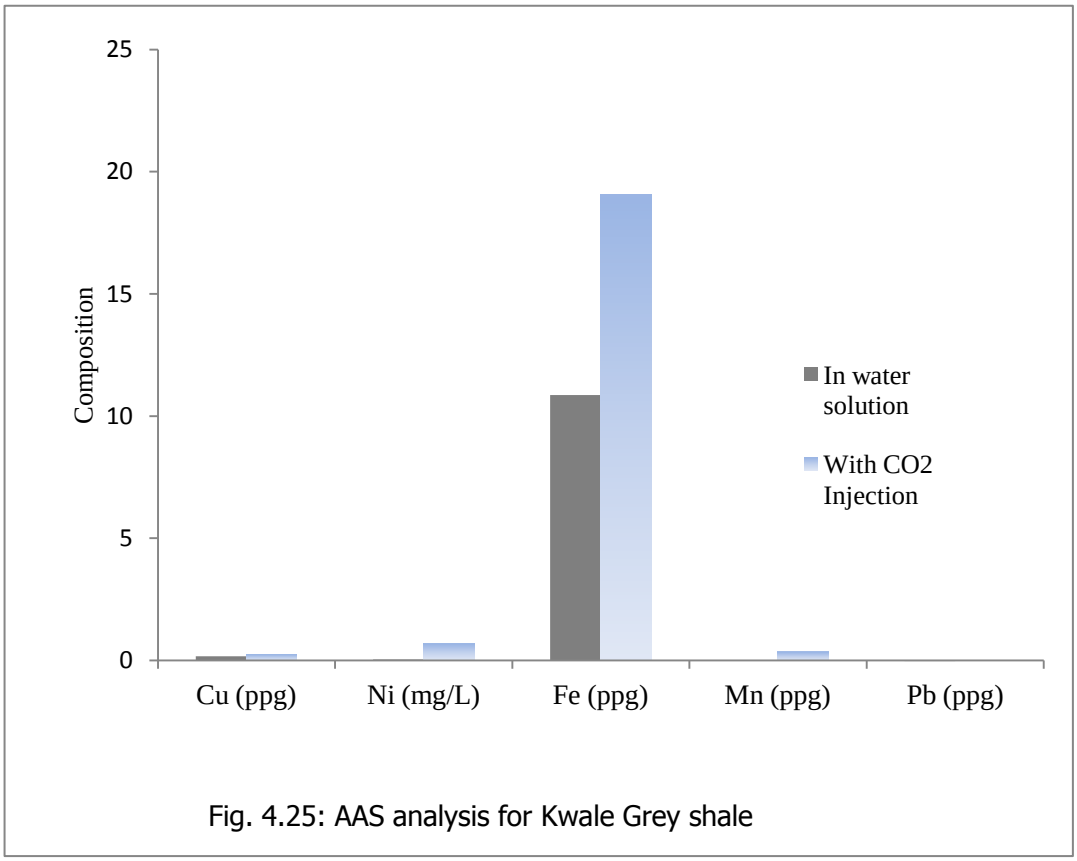

Fig. 4.25: AAS analysis for Kwale Grey shale

(Measurements are in parts-per-million, ppm, Nickel in mg/L.)

Table 4.6: AAS Analysis For Kwale Grey Shale Sample

	In water Solution		In CO_2-water solution	
	Measured content, %	Relative to Fe content	Measured content, %	Relative to Fe content
Cu (ppg)	0.1697	0.0156	0.2576	0.0135
Ni (mg/L)	0.0413	0.0038	0.6972	0.0366
Fe (ppg)	10.8544	1.0000	19.0681	1.0000
Mn (ppg)	0.0083	0.0008	0.3594	0.0188
Pb (ppg)	-0.0220	-0.0020	0.0024	0.0001

4.1.3.1. Ota Kaolinitic Clay As CO_2 Candidate Reservoir

4.1.3.1.1. Experimental Result for The Change In Physical Properties of Ota Kaolinitic Clay Injected With CO_2

Measured porosity For Ota Kaolinitic Clay is shown in fig.4.28.

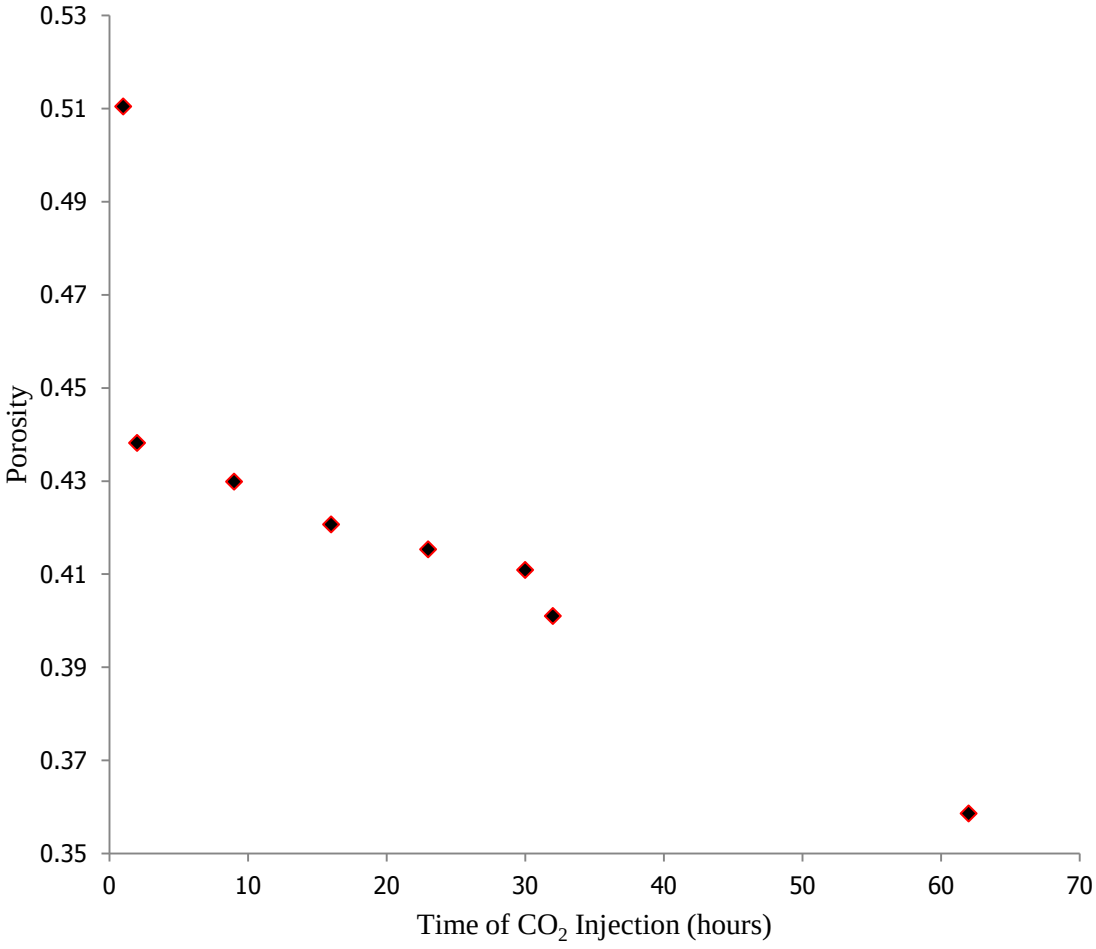

Fig. 4.26: Porosity Variation for Ota kaolinitic Clay With Time of Injection

Table 4.7: Porosity-Time Best Fit for Ota Kaolinitic Clay During CO_2 Injection.

Time (days)	Porosity	Polynomial fit		Log fit	
			Error		Error
1	0.5104546	0.487998	0.02245656	0.482	0.028455
2	0.4381905	0.480992	-0.0428015	0.468206	-0.03002
9	0.4298737	0.431838	-0.0019643	0.438275	-0.0084
16	0.4206833	0.382488	0.03819526	0.426825	-0.00614
23	0.4153322	0.332942	0.08239017	0.419604	-0.00427
30	0.4109009	0.2832	0.12770087	0.414316	-0.00342
32	0.4010112	0.268952	0.13205924	0.413032	-0.01202
62	0.3585959	0.053312	0.30528392	0.39987	-0.04127
Total error			0.66332024		-0.07709

From the above table, among the best two fits, Logarithm fit gave the better result with the lowest error but the two were employed at different time periods to obtain the porosity-time relationship.

4.1.3.1.2. S_{wirr} For Ota Kaolinitic Clay Sample

Two samples 1 and 2 were used in order to investigate the effect of the size of the sample on the irreducible water saturation measurement.

Table 4.8: S_{wirr} Determination For Kaolin 1 By Drying Rate Method

Time (mins)	Kaolin 1 Weigth (g)	water loss (g)	Drying rate (g/min)	S_w
0	24.6	0	0	1
30	24.3	0.3	0.01	0.85
40	23.9	0.7	0.0175	0.65
60	23.7	0.9	0.015	0.55
70	23.65	0.95	0.01357	0.525
75	23.6	1	0.01333	0.5
90	23.4	1.2	0.01333	0.4
150	22.6	2	0.01333	0

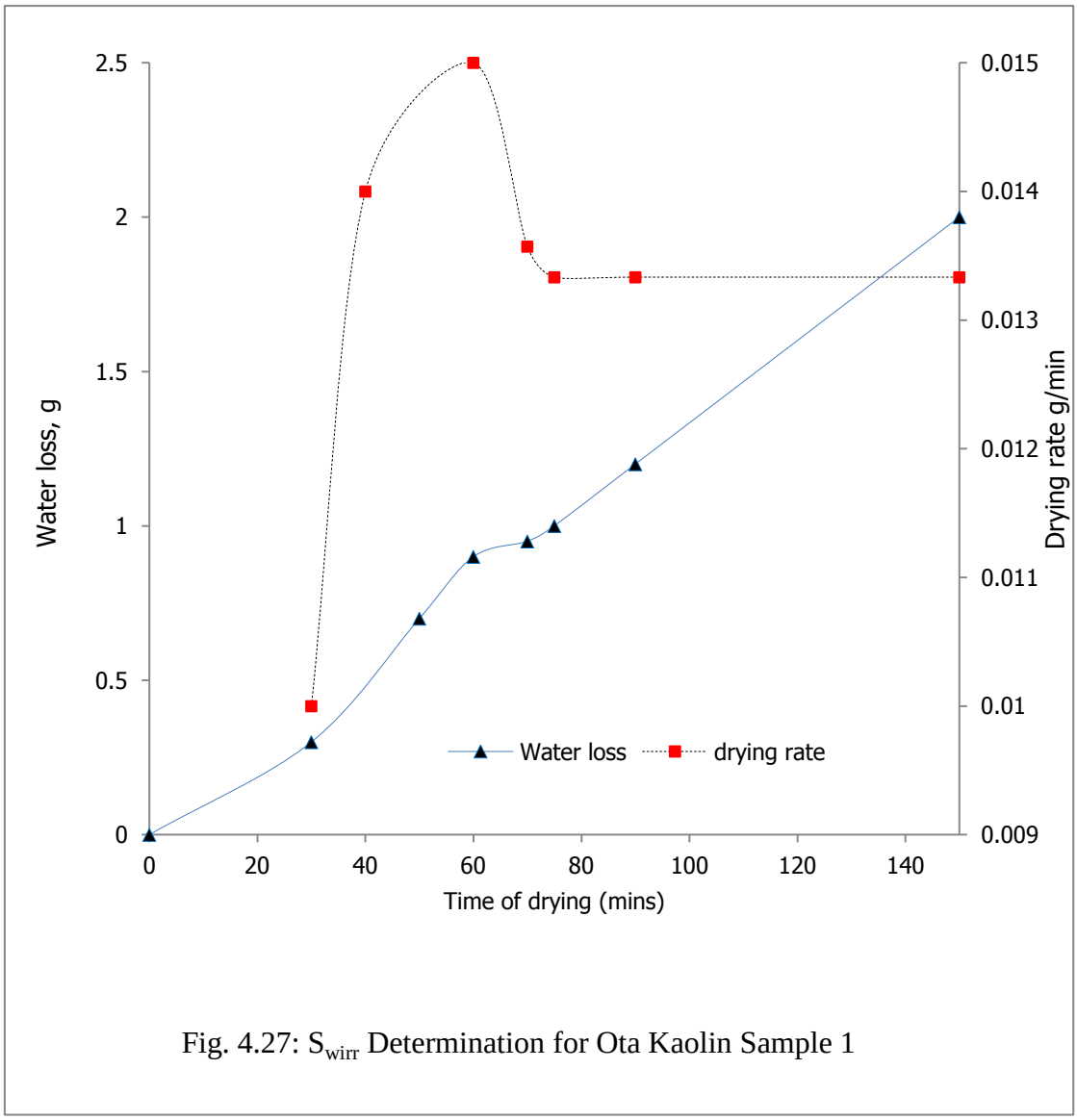

Fig. 4.27: S_{wirr} Determination for Ota Kaolin Sample 1

Table 4.9: S_{wirr} Determination For Kaolin 2 By Drying Rate Method

Time (mins)	Kaolin 2 Weight (g)	water loss (g)	drying rate (g/min)	S_w
0	12.2	0	0	1
30	12	0.2	0.00667	0.8
40	11.8	0.4	0.01	0.6
60	11.7	0.5	0.00833	0.5
70	11.7	0.5	0.00714	0.5
75	11.7	0.5	0.00667	0.5
90	11.6	0.6	0.00667	0.4
150	11.2	1	0.00667	0

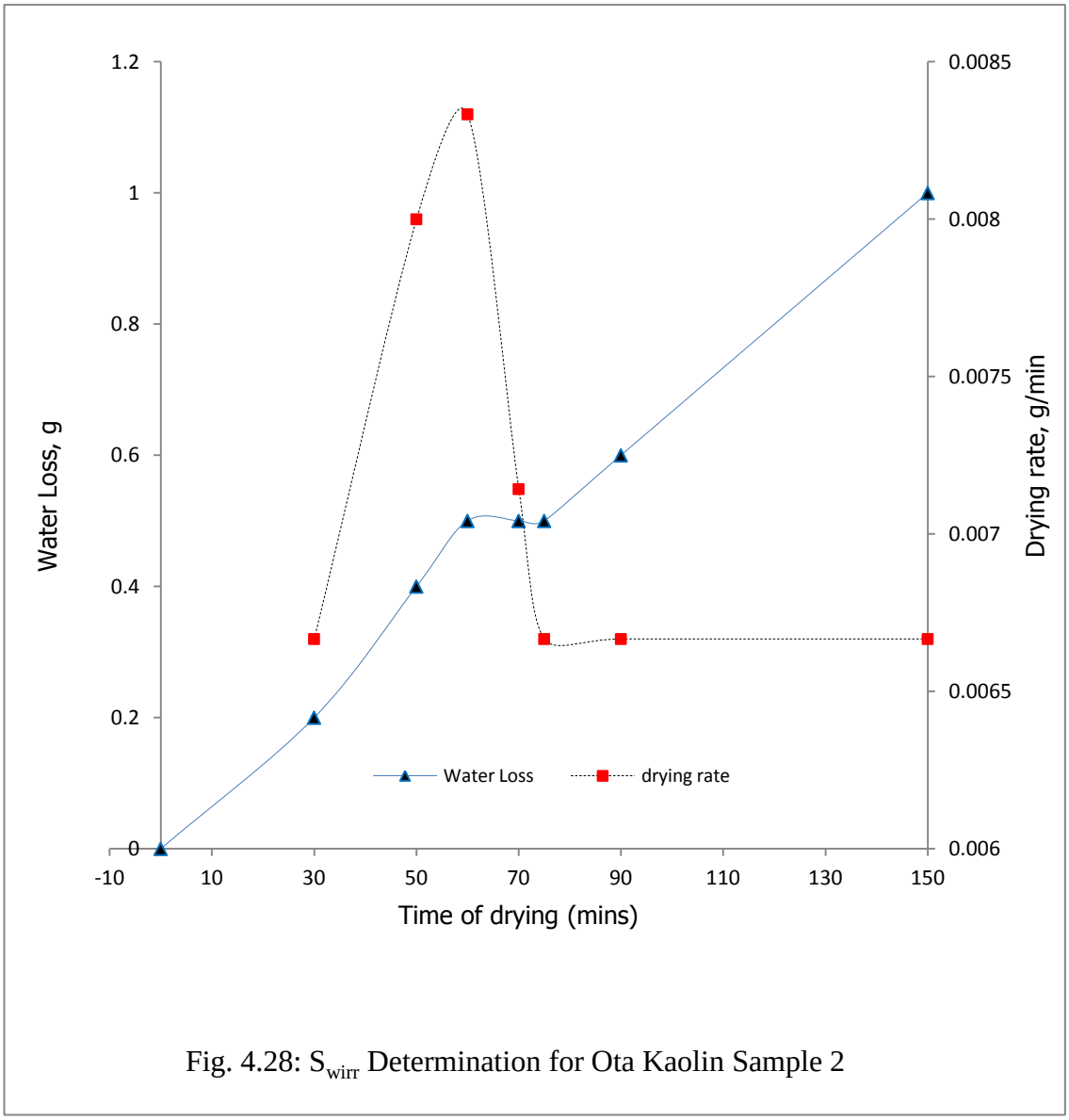

Fig. 4.28: S_{wirr} Determination for Ota Kaolin Sample 2

4.1.3.1.3. Permeability Analysis For Ota Kaolinitic Clay Sample

The obtained result for the calculated permeabilities for the Ota Kaolinitic samples using the Timur's, Tixier and Coates-Dumanior models and the proposed permeability model (modified Coates-Dumanoir) at various irreducible water saturations are as shown in figs.4.31.

Ota Kaolinitic Clay is expected to have varying properties because of locality influence that may affect the initial water saturation, but the S_{wirr} and the permeability are expected to be very similar when the clay composition is very close to one another.

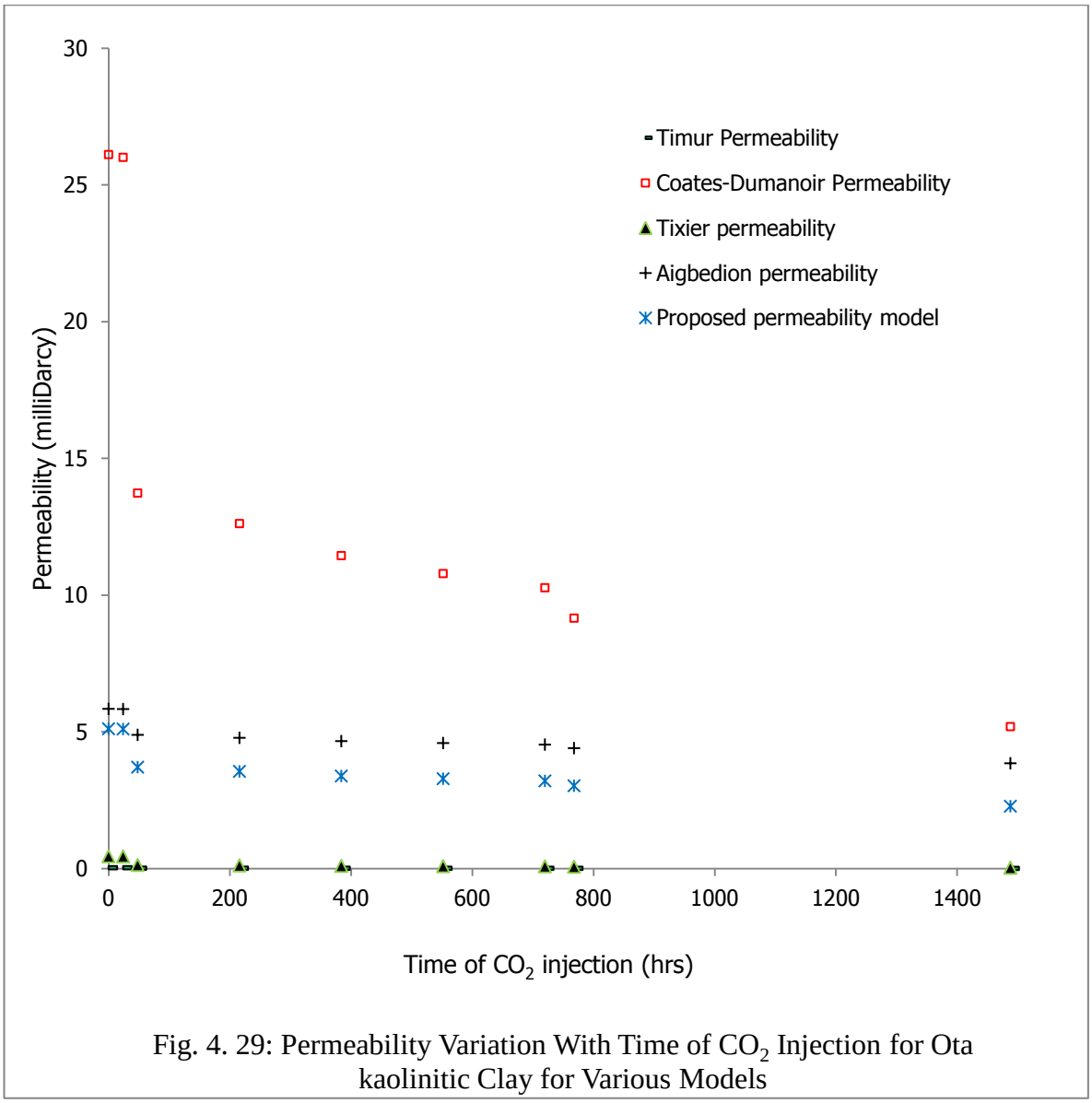

Fig. 4. 29: Permeability Variation With Time of CO_2 Injection for Ota kaolinitic Clay for Various Models

4.1.3.1.4. AAS Analysis For Ota Kaolinitic Clay Sample

Below is the summary of the AAS analysis for the various samples.

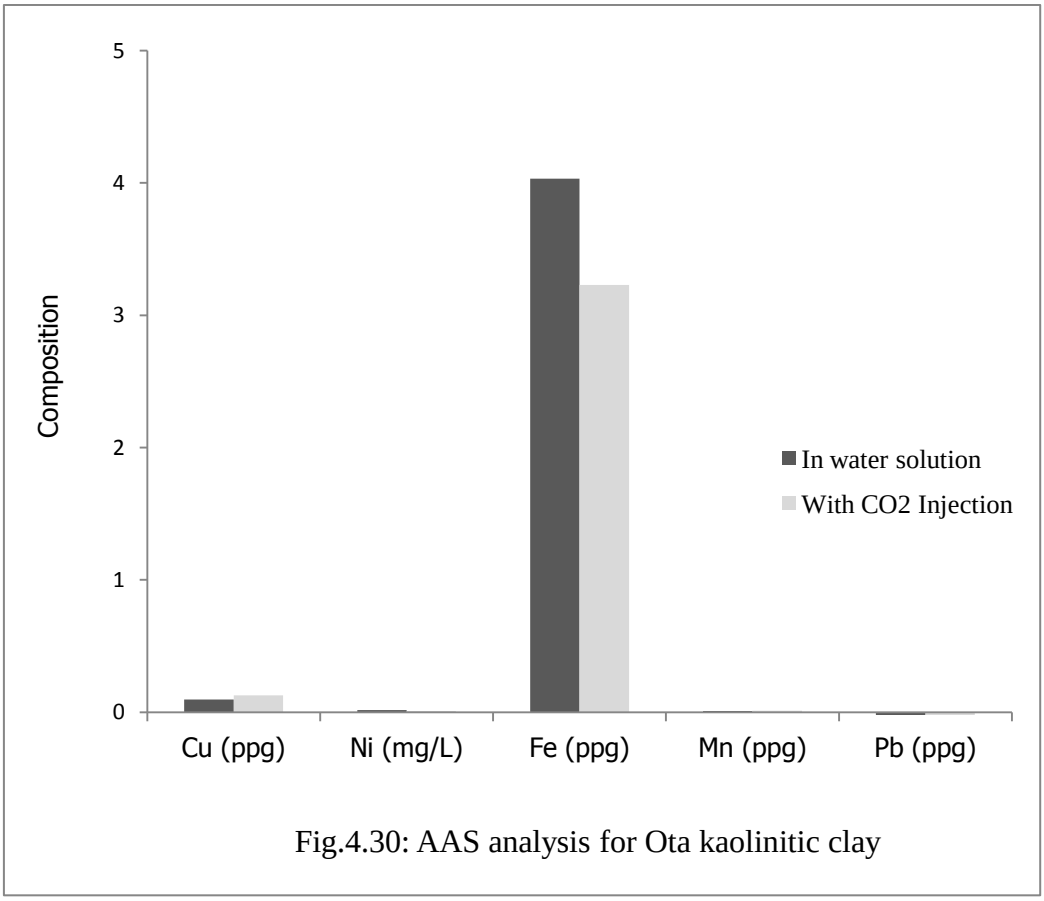

Fig.4.30: AAS analysis for Ota kaolinitic clay

(Measurements are in ppm, that of the nickel is in mg/L)

Table 4.10: S_{wirr} Determination For Ota kaolinitic clay By Drying Rate Method

	In water Solution		In CO_2-water solution	
	Measured content, %	Relative to Fe content	Measured content, %	Relative to Fe content
Cu	0.0965	0.0239	0.1281	0.0397
Ni	0.0171	0.0042	0.0099	0.0031
Fe	4.0330	1.0000	3.2284	1.0000
Mn	0.0099	0.0025	0.0115	0.0036
Pb	-0.0238	-0.0059	-0.0600	-0.0186

4.1.3.2. Experimental Result for The Change In Physical Properties of Imeri Oil Sand Sample As Possible CO_2 Gas Storage

4.1.3.2.1. Experimental Result for The Change In Porosity of Imeri Oil Sand Sample Injected With CO_2

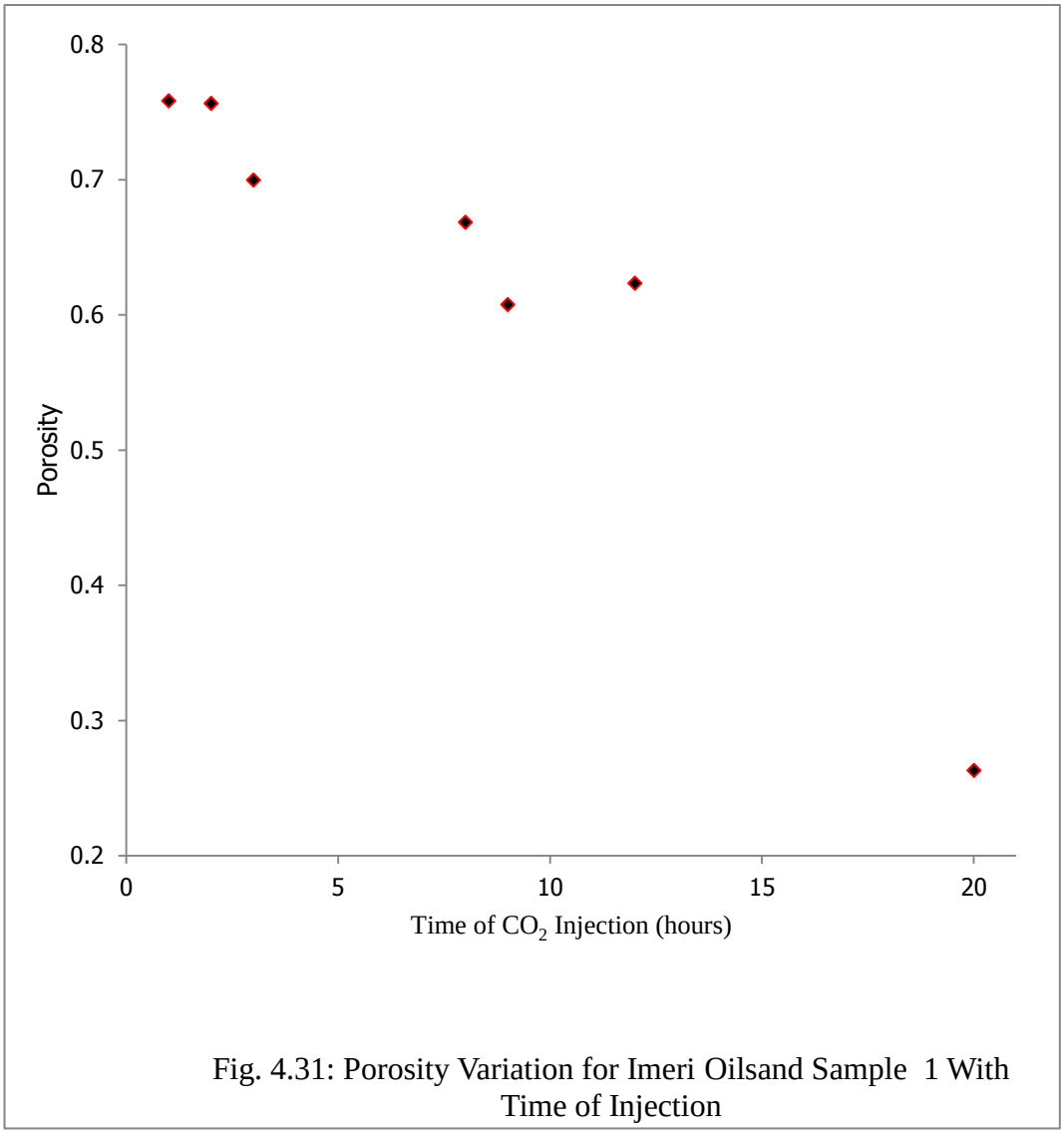

Fig. 4.31: Porosity Variation for Imeri Oilsand Sample 1 With Time of Injection

Table 4.11: Porosity Best-fit Calculations For Imeri Oil sand Sample

Time (days)	Porosity	Polynomial best fit		Log. best fit		Power fit	
			Error		Error		Error
1	0.7583	0.747	0.0113	0.84	-0.0817		
2	0.7564	0.612	0.1444	0.75336	0.00304		
3	0.6997	0.445	0.2547	0.70267	-0.003		
8	0.6685	-0.87	1.5385	0.58007	0.08843		
9	0.6076	-0.063	0.6702	0.56535	0.04225	0.552	0.0556
12	0.6234	-0.424	1.0478	0.52939	0.09401	0.57	0.0534
20	0.2631	-1.53	1.7931	0.46553	-0.2024	0.266	-0.003
Total error			5.46		-0.0594		0.1061

(The logarithm and power fits are relevant at different period of time and are therefore used for computation of the average porosity.)

4.1.3.2.2. S_{wirr} For Imeri oil Sand Sample

Table 4.12: S_{wirr} Determination For Oil sand By Drying Rate Method

Time (mins)	Oil sand Weight (g)	water loss (g)	drying rate (g/min)	S_w
0	11.2	0	0	1
30	10.8	0.4	0.01333	0.33333
40	10.7	0.5	0.0125	0.16667
60	10.7	0.5	0.00833	0.16667
70	10.7	0.5	0.00714	0.16667
75	10.7	0.5	0.00667	0.16667
90	10.7	0.5	0.00556	0.16667
150	10.6	0.6	0.004	0

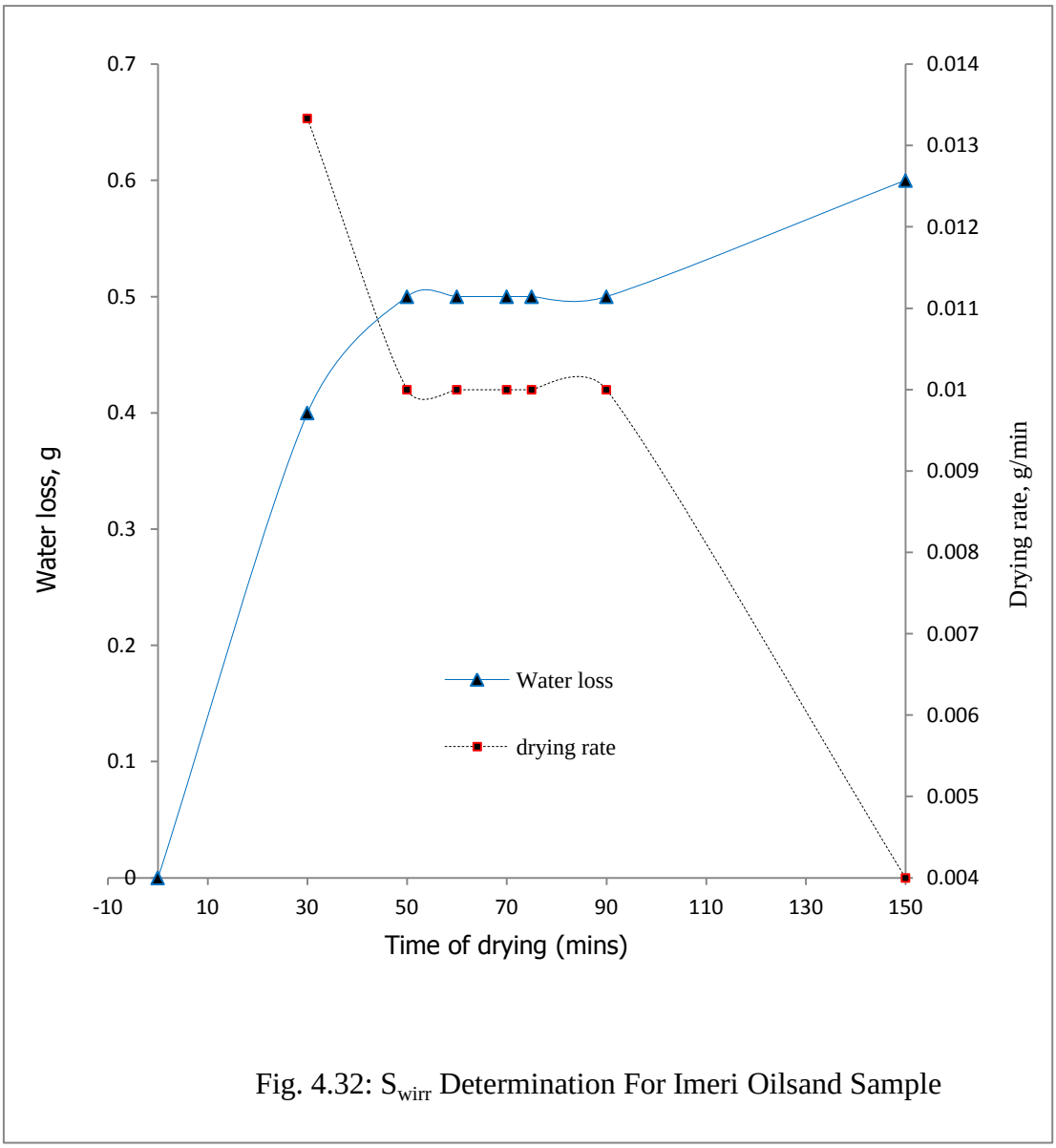

Fig. 4.32: S_{wirr} Determination For Imeri Oilsand Sample

From the Fig. 4.32 above, the S_{wirr} is at the point of rapid decline in drying rate after a constant drying rate and this correspond to 90 mins and a water saturation of 0.16667. The maximum possible S_{wirr} at the present porosity and temperature/pressure conditions is therefore 0.16667.

4.1.3.2.3. Permeability Analysis For Imeri Oilsand Sample

The result obtained for the calculated permeabilities for the Imeri Oil sand samples for the models of Timur, Tixier, Coates-Dumanoir and Aigbedion and the proposed permeability model at various irreducible water saturations are as shown in figs.4.33.

Due to observed hardening of the oil sand sample after CO_2 injection, the compressive strength of another sample of Imeri oil sand was measured before CO_2 injection and at the end of 30 days of CO_2 injection. This is as shown in fig.4.34.

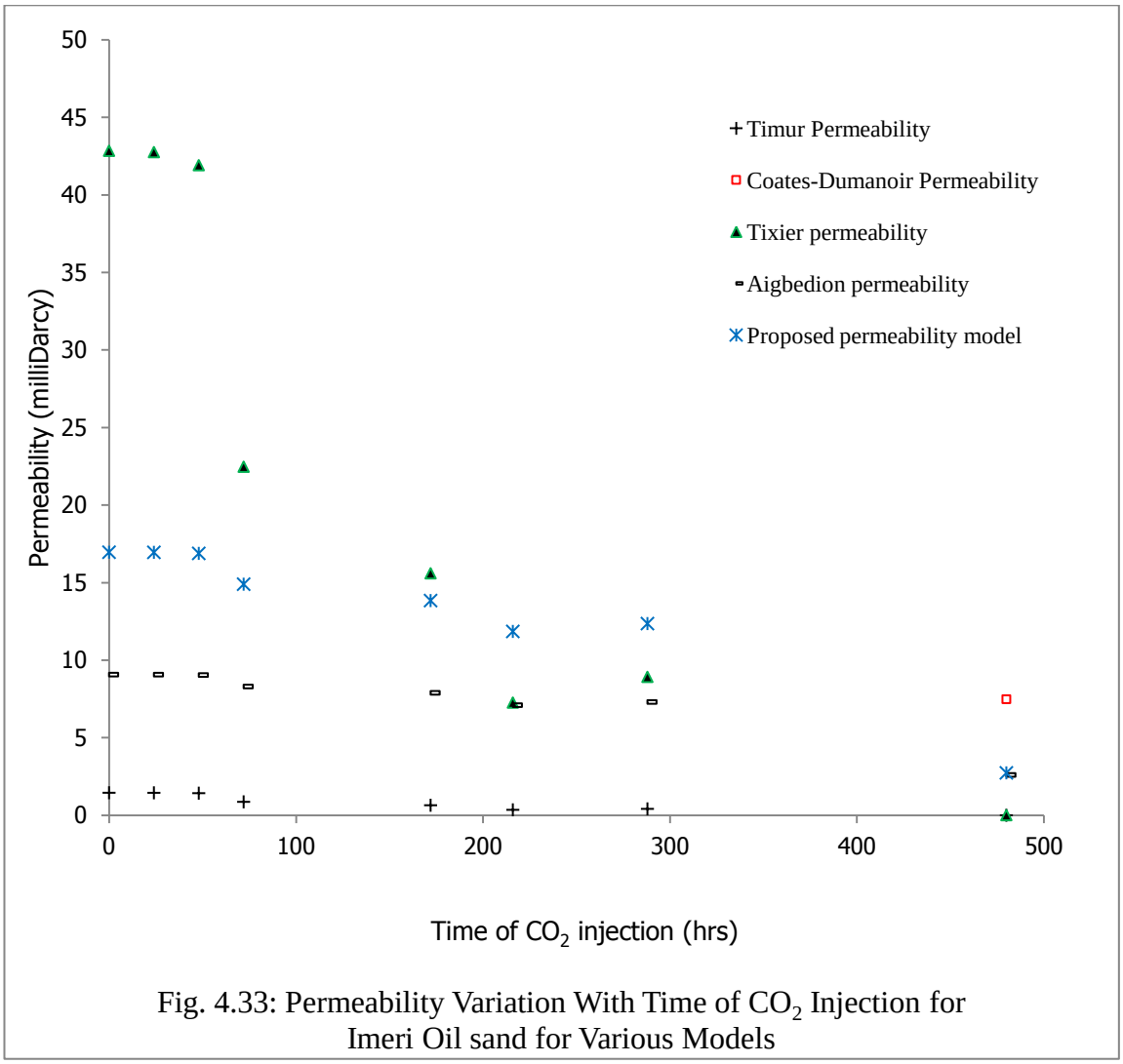

Fig. 4.33: Permeability Variation With Time of CO_2 Injection for Imeri Oil sand for Various Models

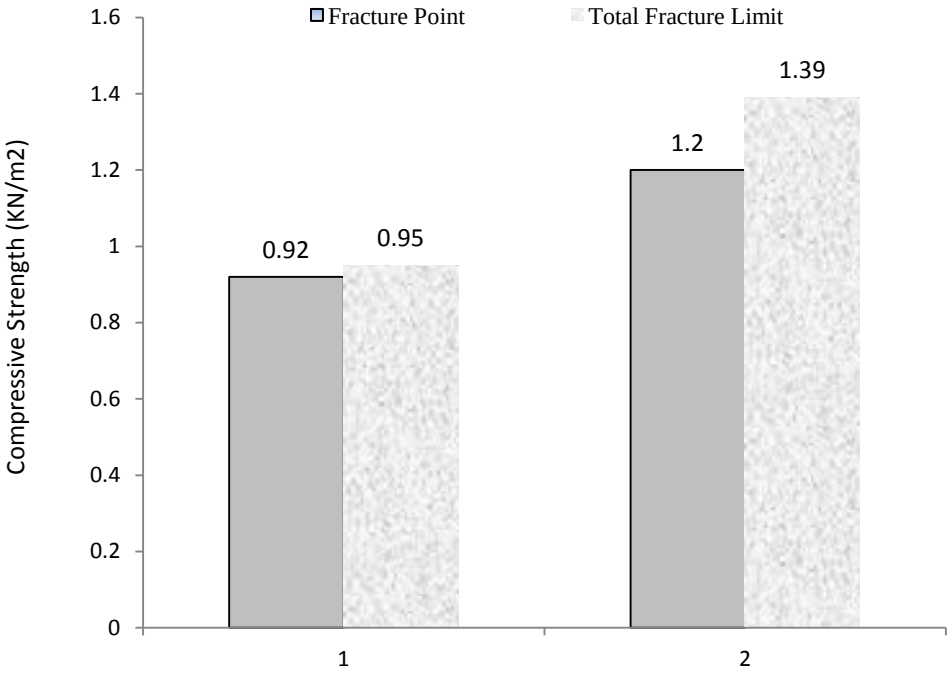

Fig. 4.34: Measured Compressive Strength of Imeri Oil sand Sample 2 Before And After CO_2 Injection

1. Before CO_2 Injection 2. After 30 days of CO_2 Injection

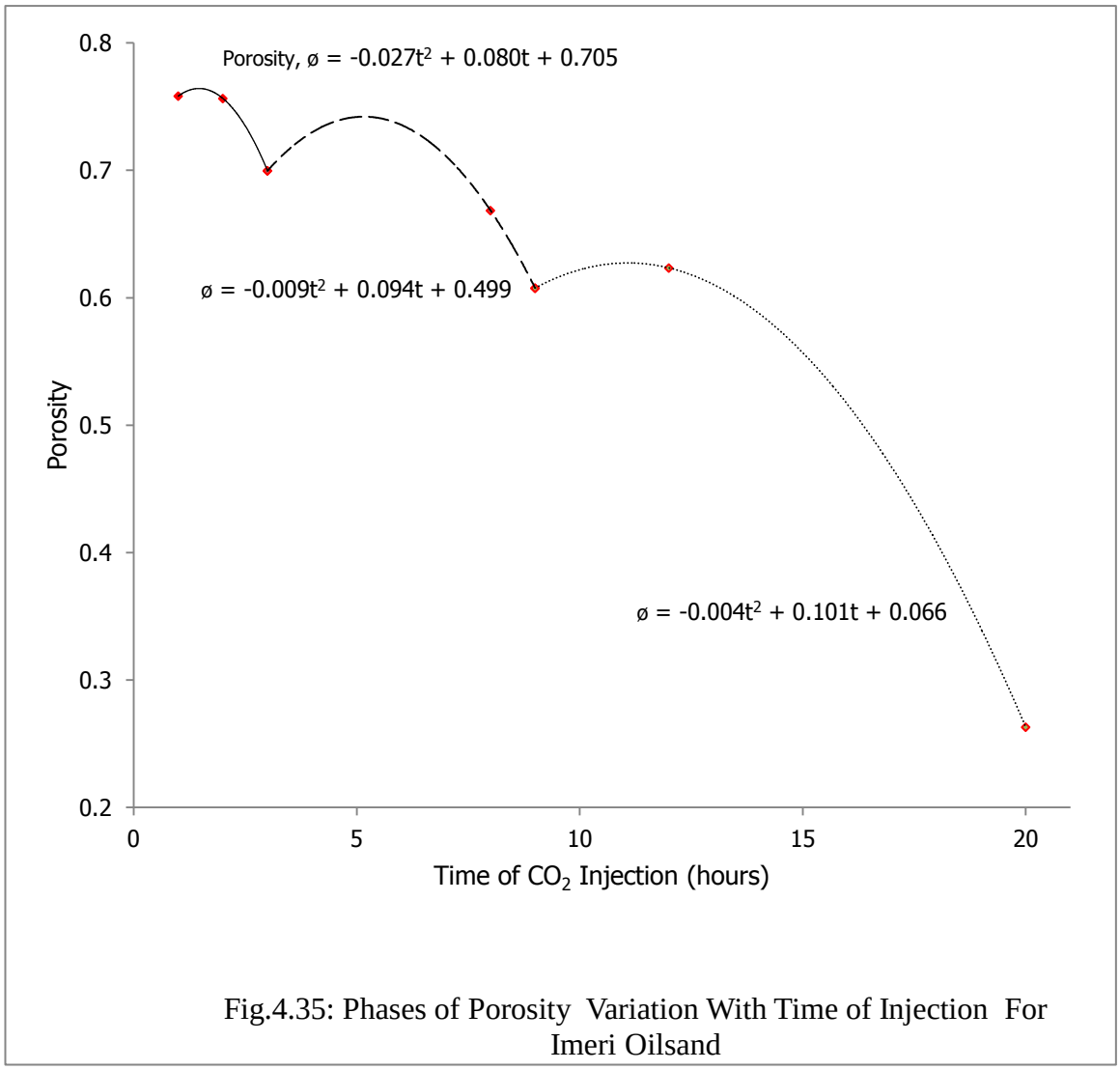

Fig.4.35: Phases of Porosity Variation With Time of Injection For Imeri Oilsand

4.1.3.2.4. AAS Analysis For Imeri Oilsand Sample

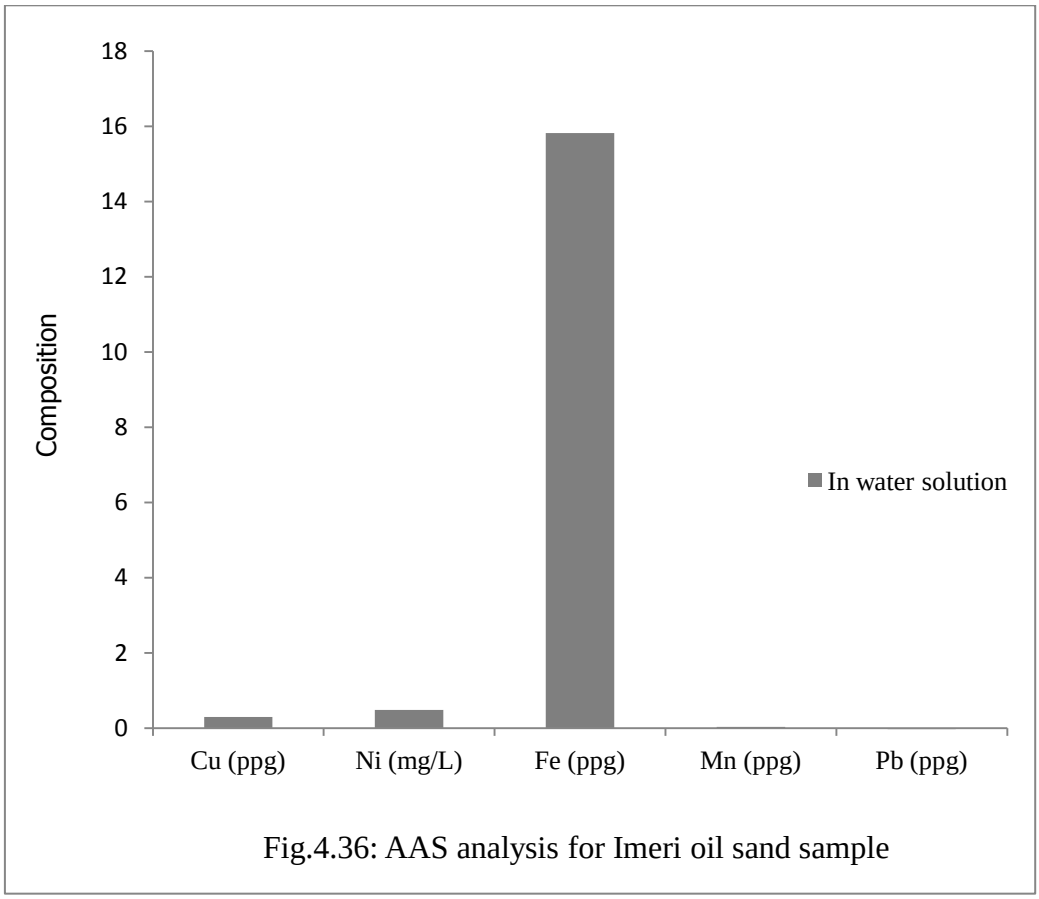

Fig.4.36: AAS analysis for Imeri oil sand sample

4.1.2. Experimental Result for The Change In Physical Properties of Fluid Sample Contaminated With CO_2

In this section the variation in properties of reservoir crude due to contamination of stored CO_2 gas and the effect of the stored gas kick on drilling mud being used in adjacent reservoir is presented.

4.1.2.1. Experimental Result for The Change In Physical Properties of Bonny Light Crude Sample Contaminated With CO_2

When CO_2 is injected in to a reservoir, it is expected to mix with the residual oil in that reservoir and alter its properties. If there is a leakage, it will affect the properties of the oil in the adjacent reservoir. In this section, the influences of the injected CO_2 on the oil properties were investigated in order to observe the effect on the flow properties of the oil in case of future production. The observed change in the viscosity of the Bonny light crude sample used is as shown in fig.4.37.

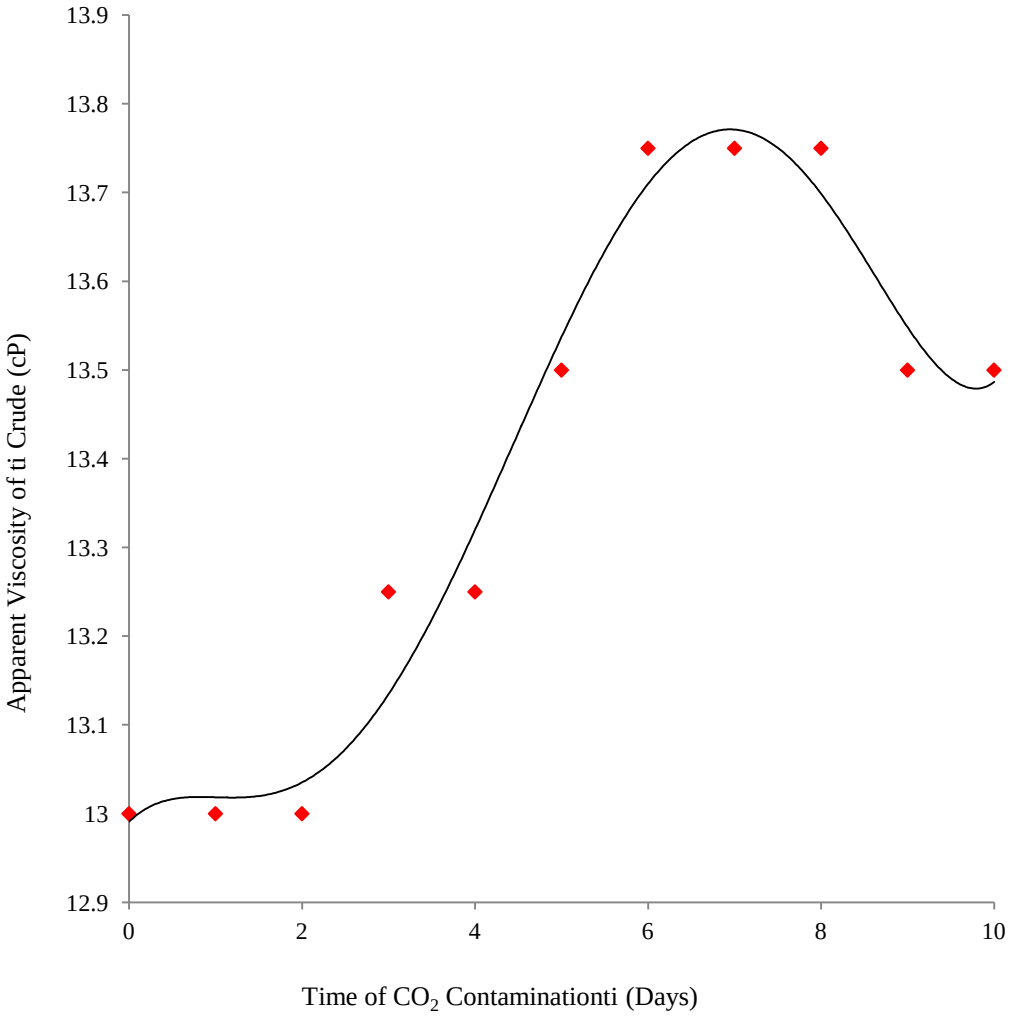

Fig.4.37: Change in Viscosity of Crude Oil Contaminated With CO_2

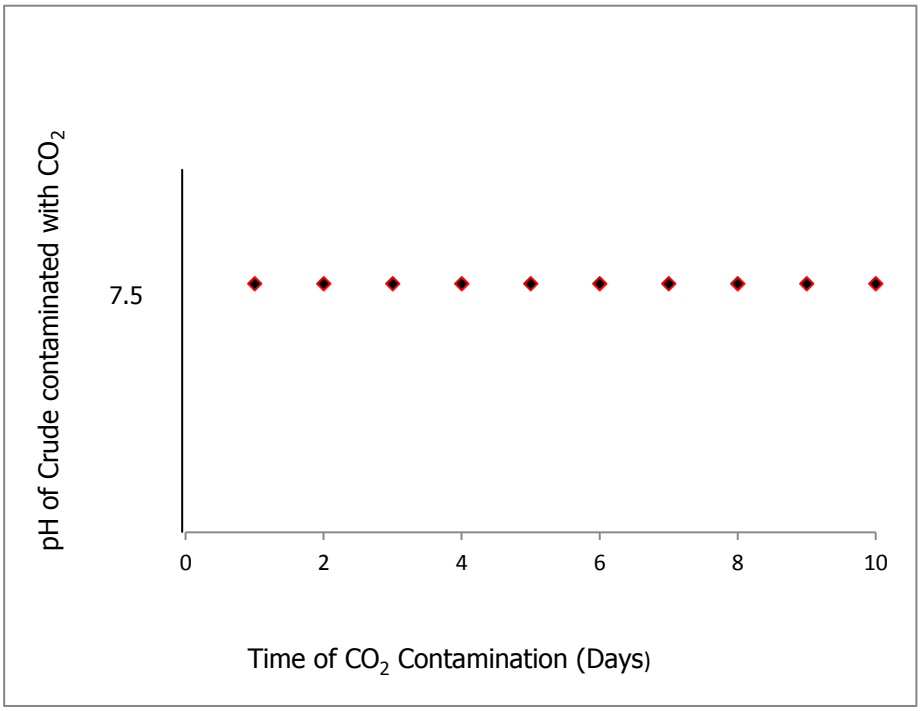

Fig. 4.38: pH Variation of Bonny Light Crude With CO_2 Contamination

4.1.2.2. Experimental Result for The Change In Properties of Drilling Mud Contaminated With CO_2 During Possible CO_2 Storage Reservoir Integrity failure.

In this section, effects of the stored CO_2 on future drilling activities in nearby reservoir when there is leakage is investigated. Leakage could be as a result of fractures due to storage reservoir structural challenges. This could be as a result of the reservoir's inability to withstand increased pressure and possible reactions between reservoir grains and stored CO_2.

4.1.2.2.1. Water-based mud

The measured data, as the shear stress and pH changes with injection of CO_2 gas into the water based mud, is as stated in Table 4.13. During the measurement, the atmospheric temperature changes erratically and is indicated against measured data.

Table.4.13: Shear Stress, pH and Temperature Measurement Variation With CO_2 Injection.

Time (days)	Temperature (^{0}C)	Shear stress		pH
		600 rpm	300 rpm	
0	29.0	52.5	45.0	7.5
3	29.8	34.0	25.0	8.5
6	29.5	24.0	15.0	8.0
7	29.4	22.0	13.0	7.5
8	29.6	21.0	14.0	7.0
9	29.5	18.0	11.0	7.0
10	29.3	15.0	9.0	6.5
11	29.2	13.0	8.0	6.0
12	29.8	13.0	8.0	6.0
13	29.5	13.0	8.0	6.0

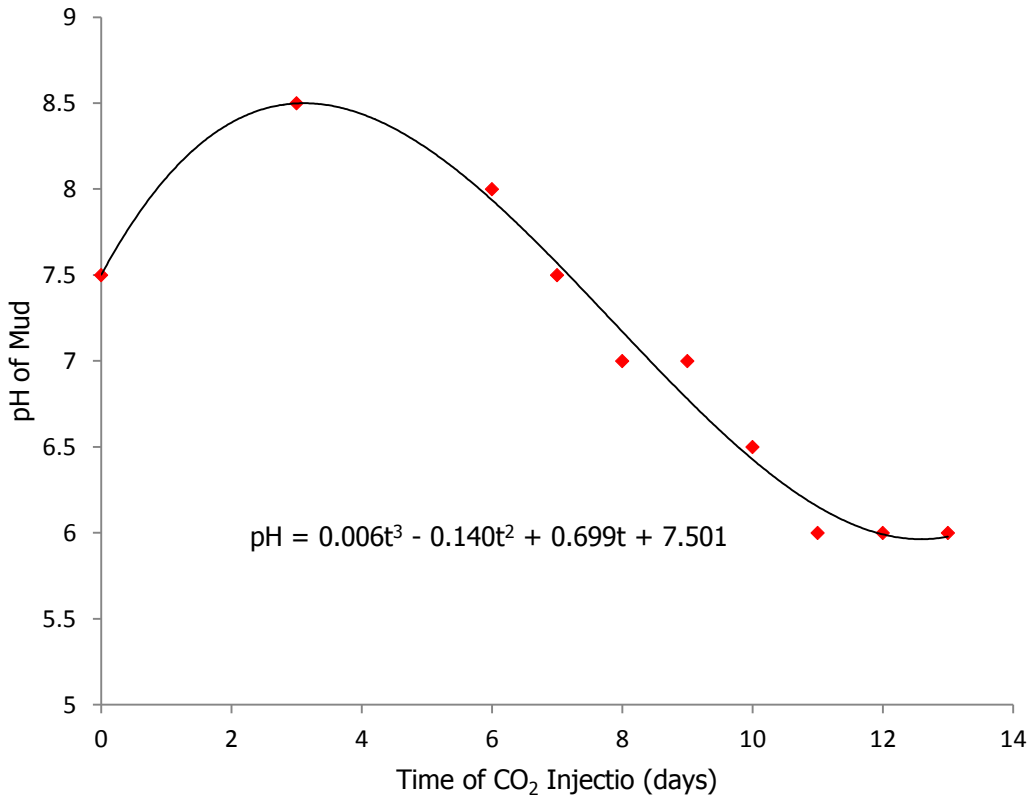

Fig. 4.39: pH Variation With Increasing Injection of CO_2 Into Water-based Mud

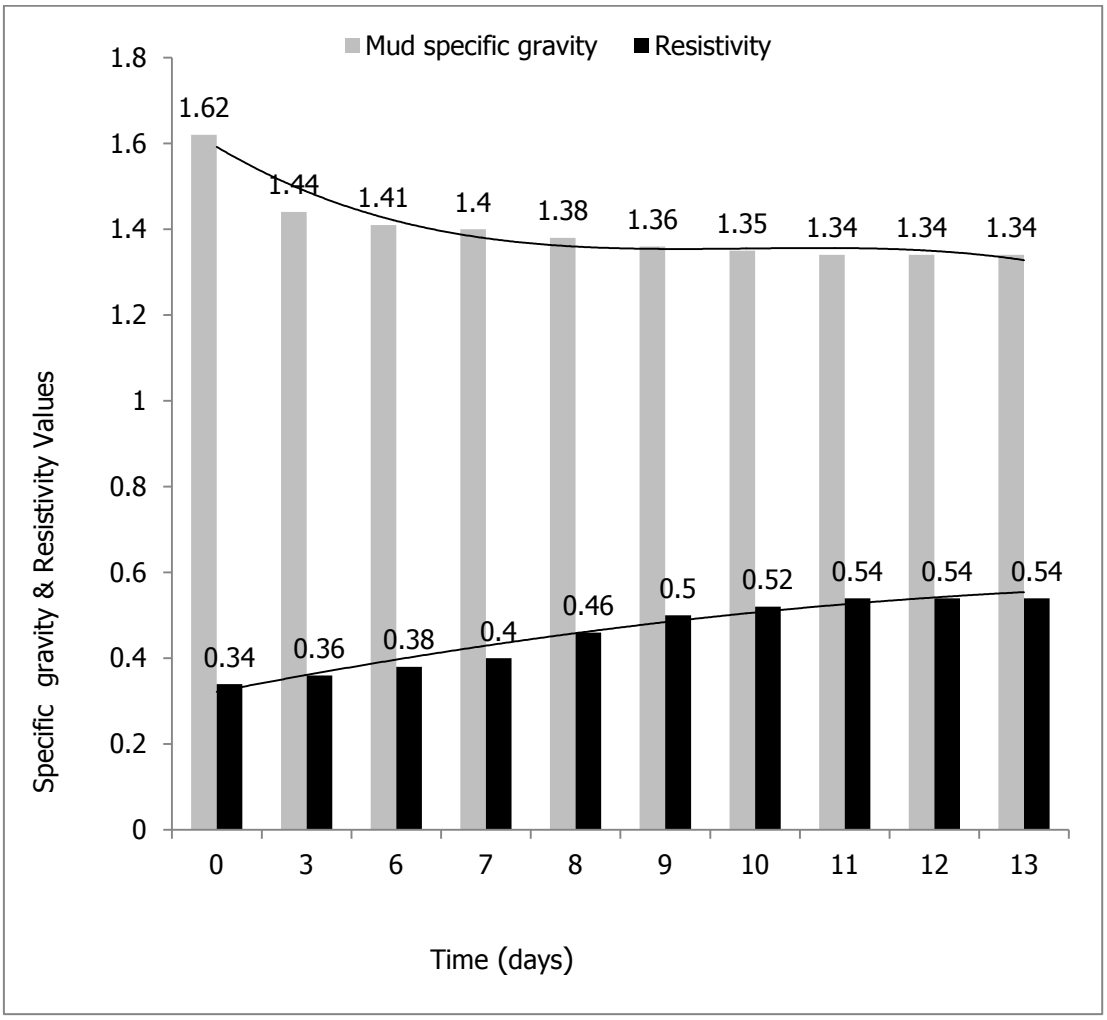

Fig. 4.40: Specific Gravity & Resistivity Values For Water-Based Mud With CO_2 Contamination

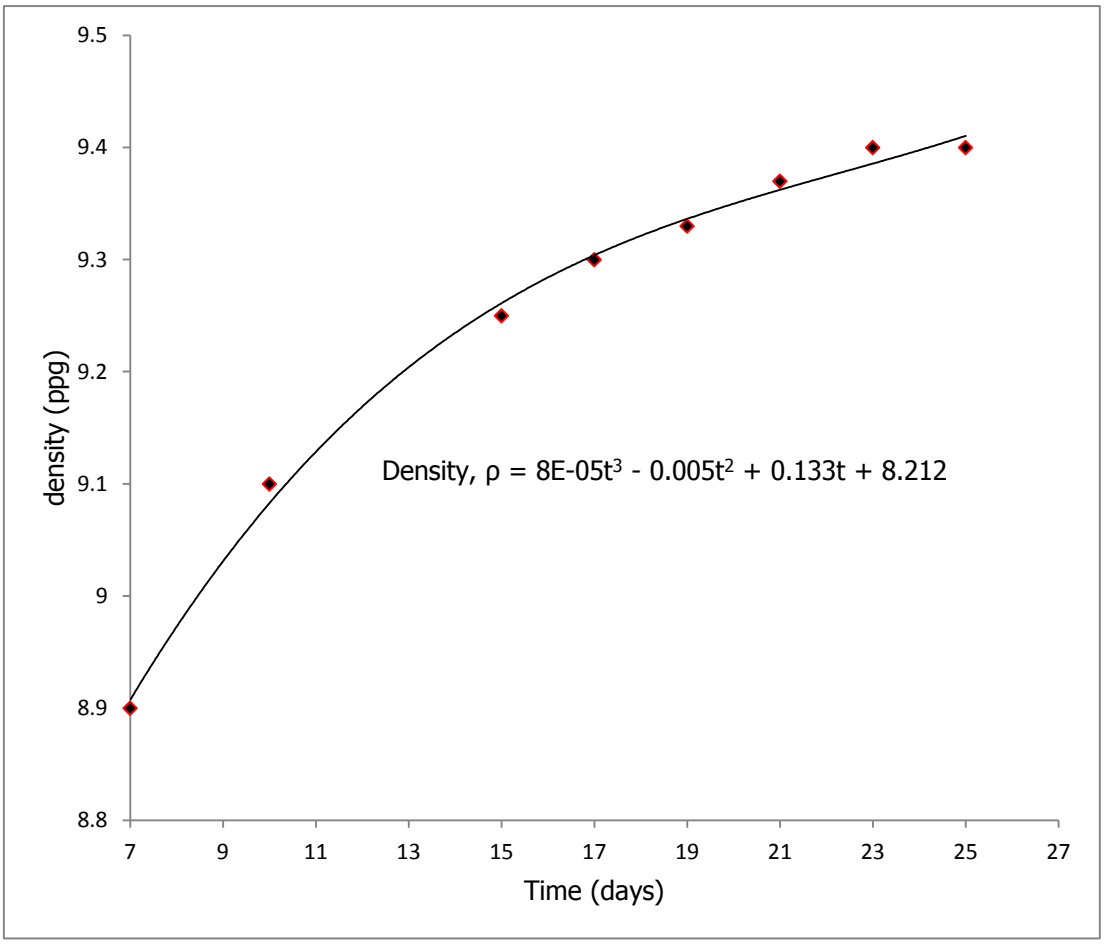

Fig. 4.41: Density of CO_2 Contaminated Water-Based Mud

4.1.2.2.2. Oil- In- Water Mud

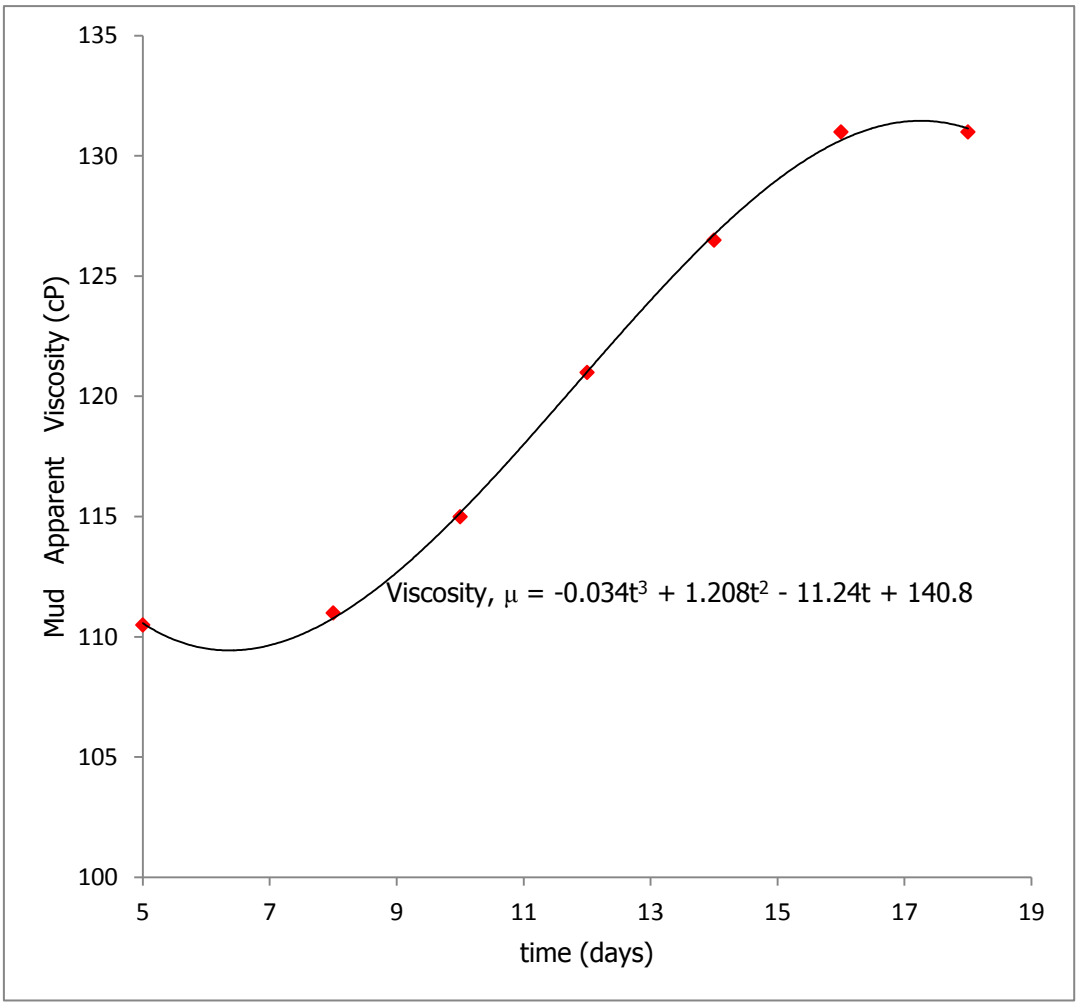

Fig. 4.42: Apparent Viscosity Change of Oil-In-Water Mud With CO_2 Contamination.

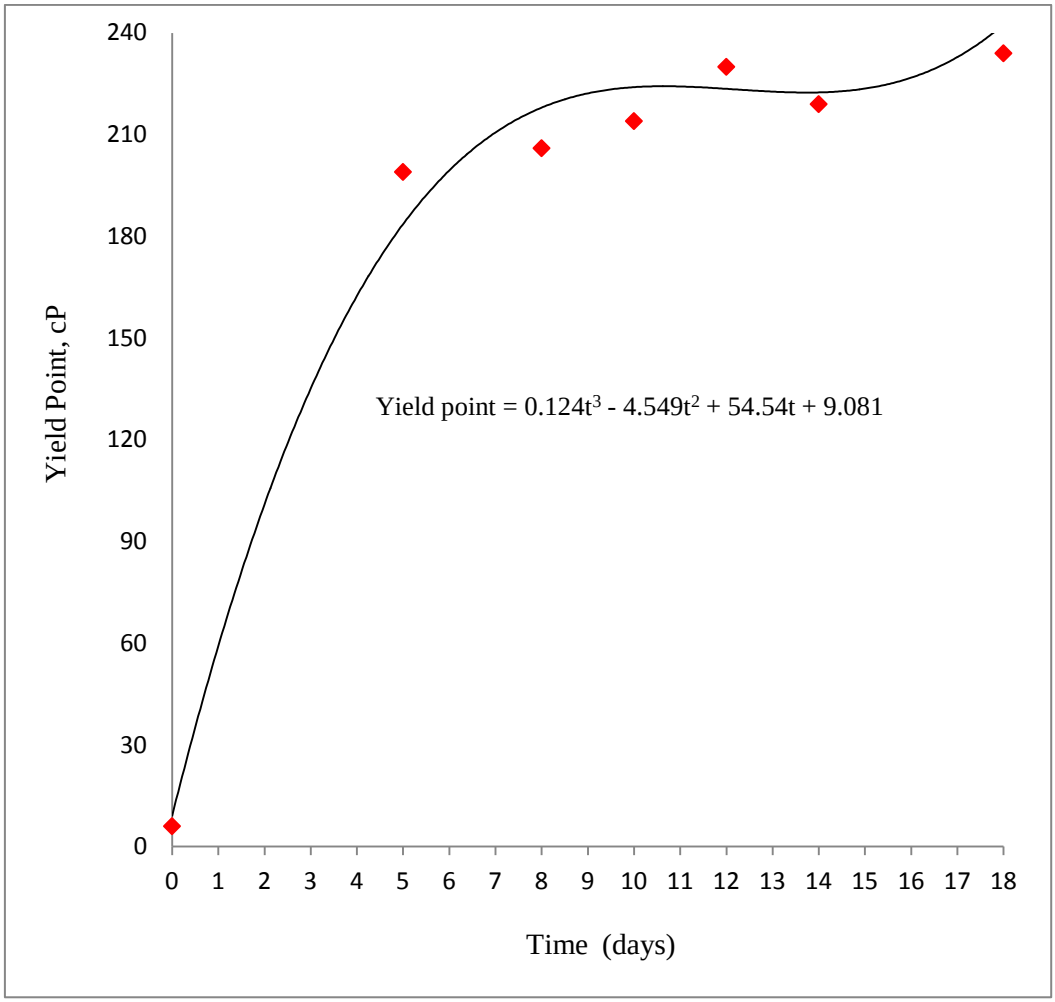

Fig. 4.43: Yield Point of Oil-In Water Mud With CO_2 Injection

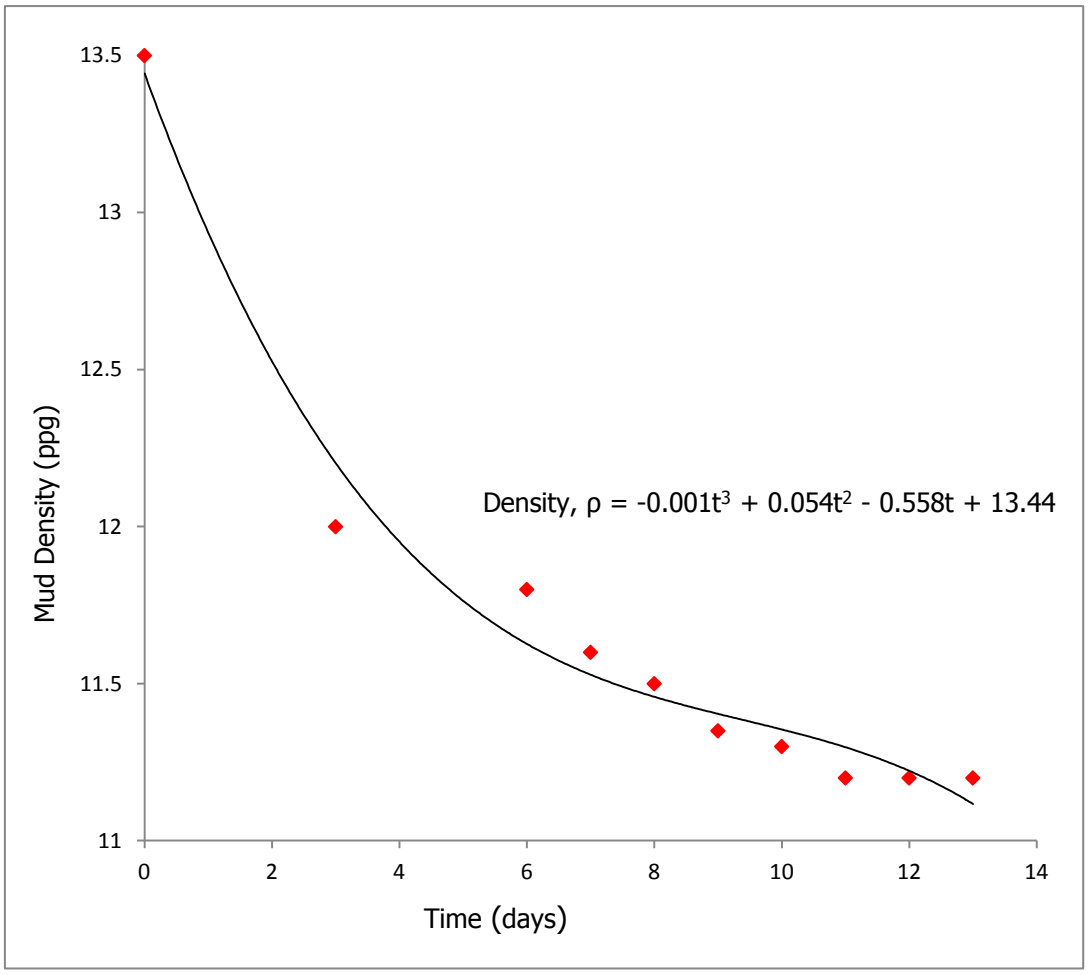

Fig. 4.44: Oil-In-Water Mud Density Change With CO_2 Injection

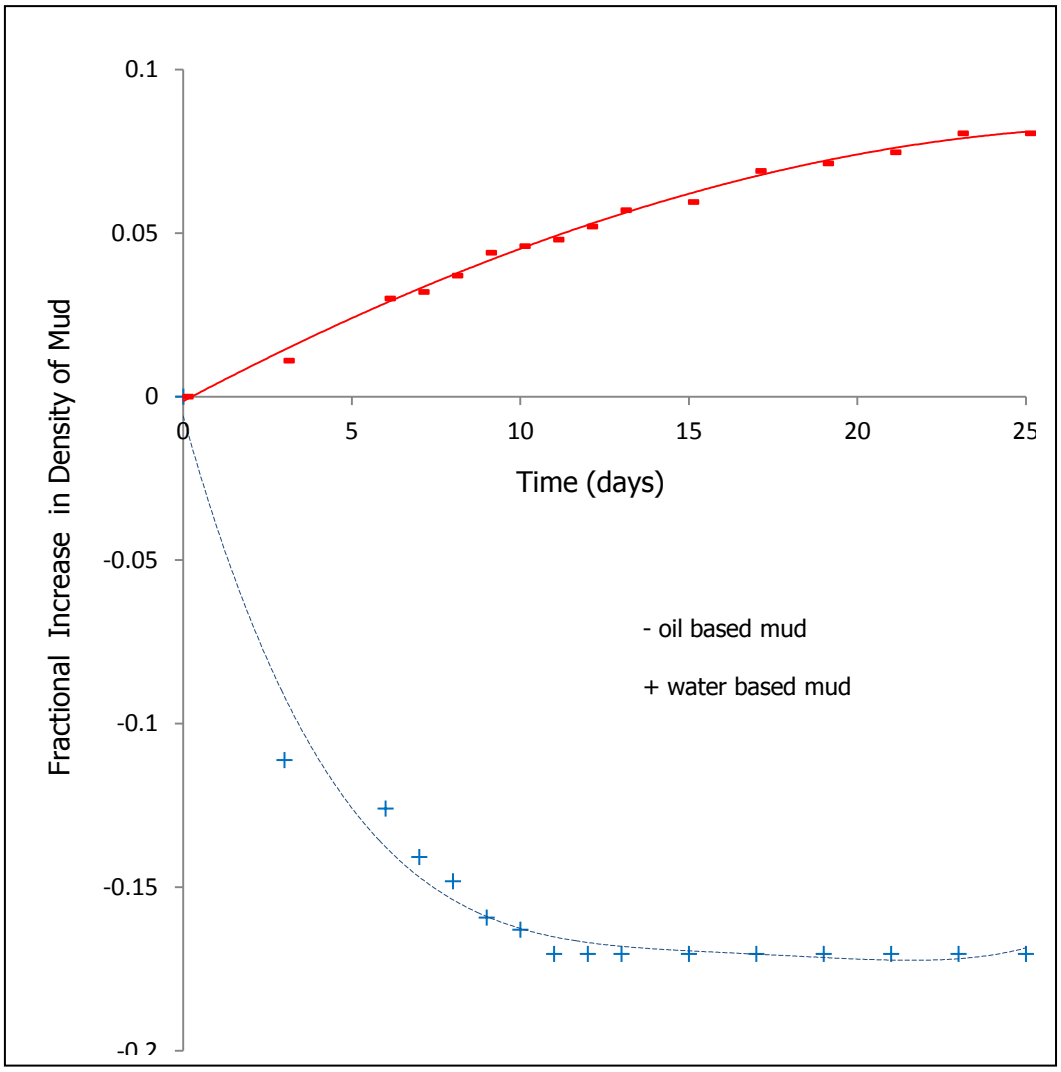

Fig. 4.45.: Fractional Change In Densities Of Drilling Fluids As Days of Contamination With CO_2 Increases

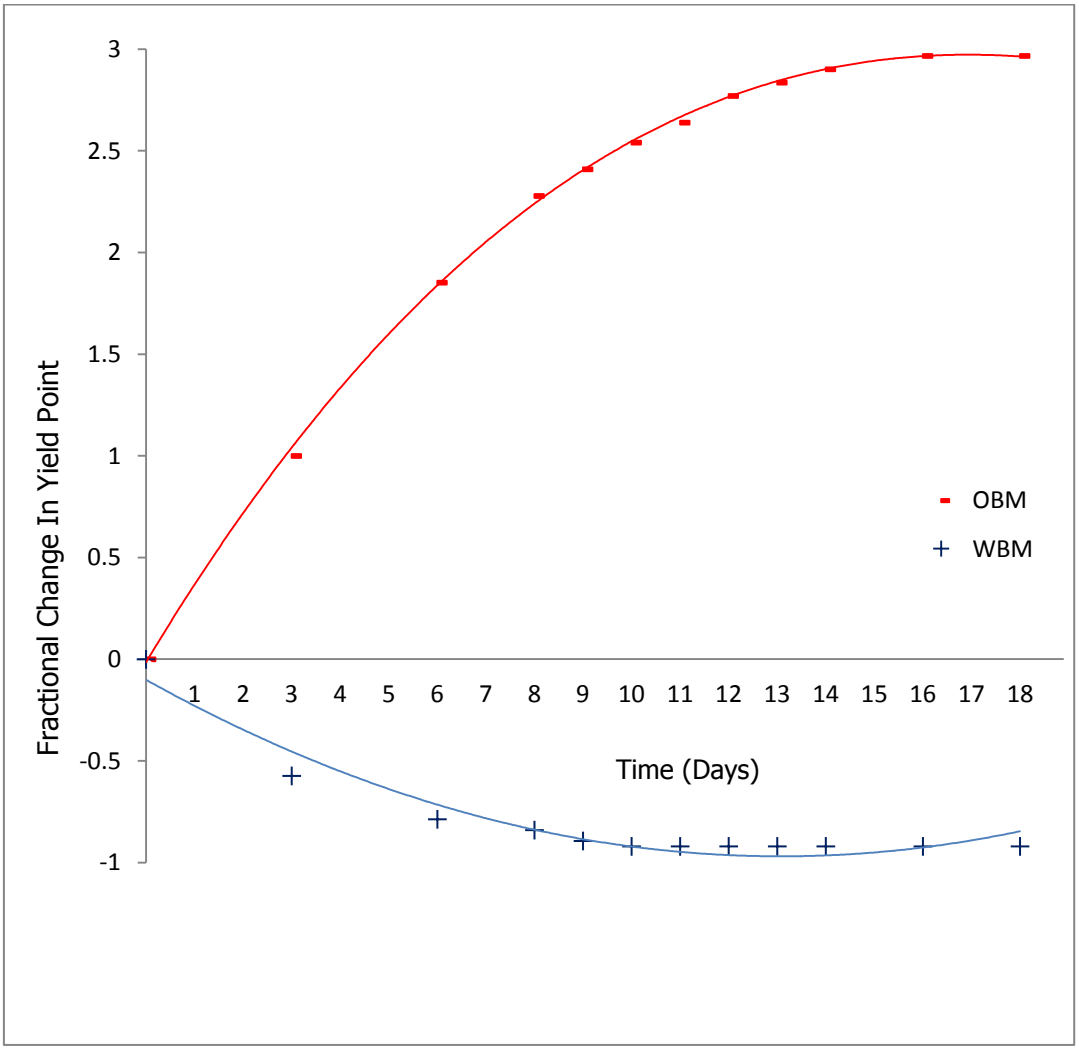

Fig. 4.46: Apparent Viscosities of Drilling Fluids As Days of Contamination With CO_2 Increases

OBM : Oil-based mud

WBM : Water-based mud

4.2. DISCUSSIONS

In this section, the results obtained in the course of this research are discussed. These include the analysis of water saturation with porosity for Kwale sands, which was used for the evaluation of the permeabilities using the four permeability models earlier discussed in chapters 2 and 4.

4.2.1 Porosity Variation With CO_2 Injection for Kwale Reservoirs.

The percentage increase in porosity is an indication of the extent of erosion and/or reaction during CO_2 injection. For Kwale Sandstone Sample 1A, there was an observed increase in the porosity of the sample from 0.281 to 0.519 (Table C1). This is an indication that the sample was much eroded. For Kwale Sandstone Sample 1B, there was an observed increase in the porosity of the sample from 0.208 to 0.428 (Table C2). This is an indication that the secondary porosity formed in the sample was higher than the primary porosity and the sample was much eroded. For Kwale Sandstone Sample 2A the observed porosity increase was from 0.210 to 0.397 (Table C3). This is an indication that the secondary porosity formed in the sample was higher than the primary porosity and the sample was much eroded. A 0.135 increase in porosity was observed for sample 2B and a 0.136 porosity increase for sample 3A while there was a 0.115 porosity increase for sample 3B (Tables C4 - C6).

For Kwale sandstone samples in crude oil, it was observed experimentally that the change in porosity is a function of the initial porosity (Table C1 and C2). It could be assumed temporarily that the lower the initial porosity, the higher the variation in porosity with increasing CO_2 injection. The implication of this is that a less porous sand may be affected more during CO_2 injection as a result of fracturing due to the pressure of injection.

The higher percentage increase in the porosity for sample 1A and that of sample 1B is an indication of instability in the rock located in an oil zone with very high hydrocarbon saturation. The inference is that, for Kwale sandstone in oil zones, there was a formation of secondary porosity with CO_2 injection.

Similarly, it was observed that, like samples 1A and 1B soaked in crude oil, there were increases in porosity of the samples 2A and 2B soaked in water. There was more variation in the porosity of sample 2A that has lower initial porosity than 2B but the

percentage increase in the 2A and 2B is far less than those of the 1A and B. This is an indication that there must be another factor apart from initial rock porosity and pressure of injection that influences variation in porosity with CO_2 injection. Comparing the bulk volume of samples used, sample 2A has lower bulk volume than that of sample 2B and hence higher injection ratio but ended up with lower porosity variation. Comparing this trend with that of samples 1A and 1B, 1B with lower injection ratio has higher porosity variation since equal volume of CO_2 was injected for each set of sample, it can be concluded that the percentage of injected CO_2 may not necessarily be a relevant factor in the variation in porosity.

For samples 3A and 3B that have same bulk volumes the trend is that rock with higher initial porosity gave higher variation in porosity with injection and this is of same trend to that of 2A and B. On comparison with sample 2A that has higher initial porosity than that of 3A and B, it is expected that the variation in its porosity will also be higher than that of 3A or 3B. This was confirmed as the variation in porosities of the 3A and 3B are actually less than that of 2A. Since this trend is contrary to that of the 1A and B, there must be another factor that influences rock porosity variation with volume of injected CO_2. Since samples 2A and 2B were soaked in water before injection and this was absent in the samples 3A and 3B, water is therefore an important factor influencing variation in porosity during CO_2 injection in Kwale sands.

Similarly, sample 2A has lower bulk volume than 1B and since the initial porosity of the two samples was close, it is expected that sample 2A should have higher porosity variation than 1B and the variation in their porosities due to CO_2 injection should be very close. Since this was not so, there must be another factor that influence variation in the porosity. The only noticeable factor is the presence of crude oil in samples 1A/1B and water in samples 2A/2B. This implies that the type of fluid presence influence the variation in porosity during CO_2 injection in Kwale reservoir sands.

In summary it can be concluded that:

1. Initial porosity of rock samples influenced the variation in porosity during CO_2 injection.
2. Volume of injected CO_2 may influence the variation in the porosity due to increasing reservoir pressure and erosion of rock matrix.

3. Presence of formation fluid influenced the porosity variation during CO_2 injection. Water caused the variation to be higher than when there is no water in the rock while the presence of crude caused highest variation in porosity.

Therefore, it can be concluded that the following holds:

$$\mathbf{\emptyset_t = function\ (\emptyset_{initial}, Vol_{CO2\ injected}, fluid\ type)}$$

Where $\emptyset_t$= porosity at time t during CO_2 injection

$\emptyset_{initial}$ =initial porosity before CO_2 injection

$Vol._{CO2}$= volume of CO_2 injected

4.2.2. CO_2 Injection Into Kwale Shales

4.2.2.1. Kwale Black Shale Sample Porosity

There was an observed increase in the porosity of the black shale from 3.17% to 20.45% with CO_2 injection in 20 days (Table C7). This is an increase of 545.9%. The increase, though on a larger scale, is similar to the one observed in the Kwale sandstone samples 1A and B. The extreme variation in the porosity means extreme erosion in the sample and this might have been due to reaction between the injected CO_2 and highly reactive shale. Confirmation of this is required with further studies involving visual monitor of the microscopic deformation in the shale during CO_2 injection over a very long period of time but this is outside the scope of the present research. AAS analysis of the sample proved the existence of traces of Fe, Cu, Pb, Ni and Mn. Black shale due to colouration is believed to contain more than 1% carbonaceous material (http://en.wikipedia.org/wiki/Shale#Composition_and _color) and also of a reducing/ oxygen-starved environment. The presence of oxygen component in the injected CO_2 gas made reactions possible and fast resulting into formation of carbonates which are actually more porous than the initial rock resulting into increase porosity.

4.2.2.2. Kwale Grey Shale Sample Porosity.

This was observed to have initial porosity of 35.19% and a final porosity of 0.86% after 20 days of injection. This is 97.6% reduction in porosity contrary to what was observed in the black shale. This reduction is an indication of blockage of the pore spaces with CO_2 injection. The inference is that new mineral must have formed that has good cementing nature as to reduce the effective porosity of the sample. The porosity versus

time graph can be fitted with three different slopes. This represented three phases of porosity variations as shown in Fig. 4.22.

Comparing this to the black shale sample, it is therefore assumed that the presence of higher carbonaceous material in the black shale and the reducing state of the shale samples have effect on the porosity variation during CO_2 injection. Further research is required for accurate determination of the reaction mechanism.

4.2.3. CO_2 injection Into Ota Kaolinitic Clay

The initial porosity value of the Kaolinitic clay sample used was 51.05% and there was a gradual decrease in the porosity as injection of CO_2 continued. At the end of 62 days there was an observed 29.75% reduction in the porosity. For the first 32 days of injection of CO_2, the observed porosity change was 21.44% (Table C.17). This was followed by a period of 29days without injection but with the CO_2 in contact with the oil sand at low pressure and an observed further reduction of 8.31% from the initial porosity was observed. This is a confirmation that not only the injection pressure caused variation in the porosity but also reaction, or interaction, between the CO_2 and the oil sand causes reduction in the porosity of the oil sand as well. It is believed that the initial reduction for the first 32 days in the porosity is higher than that of the second phase because in the first phase, both the injection pressure and possible reactions would have influenced the porosity. Although, due to the low injection pressure used (1200psi, 8273.7KN/m^2), the reaction could be rightly attributed to have contributed more to the observed change in the porosity. The expected reaction is due to the breakdown of the aluminum-silicate compound to aluminum and silicate carbonates as a result of reaction with the injected CO_2 at pressure in excess of 1000psi. The carbonates form is expected to have higher pore volume than the dissociated clay content thereby resulting into lower porosity. Observed porosity variation is in three distinct phases as shown in Fig.C5.1.

4.2.4. CO_2 injection into Imeri Oil sand

Two Imeri oil sand samples were used. The Imeri oil sand sample 1 was used for the permeability modeling while sample 2 was used to study the observed change in compressive strength with CO_2 injection. Imeri oil sand sample 1 was used for the permeability model analysis during CO_2 injection and storage in the oil sand. There was 65.03% reduction in the porosity from high value of 75.93% to 26.31% at the end of 20days (Fig. C4.1). The initial high porosity must have been due to the fact that the oil sand existed together with large water mass. There was observed porosity reduction throughout the CO_2 injection for sample 1 unlike that of the sample 2 that has initial slight increase followed by continuous decrease in the porosity. The observed difference between the two samples could be as a result of difference in the colouration of the sample due to weathering effect of seepage from the oil sand deposit. This implies that different reaction pattern with the injected CO_2 must have been followed for the two samples. Further research is required for the confirmation of this.

For the Imeri oil sand sample 2, it was observed that there was 7.888% increase in the porosity of the oil sand core 2 after 16 days of CO_2 injection, after which there was reduction in same over the next 8 days until the 24^{th} day (Table C.11). This observed reduction in the measured porosity after the 16^{th} day could be attributed to the observed hardening of the core sample after 30 days of CO_2 injection. This was also confirmed by increase in the measured compressive strength (Fig.4.36). Physical observation of the oil sand core outer surface showed a more slippery surface which is believed to have resulted in formation of seals of some grains, possibly within and, outside surface of the core that could have resulted into the reduction in measured porosity. The physical hardening of the oil sand core sample resulted in a 30.43% increase in the measured compressive strength of the core after 30 days of contamination with CO_2. This is an indication that there might have been a reduction in the porosity due to either deposition of new material in the pore spaces or that there might have been a change in the composition of the oil sand matrix due to formation of new mineral. The hardening could have also been due to reaction of this oil sand with the injected CO_2 resulting in the formation of a sealing material or a type of CO_2 hydrate. The material formed is a candidate for further investigation but is not part of the present research objective. Further comprehensive investigation is required for accurate confirmation of this.

4.2.5. *Porosity Variation Phases.*

For all the samples, it was observed that the porosity changes during CO_2 injection is in phases. The porosity measurement shows two distinct phases for the Kwale sandstone samples which is an indication of two major factors influencing porosity variation during the CO_2 injection process (Fig.C1.1-C1.6). The first phase is best described by a polynomial with second degree which is an indication of a turning point, which is a variation in the observed porosity trend. Also, as it was observed for the Kwale sandstone samples, the porosity trends observed for the two Kwale shale samples, Imeri oil sand sample and the Ota Kaolinitic clay sample were of similar phases. The porosity measurements indicated two distinct phases with a clearer intermediate phase in-between the two (Figs.C2.1, C3.1, C4.1 and C5.1) for the black shale, grey shale, Imeri oilsand and Ota Kaolinitic clay. This shows that there must have been at least two major factors that influence the porosity variation with the injection of the CO_2. The middle phase can be taken as transitional stage where the two factors have combined influence on the porosity. Each of the phases can be described by a polynomial equation. For black shale it was observed that the porosity initially reduced with CO_2 injection and then increases after the third day.

It is expected that the two major factors that can influence porosity variation on injection of CO_2 is the pressure of injection and also reaction between the injected gas and the formation rock. In this research, injection pressure was kept below 1000psi so that the effect on the rock porosity is minimized and the reaction of the rock with the injected gas will then have the dominant effect on the porosity variation. This is because, the effect of pressure of injection will mostly be felt at the rock's environment near the point of injection while away from this there is going to be a minimal pressure differential between injection pressure and the formation pressure and so the porosity variation was actually be determined by some other factors apart from the injection pressure factor.

4.2.6. Permeability Modelling

In order to carry out the permeability modeling, irreducible water saturations, S_{wirr} were computed with the Tixier, Timur and Coates-Dumanoir models. The most accurate Timur S_{wirr} was then applied in Coates-Dumanoir model to obtain a proposed model (modified Coates-Dumanoir model).

In all the computations, it was observed that the Aigbedion model is not applicable in CO_2 injection as it gave very low permeability values at high porosity and all irreducible water saturation value range from low to high values (Tables C.7- C.12, C.14 and C.16).

For the Kwale black shale, at high porosity, the Coates-Dumanoir and the proposed models gave acceptable values but at low porosity, the proposed model gave values that are closer to experimental observed values for Kwale sands (Ekine and Iyabe, 2009) as presented in appendix A. For the Tixier and Timur models, the calculated permeability was too low even when porosity increased while that of the Aigbedion gave negative values at low porosity and too low values at higher porosity for Kwale sand when compared with values obtained from literature (Ekine and Iyabe, 2009). This shows that the proposed model gave better permeability prediction for Kwale black shale better than other available models (Table C.7).

As the irreducible water saturation, S_{wirr}, increased, the calculated permeability reduced and this is because the increasing immobility of the formation water will create a restriction in the path of flow and hence a lower permeability. On the average, the proposed model gave values that are closer to published measured permeability values for Kwale sand while other methods gave permeability values that are either too low or too high. This is an indication that those other models are not applicable for permeability analysis for the Niger-Delta region when there is CO_2 injection. The highest observed permeability for the black shale is 3.776mD for the proposed model, while Tixier, Timur, Coates-Dumanoir and Aigbedion gave 0.01, 0.0027, 11.01 and 1.99mD respectively. Coates-Dumanoir model value is still reasonable but it gave too low values initially (Table C.14).

The general observation is that the Tixier and Coates-Dumanoir model gave unreasonable values at high S_{wirr} while the Aigbedion values are not affected by S_{wirr}

but gave too low values for low S_{wirr} and too high values for high S_{wirr} (Table C7 – C12). The Timur model gave values that are either too low or too high permeability values for the Kwale sandstone while the proposed model gave values ranging from 2.46 to 99mD at low sand porosity to high porosity which is in line with observed permeability values for Kwale sands.

4.2.7. CO_2 Injection into Bonny Light (Niger-Delta crude representation)

It was observed that the apparent viscosity of the oil remained constant for the first two days followed by a 5.1% increase in the same apparent viscosity over the next five days after which there was a reduction of 1.8% in the viscosity (Fig.4:39). The specific gravity varied in a similar manner as the viscosity variation as expected. It was constant for first two days and followed later by 0.6% increase within the next 7 days. (Table C.22). After the sixth day, further injection of the CO_2 made the crude denser an indication that there might have been evaporation of lighter component of the crude resulting to increasing viscosity. The observed reduction in viscosity is an abnormality and could have resulted from increased interactions between the CO_2 and the crude molecules in the mixture forming a CO_2 – crude mixture with an average density in between that of the lighter CO_2 and the density of the denser crude.

4.2.8. CO_2 Effect On A Standard Water-based and Water-in-oil Muds.

It was observed that CO_2 tends to contaminate both water-based mud and water-in-oil emulsion mud. The contamination of water-based mud resulted in 15%reduction in the mud density in the first 7 days which then stabilized at a cumulative 17% on the 15^{th} day (Table C.32- C.33) . For the oil-based mud, there was increase in its density of 3% in first 7 days and a 7% increase by the 25^{th} day (Table C.34). This implied that the oil-based mud density was more stable in CO_2 contamination than that of the water-based mud.

The yield point variation was similar to that of the density variation. There was 100% increase in the Yield Point of the oil-based mud within the first 3 days of CO_2 contamination. This went up to 250% increase by the 10^{th} day and 296% cumulative

increase by the 16th day. The yield point of that of water-based mud actually reduced by 57.3% within first 3 days and stabilized at 75% reduction by the 11th day until the 16th day. The same trend was observed for the apparent viscosities. For oil-based mud there was an increase of 242%, 334% and 394% by the 3rd, 10th and 16th day respectively while the corresponding reduction in that of the water-based mud was 35.8%, 71.69% and 75.4% respectively (Tables C.34- C.36).

A point to note is that any increase in density can be compensated by contamination with reservoir rocks and fluids. Reservoir fluid contamination during drilling will lead to average reduction in mud density while the observed reduction in density as a result of the CO_2 contamination can be compensated by suspension of drill cuttings by the mud. Hence, the change in mud density for both oil-based and water-based mud can be assumed insignificant but the variation in the yield point is a critical consideration which makes water-based mud to be considered more suitable in CO_2 contamination environment than the corresponding oil-based mud and this water-based mud is recommended with additives to enhance its viscosity.

Notwithstanding, further study is recommended to find a more suitable mud for this type of heavy CO_2 contaminated reservoir.

4.2.9. AAS Analysis of Traces of Heavy Metals In Various Samples.

For the entire sample, it was discovered that the iron content is much larger than other heavy metallic content. With relative to the iron content, the Kwale grey sample digested in water had heavy metal composition in the kaolin is in reducing volume order of Fe, Cu, Ni and Mn. For Kwale grey sample digested in water and injected with CO_2 gas for 4 days has Fe, Ni, Mn, Cu and Pb in decreasing order. This implies that the volumetric composition of the Cu reduces with the CO_2 injection while traces of Pb was discovered which seems to be absent in the sample digested in water.

The Ota Kaolinitic clay, Kwale black shale, Kwale sandstone and Imeri oil samples digested in water have Fe, Cu, Ni, Mn contents in order of reducing volumetric content. For the Ota Kaolinitic clay digested in water and injected with CO_2 intermittently for 4 days, the Ni component was higher in volumetric percentage than the Mn component.

Chapter 5.

CONCLUSIONS AND RECOMMENDATIONS

Presented in this chapter are the conclusions reached in the course of this research together with proposed recommendations.

5.1. Conclusions

Timur model was observed to be the most relevant in the computation of the irreducible water saturations, S_{wirr}, among the three models of Tixier, Timur and Coates-Dumanoir. The Coates-Dumanoir was observed to give the most appropriate permeability values for Kwale sands with no CO_2 injection. Hence, a model was proposed which was a merger of the Timur's S_{wirr} equation and the Coates-Dumanoir permeability equation to describe CO_2 injection influence on the Kwale reservoir permeability. The proposed model was observed to give values that are closest to published permeability values for Kwale sands than the Tixier, Timur, Coates-Dumanoir and the Aigbedion models. The proposed model gave permeability values ranging from 2.47 to 92.46 milliDarcy for the Kwale sandstones and 0.04 – 9.62 milliDarcy for the shales. The models gave permeabilities of 17.58 – 85.2 milliDarcy when the S_{wirr} model of Kwale sandstone was applied and 2.9 – 10.21 milliDarcy when various values of constant S_{wirr} were assumed for the Ota Kaolinitic clay. The proposed model gave 15.166 – 1.3155 milliDarcy at various assumed S_{wirr} for the Imeri oil sand samples. For all the samples, Timur model gave permeability values from 0.0 to 634 milliDarcy while Tixier values ranges from 0.0 to 10053 milliDarcy. Coates-Dumanoir gave wide range values of 6.68- 8550 milliDarcy while Aigbedion gave values ranging from -3.7 to 5.94 milliDarcy. The published measured Kwale sand permeability ranges from 0.8 to 87 milliDarcy (Appendix B). Though the proposed model gave slightly higher permeability than the published measured permeability, this is expected and is as a result of the average increase in porosity due to the CO_2 gas injection.

Injection of CO_2 into Kwale sandstones resulted in increase in the porosity of the sandstone (Tables C1 – C6) which is an indication of more space for CO_2 storage and also an indication of possible reaction between the injected CO_2 and the formation. Hence, Kwale sandstone formation is a potential CO_2 storage reservoir. It was observed that Kwale sandstone oil reservoir gave the highest potential followed by

water zone and lastly by dry reservoir zone. Hence, it is better to inject into abandoned Kwale sandstone reservoir than the water reservoirs.

This increase in the sandstone porosity is also an indication of possible erosion of cementing material content of the sandstone. This implies that any leakage of the stored CO_2 from the storage reservoir to an adjacent producing reservoir will result in erosion of the sandstone content of the producing reservoir and caused higher sand production at the active wells. This is an important consideration to be made when considering storage of CO_2 in an abandoned reservoir in the Niger-Delta sandstone formation. Unfortunately, if there is any leakage of the CO_2 from the stored reservoir to a nearby producing Kwale reservoir resulting into increase in that reservoir porosity, sand production problem will increase as the gas will react with the cementation of the reservoir matrix.

In the case of the black shale and the grey shale, it was observed that the black shale gave varying response to injection of CO_2 and the extreme variation in its porosity is an indication of lack of storage integrity as the stored gas may migrate to nearby reservoirs. The grey shale is recommended for CO_2 storage as the observed porosity reduction during the gas injection is an indication of possible reaction with the CO_2 to form new minerals which will make the gas to remain underground.

It was observed that Imeri oil sand formation is too porous for storage purpose. Though there was observed reduction in porosity as injection continues due to possible reaction between the oil sand and the injected gas but the gas will be lost to nearby formation initially until this reaction progress to a level where the oil sand property was distorted to form a material with higher compressive strength and lower porosity (Fig.4.36). This projected initial loss of the CO_2 to nearby formation has made the injection objective unrealistic.

Ota Kaolinitic clay with a moderate initial porosity coupled with reducing porosity with CO_2 injection is a potential storage reservoir for CO_2 that may be captured from Lagos/Ogun industrial zone. This is because the reduced porosity is an indication of formation of a CO_2-clay complex mineral.

It was observed that there is no single equation to describe the permeability variation with time for the considered samples since the porosity variation is divisible into three zones for each sample. Hence, permeability equation modeling can only be applicable to each type of reservoir and this is highly dependent on its reactivity with the injected CO_2 gas. Most common equation is similar to that of the sandstones where the permeability is a 2^{nd} degree polynomial in time and porosity, immediately after injection but has an exponential relationship with the time/porosity after some days of injection.

Lastly, any form of leakage from a stored reservoir will cause CO_2 gas kick in the nearby reservoir and will create drilling problem due to its side effect on drilling mud and must be specially design against possible effect of CO_2 gas kick.. Moreover, from the results obtained in this study, it was discovered that any CO_2 leakage into nearby producing reservoir will affect the property of the producing oil negatively and there may be need for further treatment of the crude at the surface.

5.2. Recommendations.

It is hereby recommended that:

1. CO_2 storage is not recommended for sandstone reservoirs adjacent to producing reservoirs in the Niger-Delta since a leakage will result in increasing sand production problems.
2. Further study is recommended for visual analysis of the reaction between CO_2 and the various rock cores. This is to be done before and intermittently during CO_2 injection, in order to know the dominant controlling factor between the pressure of injection and the reaction of the injected gas with the reservoir rock/fluids. This will enable the easy manipulation of the controlling factor to enhance the storability of the CO_2 in that formation.
3. Samples from deeper formations, especially offshore formations, should be used to analyze the suitability of the Niger-Delta offshore for CO_2 storage but with special consideration of the growth-fault nature of the Niger-Delta formation.
4. There are natural carbon sinks such as vegetation that use CO_2 for respiration purposes. Nigerian Government is encouraged to intensify efforts on her re-forestation programme this to take up the excess CO_2 being generated by automobile, animals and use of fossil fuels for small power generation units.

REFERENCES

Adebayo, Thomas Ayotunde, 2012, Comparison of Performance of Standard Water-based and Oil-based Mud For Drilling Purpose During Carbon Dioxide Gas Kick From Adjacent Reservoir, *International Journal of Engineering and Technology*, IJET UK, Vol. 2, No.5, pp.729-731

Adelere Ajayi, 2012, Nigeria: Geometric Power's Aba Plant Begins Operation Q1 2013, October 16, *This Day Publications*, Retrieved from: http://allafrica.com/stories/ 201210160400.html

Adewusi, V. A., 1992, Aspects of Tar Sands Development in Nigeria, *Energy Sources*, volume 14, Issue 3, pp. 305-315

Aigbedion, I., 2007, A Case Study of Permeability Modeling and Reservoir Performance in the Absence of Core Data in the Niger Delta, Nigeria, *Journal of Applied Sciences*, 7: 772-776.

Akinmosin, A., Adeigbe, O. C. and Oyemakinde, O. O., 2011, Scanning Electron Microscope Description Of The Afowo Oil Sand Deposits In South-Western Nigeria, *Earth Science Research Journal*, vol.15 no.1 Bogotá Jan./June

Akinmosin, A. and Gbolahan, O. O., 2010, Environmental Geochemistry of The Nigerian Tar Sand Deposits, *Journal of Applied Sciences in Environmental Sanitation*, 5 (4): 329-344, October-December, 2010

Akinmosin, A., Osinowo, O. O. and Adio, N. A., 2010, Use of Stable Carbon Isotope In Characterization of Tar Sand Deposits In South Western Nigeria, *Journal of Applied Sciences In Environmental Sanitation*, pg 317-328.

Akinmosin, A., A. A. Odewande and A. I. Akintola, 2005, Geochemical Composition And Textural Features Of Some Carbonate Rocks In Parts Of South Western Nigeria, *Ife Journal of Science*, Vol. 7(1): 101-111

Akinmosin, A., Oreddein, O. S., and Odewande, A. A., 2006, Sedimentological And Reservoir Description of Afowo Oil Sand Deposits, Southwestern Nigeria, *Ife Journal of Science*, Vol.8, No. 1.

Ako, B. D., Adegoke, O. S., and Peter S.W., 1980, Stratigraphy of the Oshosun Formation in Southwestern Nigeria, *Journal of Mineral Geoogy*., V. 17, p. 9-106.

Anomohanran O. and U. Chapele, 2012, Effectiveness of Kriging Interpolation Technique for Estimating Permeability Distribution of a Field, *Trends in Applied Sciences Research*, Vol. 7, Issue: 7, pp.523-531

Badmus B. S. and O. B. Olatinsu, 2009, Geoelectric Mapping And Characterization Of Limestone Deposits Of Ewekoro Formation, Southwestern Nigerial, *Journal of Geology and Mining Research*, Vol. 1(1) pp. 008-018 March.

BBC news, August 2006. Retrieved from http://news.bbc.co.uk/onthisday /hi/dates /stories/ august/21/newsid_3380000/3380803.stm

Beard D. C. and P. K. Weyl, 1973, Influence of Texture on Porosity and Permeability of Unconsolidated Sand, *American Association of Petroleum Geologists Bulletin*, Vol. 57, Issue 2. (February), Pages 349 - 369

Berger R. L. and Y. J. Francis, 1979, Reaction of Calcium Silicates with Carbon Dioxide and Water, *Final report of January 1976-January 1979 Researches*, Illinois University At Urbana-Champaign, US.

Bickle Mike, Andy Chadwick, Herbert E. Huppert, Mark Hallworth and Sarah Lyle, 2007, Modelling Carbon Dioxide Accumulation At Sleipner: Implications For Underground Carbon Storage, *Earth and Planetary Science Letters* 255 (2007) 164–176.

Carbon Sciences Inc., Santa Barbara, CA, 2012, Breakthrough Technology Uses Captured CO_2 and Natural Gas to Make Ultra-Clean and Environmentally Friendly Synthetic Crude Oil, Retrieved at: http://finance.yahoo.com/news/ carbon-sciences-introduces-carboncrude-tm-080100497.html, Jan 3.

Chadwick R. A., D. J. Noy and S. Holloway, 2009, Flow Processes And Pressure Evolution In Aquifers During The Injection of Supercritical CO_2 As A Greenhouse Gas Mitigation Measure, *Petroleum Geoscience*; 1 February 2009; v. 15, no. 1, pp. 59-73; DOI: 10.1144/1354-079309-793

Chang, Y. B., Coats, B. K., and Nolen, J. S., 1996, A Compositional Model for CO_2 Floods Including CO_2 Solubility in Water, *Society of Petroleum Engineers (SPE) Permian Basin Oil and Gas Recovery Conference*, Midland, Texas, 27-29 March, 1996.

Coates, G. R., Dumanoir, J. L., 1973, A New Approach To Improve Log-Derived Permeability, *Proceedings of Society of Petrophysicist and Well Log Analysts (SPWAL)*, 14th Annual Logging Symposium.

Columbia Education online, http://www.columbia.edu/~vjd1/carbon.htm. (Accessed April 12, 2013).

Cowan Richard and Timothy Gardner, 19th March 2010, Senate Climate Bill To Give Free Permits, *Reuters Edition UK,*. Available at: http://uk.reuters.com/article/2010/03/19/us-climate-usa-congress-idUKTRE62G3YG20100319

Crawford H. R., Neill G. H., Bucy, B. J., and P. B. Crawford, 1963, Carbon Dioxide: A Multipurpose Additive For Effective Well Stimulation, *Journal of Petroleum Technology*, March 1963, 237.

Daily Times Nigeria, 2013, Egbin Power Station Commences Work On Damaged Unit, *Daily Times NG, 30th Jauary*. Retrieved from: http://dailytimes.com.ng/article/egbin-power-station-commences-work-damaged-unit

Eberhard Anton and Katharine Nawaal Gratwick, 2012, Light Inside: The Experience Of Independent Power Projects In Nigeria, *Management Programme in Infrastructure Reform and Regulation*, University of Cape Town Graduate School of Business

Ehlig-Economides Christine and Michael J. Economides, 2010, Sequestering Carbon Dioxide In A Closed Underground Volume, *Journal of Petroleum Science and Engineering*, 70 (2010) 123–130.

Ekine A. S. and Iyabe Paul, 2009, Petrophysical Characterization of the Kwale Field Reservoir Sands (OML 60) from Wire-line Logs, Niger Delta, *Nigeria*, *Journal of Applied Sciences and Environmental Management*, December 2009, vol.13(4) 81-85.

Federal Republic of Nigeria, Bureau of Public Enterprises, 2011, Privatization of Generation and Distribution Companies Created out of the Power Holding Company of Nigeria Plc (PHCN): Ughelli Power PLC, *BPE Information Brochure*, http://www.nigeriaelectricityprivatisation.com/wp-content/uploads/downloads/2011/01/Ughelli-Genco-2011-01-13.pdf

Gardner Timothy, 10th August *2009, U.S. Biofuel Makers Want CO_2 Credits In Climate Bill. Reuters, Retrieved from:* www.reuters.com/.../2009/.../us-biofuels-climate-idUSTRE5795CL20090

Garner, C., G. Finqueneisel, T. Zimny, Z. Pokryszka, S. Lafortune, P.D.C. Défossez, and E.C. Gaucher, 2011, Selection Of Coals Of Different Maturities For CO_2 Storage By Modeling of CH_4 And CO_2 Adsorption Isotherms, *International Journal of Coal Geology*, v. 87, p. 80-86.

Goetz David, Rosemary Knight and Paulette Tercier, 1996, A Laboratory Procedure For Estimating Irreducible Water Saturation From Cuttings, *Society of Petrophysicists And Well Log Analysts*, vol.37. No.4.

Greenpeace, 2009, Leakages in the Utsira Formation and Their Consequences For CCS Policy, Greenpeace *Briefing*, http://static.greenpeace.org/int/pdf/081201BRUtsira.pdf (accessed, July 2013)

Greenpeace, 2008, False Hope: Why Carbon Captured and Storage W'ont Save the Climate, *Greenpeace Briefing*, May 2008, www.greenpeace.org/css (accessed July 2013)

Haroon Siddique, 2010, Senate Drops Bill To Cap Carbon Emissions, *The Guardian*, UK, 23rd July, 2010. (http://www.guardian.co.uk/environment/2010/jul/23/us-senate-climate-change-bill)

Haugan, P. M. and Joos, F, 2004, Metrics To Assess The Mitigation Of Global Warming By Carbon Capture And Storage In The Ocean And In Geological Reservoirs, *Geophysical Research Letters*, vol. 31, L18202,

Honda Hiromi and Kinji Magara, 1982, Estimation Of Irreducible Water Saturation And Effective Pore Size Of Mudstones, *Journal of Petroleum Geology*, Volume 4, Issue 4, pages 407–418, April 1982.

Houston S. J., **Yardley B. W. D.,** Smalley P. C. and I. Collins (2007), Rapid Fluid-Rock Interaction In Oilfield Reservoirs, *GEOLOGY*, **35**, pp.1143-1146. doi: 10.1130/G24264A.1

Jennie C. Stephens and David W. Keith, June 2008, Assessing Geochemical Carbon Management, *Springer online publications*, (http://www.clarku.edu /faculty/jstephens/ documents/)

Jens T. Birkholzer , Quanlin Zhou, Chin-Fu Tsang, 2009, Large-Scale Impact Of CO_2 Storage In Deep Saline Aquifers:A Sensitivity Study On Pressure Response In Stratified Systems, *International journal of Greenhouse Gas Contro*l, 3 (2009) pp. 181 – 194

Juerg M Matter, W S Broecker, M Stute, S R Gislason, E H Oelkers, A Stefánsson, D Wolff-Boenisch, E Gunnlaugsson, G Axelsson, G Björnsson, 2009, Permanent Carbon Dioxide Storage into Basalt: The CarbFix Pilot Project, Iceland, *Energy Procedia*, Volume: 1, Issue: 1, Pages: 3641-3646

Klaus S. Lackner, 2002, Carbonate Chemistry For Sequestering Fossil Carbon, *Annual Review of Energy and the Environment*, November, Vol. 27: 193-232.

Leadership, July 04, 2012, "Sapele Power Plant Begins Operation, Supplies 225 Mws To National Grid, Says Maku", http://www.leadership.ng/nga/ articles/17117/2012/02/22/sapele_power_plant_begins_operation_supplies_225_m ws_ national_grid_says_maku.html

Liptow Christin and Anne-Marie Tillman, 2012, A Comparative Life Cycle Assessment Study of Polyethylene Based on Sugarcane and Crude Oil, *Journal of Industrial Ecology*, Volume 16, Issue 3, pages 420–435,

National Energy Technology Laboratory (**NETL**), 2006, Evaluating The Influence Of Pore Architecture And Initial Saturation On Wettability And Relative Permeability. Retrieved from: http://www.netl.doe.gov/kmd/cds/disk41/B-Reservoir_ Characterization/ 15516_Fact_Sheet_2006_Aug.pdf

Nazir S., M. Tufail, W. Nisa and M. Ghouri, 2011, Modelling For Capture of Carbon Dioxide Using Aqueous Ammonia From Flue Gases of a Brick Kiln, *International Journal of Chemical and* Environment, June 2011, volume 2, No. 3.

Nicot, J. P., 2008, Evaluation Of Large-Scale CO_2 Storage On Fresh-Water Sections Of Aquifers: An Example From The Texas Gulf Coast Basin. *Int. J. Greenhouse Gas Control*, 2: 582–593.

Niger-Delta Power Holding Company Pamphlet, 2013. Retrieved from: http://www.nidelpower.com/main/alaoji

Nigerian Federal Ministry of information, 16th Feb. 2013, NGGT Rivers: Maku Urges States To Key Into Power Road-Map, Commends Rivers Govt's Power Plants. Retrieved from: http://fmi.gov.ng/nggt-rivers-maku-urges-states-to-key-into-power-road-map-commends-rivers-govts-power-plants/

Odd Magne Mathiassen, 2003, CO_2 as Injection Gas for Enhanced Oil Recovery and Estimation of the Potential on the Norwegian Continental Shelf, Postgraduate Thesis, Norwegian University of Science and Technology.

Okechukwu Ukwuoma, 1999, Study Of Composition Of Nigerian Tar Sand Bitumen, *Petroleum Science and Technology*, volume 17, issue 1-2, Pages 57-65

Ola S. A, 1991, Geotechnical Properties And Behaviour Of Nigerian Tarsand, *Engineering Geology*, Volume 31, Issues 3–4, December, Page 383

Olotu A. James, 2012, National Integrated Power Project: Integrating NIPP for 2012, Issues and Challenges, *Uyo Feb. 12 – 14 Power Summit.* Retrieved from:http://www.nigeriapowerreform.org/index.php?option=com_rokdownloads&view=file&task=download&id=79%3Auyo-summit-feb-24-25-2012-ndphc-presentation&Itemid=82

Petroleum Exploration And Production. Retrieved from: http://www.online nigeria.com / links/petradv.asp?blurb=485

Qi Ran, 2009, Simulation Of Geological Carbon Dioxide Storage, Ph.D. Dissertation, Department of Earth Science and Engineering, Imperial College London, UK .

Rayward-Smith W. J. and Woods Andrew W., 2011, Some Implications Of Cold CO_2 Injection Into Deep Saline Aquifers, *Geophysical Research Letters*, Vol. 38, L06407, 6 PP.

Robert Stavins, Ruben Lubowski and Andrew Plantinga, 2006, Land-Use Change and Carbon Sinks: Econometric Estimation of the Carbon Sequestration Supply Function, *Journal of Environmental Economics and Management,* 51: 135-152.

Robert Stavins, and Richard Newell, 2000, Climate Change and Forest Sinks: Factors Affecting the Costs of Carbon Sequestration, *Journal of Environmental Economics and Management*, 40:211-235.

Robert Stavins, 1999, The Costs of Carbon Sequestration: A Revealed-Preference Approach, *American Economic Review*, volume 89, number 4, September, pp. 994-1009.

Rochelle C. A., I. Czernichow-Lauriol and A. E. Milodowski, 2004, The Impact of Chemical Reaction on CO_2 Storage In Geological Formations: A Brief Review, *Geological Society London, Special Publications*, vol.233: pp.87-106.

Sarah Pistone, Robert Stacey, and Roland Horne, 2011, The Significance Of CO_2 Solubility In Geothermal Reservoirs, *Proceedings Thirty-Sixth Workshop on Geothermal Reservoir Engineering*, Stanford University, Stanford, California, January 31 - February 2.

Scottish Centre for Carbon Storage. Retrieved from: www.geos.ed.ac.uk/sccs /capture /postcombustion.html

Semere Solomon, 2007, Security of CO_2 Storage In Norway, *The Bellona Foundation Fact Sheet: Security of CO_2 Storage*. Retrieved from http://www.bellona.org/filearchive/fil_Factsheet_Security_of_CO_2_storage_in_Norway_-_english_-_rev_16aug07.pdf

Singleton G. R., 2007, Geological Storage of Carbon Dioxide: Risk Analyses and Implications For Public Acceptance, *Masters thesis*, Massachesetts Institute of Technology.

Solomon D. H. and H. H. Murray, 1972, Acid-Base Interactions And The Properties Of Kaolinite In Non-Aqueous Media, *Clays and Clay Minerals*, Vol. 20, pp. 135-141.

Soren Anderson and Richard Newell, 2004, Prospects For Carbon Capture And Storage Technologies, *Annual Review of Environment and Resources*, Vol. 29: 109-142.

Srivastava M. , S. Harpalani, 2004, Permeability Variations with CO_2 Injection in Coalgas Reservoirs and its Impact on Methane Production, *Third Annual Conference on Carbon Capture & Sequestration*, May 3–6, 2004. Alexandria, Virginia.

This Day Live, 15th May 2012, Ibom Power Plant and Challenges of Electricity Evacuation. Retrieved from: http://www.thisdaylive.com/articles/ibom-power-plant-and-challenges-of-electricity-evacuation/115792/

Timur, A., 1968, An Investigation Of Permeability, Porosity And Residual Water Saturation Relationships For Sandstone Reservoirs, *The Log Analyst*, July – August, 9(#4): 3 – 5.

Tixier, M. P., 1949. Evaluation Of Permeability From Electric Log Resistivity Gradient. *Earth Science Journal*, 2: 113-113.

Watson, T. L. and Bachu, S., 2007, Evaluation Of The Potential For Gas And CO_2 Leakage Along Wellbores. *Society of Petroleum Engineers E&P Environmental and Safety Conference*, 5–7 March 2007, Galveston, Texas, U.S.A

Weiss Martin, Juliane Haufe, Michael Carus, Miguel Brandão, Stefan Bringezu, Barbara Hermann and Martin K. Patel, 2012, A Review of the Environmental Impacts of Biobased Materials, *Journal of Industrial Ecology*, Volume 16, Issue Supplement s1, pages S169–S181

Zahidad M Zain, Nor I. Kechut, Ganesan Nadeson, Noraini Ahmad and D. M. Anwar Raja, 2001, Evaluation of CO2 Gas Injection for Major Oil Production Fields in Malaysia – Experimental Approach Case Study: Dulang Field, *SPE Asia Pacific Improved Oil Recovery Conference*, 6-9 October, Kuala Lumpur, Malaysia

Zekri, A.Y., Shedid, A. Shedid, and Almehaideb, Reyadh, 2009, Investigation Of Supercritical Carbon Dioxide, Aspheltenic Crude Oil, And Formation Brine Interactions In Carbonate Formations, *Journal of Petroleum Science and Engineering*, Volume 69, Issues 1-2, Pages 1-162 (November) Pages 63-70

Zweigel Peter, Rob Arts, Ane E. Lothe & Erik B. G. Lindeberg, 2004, Reservoir Geology Of The Utsira Formation At The First Industrial-Scale Underground CO_2 Storage Site (Sleipner area, North Sea), *Geological Society*, London, Special Publications; v. 233; p. 165-180.

APPENDIX A

Power station	Community	Type	Capacity	Year completed	Additional description
Olorunsogo Power Station	Olorunsogo	Gas turbine	160 MW	2007	336 MW total capacity but working below capacity since its inauguration due to gas supply issues
Afam Power Station	Afam	Gas turbine	420 MW		
Egbin Thermal Power Station	Egbin	Gas-fired steam turbine	1,320 MW	1985-1986	Have six 220-MW independent units.

Table A.1: Power Generation Plants In Nigeria

Hydroelectric

Hydroelectric station	Type	Capacity	Year completed	Name of reservoir	River
Kainji Power Station	Reservoir	800 MW	1968[7]	Kainji Lake	Niger River
Jebba Power Station	Reservoir	540 MW	1985	Lake Jebba	Niger River
Shiroro Power Station	Reservoir	600 MW	1990	Lake Shiroro	Kaduna River
Kano Power Station	Reservoir	100 MW	2015[8]		Hadejia River
Zamfara Power Station	Reservoir	100 MW	2012[9]	Gotowa Lake	Bunsuru River
Kiri Power Station	Reservoir	35 MW	2016		Benue River

Table A.2: Power Generation Plants In Nigeria

(Source: http://en.wikipedia.org/wiki/List_of_power_stations_in_Nigeria)

APPENDIX B

In this section, S_{wirr} model analysis is presented. The data of Ekine and Iyabe (2009) for some sands in Kwale reservoir was used as basis for the analysis for accurate choice of a permeability model to be adopted and modified for CO_2 injection. The S_{wirr}, for Kwale sand is computed as follows using the Tixier, Timur, Coated-Dumanoir and Aigbedion models for no CO_2 injection.

Table B. 1: Properties of Kwale Well 1

(Ekine and Iyabe, 2009)

Sand	Permeability	Porosity	S_w
B	28	19	45
C	87	21	32
D	31	20	48
F	16	17	53
G	18	17	50
H	27	17	36
L	16	16	41
M	4.6	14	57

Table B. 2: Properties of Kwale Well 2

(Ekine and Iyabe, 2009)

Sand	Permeability	Porosity	S_w
A	16	21	74
B	8.1	18	75
C	8.6	19	82
D	10	20	85
F	5.2	18	93
G	8.1	19	75
H	4.3	17	91
I	4.8	16	75
J	4	16	82
K	10.2	19	75
L	5.4	17	81

Table B. 3.: Properties of Kwale Well 5

(Ekine and Iyabe, 2009)

Sand	Permeability	Porosity	S_w
B	12	19	69
C	9.4	19	77
B	10.8	18	73
F	9.4	17	78
G	5.2	17	82
H	5.2	11	89
I	6.5	17	71
J	6.9	14	90
K	1.8	13	74
L	1.9	13	66
M	1.9	11	51

Table B. 4.: Properties of Kwale Well 6

(Ekine and Iyabe, 2009)

Sand	Permeability	Porosity	S_w
B	10	19	76
C	7	17	71
D	6.4	17	74
F	7.4	17	69
G	7.4	17	74
H	6	16	67
I	5.1	15	63
J	1.8	14	90
K	2	13	73
L	0.8	11	81
M	2.5	12	55

Table B. 5.: Properties of Kwale Well 8

(Ekine and Iyabe, 2009)

Sand	Permeability	Porosity	S_w
H	1.9	13	76
I	1.1	12	92
J	1.1	12	92
K	1.1	12	92
M	3.7	11	54

Table B. 6.: Properties of Kwale Well 10

(Ekine and Iyabe, 2009)

	Permeability	Porosity	S_w
A	37	17	17
B	27	17	17
D	24	18	18
F	13	17	17
G	68	16	16

B1. Porosity-Permeability Relationship For Kwale Sands

The porosity-permeability versus water saturation for the Kwale sands based on the published measured data is as shown in Figs.B1-B10.

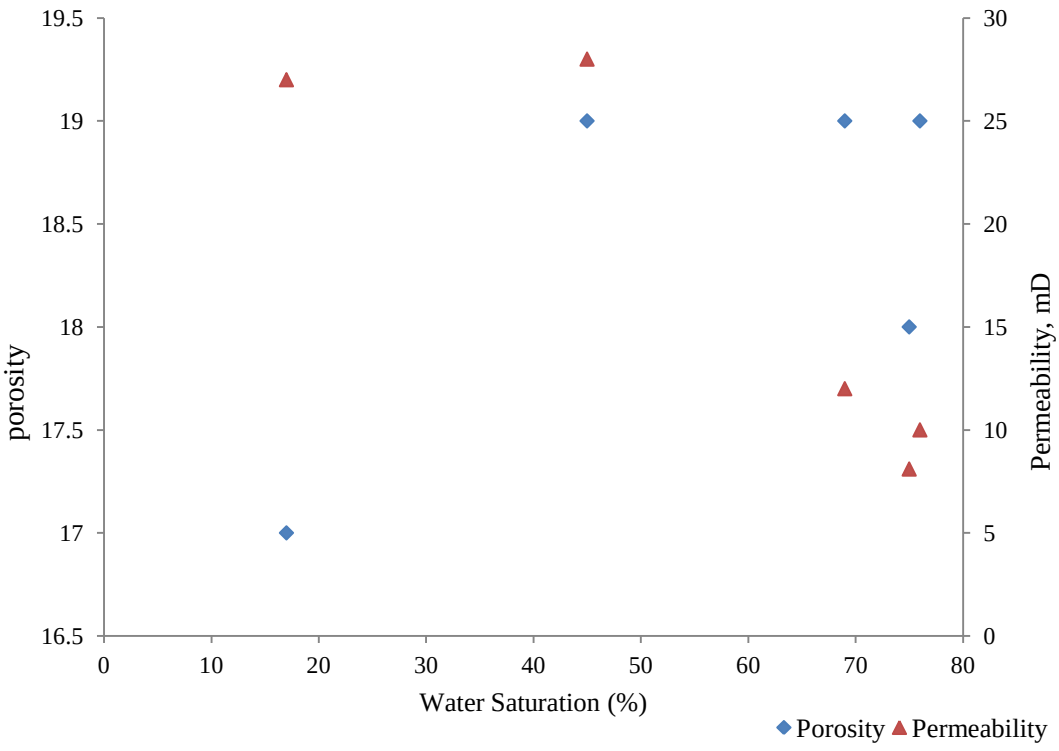

Fig. B1: porosity-Permeability Versus Water Saturation plot For Kwale Sand B

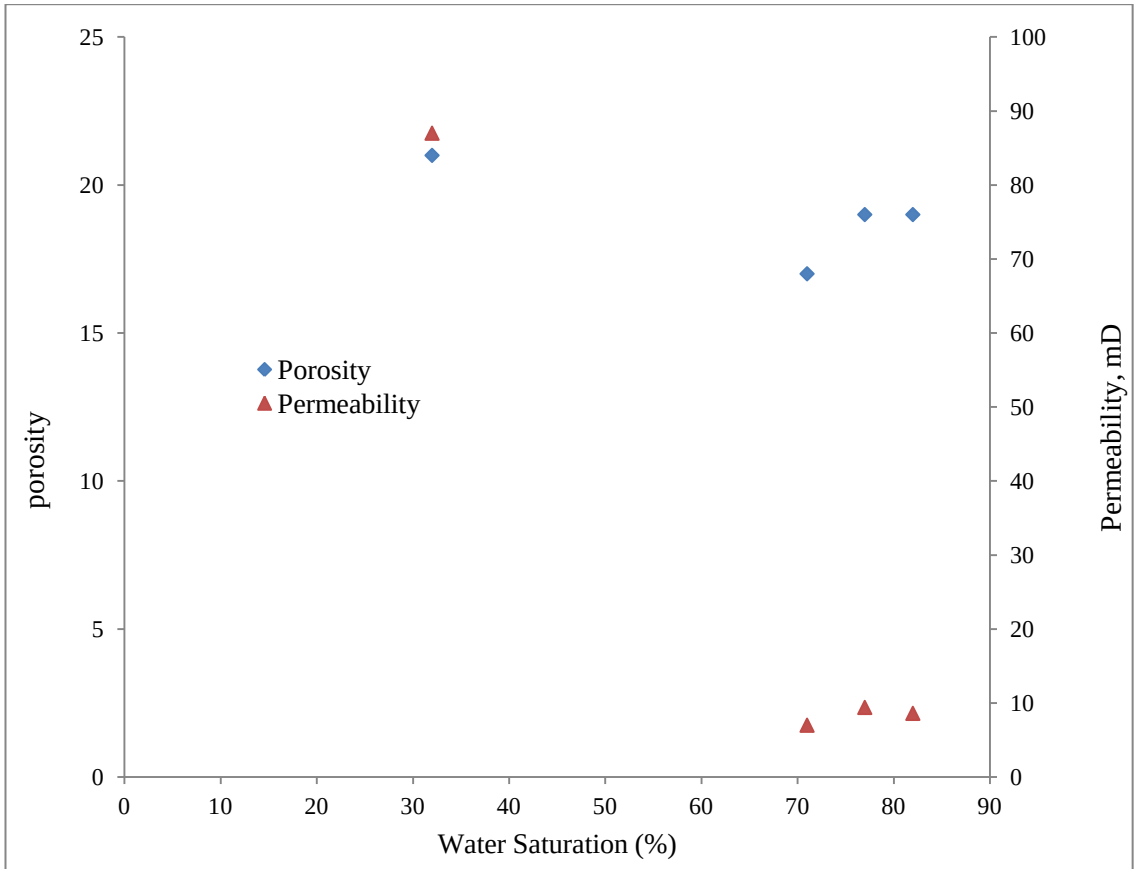

Fig.B2: Porosity-Permeability Versus Water Saturation plot For Kwale Sand C

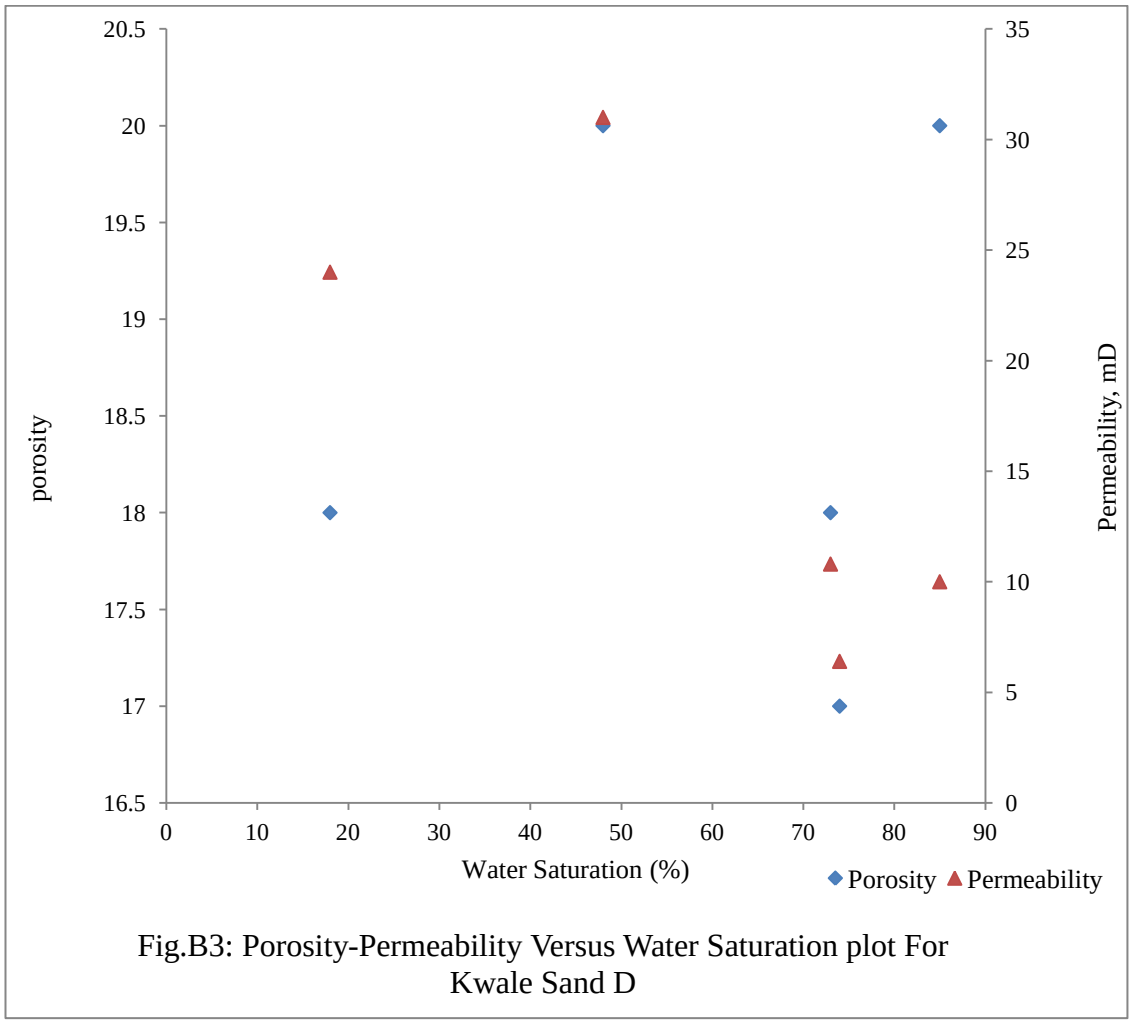

Fig.B3: Porosity-Permeability Versus Water Saturation plot For Kwale Sand D

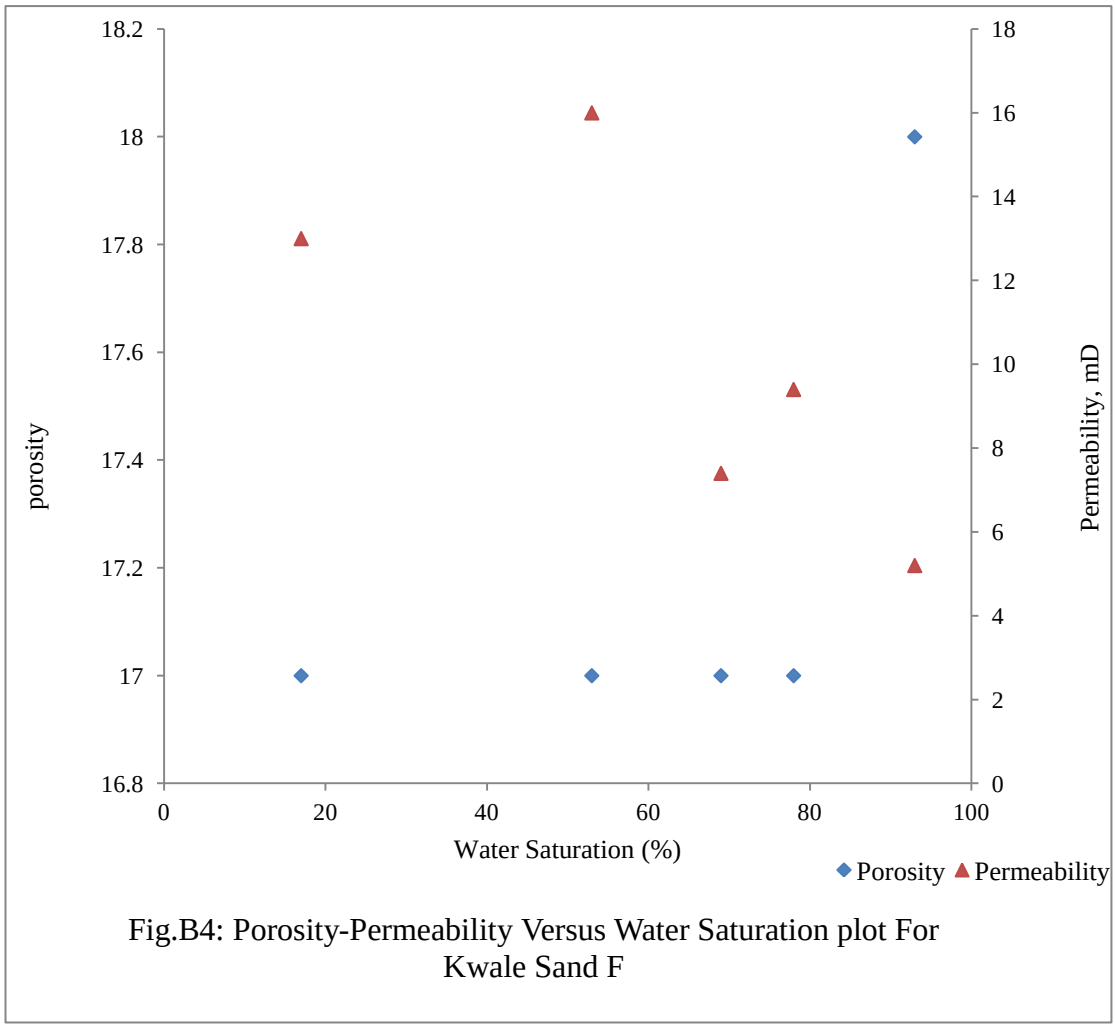

Fig.B4: Porosity-Permeability Versus Water Saturation plot For Kwale Sand F

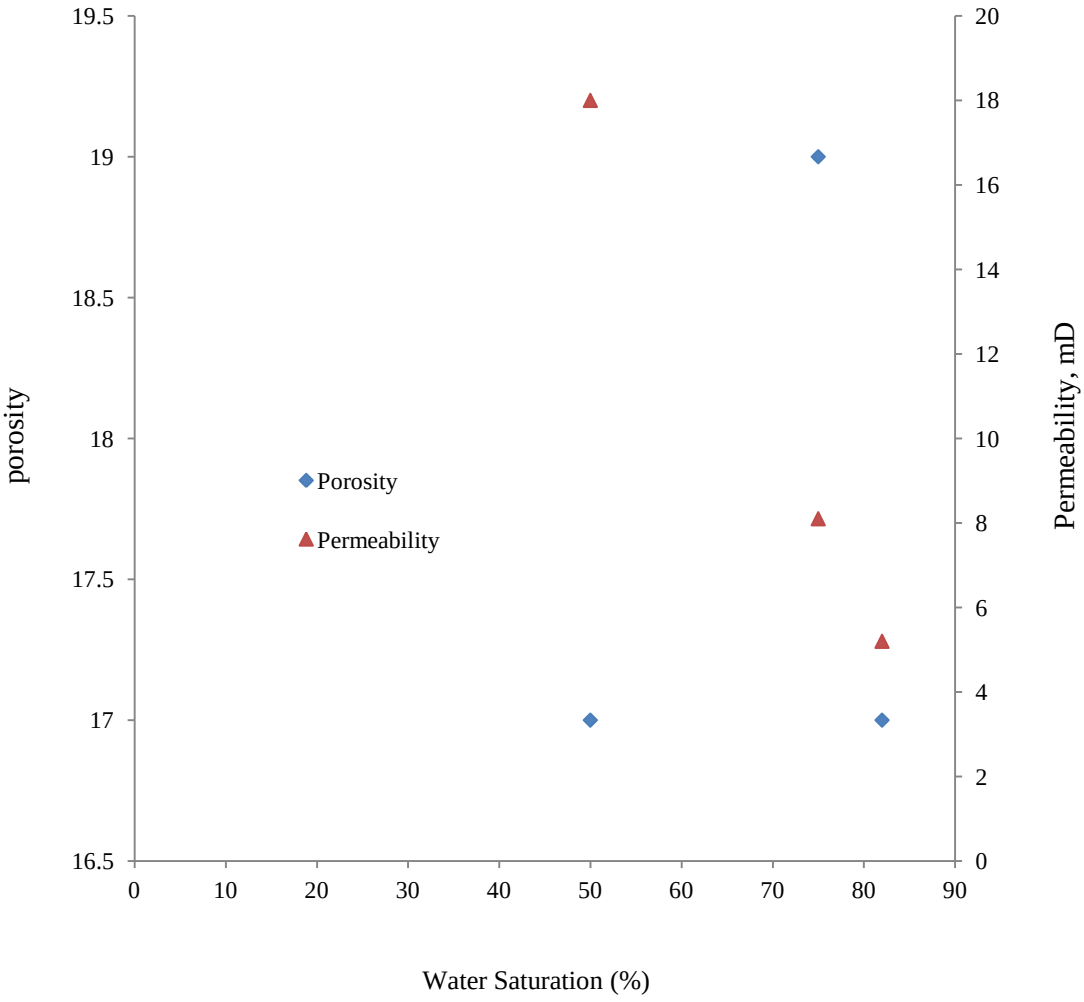

Fig.B5: Porosity-Permeability Versus Water Saturation plot For Kwale Sand G

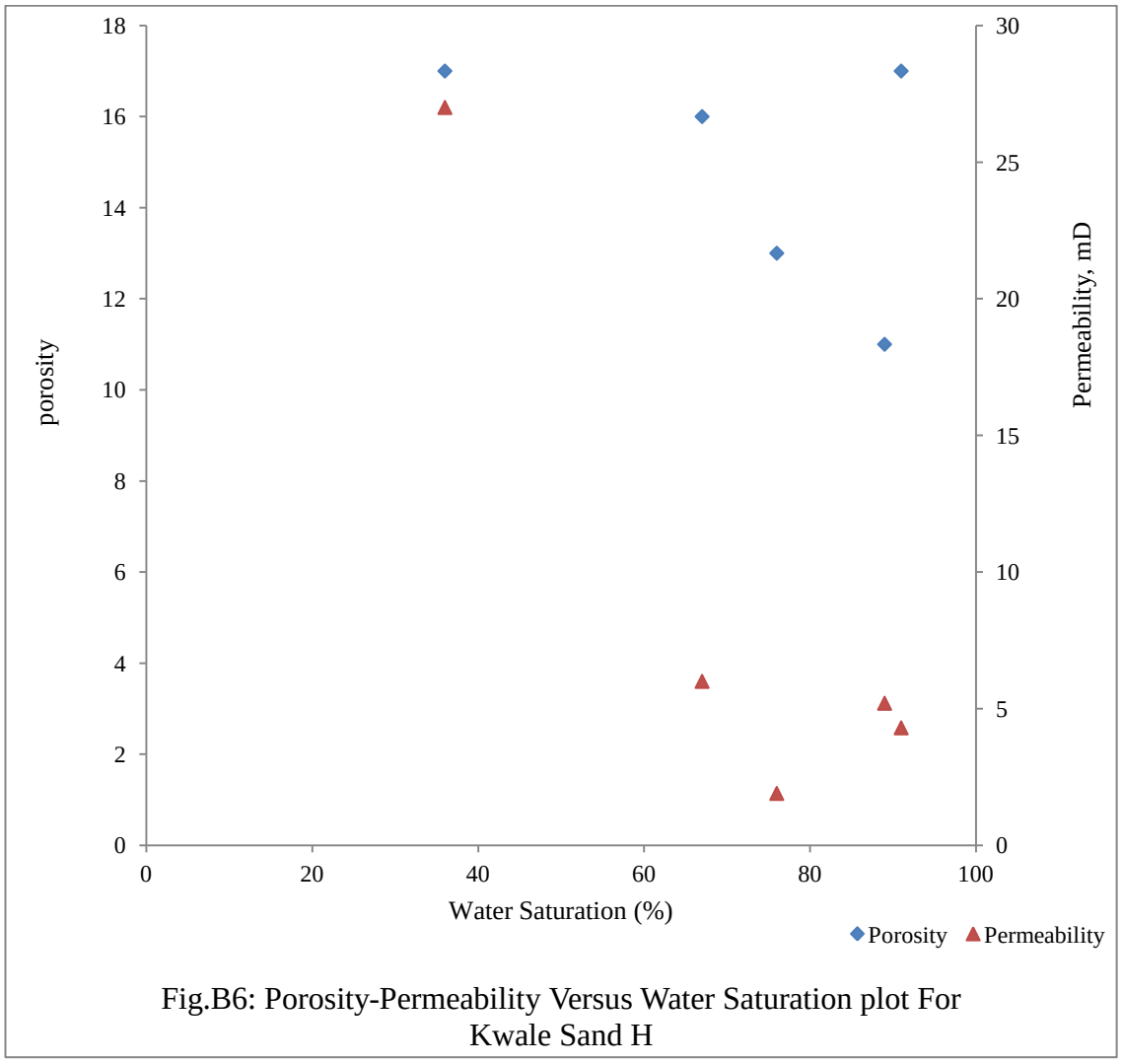

Fig.B6: Porosity-Permeability Versus Water Saturation plot For Kwale Sand H

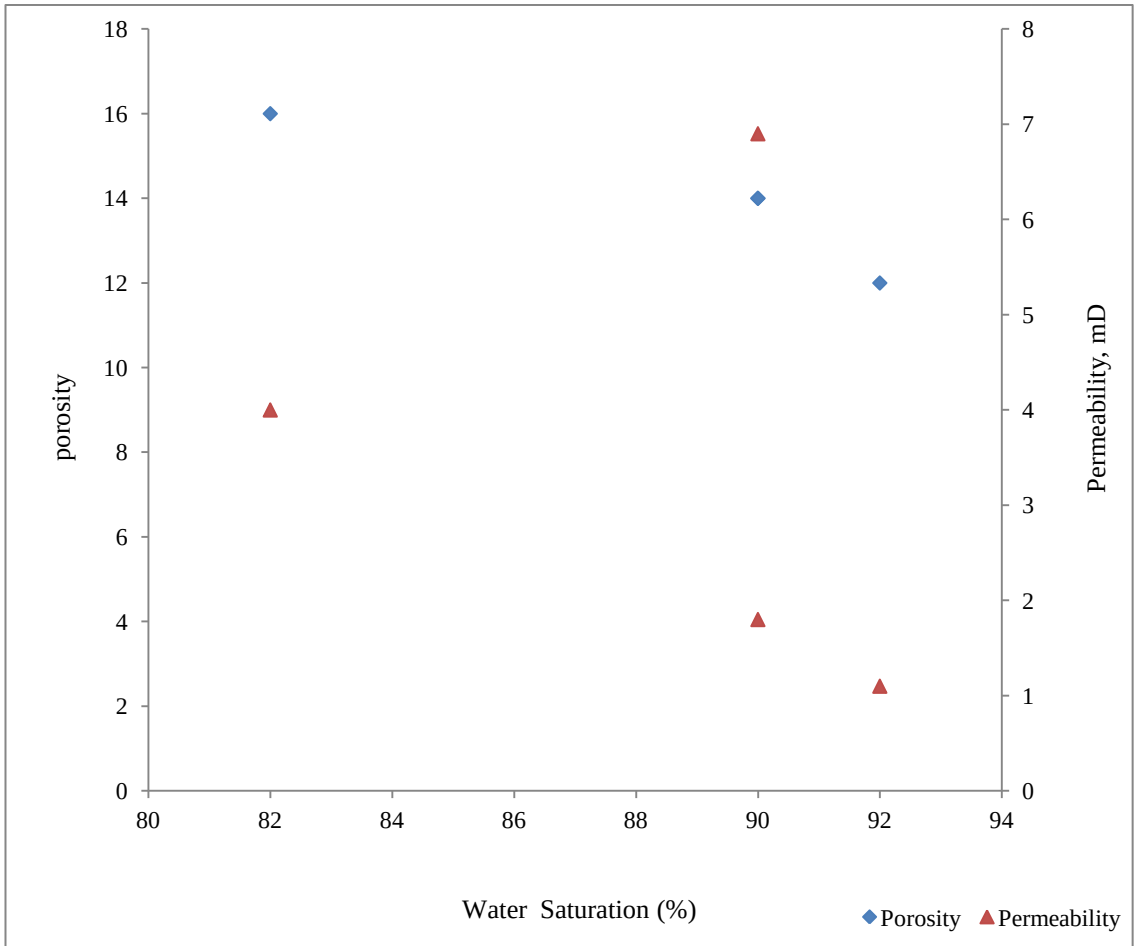

Fig.B7: Porosity-Permeability Versus Water Saturation plot For Kwale Sand J

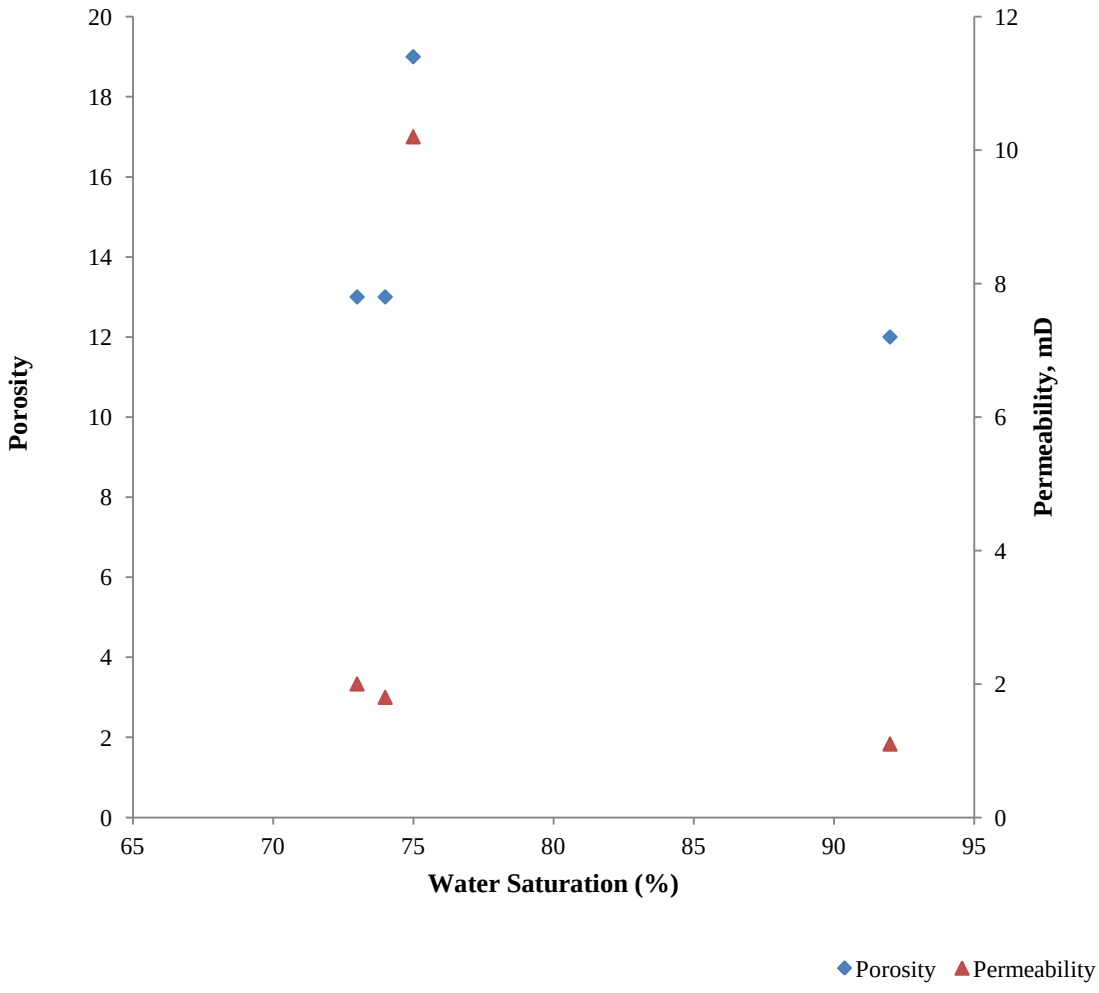

Fig.B8: Porosity-Permeability Versus Water Saturation plot For Kwale Sand K

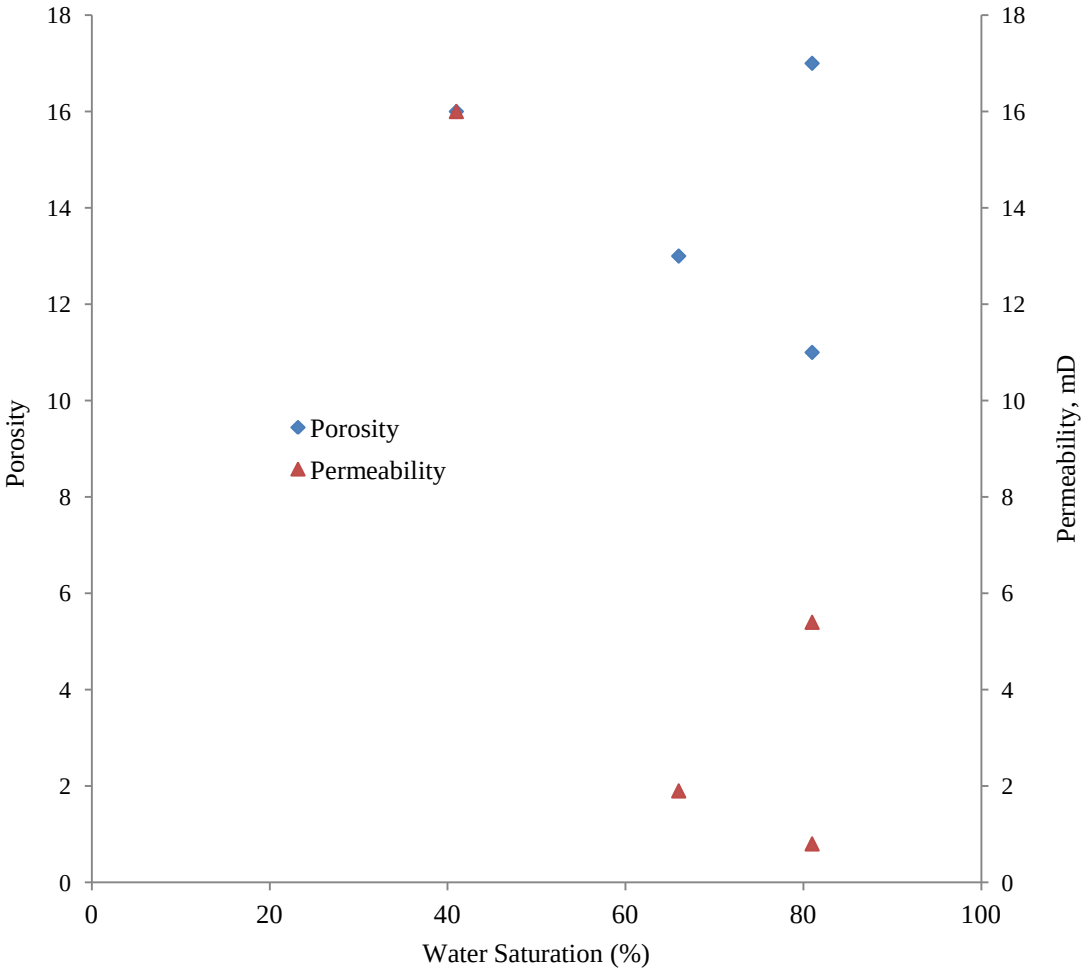

Fig.B9: Porosity-Permeability Versus Water Saturation plot For Kwale Sand L

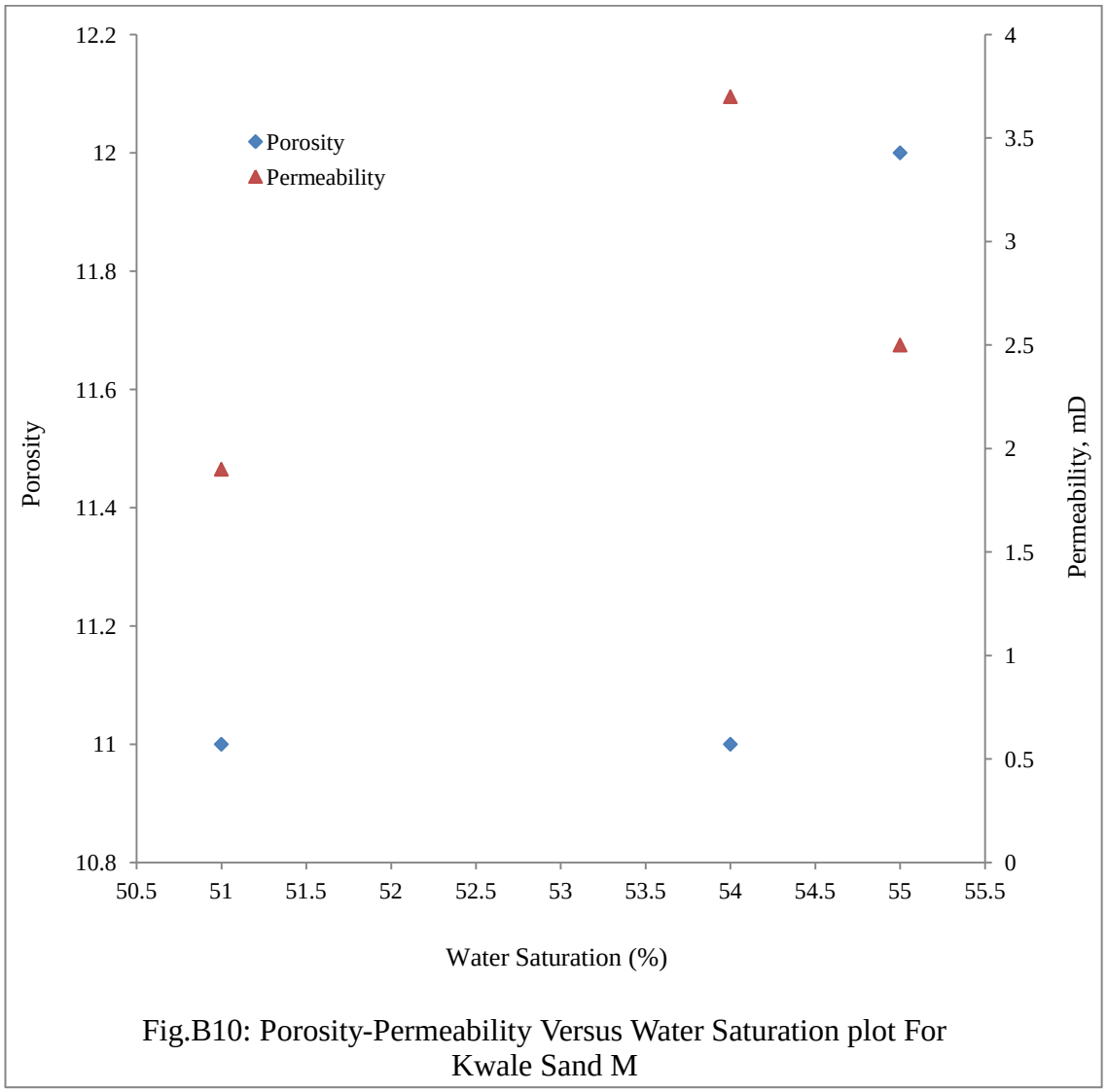

Fig.B10: Porosity-Permeability Versus Water Saturation plot For Kwale Sand M

B2: Best –fit Curves For Porosity-Water Saturation Plots For Kwale Sands.

The best-fit curves for the porosity-water saturation for the Kwale sands are as stated in Figs. B11 – B20. This was done for only Kwale sands with sufficient data, the relationship between the porosity and permeability is established graphically below with the equation that best described the relationship on each plot.

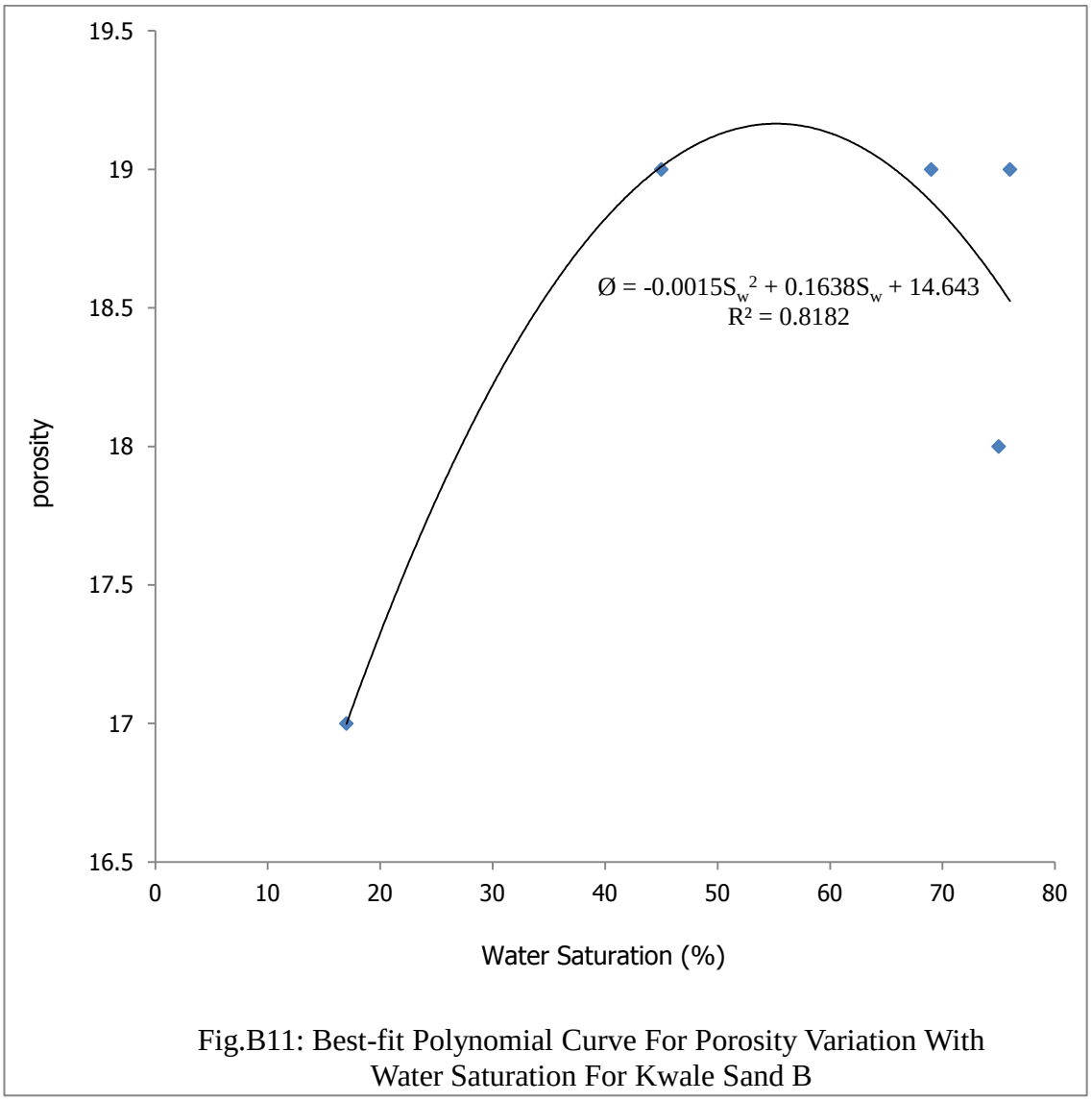

Fig.B11: Best-fit Polynomial Curve For Porosity Variation With Water Saturation For Kwale Sand B

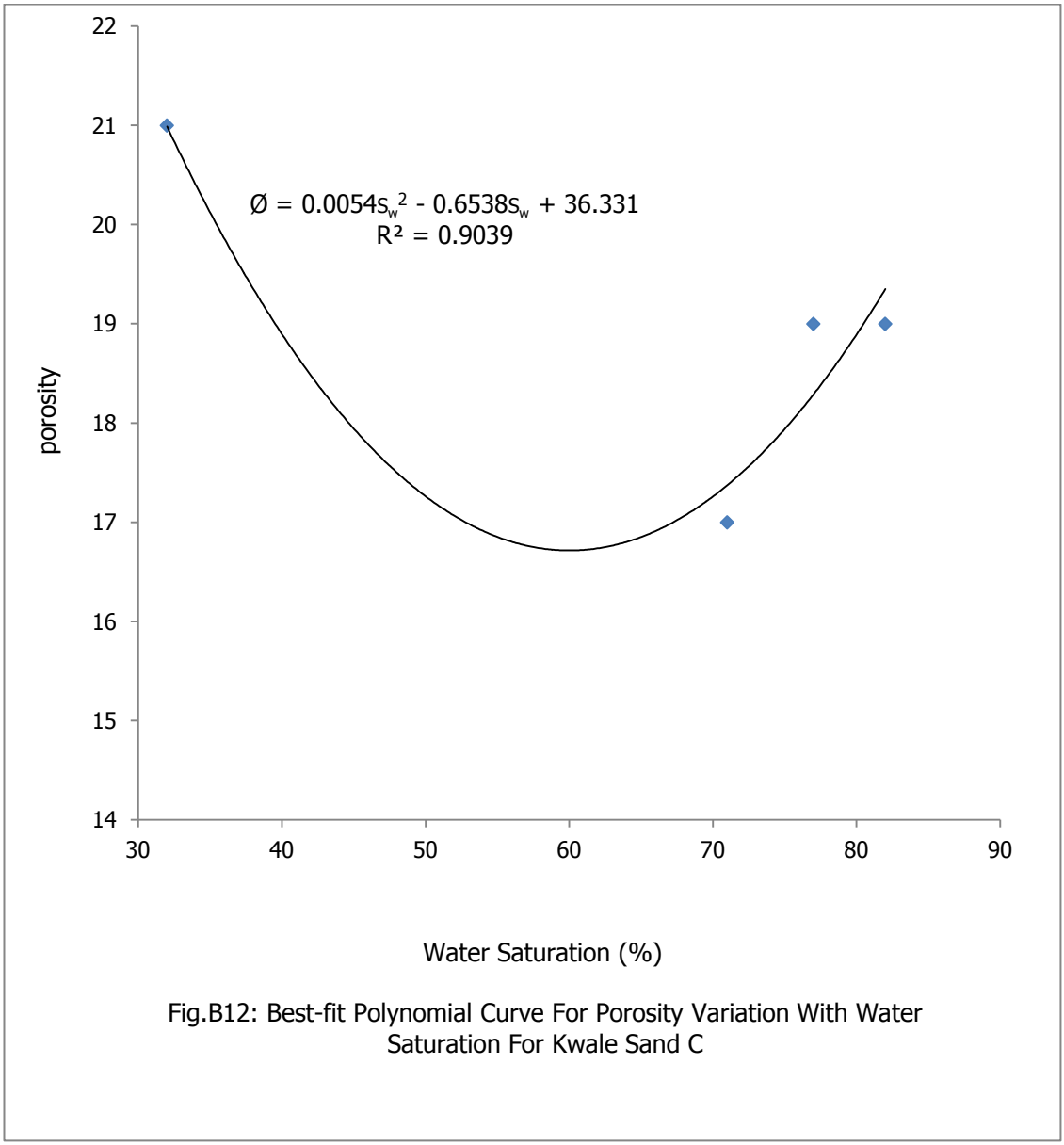

Fig.B12: Best-fit Polynomial Curve For Porosity Variation With Water Saturation For Kwale Sand C

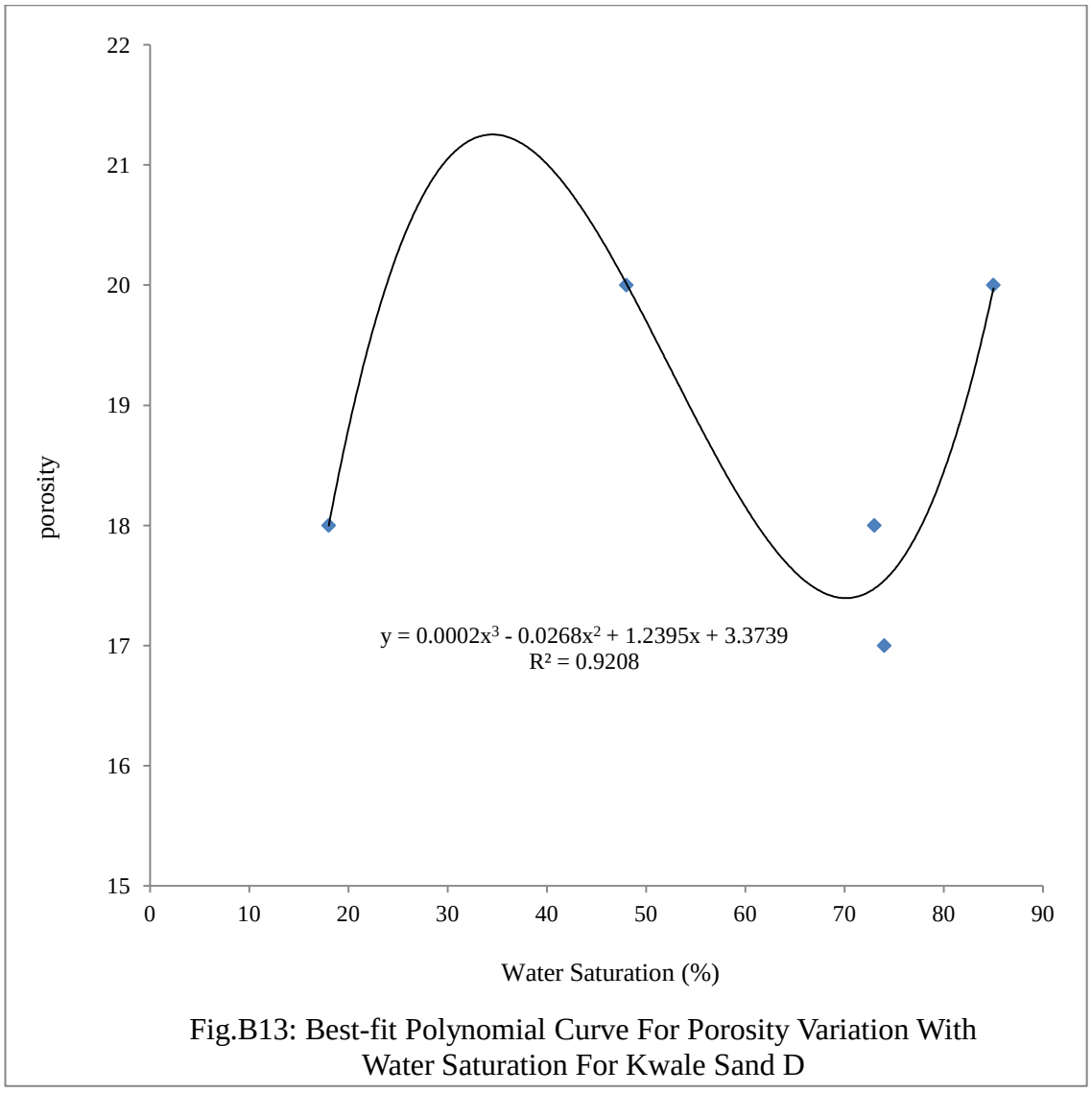

Fig.B13: Best-fit Polynomial Curve For Porosity Variation With Water Saturation For Kwale Sand D

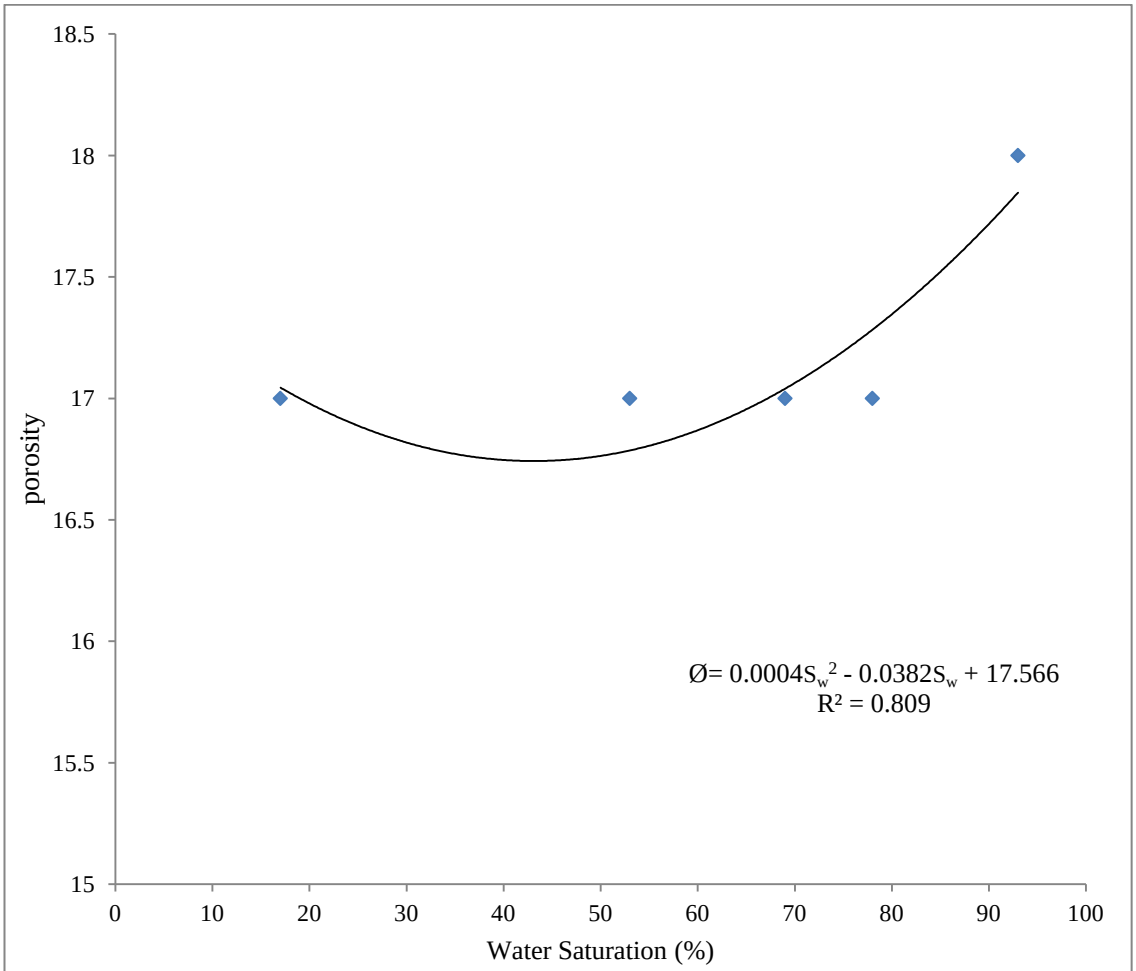

Fig.B14: Best-fit Polynomial Curve For Porosity Variation With Water Saturation For Kwale Sand F

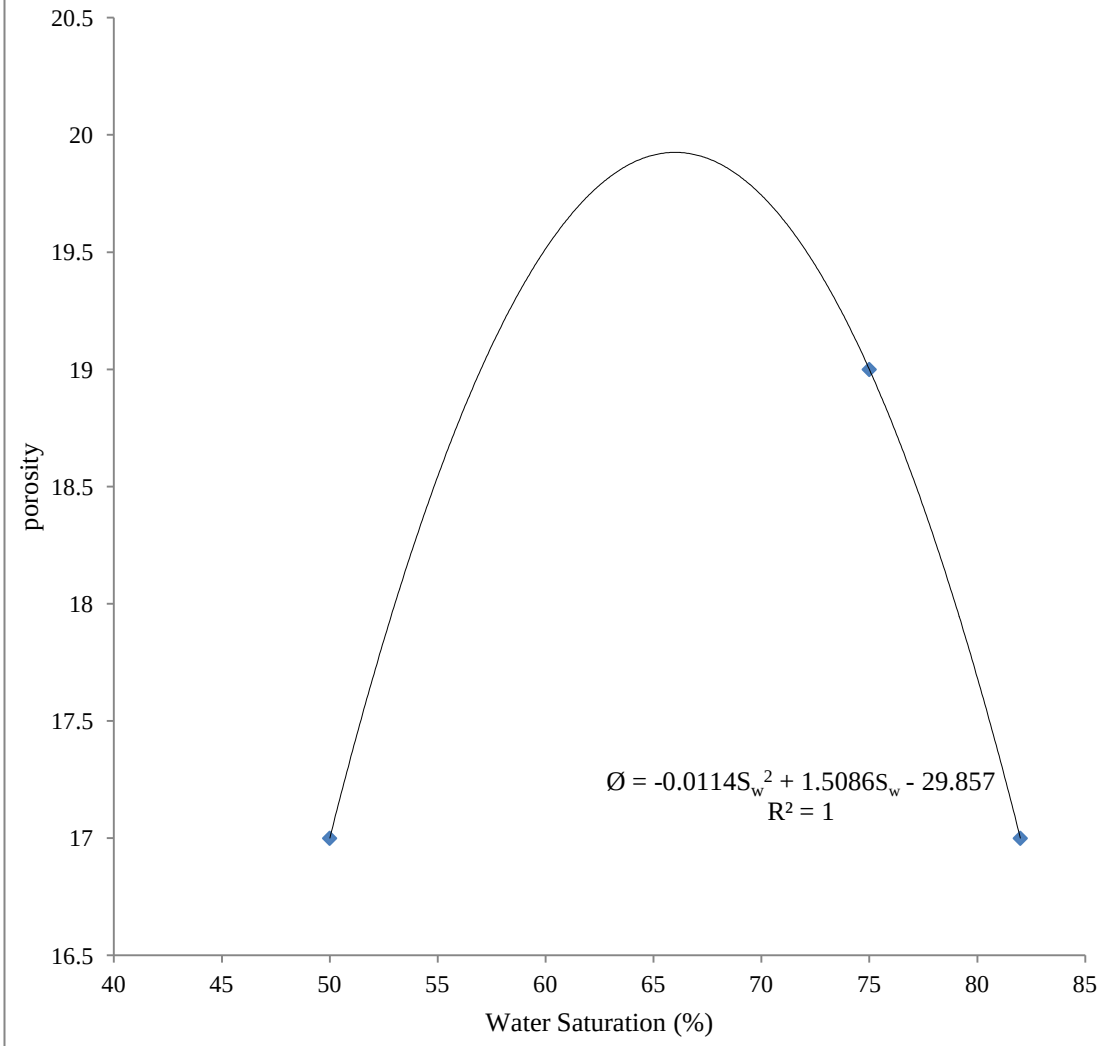

Fig.B15: Best-fit Polynomial Curve For Porosity Variation With Water Saturation For Kwale Sand G

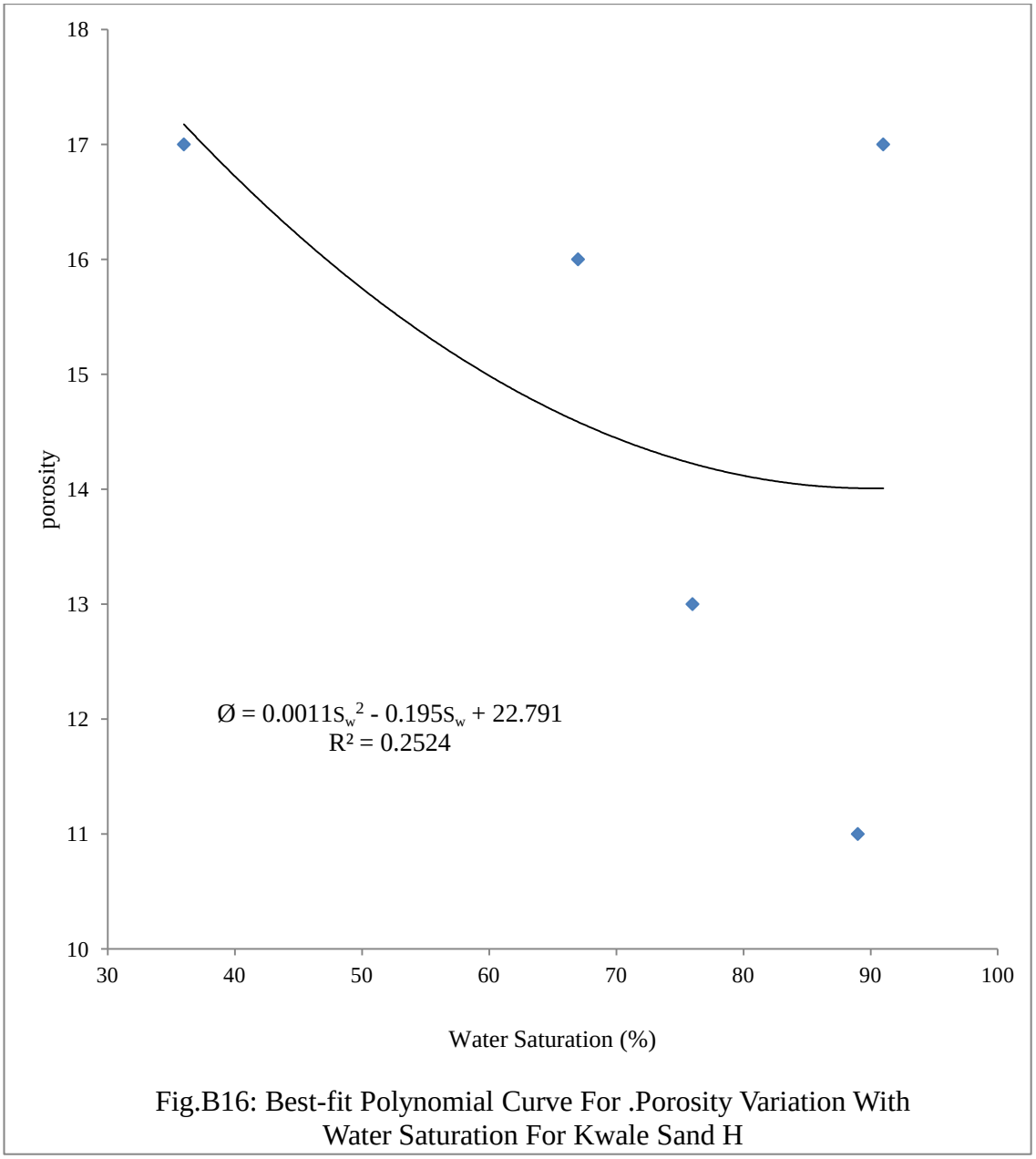

Fig.B16: Best-fit Polynomial Curve For .Porosity Variation With Water Saturation For Kwale Sand H

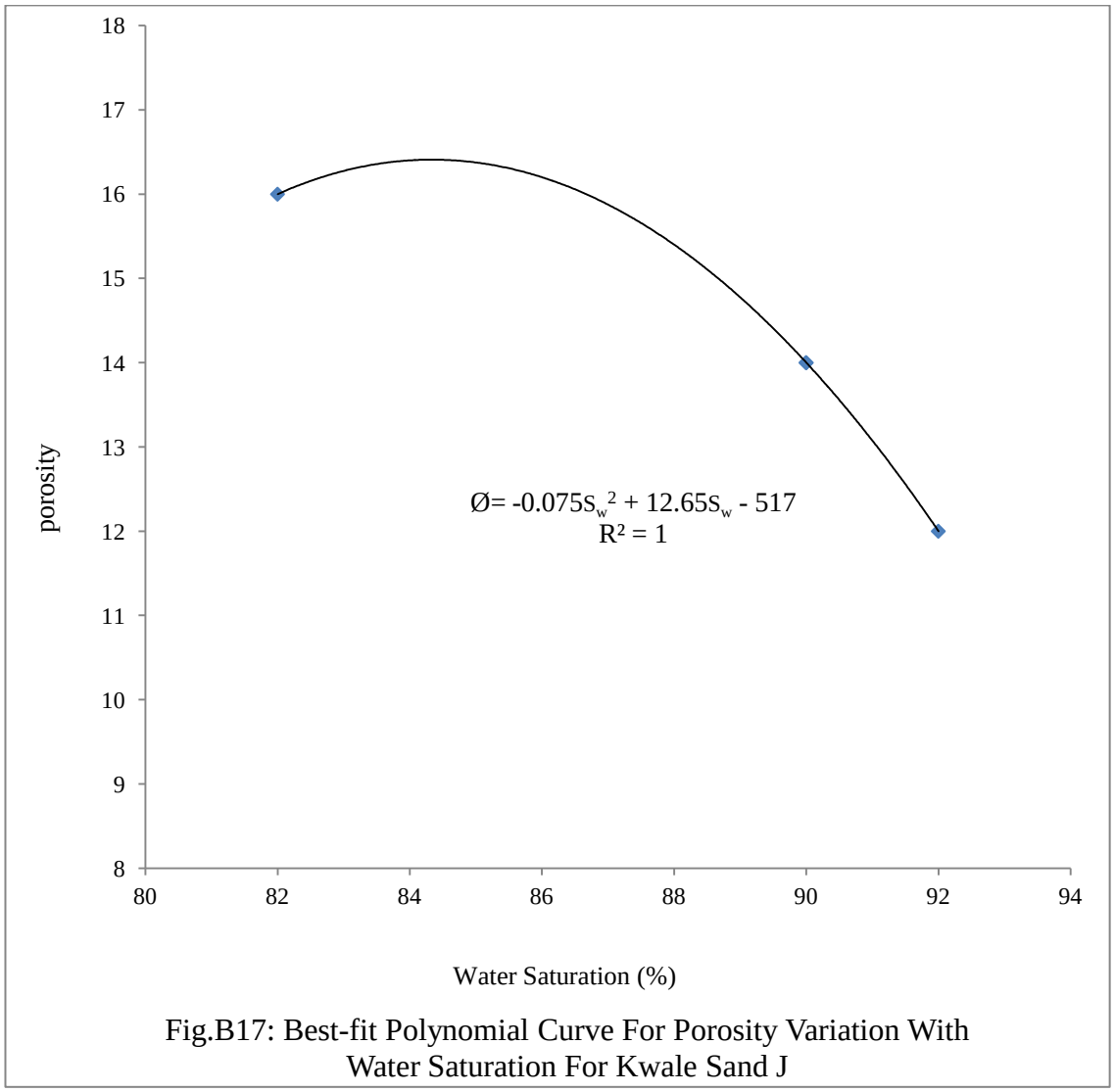

Fig.B17: Best-fit Polynomial Curve For Porosity Variation With Water Saturation For Kwale Sand J

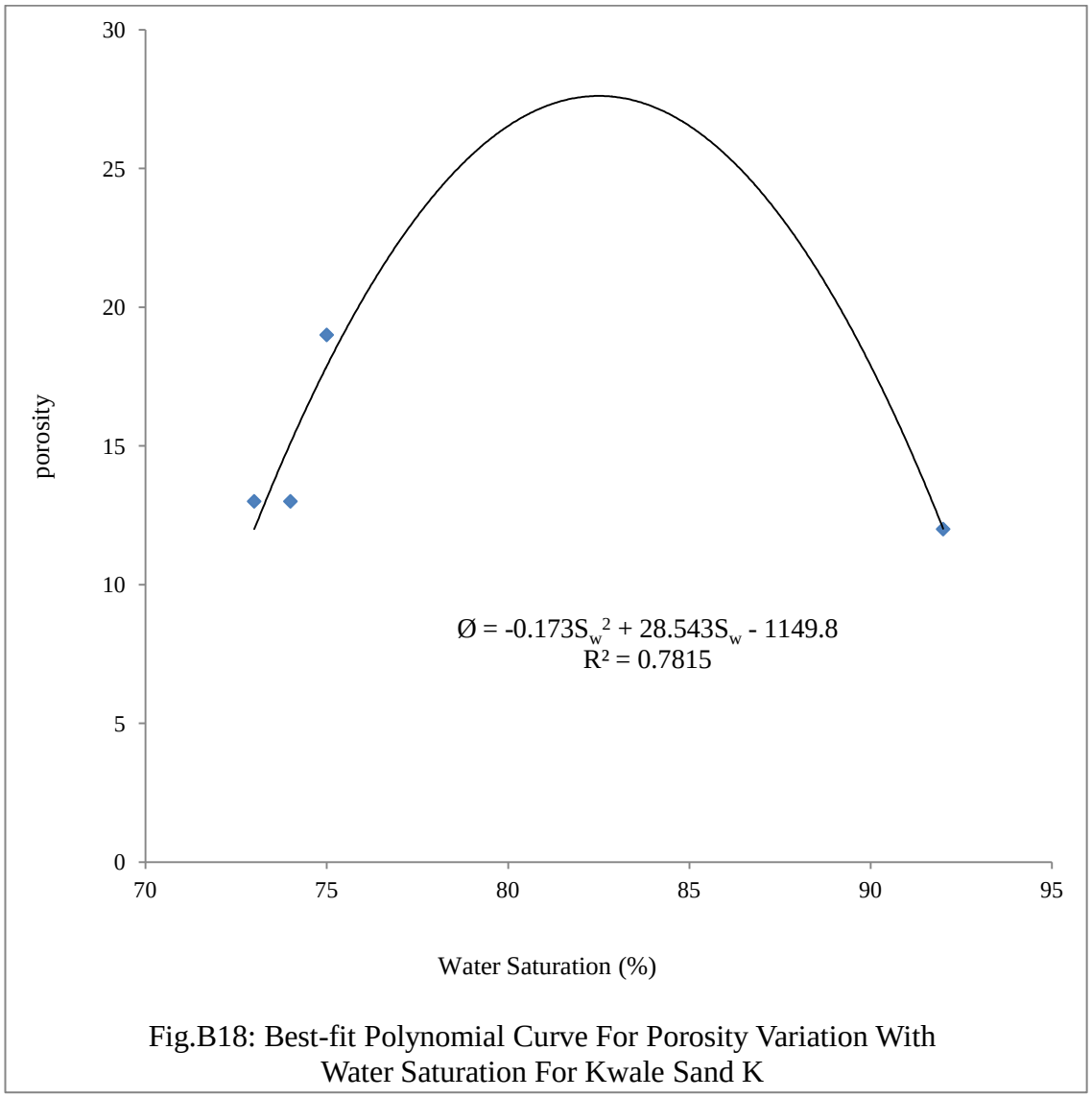

Fig.B18: Best-fit Polynomial Curve For Porosity Variation With Water Saturation For Kwale Sand K

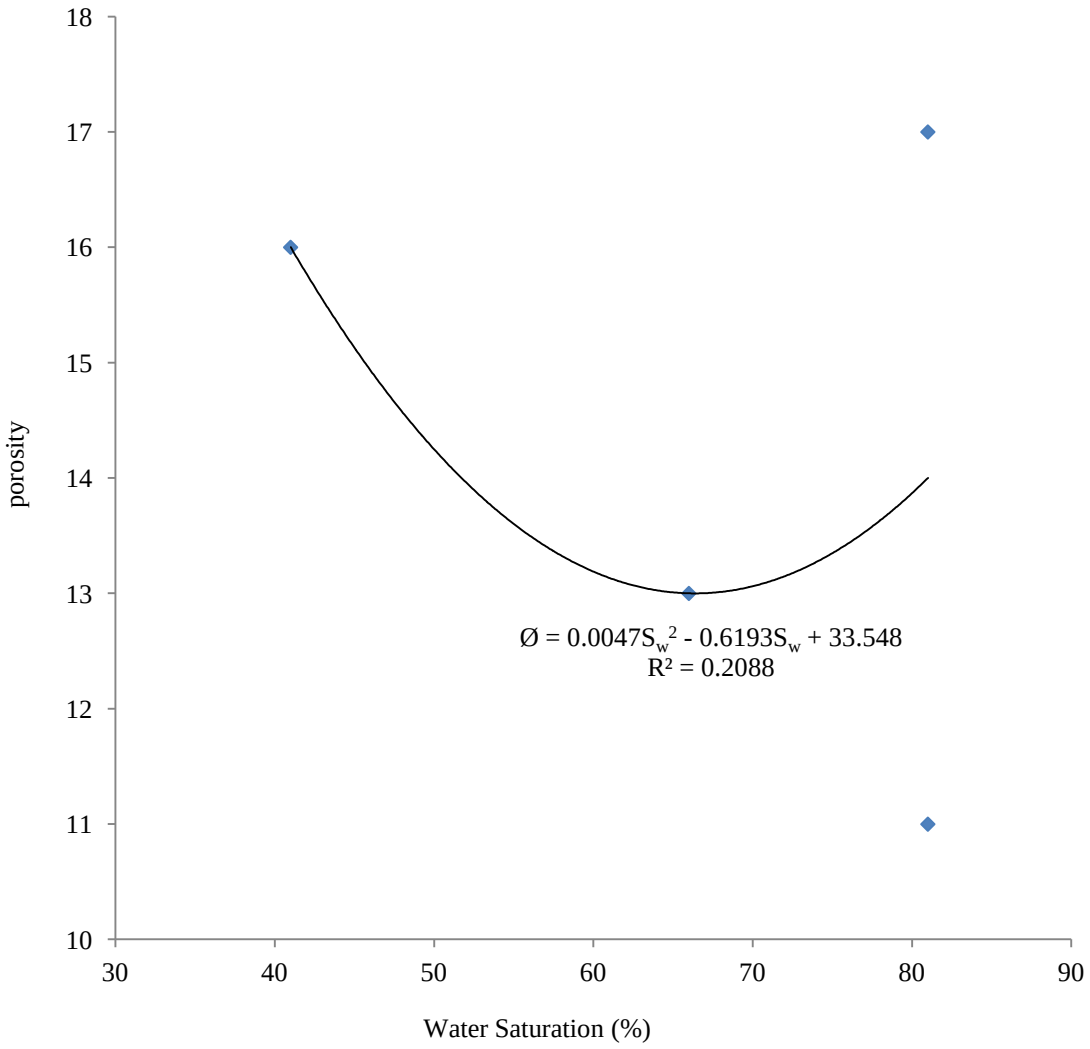

Fig.B19: Best-fit Polynomial Curve For Porosity Variation With Water Saturation For Kwale Sand L

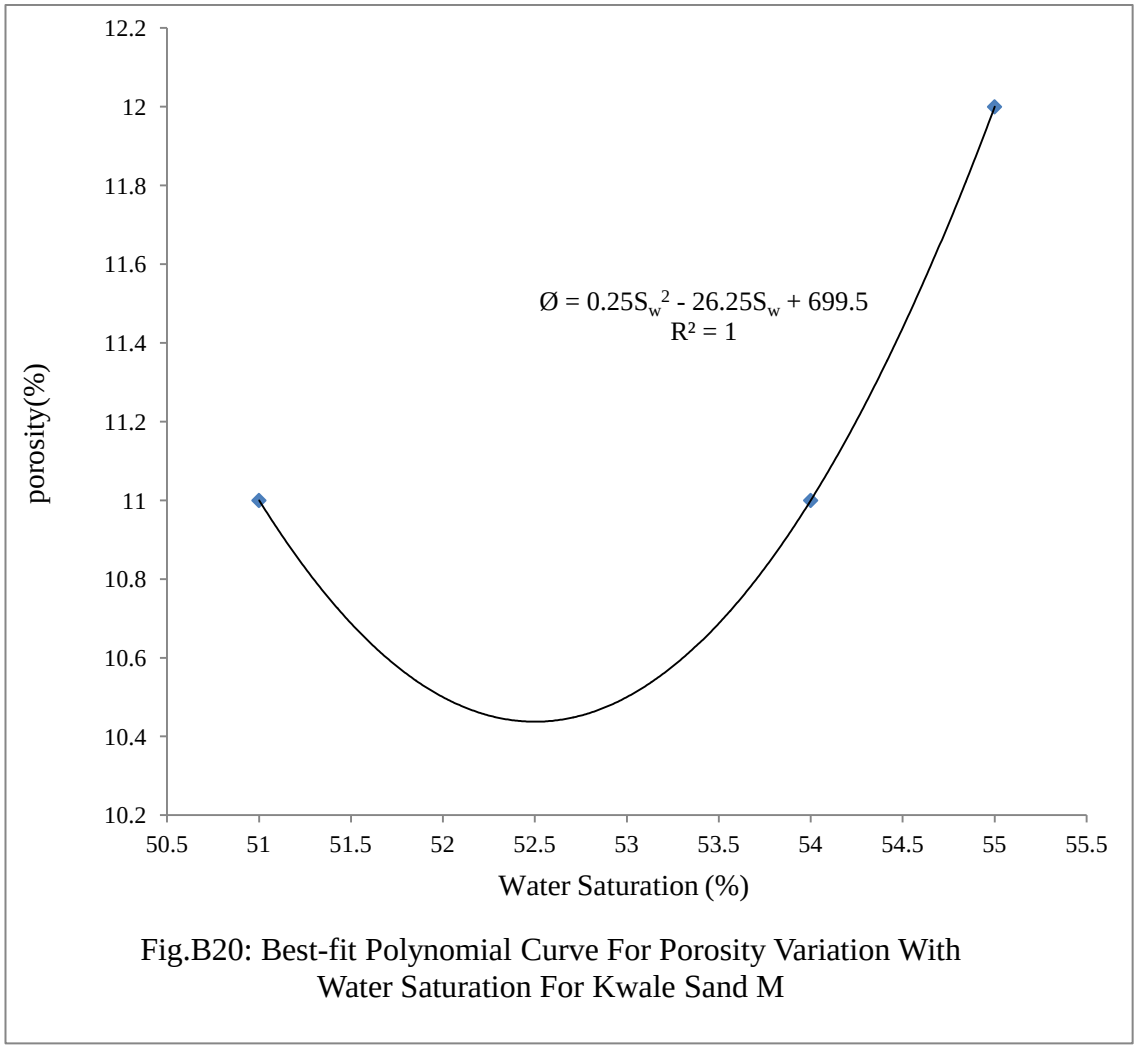

Fig.B20: Best-fit Polynomial Curve For Porosity Variation With Water Saturation For Kwale Sand M

B3. Irreducible Water Saturation Computation For Kwale Sands Using Timur, Tixier and Coates-Dumanoir Models

In this section, the models of Timur, tixier, Coates-Dumanoir and Aigbedion were used to compute the irreducible water saturation for the Kwale sands in order to know the most appropriate model for the sands in the absence of CO2 injection or changing porosity.

Table B.7.: Computed Irreducible Water Saturation For Kwale Well 1

Kwale-1						
Sand	Permeability	Porosity	Irreducible Water Saturation			Sw
			Timur Model	Tixier Model	Coates - Dumanior Model	
B	28	19	43.5443	32.4057	99.9853	45
C	87	21	32.9807	24.8221	99.9789	32
D	31	20	44.8553	35.9211	99.9861	48
F	16	17	46.0968	30.7063	99.9862	53
G	18	17	44.1948	28.9501	99.9853	50
H	27	17	38.2154	23.6377	99.9820	36
L	16	16	42.6332	25.6000	99.9844	41
M	4.6	14	56.0459	31.9849	99.9891	57

Table B. 8: Computed Irreducible Water Saturation For Kwale Well 2

Kwale-2						
Sand	Permeability	Porosity	Irreducible Water Saturation			Sw
			Timur Model	Tixier Model	Coates & Dumanior Model	
A	16	21	60.4642	57.8813	99.9909	74
B	8.1	18	63.2306	51.2289	99.9912	75
C	8.6	19	66.3322	58.4725	99.9919	82
D	10	20	67.1343	63.2456	99.9921	85
F	5.2	18	74.0085	63.9375	99.9930	93
G	8.1	19	67.7587	60.2502	99.9921	75
H	4.3	17	73.5967	59.2315	99.9928	91
I	4.8	16	65.5005	46.7390	99.9914	75
J	4	16	69.8824	51.2000	99.9922	82
K	10.2	19	62.4289	53.6909	99.9912	75
L	5.4	17	67.8804	52.8555	99.9920	81

Table B. 9.: Computed Irreducible Water Saturation For Kwale Well 5

Kwale-5						
Sand	Permeability	Porosity	Irreducible Water Saturation			Sw
			Timur Model	Tixier Model	Coates & Dumanior Model	
B	12	19	58.9217	49.5006	99.9904	69
C	9.4	19	64.2684	55.9290	99.9915	77
D	10.8	18	57.0782	44.3655	99.9899	73
F	9.4	17	55.7334	40.0611	99.9894	78
G	5.2	17	68.7963	53.8623	99.9921	82
H	5.2	11	39.3294	14.5921	99.9812	89
I	6.5	17	63.5526	48.1759	99.9912	71
J	6.9	14	48.4985	26.1156	99.9866	90
K	1.8	13	71.1591	40.9387	99.9921	74
L	1.9	13	69.8065	39.8468	99.9918	66
M	1.9	11	56.3666	24.1402	99.9886	51

Table B. 10.: Computed Irreducible Water Saturation For Kwale Well 6

Kwale-6						
Sand	Permeability	Porosity	Irreducible Water Saturation			Sw
			Timur Model	Tixier Model	Coates & Dumanior Model	
B	10	19	62.8701	54.2252	99.9912	76
C	7	17	61.8998	46.4235	99.9908	71
D	6.4	17	63.9039	48.5508	99.9912	74
F	7.4	17	60.6883	45.1514	99.9906	69
G	7.4	17	60.6883	45.1514	99.9906	74
H	6	16	60.5044	41.8046	99.9904	67
I	5.1	15	59.0197	37.3619	99.9900	63
J	1.8	14	78.2217	51.1314	99.9932	90
K	2	13	68.5466	38.8378	99.9916	73
L	0.8	11	76.6500	37.2026	99.9926	81
M	2.5	12	57.1510	27.3221	99.9890	55

Table B. 11.: Computed Irreducible Water Saturation For Kwale Well 8

Kwale-8						
Sand	Permeability	Porosity	Irreducible Water Saturation			Sw
			Timur Model	Tixier Model	Coates & Dumanior Model	
H	1.9	13	69.8065	39.8468	99.9918	76
I	1.1	12	76.5084	41.1896	99.9927	92
J	1.1	12	76.5084	41.1896	99.9927	92
K	1.1	12	76.5084	41.1896	99.9927	92
M	3.7	11	44.4310	17.2988	99.9841	54

Table B. 12.: Computed Irreducible Water Saturation For Kwale Well 10

Kwale-10						
	Permeability	Porosity	Irreducible Water Saturation			Sw
			Timur Model	Tixier Model	Coates & Dumanior Model	
A	37	17	34.1207	20.1923	99.9790	17
B	27	17	38.2154	23.6377	99.9820	17
D	24	18	42.9175	29.7613	99.9849	18
F	13	17	49.6470	34.0655	99.9875	17
G	68	16	25.2955	12.4178	99.9678	16

From Tables B7 to B12 above, it was discovered that Timur and Tixier gave reasonable irreducible water saturation values for a hydrocarbon-water reservoir for all the sands. Coates-Dumanior gave impracticable irreducible water saturation. With consideration to the values of measured water saturation, on the average, Timur gave more acceptable irreducible water saturation than that of Tixier. Timur model is therefore adopted for the irreducible water saturation computation for the Kwale reservoir.

The petro-physical geometric average values for the Kwale sand is calculated as follows.

Table B13: Calculated Geometric Average Properties For Kwale Sands

Sand	Porosity Ø	Permeability K	Water Saturation	Timur Swirr
B	18.270	16.900	57.054	53.538
C	20.429	30.105	64.474	51.283
D	18.920	16.723	59.742	58.121
F	17.102	10.142	62.360	59.760
G	16.515	20.490	60.267	38.932
H	15.991	9.595	70.243	53.001
J	14.420	3.554	88.143	69.371
K	16.980	4.498	77.895	88.332
L	15.822	6.689	66.351	62.004
M	11.309	2.694	53.382	46.673

With consideration to the average initial porosity for the Kwale sandstone samples used in this research, sand C, according to Table B7, has closest porosity values to the measured porosity of the samples 1A, 1B, 2A and 2B and its irreducible water saturation equation based on Timur model analysis is therefore adopted for the analysis of the irreducible water saturation equation for the samples used in this research.

Table B14: Kwale Sand C Permeability, Porosity & Irreducible water Saturation

Water Saturation, Sw	Permeability K	Porosity Ø	Timur Irreducible Water Saturation, S_{wirr}
32	87	0.21	0.32981
82	8.6	0.19	0.66332
77	9.4	0.19	0.64268
71	7	0.17	0.619

The best-fit curve and equation for the Kwale sand C is as shown in Fig.B16.

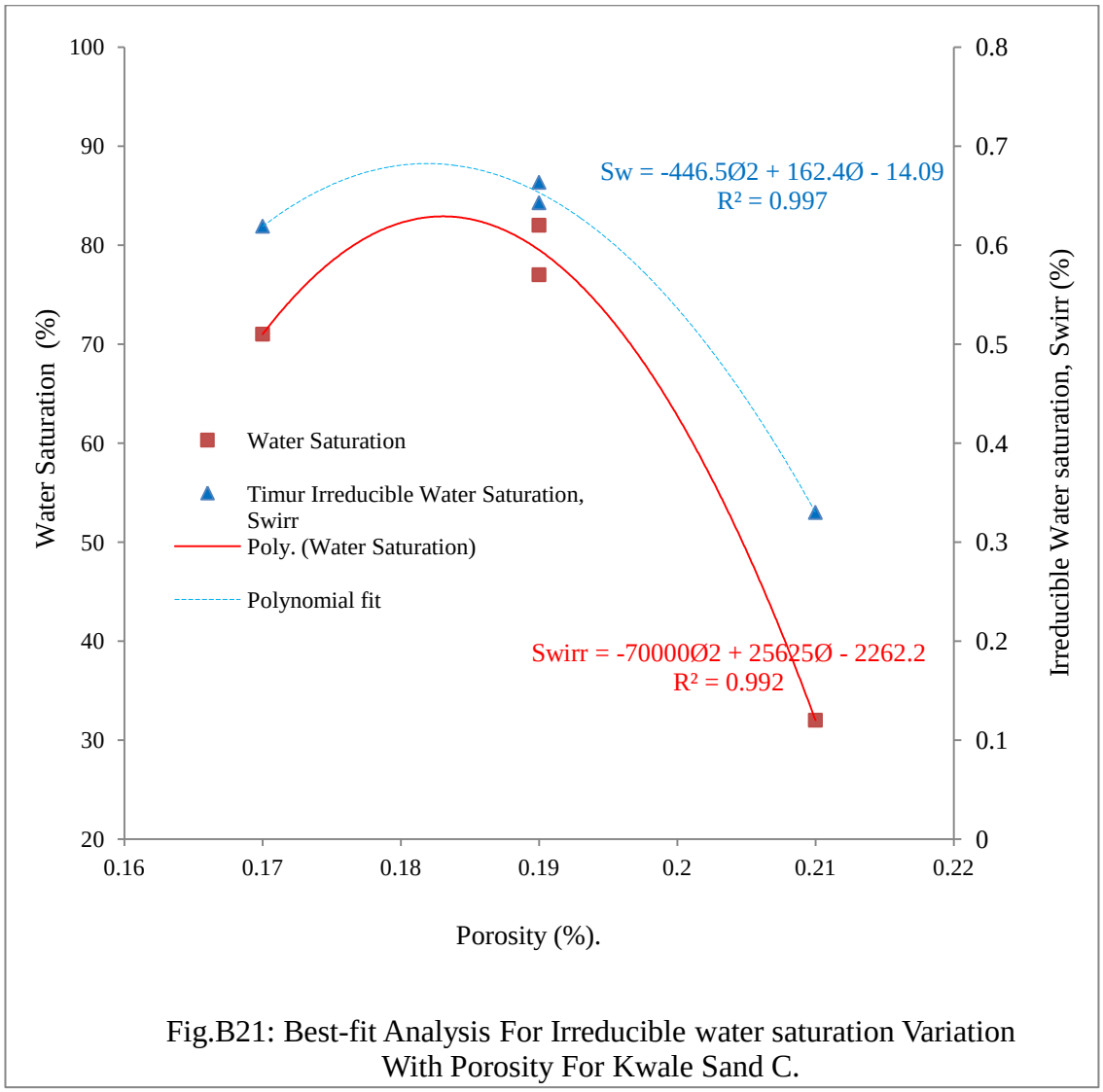

Fig.B21: Best-fit Analysis For Irreducible water saturation Variation With Porosity For Kwale Sand C.

From the above, exponential fit is more applicable practically, though it gave less root mean square than that of polynomial fit, but it shows the expected decrease in irreducible water saturation as porosity increases in non- producing storage reservoir. Volume of water is expected to either remain constant or reduce while the volume of injected fluid increases in that reservoir. This will result into lower water saturation and corresponding lower irreducible water saturation with increasing formation of secondary porosity. All this is based on the assumption that there was no water encroachment from nearby reservoir and this is the expected situation in this research as a link to the reservoir will result in escape of injected or stored CO_2.

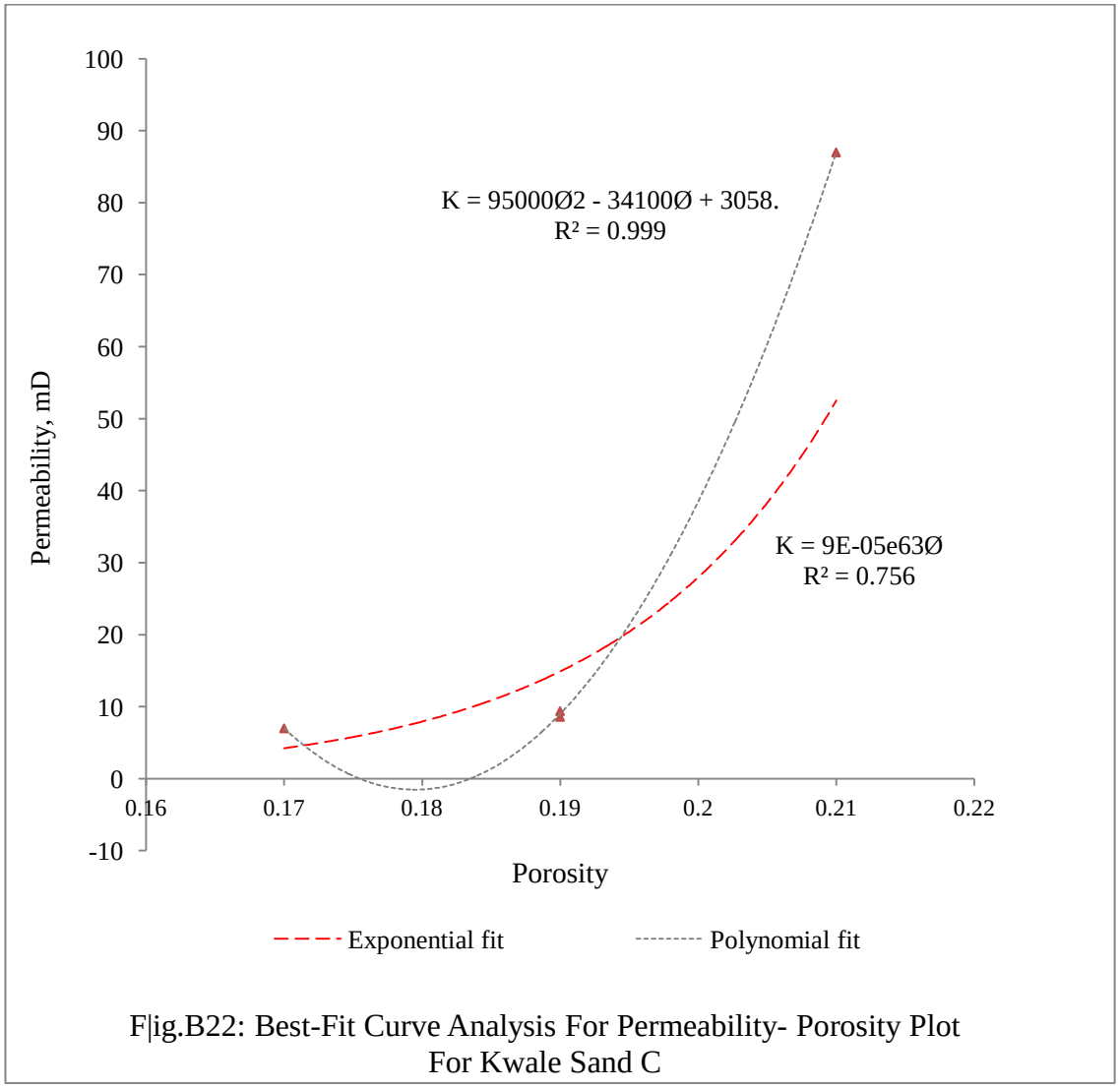

F|ig.B22: Best-Fit Curve Analysis For Permeability- Porosity Plot For Kwale Sand C

Analysis of available data for some well in Kwale field shows that Kwale Sands have unique relationship between the porosity and water saturations. Model equations are being proposed from the analysis of the available data and these are as stated below.

For Kwale Sand B, the porosity variation with water saturation is best described by a proposed model equation of 4.1

$$\varphi = -0.0015Sw^2 + 0.1638Sw + 14.643 \quad 4.1$$

For Kwale sand C, the porosity reduces with increasing water saturation until a minimum at Sw of 0.6 and thereafter increases. Proposed model equation is as follows

$$\varphi = 0.0054Sw^2 - 0.6538Sw + 36.331 \quad 4.2$$

For Kwale sand D, the analysis shows that the porosity reduces with increasing water saturation until a minimum at S_w of 0.7 and thereafter increases

$$\varphi = 0.0002Sw^3 - 0.0268Sw^2 + 1.2395Sw + 3.3739 \quad 4.3$$

For Kwale sand F, porosity increases gradually with water saturation. The proposed model equation is as follows:

$$\varphi = 0.0004Sw^2 - 0.0382Sw + 17.566 \quad 4.4$$

For Kwale sand G, porosity also increases gradually with water saturation. The proposed model equation is as follows:

$$\varphi = -0.0004Sw^2 + 0.069Sw + 14.953 \quad 4.6$$

Kwale Sand H has porosity reducing sharply with increasing water saturation until a minimum at S_w=0.8 after which it increases again. The proposed model equation is:

$$\varphi = 0.0008Sw^3 - 0.1501Sw^2 + 9.1334Sw - 153.25 \quad 4.7$$

Kwale Sand I has high water saturation and the porosity was observed to increase with water saturation between Sw of 0.6 and 0.7 and then drops. The proposed model equation is

$$\varphi = -0.0129Sw^2 + 1.8974Sw - 53.012 \quad 4.8$$

Like Sand I, Kwale Sand J has high water saturation but the porosity was observed to decrease sharply with water saturation and the model equation for the Sand is

$$\varphi = -0.075Sw^2 + 12.65Sw – 517 \quad 4.9$$

Kwale Sank K has almost constant porosity of 13% for water saturation range except an observed abnormality at S_w of 0.75. The sand was observed to have very high S_w with a minimum of 75%. The proposed model equation is

$$\varphi = -0.0551Sw + 17.076 \quad 4.10$$

APPENDIX C

Presented in this appendix are the measured porosity data and calculated average porosity and permeability data for the various samples used in the research.

C.1. Measured/calculated Properties Kwale Sandstone Samples

Table C 1: Porosity Variation With Time For Kwale Sandstone rock Sample 1A in Crude Oil Zone

Time (hours)	Grain volume, cc	Pore volume. cc	Porosity
24	3.84	1.5	0.280899
48	3.7	1.64	0.307116
72	3.56	1.78	0.333333
96	3.51	1.83	0.342697
120	3.49	1.85	0.346442
144	3.43	1.91	0.357678
168	3.3	2.04	0.382022
192	3.2	2.14	0.400749
216	3.1	2.24	0.419476
240	2.99	2.35	0.440075
264	2.89	2.45	0.458801
288	2.82	2.52	0.47191
312	2.68	2.66	0.498127
336	2.57	2.77	0.518727

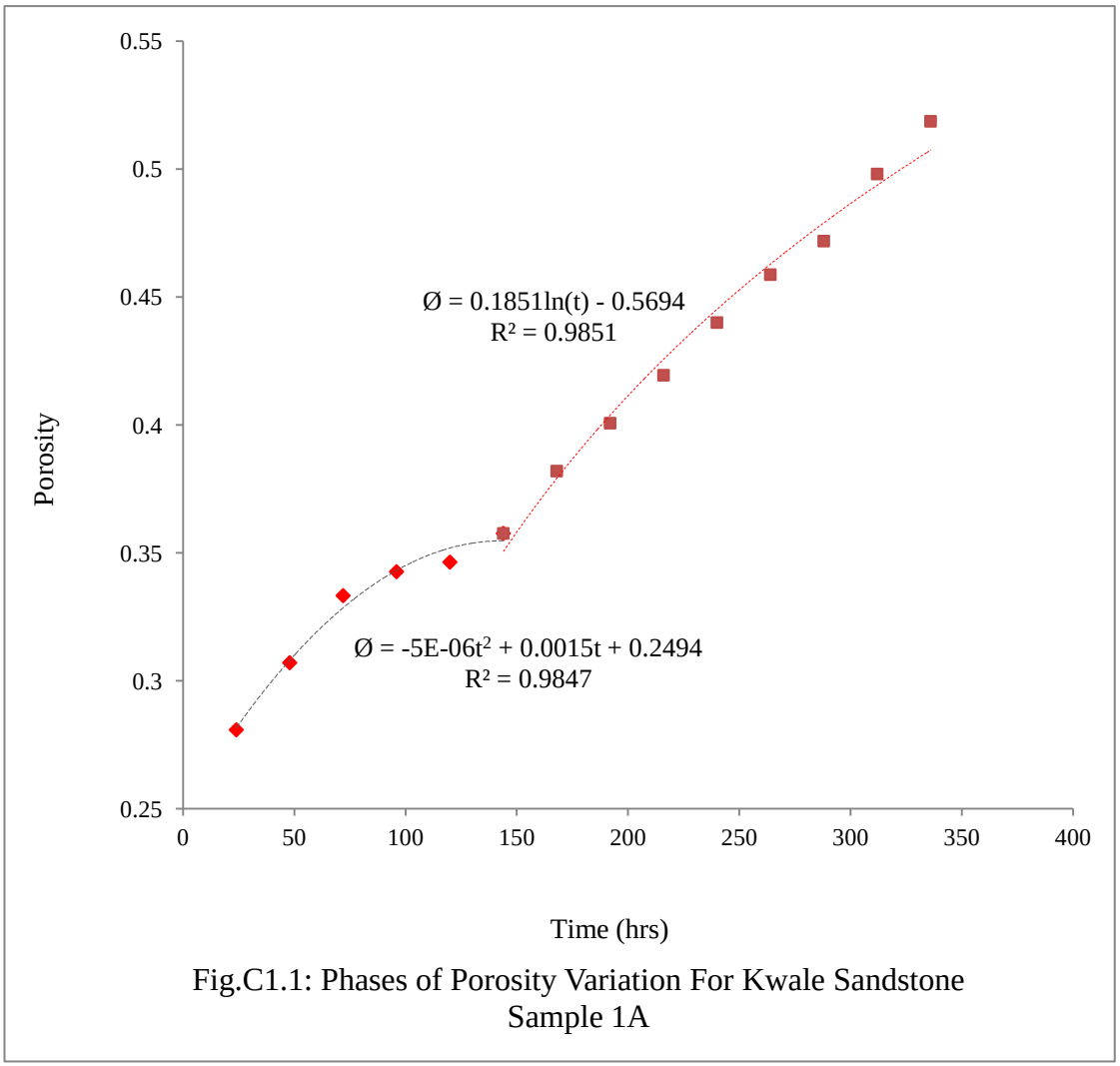

Fig.C1.1: Phases of Porosity Variation For Kwale Sandstone Sample 1A

Sample 1B: Bulk volume was 9.25cc.

Table C 2: Porosity Variation With Time For Kwale Sandstone rock Sample 1B in Crude Oil Zone

Time (hours)	Grain volume, cc	Pore volume. cc	Porosity
0	7.33	1.92	0.207568
24	7.33	1.92	0.207568
48	7.29	1.96	0.211892
72	7.23	2.02	0.218378
96	7.19	2.06	0.222703
120	7.07	2.18	0.235676
144	6.84	2.41	0.260541
168	6.61	2.64	0.285405
192	6.37	2.88	0.311351
216	6.14	3.11	0.336216
240	5.91	3.34	0.361081
264	5.68	3.57	0.385946
288	5.52	3.73	0.403243
312	5.37	3.88	0.419459
336	5.29	3.96	0.428108

The porosity variation for sample 1B is shown in Fig.4.2 and the comparison between porosity variation for 1A and 1B is shown in Fig.4.3.

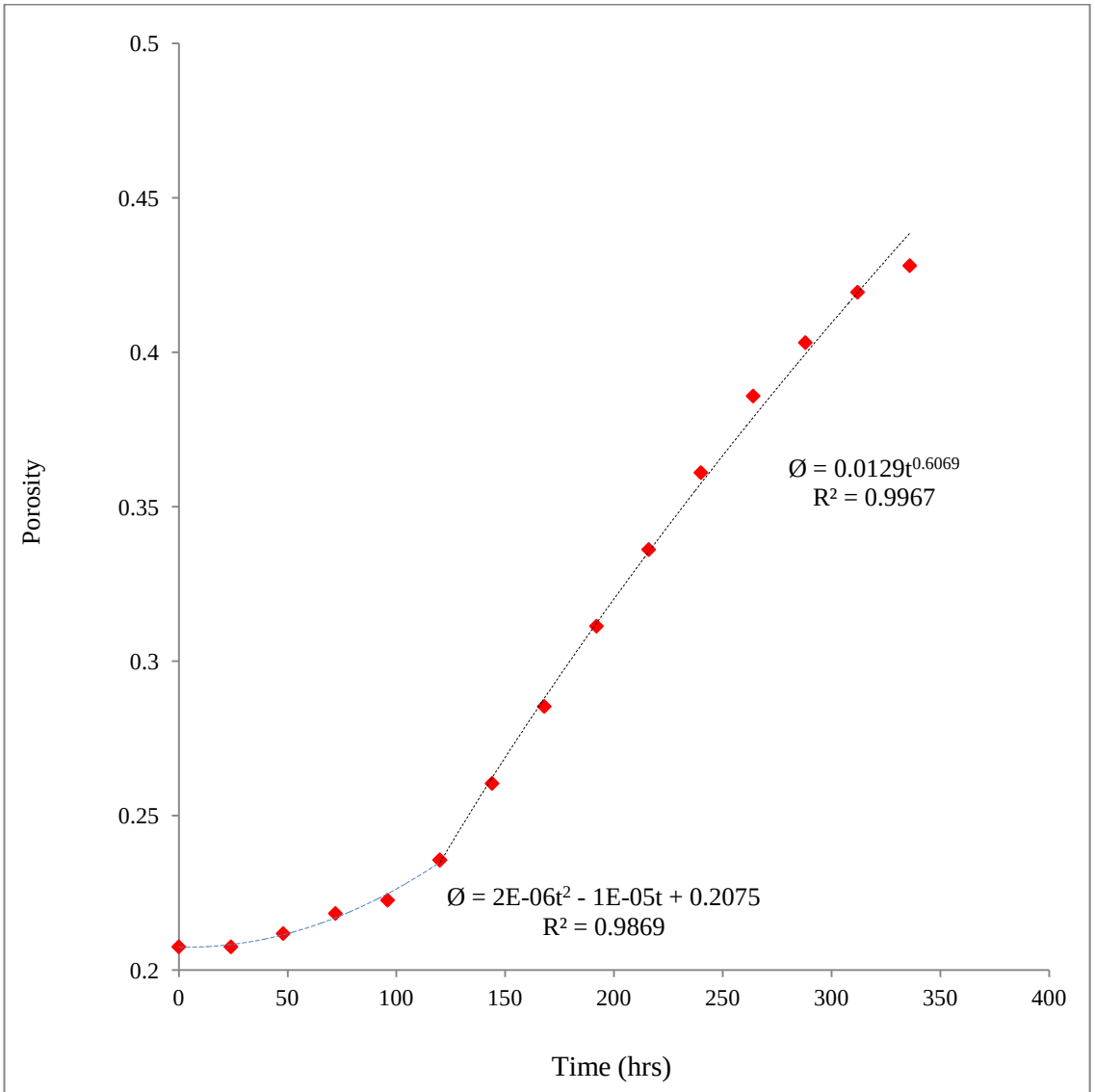

Fig.C1.2: Phases of Porosity Variation For Kwale Sandstone Sample 1B

Table C 3: Porosity Variation With Time For Kwale Sandstone Rock Sample 2A in Water Zone

Time (hours)	Grain volume, cc	Pore volume. cc	Porosity
0	4.81	1.28	0.210181
24	4.81	1.28	0.210181
48	4.73	1.36	0.223317
72	4.59	1.5	0.246305
96	4.49	1.6	0.262726
120	4.43	1.66	0.272578
144	4.34	1.75	0.287356
168	4.25	1.84	0.302135
192	4.17	1.92	0.315271
216	4.08	2.01	0.330049
240	3.98	2.11	0.34647
264	3.89	2.2	0.361248
288	3.8	2.29	0.376026
312	3.71	2.38	0.390805
336	3.67	2.42	0.397373

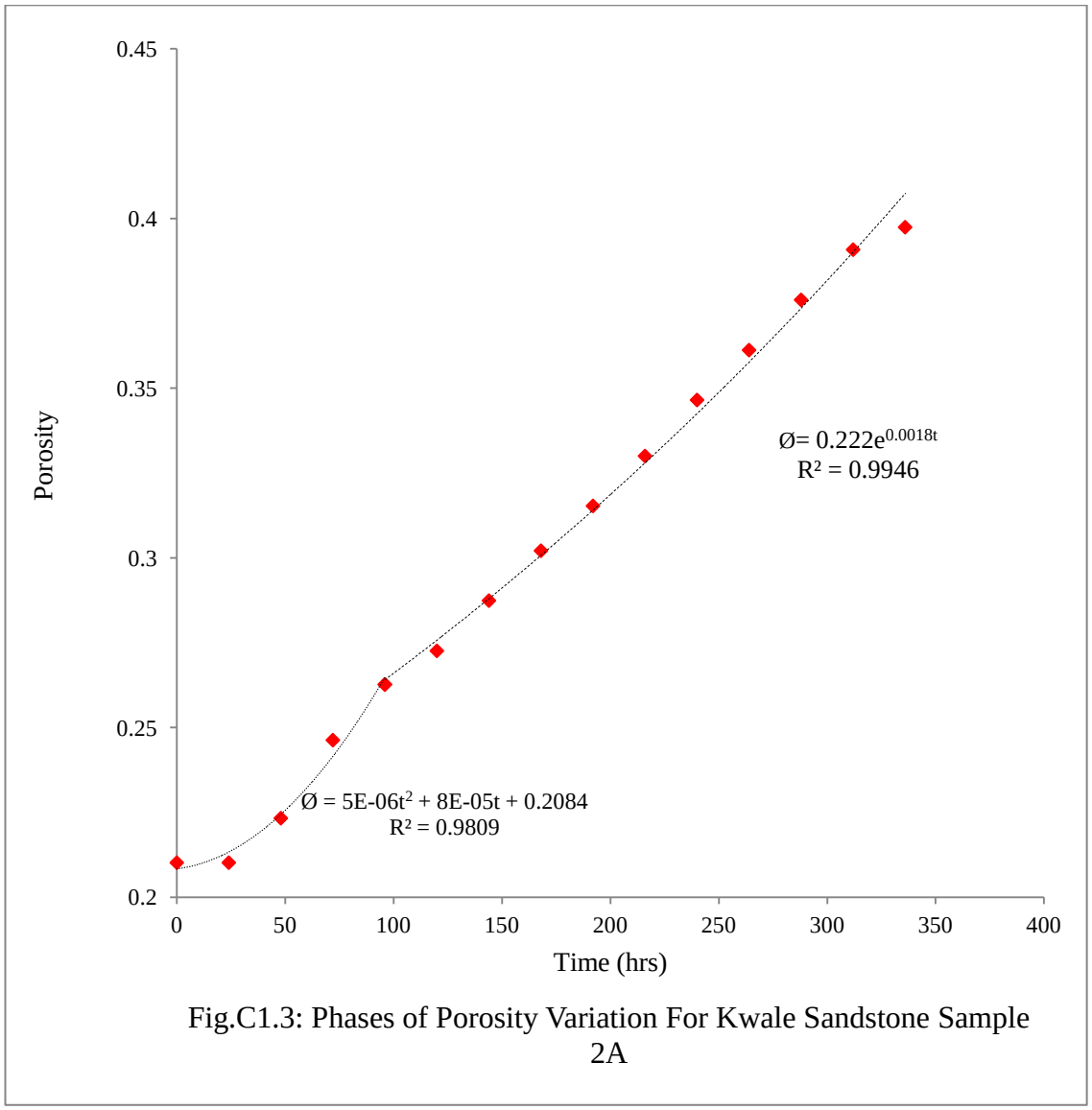

Fig.C1.3: Phases of Porosity Variation For Kwale Sandstone Sample 2A

Sample 2B

Table C 4: Porosity Variation With Time For Kwale Sandstone rock Sample 2B in Water Zone

Time (hours)	Grain volume, cc	Pore volume. cc	Porosity
0	3.13	2.96	0.37468
24	3.13	2.96	0.37468
48	3.07	3.02	0.38228
72	2.9	3.19	0.4038
96	2.73	3.36	0.42532
120	2.66	3.43	0.43418
144	2.56	3.53	0.44684
168	2.47	3.62	0.45823
192	2.44	3.65	0.46203
216	2.36	3.73	0.47215
240	2.28	3.81	0.48228
264	2.14	3.95	0.5
288	2.08	4.01	0.50759
312	2.06	4.03	0.51013
336	2.06	4.03	0.51013

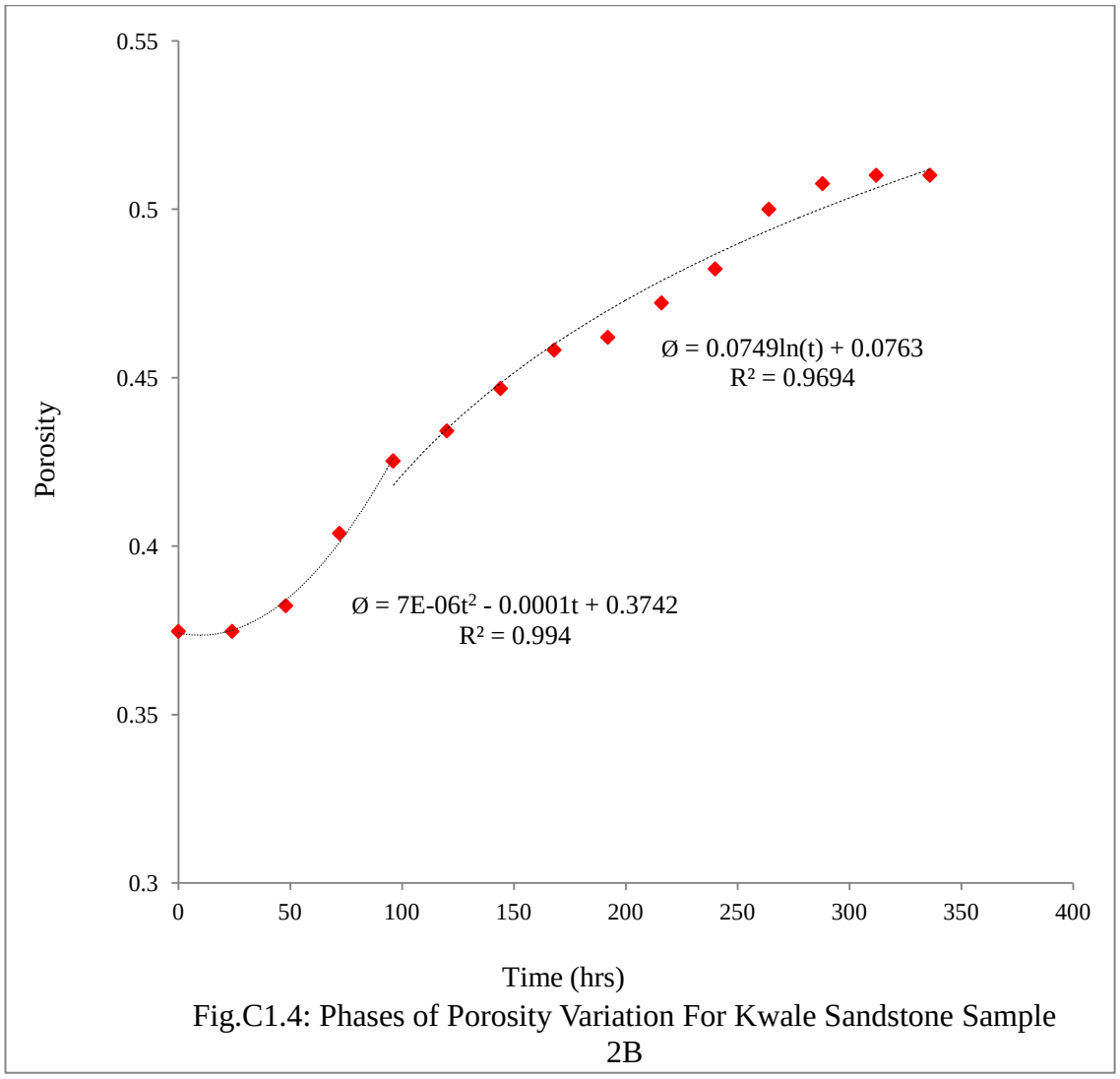

Fig.C1.4: Phases of Porosity Variation For Kwale Sandstone Sample 2B

Sample 3A

Table C 5: Porosity Variation With Time For Kwale Sandstone Dry Rock Sample 3A

Time (hours)	Grain volume, cc	Pore volume. cc	Porosity
0	2.69	1.63	0.377315
24	2.63	1.69	0.391204
48	2.57	1.75	0.405093
72	2.52	1.8	0.416667
96	2.46	1.86	0.430556
120	2.39	1.93	0.446759
144	2.35	1.97	0.456019
168	2.27	2.05	0.474537
192	2.25	2.07	0.479167
216	2.24	2.08	0.481481
240	2.22	2.1	0.486111
264	2.16	2.16	0.5
288	2.14	2.18	0.50463
312	2.1	2.22	0.513889
336	2.1	2.22	0.513889

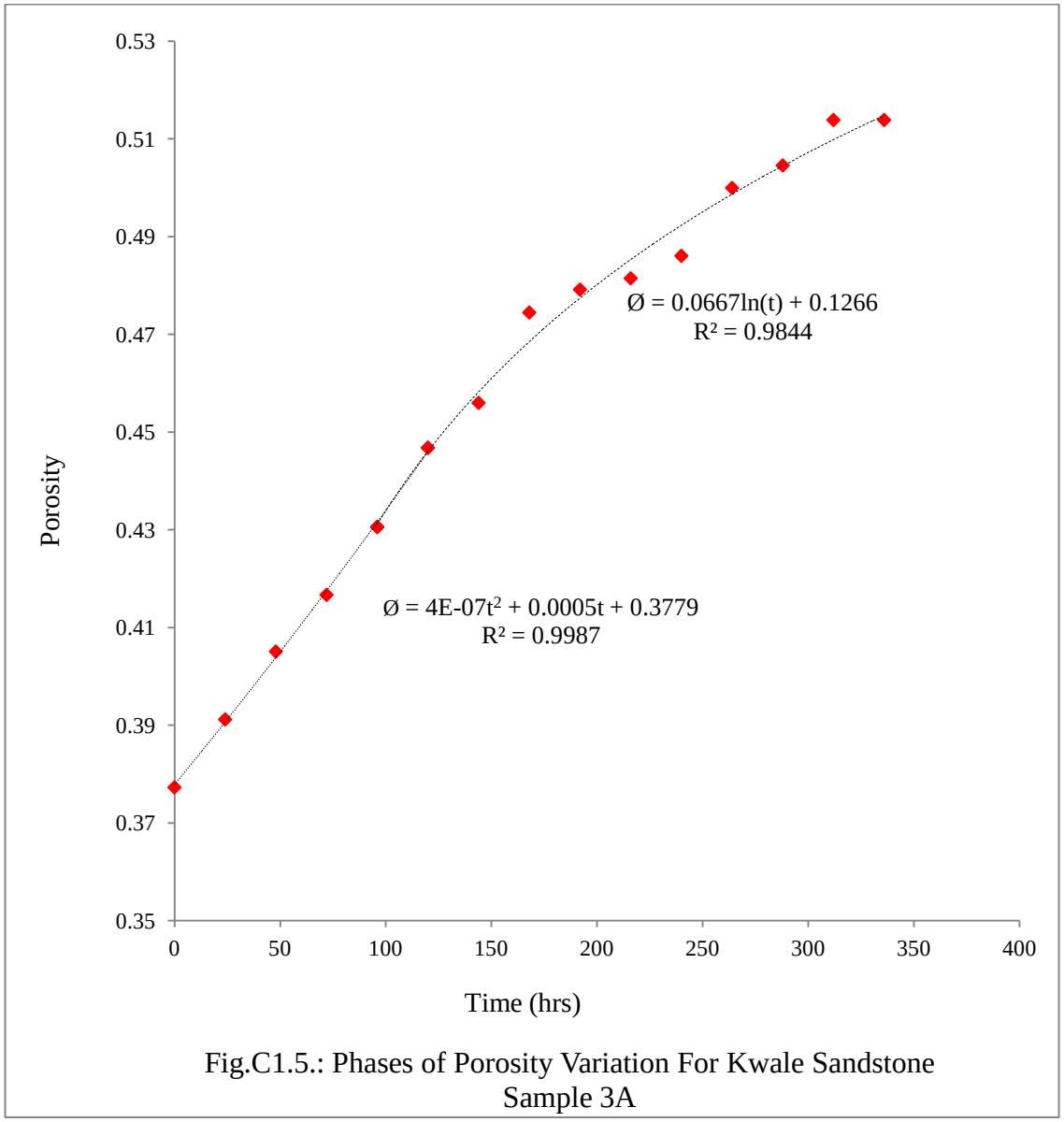

Fig.C1.5.: Phases of Porosity Variation For Kwale Sandstone Sample 3A

Sample 3B

Table C 6: Porosity Variation With Time For Kwale Sandstone Rock Sample 3B

Time (hours)	Grain volume, cc	Pore volume. cc	Porosity
0	2.71	1.61	0.372685
24	2.7	1.62	0.375
48	2.65	1.67	0.386574
72	2.59	1.73	0.400463
96	2.56	1.76	0.407407
120	2.53	1.79	0.414352
144	2.49	1.83	0.423611
168	2.45	1.87	0.43287
192	2.41	1.91	0.44213
216	2.37	1.95	0.451389
240	2.33	1.99	0.460648
264	2.29	2.03	0.469907
288	2.25	2.07	0.479167
312	2.21	2.11	0.488426
336	2.21	2.11	0.488426

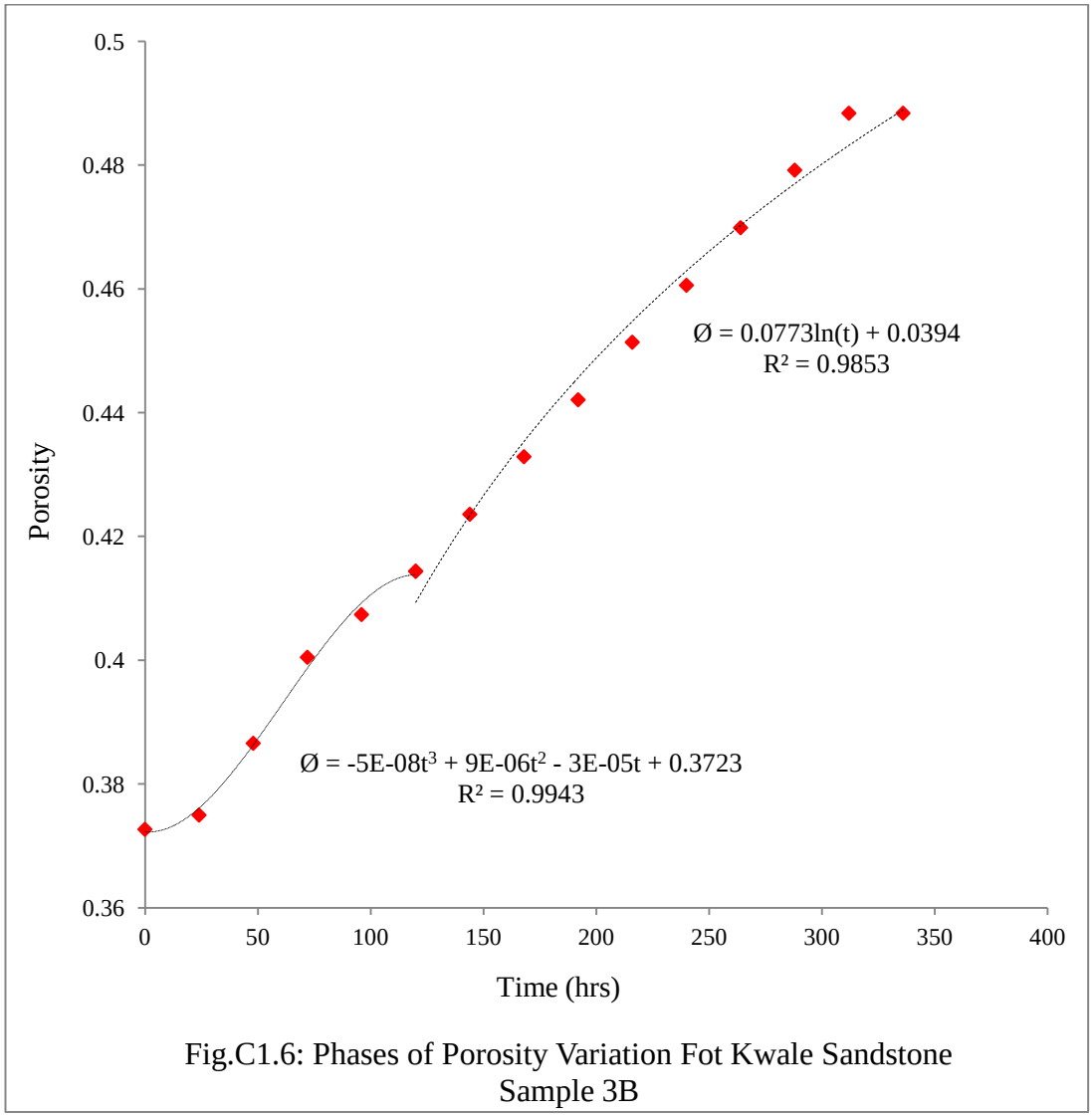

Fig.C1.6: Phases of Porosity Variation Fot Kwale Sandstone Sample 3B

Table C.7: Permeability Variation For Rock Sample 1A Soaked In Crude Oil

Time (hours)	Porosity φ	Computed Swirr (proposed model)	Timur Permeability	Model Average porosity (φ)	Proposed Model Permeability	Model Permeability Based on Actual φ
24	0.2809	0.2980	362.0156	0.2773	812.3566	872.7956
48	0.3071	0.2980	536.0893	0.2782	826.6186	1377.2195
72	0.3333	0.2980	768.7249	0.2796	850.6670	1996.9914
96	0.3427	0.2980	868.3838	0.2816	884.9194	2246.3142
120	0.3464	0.2980	910.9211	0.2842	929.9605	2350.1468
144	0.3577	0.2980	1048.2677	0.2874	986.5418	2675.7965
168	0.3820	0.2980	1400.5391	0.2911	1055.5822	3454.0310
192	0.4007	0.2980	1728.8016	0.2954	1138.1672	4120.3810
216	0.4195	0.2980	2113.5752	0.3003	1235.5497	4845.5856
240	0.4401	0.2980	2609.8999	0.3058	1349.1495	5711.2570
264	0.4588	0.2980	3135.1155	0.3118	1480.5535	6560.0071
288	0.4719	0.2980	3548.8429	0.3185	1631.5154	7189.1861
312	0.4981	0.2980	4501.9715	0.3257	1803.9563	8534.0082
336	0.5187	0.2980	5380.6821	0.3334	1999.9641	9671.6272

Table C.8: Permeability Variation For Rock Sample 1B Soaked In Crude Oil

Time (hours)	Porosity φ	Computed Swirr (proposed model)	Timur Permeability	Model Average porosity (φ)	Proposed Model Permeability	Model Permeability Based on Actual φ
0	0.2076	0.4850	36.1045	0.1930	23.2636	74.4215
24	0.2076	0.4850	36.1045	0.1936	24.6100	74.4215
48	0.2119	0.4850	39.5330	0.1953	28.9835	96.4604
72	0.2184	0.4850	45.1413	0.1982	37.3861	135.4021
96	0.2227	0.4850	49.2096	0.2022	51.4883	165.2926
120	0.2357	0.4850	63.1310	0.2074	73.6285	273.7804
144	0.2605	0.4850	98.1545	0.2137	106.8134	560.6620
168	0.2854	0.4850	146.5839	0.2212	154.7179	951.2836
192	0.3114	0.4850	214.9595	0.2299	221.6847	1469.5237
216	0.3362	0.4850	301.4229	0.2397	312.7251	2072.1854
240	0.3611	0.4850	412.5873	0.2506	433.5182	2778.6048
264	0.3859	0.4850	553.0600	0.2627	590.4114	3588.7820
288	0.4032	0.4850	670.7328	0.2759	790.4202	4213.5643
312	0.4195	0.4850	797.7913	0.2903	1041.2283	4844.9006
336	0.4281	0.4850	872.7506	0.3059	1351.1874	5199.6769

Table C.9: Permeability Variation For Rock Sample 2A Soaked In Brine

Time (hours)	Porosity φ	Computed Swirr (proposed model)	Timur Permeability	Model Average porosity (φ)	Proposed Model Permeability	Model Permeability Based on Actual φ
0	0.2102	0.4850	38.1475	0.2190	139.5075	87.3645
24	0.2102	0.4850	38.1475	0.2190	139.5190	87.3645
48	0.2233	0.4850	49.8094	0.2190	139.5535	169.7905
72	0.2463	0.4850	76.6545	0.2190	139.6110	383.7164
96	0.2627	0.4850	101.8284	0.2190	139.6915	590.8310
120	0.2726	0.4850	119.7333	0.2190	139.7951	736.8117
144	0.2874	0.4850	151.0444	0.2191	139.9217	986.3243
168	0.3021	0.4850	188.3389	0.2191	140.0714	1272.5077
192	0.3153	0.4850	227.1251	0.2191	140.2443	1557.6448
216	0.3300	0.4850	277.8437	0.2191	140.4403	1913.0380
240	0.3465	0.4850	344.0204	0.2192	140.6596	2350.9320
264	0.3612	0.4850	413.4276	0.2192	140.9022	2783.7001
288	0.3760	0.4850	493.1898	0.2192	141.1681	3253.1182
312	0.3908	0.4850	584.3592	0.2193	141.4574	3759.2220
336	0.3974	0.4850	628.8227	0.2193	141.7703	3995.9065

Table C.10: Permeability Variation For Rock Sample 2B Soaked In Brine

Time (hours)	Porosity φ	Computed Swirr (proposed model)	Timur Permeability	Model Average porosity (φ)	Proposed Model Permeability	Model Permeability Based on Actual φ
0	0.3747	0.3700	834.1453	0.3747	3209.5016	3208.8459
24	0.3747	0.3700	834.1453	0.3744	3200.0673	3208.8459
48	0.3823	0.3700	911.2014	0.3735	3171.8479	3462.8114
72	0.4038	0.3700	1159.4906	0.3721	3125.0940	4234.5181
96	0.4253	0.3700	1457.0854	0.3701	3060.2231	5083.9439
120	0.4342	0.3700	1595.4480	0.3675	2977.8199	5456.2468
144	0.4468	0.3700	1810.5247	0.3643	2878.6361	6011.0889
168	0.4582	0.3700	2022.5671	0.3606	2763.5903	6533.2568
192	0.4620	0.3700	2097.4143	0.3563	2633.7684	6712.3091
216	0.4722	0.3700	2307.2116	0.3514	2490.4229	7200.9740
240	0.4823	0.3700	2533.0990	0.3459	2334.9738	7707.3344
264	0.5000	0.3700	2968.9541	0.3399	2169.0079	8634.5000
288	0.5076	0.3700	3172.4363	0.3332	1994.2791	9047.7518
312	0.5101	0.3700	3242.8829	0.3260	1812.7083	9188.2059
336	0.5101	0.3700	3242.8829	0.3183	1626.3834	9188.2059

Table C.11: Permeability Variation For Dry Rock Sample 3A

Time (hours)	Porosity φ	Computed Swirr (proposed model)	Timur Permeability	Model Average porosity (φ)	Proposed Model Permeability	Model Permeability Based on Actual φ
0	0.3773	0.3700	860.2672	0.3773	3295.8007	3295.8007
24	0.3912	0.3700	1008.5790	0.3778	3311.1267	3773.3938
48	0.4051	0.3700	1175.9160	0.3792	3357.3187	4283.3601
72	0.4167	0.3700	1331.0903	0.3815	3435.0180	4733.0549
96	0.4306	0.3700	1537.6798	0.3847	3545.2937	5302.3717
120	0.4468	0.3700	1809.0811	0.3888	3689.6424	6007.4534
144	0.4560	0.3700	1979.9781	0.3939	3869.9883	6430.1919
168	0.4745	0.3700	2358.9776	0.3999	4088.6834	7318.7402
192	0.4792	0.3700	2461.9420	0.4068	4348.5071	7549.8944
216	0.4815	0.3700	2514.6858	0.4146	4652.6664	7666.7698
240	0.4861	0.3700	2622.8378	0.4234	5004.7962	7903.3195
264	0.5000	0.3700	2968.9541	0.4331	5408.9587	8634.5000
288	0.5046	0.3700	3091.8396	0.4437	5869.6438	8885.4391
312	0.5139	0.3700	3349.3496	0.4552	6391.7691	9398.0537
336	0.5139	0.3700	3349.3496	0.4676	6980.6797	9398.0537

Table C.12: Permeability Variation For Dry Rock Sample 3B

Time (hours)	Porosity φ	Computed Swirr (proposed model)	Timur Permeability	Model Average porosity (φ)	Proposed Model Permeability	Model Permeability Based on Actual φ
0	0.3727	0.3700	814.7791	0.3727	3143.7862	3143.7862
24	0.3750	0.3700	837.2845	0.3727	3145.4683	3219.3438
48	0.3866	0.3700	957.1039	0.3729	3150.5174	3610.5875
72	0.4005	0.3700	1117.9181	0.3732	3158.9415	4109.7620
96	0.4074	0.3700	1205.7598	0.3735	3170.7543	4371.4700
120	0.4144	0.3700	1298.8560	0.3740	3185.9746	4641.3096
144	0.4236	0.3700	1431.4997	0.3746	3204.6267	5013.6462
168	0.4329	0.3700	1574.3758	0.3752	3226.7406	5400.3698
192	0.4421	0.3700	1728.0464	0.3760	3252.3512	5801.5246
216	0.4514	0.3700	1893.0398	0.3769	3281.4993	6217.0239
240	0.4606	0.3700	2069.9502	0.3779	3314.2309	6646.9102
264	0.4699	0.3700	2259.3727	0.3790	3350.5972	7091.1836
288	0.4792	0.3700	2461.9420	0.3801	3390.6553	7549.8944
312	0.4884	0.3700	2678.2435	0.3814	3434.4672	8022.9434
336	0.4884	0.3700	2678.2435	0.3828	3482.1007	8022.9434

C.2. Measured/Calculated Properties For Kwale Black Shales

Table C.13.: Measured Porosity For Black Kwale Shale.

DAY	Bulk Volume cc	Grain volume	Corrected Porosity
1	11	8.265467	0.031667
2	11	7.7768	0.024346
3	11	8.558667	0.012265
8	11	7.615034	0.079629
9	11	5.744418	0.216002
12	11	5.792598	0.216482
20	11	5.995472	0.204533

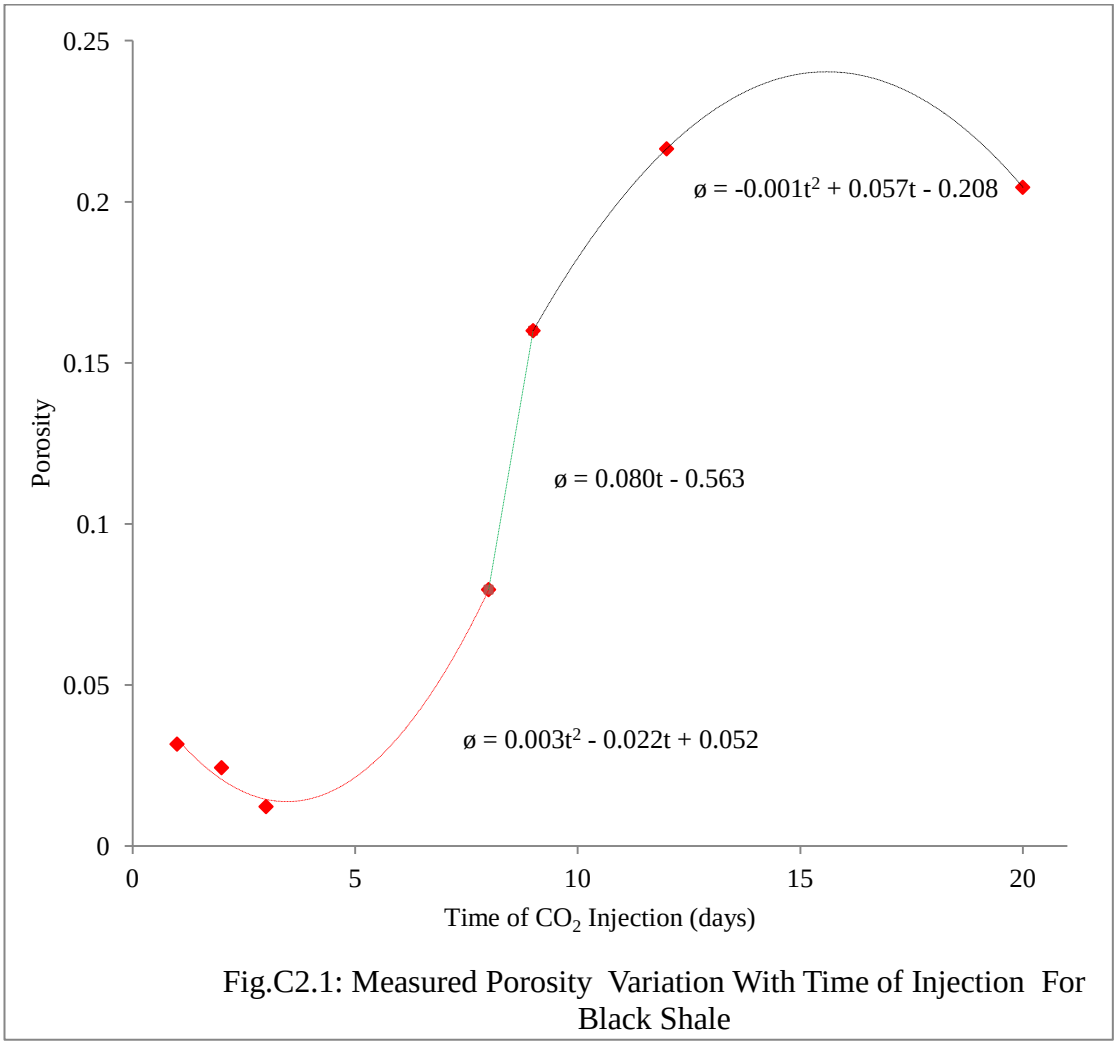

Fig.C2.1: Measured Porosity Variation With Time of Injection For Black Shale

. The graph of average S_{wirr} against average porosity was obtained for the Kwale sand and a model equation was obtained which was then used for the computation of the S_{wirr} for the Kwale shales. This is as shown in Fig.C2.2.

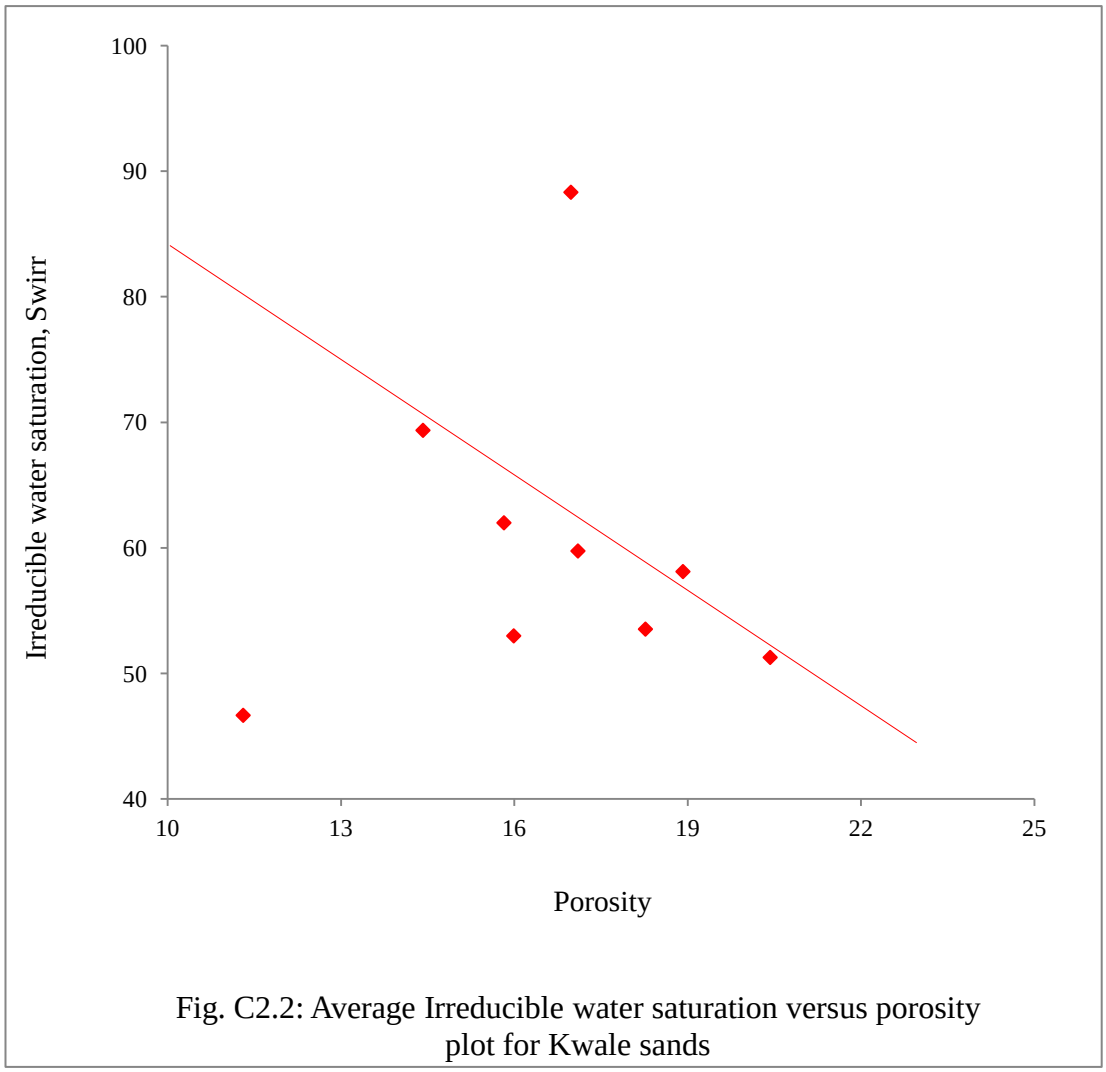

Fig. C2.2: Average Irreducible water saturation versus porosity plot for Kwale sands

The best-fit exponential equation for above is $S_{wirr}=0.849e^{-5.61Ø}$ and when this was applied into the S_{wirr} calculation for the black shale an equation relating S_{wirr} and porosity for the shale was obtained (Fig. C2.3) such that the following equation was obtained:

$$\mathbf{S_{wirr} = 0.848e^{-5.61Ø}}$$

This is very similar to that of the S_{wirr} equation obtained for the sandstone.

Calculated Permeability For Black Kwale Shales.

Table C.14: Permeability Variation For Kwale Black Shale Sample

Time (hrs)	Porosity φ	Computed Swirr	Timur Permeability	Dumanoir Permeability	Tixier Permeability	Aigbedion Permeability	Model Permeability
0	0.03167	0.3333	0.0000	0.20	0.00	-0.4221	0.4479
24	0.02435	0.4354	0.0000	0.08	0.00	-0.5177	0.2772
48	0.01227	0.8642	0.0000	0.00	0.00	-0.6755	0.0486
36	0.07963	0.1331	0.0001	4.13	0.00	0.20430	2.0321
216	0.21600	0.0491	0.0666	90.41	0.26	1.98534	9.5084
288	0.21648	0.0490	0.0676	91.02	0.27	1.99160	9.5407
480	0.20453	0.0518	0.0470	76.54	0.17	1.83556	8.7486

C.3. Measured/calculated Properties Kwale Grey Shales

Table C.15.: Measured Porosity For Grey Kwale Shale

Time (days)	Grain volume	Corrected Porosity
1	12.648	0.35186
2	7.9568	0.34703
3	8.738667	0.33737
8	12.9412	0.129645
12	5.924418	0.01834
20	15.2053	0.0086

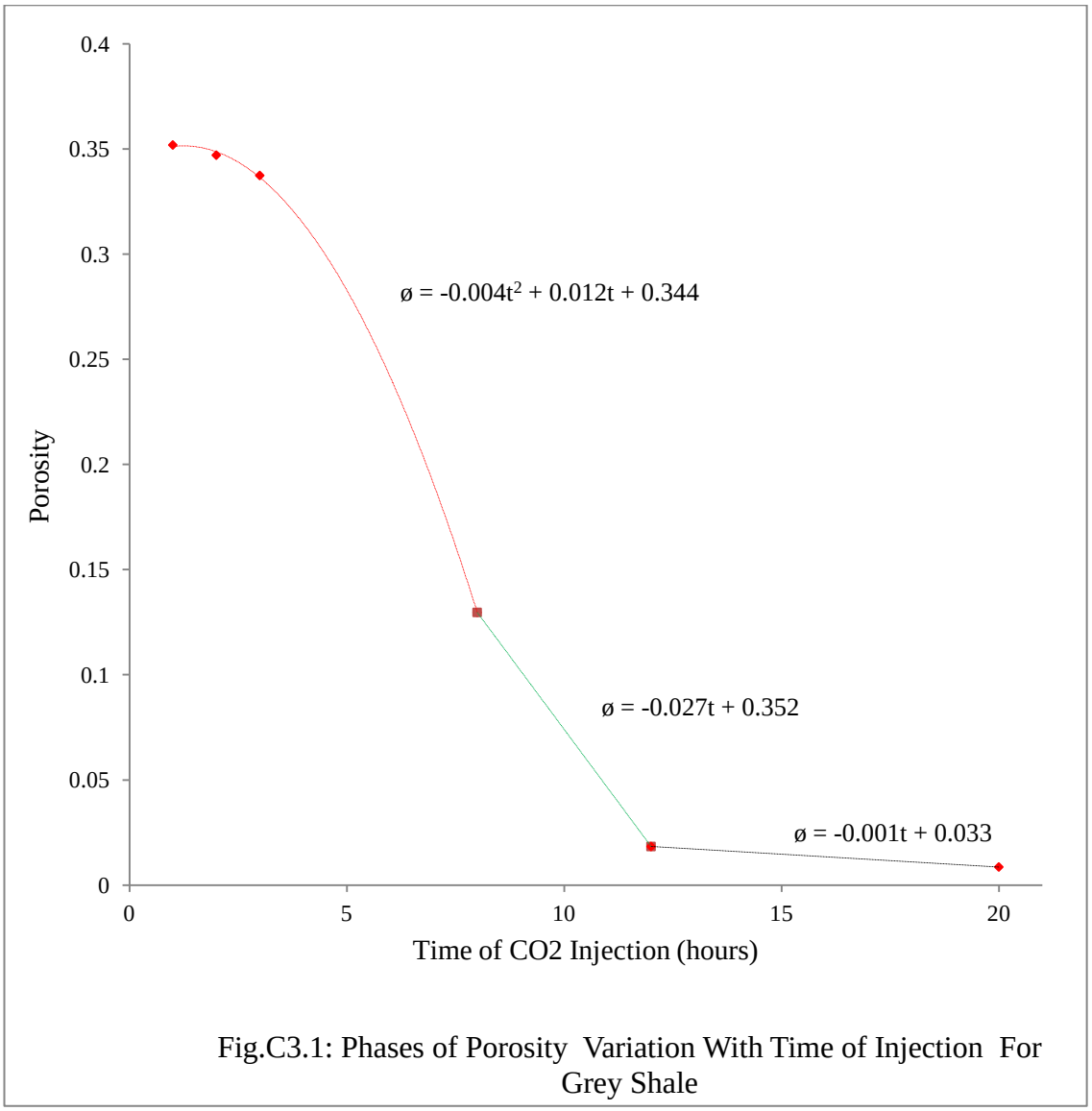

Fig.C3.1: Phases of Porosity Variation With Time of Injection For Grey Shale

Table C.16: Permeability Variation For Kwale Grey Shale Sample

Time (days)	Corrected Porosity	Computed Swirr	Timur Permeability	Dumanoir Permeability	Tixier Permeability	Aigbedion Permeability	Proposed Model Permeability
0	0.352	0.1173	0.0999	93.2396	0.8641	3.7615	9.6561
24	0.3519	0.1173	0.0998	93.1880	0.8624	3.7596	9.6534
48	0.3470	0.3380	0.0113	23.5860	0.0955	3.6966	4.8565
36	0.3374	0.3477	0.0094	21.3538	0.0762	3.5704	4.6210
216	0.1296	0.9048	0.0000	0.1769	0.0000	0.8575	0.4206
288	0.0183	1.0000	0.0000	0.0000	0.0000	-0.5961	0.0000
480	0.0086	1.0000	0.0000	0.0000	0.0000	-0.7233	0.0000

C.4. Measured/Calculated Properties For Imeri Oil Sand

Table C.17. Measured Porosity For Imeri Oil sand

DAY	Grain volume	Corrected Porosity
1	10.08427	0.7583
2	6.9568	0.7564
3	7.738667	0.6997
8	11.9412	0.6685
9	4.924418	0.6076
12	14.2053	0.6234
20	32.29856	0.2631

Bulk volume was 48.7cc and Porosimeter constant of 58.64.

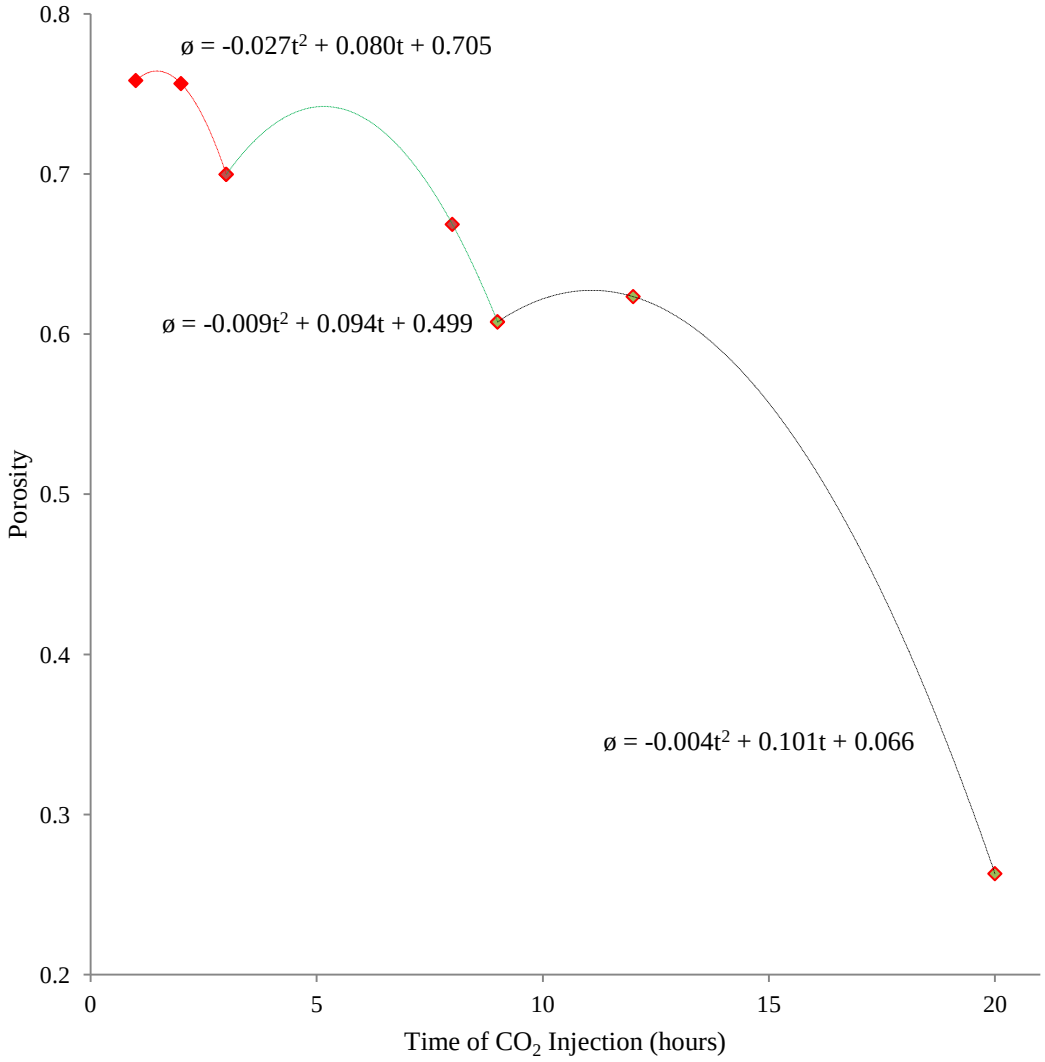

Fig.C4.1: Phases of Porosity Variation With Time of Injection For Imeri Oilsand

Table C.18: Permeability Variation For Imeri Oil sand

Time (hours)	Porosity φ	Computed Swirr	Timur Permeability	Dumanoir Perm.	Tixier Perm.	Aigbedion Perm.	Proposed Model Perm.
0	0.7584	0.1666	1.4512	287.72	42.85	9.06905	16.9624
24	0.7583	0.1667	1.4487	287.44	42.76	9.06775	16.9541
48	0.7564	0.1671	1.4258	285.17	41.92	9.04293	16.8868
72	0.6997	0.1806	0.8659	222.05	22.47	8.30243	14.9015
172	0.6685	0.1891	0.6467	191.66	15.60	7.89496	13.8442
216	0.6076	0.2080	0.3509	140.54	7.27	7.09961	11.8551
288	0.6234	0.2028	0.4136	152.81	8.92	7.30595	12.3615
480	0.2631	0.4804	0.0017	7.49	0.01	2.60044	2.7361

C.5. Measured/Calculated Properties For Ota Kaolinitic Clay

Table C.19. Measured Porosity For Ota Kaolinitic Clay

Time of Injection (days)	Grain volume	Corrected porosity
1	23.84086	0.35186
2	27.36012	0.34703
9	27.76515	0.33737
16	28.08611	0.129645
23	28.3467	0.01834
30	28.56251	0.4135
32	29.17075	0.40101
62	31.23638	0.3586

Porosimeter constant was 57.1cc and bulk volume of 47.1cc.

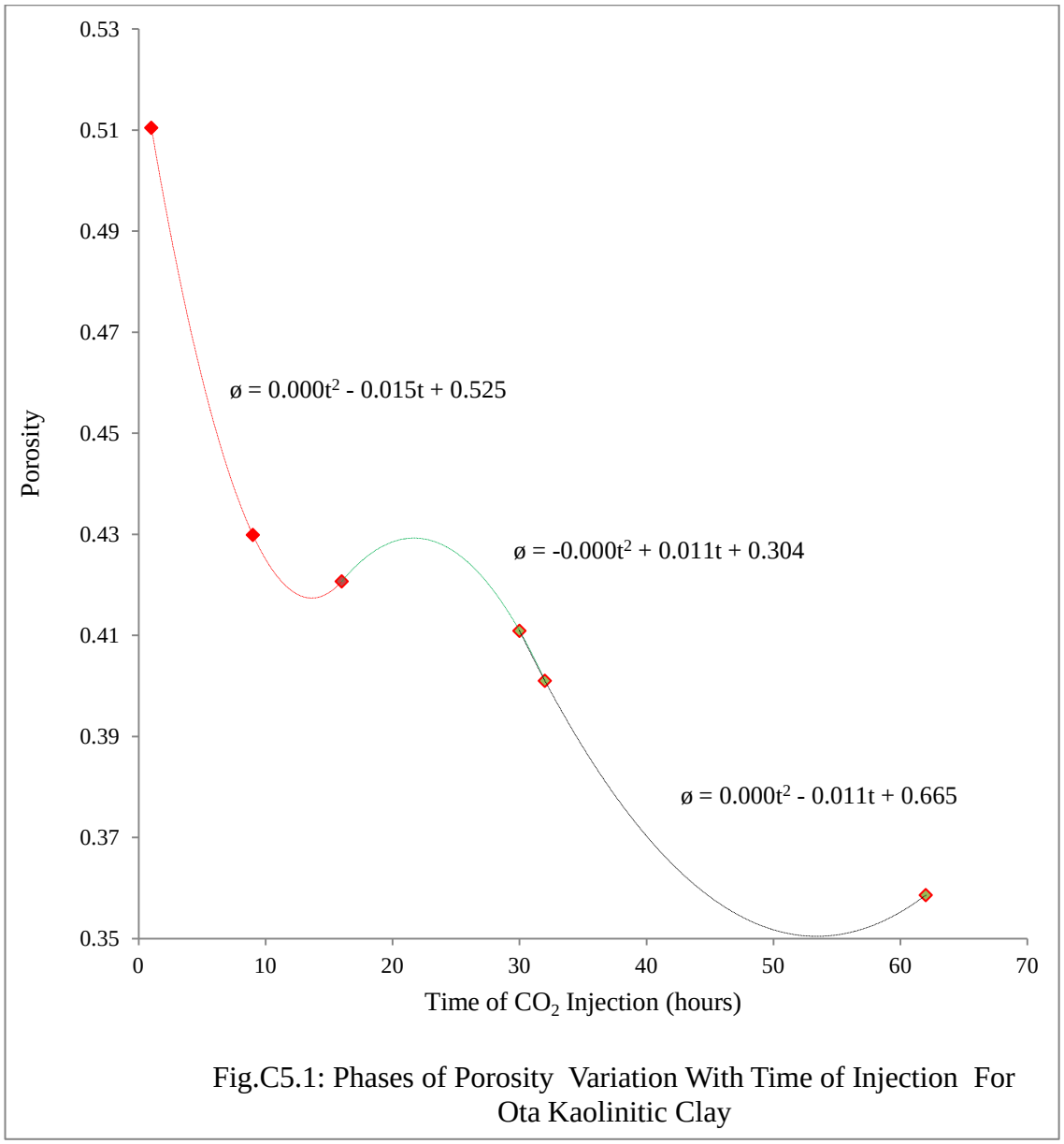

Fig.C5.1: Phases of Porosity Variation With Time of Injection For Ota Kaolinitic Clay

Table C.20: Permeability Variation For Ota Kaolinitic Clay At Varying S_{wirr}

Time (hours)	Porosity φ	Computed Swirr	Timur Permeability	Coates Dumanoir Perm.	Tixier Perm.	Aigbedion Perm.	Proposed Model Perm.
0	0.511	0.5000	0.0284	26.11	0.45	5.8380	5.1100
24	0.5105	0.5005	0.0282	26.01	0.44	5.8315	5.1000
48	0.4382	0.5831	0.0106	13.73	0.13	4.8872	3.7055
216	0.4299	0.5943	0.0094	12.62	0.11	4.7788	3.5518
384	0.4207	0.6073	0.0082	11.44	0.09	4.6587	3.3828
552	0.4153	0.6152	0.0075	10.79	0.08	4.5882	3.2844
720	0.4109	0.6218	0.0070	10.27	0.08	4.5307	3.2045
768	0.401	0.6372	0.0060	9.16	0.06	4.4014	3.0261
1488	0.3586	0.7125	0.0029	5.19	0.03	3.8477	2.2779

C.6. Measured Properties For Bonny Light Crude Sample

Table C.21.: Measured Crude Oil Shear Stress With CO_2 Injection

TIME (Days)	600RPM READING (cP)	300RPM READING (cP)	Apparent Viscosity (cp)
0	26	13	13
1	26	13	13
2	26	13	13
3	26.5	14	13.25
4	26.5	13.5	13.25
5	27	13.5	13.5
6	27.5	13.5	13.75
7	27.5	13.5	13.75
8	27.5	13.5	13.75
9	27	13	13.5
10	27	13	13.5

Table C.22.: Variation In Bonny Light Crude Density With CO_2 Injection

TIME (DAYS)	ρ (ppg)	ρ (specific gravity)
0	7.46	0.895
2	7.46	0.895
3	7.44	0.893
4	7.41	0.89
5	7.41	0.89
6	7.41	0.89
7	7.41	0.89
8	7.47	0.897
9	7.50	0.9
10	7.50	0.9

C.7. Measured Properties Of CO_2 Contaminated Water-Based And Oil-Based Muds.

C7.1. Measured Properties of Water-Based Mud During CO_2 Contamination

Table C.23.: Density and Resistivity Measurement for CO_2 contaminated Water-based mud.

Time (days)	Density		Specific Gravity	Resistivity (Ωm)
	(ppg)	(lb/ft^3)		
0	13.5	101.0	1.62	0.34
3	12.0	90.0	1.44	0.36
6	11.8	88.0	1.41	0.37
7	11.6	87.0	1.4	0.40
8	11.5	86.0	1.38	0.46
9	11.35	85.0	1.36	0.50
10	11.3	84.5	1.35	0.52
11	11.2	84.0	1.34	0.54
12	11.2	84.0	1.34	0.54
13	11.2	84.0	1.34	0.54

Table C.24.: Measured Density of Water-in-oil Mud Contaminated With CO_2

Time (days)	**Density (ppg)**
0	8.7
7	8.9
10	9.1
15	9.2
17	9.3
19	9.32
21	9.35
23	9.4
25	9.4

C7.2. Measured Oil-In-Water Emulsion Mud Properties During CO_2 Contamination

Table C.25.: Shear Stress of CO_2 Contaminated Oil-in-water Mud

Time (days)	Shear stress		Yield point	Apparent viscosity
	600 rpm	300 rpm		
0	122	114	6	61
5	221	210	199	110.5
8	222	214	206	111
10	230	222	214	115
12	242	236	230	121
14	253	241	219	126.5
16	262	255	242	131
18	262	258	234	131

C7.3. Comparison Between The Effect of CO_2 Contamination on Water and Oil-in-water Emulsion Muds.

Table C26: Fractional Change In Mud Density Due To Contamination By CO_2

Time (days)	Fractional Change in Mud Density	
	Water-based Mud (WBM)	Water-in-oil Mud (OBM)
0	0.0000	0.0000
3	-0.1111	0.0110
6	-0.1259	0.0300
7	-0.1407	0.0320
8	-0.1481	0.0370
9	-0.1593	0.0440
10	-0.1630	0.0460
11	-0.1704	0.0480
12	-0.1704	0.0520
13	-0.1704	0.0570
15	-0.1704	0.0595
17	-0.1704	0.0690
19	-0.1704	0.0713
21	-0.1704	0.0747
23	-0.1704	0.0805
25	-0.1704	0.0805

Table C27: Fractional Change In Yield Point and Apparent Viscosity of Drilling Mud Due To Contamination By CO_2 Gas

Time	Fractional Change In Yield Point		Fractional Change In Apparent Viscosity	
(days)	OBM	WBM	OBM	WMB
0	0.000	0.000	0.000	0.000
3	1.000	-0.573	2.423	-0.358
6	1.852	-0.787	2.981	-0.585
8	2.279	-0.840	3.189	-0.604
9	2.410	-0.893	3.226	-0.660
10	2.541	-0.920	3.340	-0.717
11	2.639	-0.920	3.415	-0.755
12	2.770	-0.920	3.566	-0.755
13	2.836	-0.920	3.642	-0.755
14	2.902	-0.920	3.774	-0.755
16	2.967	-0.920	3.943	-0.755
18	2.967	-0.920	3.943	-0.755

The fractional (percentage) change in the yield point of the mud when it was contaminated with CO_2 gas is in the appendix B.

C.8. Measured Metal Composition of Samples Using Atomic Absorption Spectrometer (AAS)

C.8.1. Test Result For Copper Using Atomic Absorption Spectrometer (AAS)

SEQUENCE TABLE Shared Standards: Yes

Action	Solution ID	Cu (copper)
Calibration		X
Sample 1	GREY COLOURED SHALE CA	X
Sample 2	KAOLIN	X
Sample 3	GREY SHALE WATER	X
Sample 4	KAOLIN CA	X
Sample 5	SANDSTONE CA	X
Sample 6	BLACK SHALE WATER	X
Sample 7	OIL SAND CA	X
Reblank		X

SAMPLE DETAILS Nominal Mass: 1.0000

No.	Sample Id	Sample Mass	Dilution Ratio
1	GREY SHALE CA	1.0000	1.0000
2	KAOLIN	1.0000	1.0000
3	GREY SHALE WATER	1.0000	1.0000
4	KAOLIN CA	1.0000	1.0000
5	SANDSTONE CA	1.0000	1.0000
6	BLACK SHALE WATER	1.0000	1.0000
7	OIL SAND CA	1.0000	1.0000

ANALYSIS AUDIT TRAIL OPERATOR ACTION TIME DATE

Valued coy:AUTHORIS-086FA7 Record created 12:59:06 4/3/2013

Valued coy:AUTHORIS-086FA7 Error MD147 - Activity manually aborted by user. 1:06:08 4/3/2013

ELEMENT AUDIT TRAIL OPERATOR ACTION TIME DATE

No changes for element

SPECTROMETER PARAMETERS Element: Cu Measurement Mode: Absorbance

Wavelength: 324.8 Bandpass: 0.5nm Lamp Current: % 50

Background Correction: D2 High Resolution: Off Optimize Spectrometer Parameters: No

Signal Type: Continuous Resamples: Fast Number Of Resamples: 3

Measurement Time: secs 4.0 Flier Mode: No

Use RSD Test: No

FLAME PARAMETERS Flame Type: Air-C2H2 Fuel Flow: L/min 1.1

Auxilary Oxidant: Off

Nebuliser Uptake: secs 4 Burner Stabilization: mins 0

Optimize Fuel Flow: No

Burner Height: mm 7.0 Optimize Burner Height: No

SAMPLING PARAMETERS Sampling: None

CALIBRATION PARAMETERS Calibration Mode: Normal Line Fit: Segmented Curve Use Stored Calibration: No

Concentration Units: ppm Scaled Units: ppm Scaling Factor: 1.0000

Excess Curvature Limits: -10% to +40% Rescale Limit: % 10.0

Failure Action: Flag and Continue

Master Standard 4.0000

Standard 1 1.0000

Standard 2 2.0000

Standard 3 4.0000

RESULTS FOR ELEMENT Cu

SAMPLE ID	RESULT TYPE	SIGNAL		Rsd	FLAGS
CONC.	CORRECTED CONC.		TIME	DATE	
	Abs	%	ppm	ppm	
GREY SHALE CA	Mean	-0.002	30.9	0.1697	0.1697
GREY SHALE CA	Resample 1 of 3		-0.001		
1:02:12	4/3/2013				
GREY SHALE CA	Resample 2 of 3		-0.002		1:02:16
4/3/2013					
GREY SHALE CA	Resample 3 of 3		-0.002		1:02:21
4/3/2013					
KAOLIN	Mean	-0.003	21.8	0.0965	0.0965

KAOLIN	Resample 1 of 3		-0.003			1:02:40 4/3/2013
KAOLIN	Resample 2 of 3		-0.003			1:02:44 4/3/2013
KAOLIN	Resample 3 of 3		-0.004			1:02:48 4/3/2013
GREY SHALE WATER	Mean	-0.000	979.9	0.2576	0.2576	
GREY SHALE WATER	Resample 1 of 3		0.001			1:03:17 4/3/2013
GREY SHALE WATER	Resample 2 of 3		-0.000			1:03:21 4/3/2013
GREY SHALE WATER	Resample 3 of 3		-0.001			1:03:26 4/3/2013
KAOLIN CA	Mean	-0.003	12.5	0.1281	0.1281	
KAOLIN CA	Resample 1 of 3		-0.002			1:03:43 4/3/2013
KAOLIN CA	Resample 2 of 3		-0.003			1:03:48 4/3/2013
KAOLIN CA	Resample 3 of 3		-0.003			1:03:52 4/3/2013
SANDSTONE CA	Mean	-0.001	41.1	0.1997	0.1997	
SANDSTONE CA	Resample 1 of 3		-0.001			1:04:22 4/3/2013
SANDSTONE CA	Resample 2 of 3		-0.001			1:04:26 4/3/2013
SANDSTONE CA	Resample 3 of 3		-0.002			1:04:30 4/3/2013
BLACK SHALE WATER	Mean	-0.002	13.4	0.1536	0.1536	
BLACK SHALE WATER	Resample 1 of 3		-0.002			1:04:55 4/3/2013
BLACK SHALE WATER	Resample 2 of 3		-0.002			1:05:00 4/3/2013
BLACK SHALE WATER	Resample 3 of 3		-0.002			1:05:04 4/3/2013
OIL SAND CA	Mean	0.001	77.2	0.2958	0.2958	

OIL SAND CA 4/3/2013	Resample 1 of 3	0.001	1:05:25
OIL SAND CA 4/3/2013	Resample 2 of 3	0.001	1:05:30
OIL SAND CA 4/3/2013	Resample 3 of 3	0.000	1:05:34

C.8.2. Test Result For Nickel (Ni) Using Atomic Absorption Spectrometer (AAS)

ANALYSIS INFORMATION NAME OPERATOR TIME DATE

Spectrometer:

Analysis 49 Valued coy 1:21:05 4/3/2013 S Series 712118 v1.27

GENERAL PARAMETERS Instrument Mode: Flame Autosampler : None

Dilution: None Use SFI: No

METHOD AUDIT TRAIL OPERATOR ACTION TIME DATE

Valued coy:AUTHORIS-086FA7 Record created 12:07:49 9/23/2010

SEQUENCE TABLE Shared Standards: Yes

Action Solution ID	NiCKEL		
Calibration	X		
Sample 1	GREY SHALE CA	X	
Sample 2	KAOLIN WATER	X	
Sample 3	GREY SHALE WATER		X
Sample 4	KAOLIN CA	X	
Sample 5	BLACK SHALE	X	
Sample 6	BLACK SHALE REAL		X
Sample 7	OIL SAND	X	
Reblank	X		
Reblank	X		

SAMPLE DETAILS Nominal Mass: 1.0000

No.	Sample Id	Sample Mass	Dilution Ratio
1	GREY SHALE CA	1.0000	1.0000
2	KAOLIN WATER	1.0000	1.0000
3	GREY SHALE WATER	1.0000	1.0000
4	KAOLIN CA	1.0000	1.0000
5	BLACK SHALE	1.0000	1.0000
6	BLACK SHALE REAL	1.0000	1.0000
7	OIL SAND	1.0000	1.0000

ANALYSIS AUDIT TRAIL OPERATOR ACTION TIME DATE

Valued coy:AUTHORIS-086FA7 Record created 1:21:05 4/3/2013

Valued coy:AUTHORIS-086FA7 Error MD147 - Activity manually aborted by user. 1:27:31 4/3/2013

ELEMENT AUDIT TRAIL OPERATOR ACTION TIME DATE

No changes for element

SPECTROMETER PARAMETERS Element: Ni Measurement Mode: Absorbance

Wavelength: 232.0 Bandpass: 0.2nm Lamp Current: % 50

Background Correction: D2 High Resolution: Off Optimize Spectrometer Parameters: No

Signal Type: Continuous Resamples: Fast Number Of Resamples: 2

Measurement Time: secs 4.0 Flier Mode: No

Use RSD Test: No

FLAME PARAMETERS Flame Type: Air-C2H2 Fuel Flow: L/min 0.9

Auxilary Oxidant: Off

Nebuliser Uptake: secs 4 Burner Stabilization: mins 0

Optimize Fuel Flow: No

Burner Height: mm 7.0 Optimize Burner Height: No

SAMPLING PARAMETERS Sampling: None

CALIBRATION PARAMETERS Calibration Mode: Normal Line Fit: Segmented Curve Use Stored Calibration: No

Concentration Units: mg/L Scaled Units: mg/L Scaling Factor: 1.0000

Excess Curvature Limits: -10% to +40% Rescale Limit: % 10.0

Failure Action: Flag and Continue

Master Standard 5.0000

Standard 1 0.1000

Standard 2 0.2000

Standard 3 0.4000

QC TEST SUMMARY QC ACTION QC SUMMARY RESULT

Over/Under Calibration 2 of 13 solutions

RESULTS FOR ELEMENT Ni

SAMPLE ID	RESULT TYPE			SIGNAL		Rsd	FLAGS	
CONC.	CORRECTED CONC.				TIME	DATE		
	Abs	%		mg/L	mg/L			
GREY SHALE CA	Mean	0.001		52.2		0.0413	0.0413	
GREY SHALE CA	Resample 1 of 2				0.001			1:23:58
4/3/2013								
GREY SHALE CA	Resample 2 of 2				0.001			1:24:03
4/3/2013								
KAOLIN WATER	Mean	-0.000		609.0		0.0171	0.0171	
KAOLIN WATER	Resample 1 of 2				-0.000			1:24:21
4/3/2013								
KAOLIN WATER	Resample 2 of 2				0.000			1:24:25
4/3/2013								
GREY SHALE WATER		Mean	0.026	0.7	C	0.6972	0.6972	
GREY SHALE WATER		Resample 1 of 2			0.026			1:24:44
4/3/2013								
GREY SHALE WATER		Resample 2 of 2			0.026			1:24:49
4/3/2013								
KAOLIN CA	Mean	-0.000		27.6		0.0099	0.0099	
KAOLIN CA	Resample 1 of 2			-0.000			1:25:10	
4/3/2013								
KAOLIN CA	Resample 2 of 2			-0.000			1:25:14	
4/3/2013								
BLACK SHALE	Mean	0.004		8.4		0.1191	0.1191	
BLACK SHALE	Resample 1 of 2				0.004			1:25:40
4/3/2013								
BLACK SHALE	Resample 2 of 2				0.004			1:25:44
4/3/2013								
BLACK SHALE REAL		Mean	0.001	29.0		0.0467	0.0467	
BLACK SHALE REAL		Resample 1 of 2			0.001			1:26:12
4/3/2013								
BLACK SHALE REAL		Resample 2 of 2			0.001			1:26:17
4/3/2013								
OIL SAND	Mean	0.018	1.7	C	0.4832	0.4832		

OIL SAND 4/3/2013	Resample 1 of 2	0.018	1:26:37
OIL SAND 4/3/2013	Resample 2 of 2	0.018	1:26:41

C.8.3. Test Result For Iron (Fe) Using Atomic Absorption Spectrometer (AAS)

SEQUENCE TABLE Shared Standards: Yes

Action	Solution ID	Fe
Calibration		X
Sample 1	GREY COLOURED SHALE	X
Sample 2	KAOLIN IN WATER	X
Sample 3	GREY SHALE IN H2O	X
Sample 4	GREY SHALE (WATER)	X
Sample 5	KAOLIN IN ACID	X
Sample 6	SANDSTONE	X
Sample 7	BLACK SHALE H2O	X
Sample 8	OILSAND IN CA	X
Sample 9	Sample ID 9	X
Reblank		X
Reblank		X
Reblank		X

SAMPLE DETAILS Nominal Mass: 1.0000

No.	Sample Id	Sample Mass	Dilution Ratio
1	GREY COLOURED SHALE	1.0000	1.0000
2	KAOLIN IN WATER	1.0000	1.0000
3	GREY SHALE IN H2O	1.0000	1.0000
4	GREY SHALE (WATER)	1.0000	1.0000
5	KAOLIN IN ACID	1.0000	1.0000
6	SANDSTONE	1.0000	1.0000
7	BLACK SHALE H2O	1.0000	1.0000
8	OILSAND IN CA	1.0000	1.0000
9	Sample ID 9	1.0000	1.0000

ANALYSIS AUDIT TRAIL OPERATOR ACTION TIME DATE

Valued coy:AUTHORIS-086FA7 Record created 12:10:57 4/3/2013

Valued coy:AUTHORIS-086FA7 Error MD147 - Activity manually aborted by user. 12:28:21 4/3/2013

ELEMENT AUDIT TRAIL OPERATOR ACTION TIME DATE

No changes for element

SPECTROMETER PARAMETERS Element: Fe Measurement Mode: Absorbance

Wavelength: 248.3 Bandpass: 0.2nm Lamp Current: % 50

Background Correction: D2 High Resolution: Off Optimize Spectrometer Parameters: No

Signal Type: Continuous Resamples: Fast Number Of Resamples: 2

Measurement Time: secs 4.0 Flier Mode: No

Use RSD Test: No

FLAME PARAMETERS Flame Type: Air-C2H2 Fuel Flow: L/min 0.9

Auxilary Oxidant: Off

Nebuliser Uptake: secs 4 Burner Stabilization: mins 0

Optimize Fuel Flow: No

Burner Height: mm 7.0 Optimize Burner Height: No

SAMPLING PARAMETERS Sampling: None

CALIBRATION PARAMETERS Calibration Mode: Normal Line Fit: Segmented Curve Use Stored Calibration: No

Concentration Units: ppm Scaled Units: ppm Scaling Factor: 1.0000

Excess Curvature Limits: -10% to +40% Rescale Limit: % 10.0

Failure Action: Flag and Continue

Master Standard 5.0000

Standard 1 0.5000

Standard 2 1.0000

Standard 3 2.0000

QC TEST SUMMARY QC ACTION QC SUMMARY RESULT

Excess Curvature 10 of 16 solutions

Over/Under Calibration 3 of 16 solutions

RESULTS FOR ELEMENT Fe

SAMPLE ID	RESULT TYPE	SIGNAL	Rsd	FLAGS	CONC.	CORRECTED CONC.	TIME	DATE
	Abs	%			ppm	ppm		
GREY COLOURED SHALE	Mean	0.034	2.7	X	10.8544	10.8544		

GREY COLOURED SHALE Resample 1 of 2 0.035 12:16:17 4/3/2013

GREY COLOURED SHALE Resample 2 of 2 0.033 12:16:22 4/3/2013

KAOLIN IN WATER Mean 0.005 28.3 X 4.0330 4.0330

KAOLIN IN WATER Resample 1 of 2 0.006 12:17:53 4/3/2013

KAOLIN IN WATER Resample 2 of 2 0.004 12:17:57 4/3/2013

GREY SHALE IN H2O Mean 0.034 0.8 X 10.7821 10.7821

GREY SHALE IN H2O Resample 1 of 2 0.034 12:20:04 4/3/2013

GREY SHALE IN H2O Resample 2 of 2 0.034 12:20:08 4/3/2013

GREY SHALE (WATER) Mean 1.100 0.2 CX 19.0681 19.0681

GREY SHALE (WATER) Resample 1 of 2 1.102 12:22:35 4/3/2013

GREY SHALE (WATER) Resample 2 of 2 1.099 12:22:40 4/3/2013

KAOLIN IN ACID Mean 0.003 14.7 X 3.2284 3.2284

KAOLIN IN ACID Resample 1 of 2 0.004 12:23:56 4/3/2013

KAOLIN IN ACID Resample 2 of 2 0.003 12:24:00 4/3/2013

SANDSTONE Mean 0.456 1.2 CX 8.4879 8.4879

SANDSTONE Resample 1 of 2 0.460 12:24:56 4/3/2013

SANDSTONE Resample 2 of 2 0.452 12:25:00 4/3/2013

BLACK SHALE H2O Mean 0.009 2.8 X 5.2145 5.2145

BLACK SHALE H2O Resample 1 of 2 0.009 12:25:50 4/3/2013

BLACK SHALE H2O Resample 2 of 2 0.008 12:25:54 4/3/2013

OILSAND IN CA Mean 0.902 0.2 CX 15.8146 15.8146

OILSAND IN CA		Resample 1 of 2		0.901	12:26:24 4/3/2013
OILSAND IN CA		Resample 2 of 2		0.903	12:26:28 4/3/2013
Sample ID 9	Mean	-0.001	69.6	0.3453	0.3453
Sample ID 9	Resample 1 of 2		-0.001	12:27:09	4/3/2013
Sample ID 9	Resample 2 of 2		-0.002	12:27:13	4/3/2013

C.8.4. Test Result For Manganese (Mn) Using Atomic Absorption Spectrometer (AAS)

ANALYSIS INFORMATION NAME OPERATOR TIME DATE

Spectrometer:

Analysis 45 Valued coy 12:48:39 4/3/2013 S Series 712118 v1.27

GENERAL PARAMETERS Instrument Mode: Flame Autosampler : None

Dilution: None Use SFI: No

SEQUENCE TABLE Shared Standards: Yes

Action	Solution ID	Mn
Calibration		X
Sample 1	SHALE IN CA	X
Sample 2	KAOLIN IN WATER	X
Sample 3	GREY SHALE IN W	X
Sample 4	KAOLIN IN CA	X
Sample 5	SANDSTONE IN CA	X
Sample 6	BLACK SHALE	X
Sample 7	OIL SAND	X
Reblank		X
Reblank		X
Sample 8	Sample ID 8	X

SAMPLE DETAILS Nominal Mass: 1.0000

No.	Sample Id	Sample Mass	Dilution Ratio
1	SHALE IN CA	1.0000	1.0000
2	KAOLIN IN WATER	1.0000	1.0000
3	GREY SHALE IN W	1.0000	1.0000
4	KAOLIN IN CA	1.0000	1.0000
5	SANDSTONE IN CA	1.0000	1.0000
6	BLACK SHALE	1.0000	1.0000
7	OIL SAND	1.0000	1.0000
8	Sample ID 8	1.0000	1.0000

ANALYSIS AUDIT TRAIL OPERATOR ACTION TIME DATE

Valued coy:AUTHORIS-086FA7 Record created 12:48:39 4/3/2013

Valued coy:AUTHORIS-086FA7 Error MD147 - Activity manually aborted by user. 12:55:41 4/3/2013

ELEMENT AUDIT TRAIL OPERATOR ACTION TIME DATE

No changes for element

SPECTROMETER PARAMETERS Element: Mn Measurement Mode: Absorbance

Wavelength: 279.5 Bandpass: 0.2nm Lamp Current: % 75

Background Correction: D2 High Resolution: Off Optimize Spectrometer Parameters: No

Signal Type: Continuous Resamples: Fast Number Of Resamples: 3

Measurement Time: secs 4.0 Flier Mode: No

Use RSD Test: No

FLAME PARAMETERS Flame Type: Air-C2H2 Fuel Flow: L/min 1.0

Auxilary Oxidant: Off

Nebuliser Uptake: secs 4 Burner Stabilization: mins 0

Optimize Fuel Flow: No

Burner Height: mm 7.0 Optimize Burner Height: No

SAMPLING PARAMETERS Sampling: None

CALIBRATION PARAMETERS Calibration Mode: Normal Line Fit: Segmented Curve Use Stored Calibration: No

Concentration Units: ppm Scaled Units: ppm Scaling Factor: 1.0000

Excess Curvature Limits: -10% to +40% Rescale Limit: % 10.0

Failure Action: Flag and Continue

Master Standard 4.0000

Standard 1 1.0000

Standard 2 2.0000

Standard 3 4.0000

QC TEST SUMMARY QC ACTION QC SUMMARY RESULT

No QC actions performed

RESULTS FOR ELEMENT Mn

SAMPLE ID	RESULT TYPE		SIGNAL		Rsd	FLAGS
CONC.	CORRECTED CONC.			TIME	DATE	
	Abs	%	ppm	ppm		
SHALE IN CA	Mean	-0.002	21.0		0.0083	0.0083
SHALE IN CA	Resample 1 of 3			-0.002	12:51:38	
4/3/2013						
SHALE IN CA	Resample 2 of 3			-0.002	12:51:42	
4/3/2013						
SHALE IN CA	Resample 3 of 3			-0.002	12:51:47	
4/3/2013						
KAOLIN IN WATER	Mean	-0.002	3.1		0.0099	0.0099
KAOLIN IN WATER	Resample 1 of 3			-0.002	12:52:06	4/3/2013
KAOLIN IN WATER	Resample 2 of 3			-0.002	12:52:10	4/3/2013
KAOLIN IN WATER	Resample 3 of 3			-0.002	12:52:14	4/3/2013
GREY SHALE IN W	Mean	0.014	3.0		0.3594	0.3594
GREY SHALE IN W	Resample 1 of 3			0.014	12:52:35	4/3/2013
GREY SHALE IN W	Resample 2 of 3			0.014	12:52:39	4/3/2013
GREY SHALE IN W	Resample 3 of 3			0.015	12:52:44	4/3/2013
KAOLIN IN CA	Mean	-0.002	28.4		0.0115	0.0115
KAOLIN IN CA	Resample 1 of 3			-0.001	12:53:02	
4/3/2013						
KAOLIN IN CA	Resample 2 of 3			-0.002	12:53:06	
4/3/2013						
KAOLIN IN CA	Resample 3 of 3			-0.002	12:53:10	
4/3/2013						
SANDSTONE IN CA	Mean	0.001	22.0		0.0821	0.0821
SANDSTONE IN CA	Resample 1 of 3			0.002	12:53:34	4/3/2013
SANDSTONE IN CA	Resample 2 of 3			0.001	12:53:38	4/3/2013
SANDSTONE IN CA	Resample 3 of 3			0.001	12:53:42	4/3/2013
BLACK SHALE	Mean	-0.001	23.1		0.0237	0.0237
BLACK SHALE	Resample 1 of 3			-0.001	12:54:03	
4/3/2013						
BLACK SHALE	Resample 2 of 3			-0.001	12:54:08	
4/3/2013						

BLACK SHALE	Resample 3 of 3	-0.001	12:54:12	4/3/2013	
OIL SAND	Mean	-0.001	69.9	0.0340	0.0340
OIL SAND	Resample 1 of 3	-0.001	12:54:32	4/3/2013	
OIL SAND	Resample 2 of 3	-0.001	12:54:36	4/3/2013	
OIL SAND	Resample 3 of 3	-0.000	12:54:41	4/3/2013	
Blank	Mean	-0.002	9.5	0.0000	

C.8.5. Test Result For Lead (Pb) Using Atomic Absorption Spectrometer (AAS)

ANALYSIS INFORMATION NAME OPERATOR TIME DATE

Spectrometer:

Analysis 44 Valued coy 12:34:37 4/3/2013 S Series 712118 v1.27

GENERAL PARAMETERS Instrument Mode: Flame Autosampler : None

Dilution: None Use SFI: No

SEQUENCE TABLE Shared Standards: Yes

Action Solution ID	Pb		
Calibration	X		
Sample 1	GREY COLOURED SHALE	X	
Sample 2	KAOLIN WATER	X	
Sample 3	GREY SHALE H20	X	
Sample 4	KAOLIN IN CA	X	
Sample 5	SANDSTONE	X	
Sample 6	BLACK SHALE H2O	X	
Sample 7	OILSAND IN CA	X	
Sample 8	Sample ID 8	X	
Reblank	X		

SAMPLE DETAILS Nominal Mass: 1.0000

No.	Sample Id	Sample Mass	Dilution Ratio
1	GREY COLOURED SHALE	1.0000	1.0000
2	KAOLIN WATER	1.0000	1.0000
3	GREY SHALE H20	1.0000	1.0000
4	KAOLIN IN CA	1.0000	1.0000
5	SANDSTONE	1.0000	1.0000
6	BLACK SHALE H2O	1.0000	1.0000
7	OILSAND IN CA	1.0000	1.0000
8	Sample ID 8	1.0000	1.0000

ANALYSIS AUDIT TRAIL OPERATOR ACTION TIME DATE

Valued coy:AUTHORIS-086FA7 Record created 12:34:37 4/3/2013

Valued coy:AUTHORIS-086FA7 Error MD147 - Activity manually aborted by user. 12:44:01 4/3/2013

ELEMENT AUDIT TRAIL OPERATOR ACTION TIME DATE

No changes for element

SPECTROMETER PARAMETERS Element: Pb Measurement Mode: Absorbance

Wavelength: 217.0 Bandpass: 0.5nm Lamp Current: % 75

Background Correction: D2 High Resolution: Off Optimize Spectrometer Parameters: No

Signal Type: Continuous Resamples: Fast Number Of Resamples: 3

Measurement Time: secs 4.0 Flier Mode: No

Use RSD Test: No

FLAME PARAMETERS Flame Type: Air-C2H2 Fuel Flow: L/min 1.1

Auxilary Oxidant: Off

Nebuliser Uptake: secs 4 Burner Stabilization: mins 0

Optimize Fuel Flow: No

Burner Height: mm 7.0 Optimize Burner Height: No

SAMPLING PARAMETERS Sampling: None

CALIBRATION PARAMETERS Calibration Mode: Normal Line Fit: Segmented Curve Use Stored Calibration: No

Concentration Units: ppm Scaled Units: ppm Scaling Factor: 1.0000

Excess Curvature Limits: -10% to +40% Rescale Limit: % 10.0

Failure Action: Flag and Continue

Master Standard 7.0000

Standard 1 1.0000

Standard 2 2.0000

Standard 3 4.0000

QC TEST SUMMARY QC ACTION QC SUMMARY RESULT

Excess Curvature 2 of 13 solutions

Over/Under Calibration 7 of 13 solutions

RESULTS FOR ELEMENT Pb

SAMPLE ID RESULT TYPE SIGNAL Rsd FLAGS CONC. CORRECTED CONC. TIME DATE

		Abs	%		ppm	ppm		
Blank	Mean	-0.001	8.6		0.0000			
GREY COLOURED SHALE				Mean	-0.001	13.6	C	-0.0220
-0.0220								
GREY COLOURED SHALE				Resample 1 of 3		-0.001	12:38:01	
4/3/2013								
GREY COLOURED SHALE				Resample 2 of 3		-0.001	12:38:05	
4/3/2013								
GREY COLOURED SHALE				Resample 3 of 3		-0.002	12:38:10	
4/3/2013								
KAOLIN WATER		Mean	-0.001	29.3	C	-0.0238		-0.0238
KAOLIN WATER		Resample 1 of 3			-0.002		12:38:37	
4/3/2013								
KAOLIN WATER		Resample 2 of 3			-0.001		12:38:41	
4/3/2013								
KAOLIN WATER		Resample 3 of 3			-0.002		12:38:46	
4/3/2013								
GREY SHALE H20		Mean	-0.001	22.0		0.0024	0.0024	
GREY SHALE H20		Resample 1 of 3			-0.001		12:39:13	
4/3/2013								
GREY SHALE H20		Resample 2 of 3			-0.001		12:39:17	
4/3/2013								
GREY SHALE H20		Resample 3 of 3			-0.001		12:39:22	
4/3/2013								
KAOLIN IN CA		Mean	-0.002	17.6	C	-0.0600		-0.0600
KAOLIN IN CA		Resample 1 of 3			-0.001		12:39:42	
4/3/2013								
KAOLIN IN CA		Resample 2 of 3			-0.002		12:39:46	
4/3/2013								
KAOLIN IN CA		Resample 3 of 3			-0.002		12:39:51	
4/3/2013								
SANDSTONE	Mean	-0.002	8.5	C	-0.1228		-0.1228	
SANDSTONE	Resample 1 of 3				-0.002		12:40:15	4/3/2013
SANDSTONE	Resample 2 of 3				-0.002		12:40:19	4/3/2013

SANDSTONE Resample 3 of 3 -0.003 12:40:23 4/3/2013

BLACK SHALE H2O Mean -0.002 12.9 C -0.0791 -0.0791

BLACK SHALE H2O Resample 1 of 3 -0.002 12:40:49 4/3/2013

BLACK SHALE H2O Resample 2 of 3 -0.002 12:40:54 4/3/2013

BLACK SHALE H2O Resample 3 of 3 -0.002 12:40:58 4/3/2013

OILSAND IN CA Mean -0.001 39.1 C -0.0300 -0.0300

OILSAND IN CA Resample 1 of 3 -0.002 12:41:25 4/3/2013

OILSAND IN CA Resample 2 of 3 -0.001 12:41:29 4/3/2013

OILSAND IN CA Resample 3 of 3 -0.001 12:41:34 4/3/2013

`Sample ID 8 Mean -0.003 11.7 C -0.1919 -0.1919

Sample ID 8 Resample 1 of 3 -0.004 12:43:19 4/3/2013

Sample ID 8 Resample 2 of 3 -0.003 12:43:23 4/3/2013

Sample ID 8 Resample 3 of 3 -0.003 12:43:28 4/3/2013

Blank Mean -0.003 15.0 0.0000

Blank Resample 1 of 3 -0.003 12:43:46 4/3/2013

Blank Resample 2 of 3 -0.003 12:43:50 4/3/2013

Blank Resample 3 of 3 -0.002 12:43:54 4/3/2013